AD-A049 794 LITTLE (ARTHUR D) INC CAMBRIDGE MASS F/G 6/6
THEORETICAL STUDY TO DETERMINE THE SEA STATE LIMIT FOR THE SURV--ETC(U)
JUN 77 P P RAJ DOT-CG-61505-A
UNCLASSIFIED ADL-79299-F USCG-D-90-77 NL

1 OF 3
AD A049794

DDC
RECEIVED
FEB 10 1978
F

(12) 275 p.

Technical Report Documentation Page

1. Report No. (19)	2. Government Accession No.	3. Recipient's Catalog No.
(18) USCG D-90-77	/	(14) ADL-79299-F

4. Title and Subtitle	5. Report Date
(6) Theoretical Study to Determine the Sea State Limit for the Survival of Oil Slicks on the Ocean.	(11) June 1977
	6. Performing Organization Code: DOT/USCG
7. Author(s): (10) PHANI P.K. RAJ	8. Performing Organization Report No.
9. Performing Organization Name and Address: Arthur D. Little, Inc., Acorn Park, Cambridge, Mass. 02140	10. Work Unit No. (TRAIS): 4714.21
	11. Contract or Grant No.: (15) DOT-CG-61,505A
12. Sponsoring Agency Name and Address: Office of Research and Development, United States Coast Guard, 400 Seventh Street, S.W., Washington, D.C. 20590	13. Type of Report and Period Covered: (9) FINAL REPORT.
	14. Sponsoring Agency Code: G-DOE

15. Supplementary Notes

16. Abstract

Limiting sea state condition for the globular dispersion of oil slicks on the ocean have been obtained from simple considerations. Models have been derived for determining the conditions under which breaking waves will disperse an oil slick. Two types of dispersions are considered, viz., surface dispersion and globular dispersion within the water column, with emphasis on the latter type of dispersion.

The results indicate that a 3 m significant wave height sea state will tend to initiate globular dispersion and that breaking waves of large crest lengths are essential for a surface dispersion to take place. The depth of penetration of globules of oil formed under breaking waves is calculated to be relatively shallow.

The large number of assumptions made and their effects on the results are discussed. Several of the unknown physical parameters of importance are identified and recommendations have been made for experimental determination of some of these parameters.

17. Key Words	18. Distribution Statement
OIL SLICK, SEA-STATE, BREAKING-WAVE, TURBULENCE, GLOBULATION	Document is available to the Public through the National Technical Information Service, Springfield, Virginia 22161

19. Security Classif. (of this report)	20. Security Classif. (of this page)	21. No. of Pages	22. Price
Unclassified	Unclassified	276	

Form DOT F 1700.7 (8-72) Reproduction of completed page authorized

208850

METRIC CONVERSION FACTORS

Approximate Conversions to Metric Measures

Symbol	When You Know	Multiply by	To Find	Symbol
		LENGTH		
in	inches	*2.5	centimeters	cm
ft	feet	30	centimeters	cm
yd	yards	0.9	meters	m
mi	miles	1.6	kilometers	km
		AREA		
in^2	square inches	6.5	square centimeters	cm^2
ft^2	square feet	0.09	square meters	m^2
yd^2	square yards	0.8	square meters	m^2
mi^2	square miles	2.6	square kilometers	km^2
	acres	0.4	hectares	ha
		MASS (weight)		
oz	ounces	28	grams	g
lb	pounds	0.45	kilograms	kg
	short tons (2000 lb)	0.9	tonnes	t
		VOLUME		
tsp	teaspoons	5	milliliters	ml
Tbsp	tablespoons	15	milliliters	ml
fl oz	fluid ounces	30	milliliters	ml
c	cups	0.24	liters	l
pt	pints	0.47	liters	l
qt	quarts	0.95	liters	l
gal	gallons	3.8	liters	l
ft^3	cubic feet	0.03	cubic meters	m^3
yd^3	cubic yards	0.76	cubic meters	m^3
		TEMPERATURE (exact)		
°F	Fahrenheit temperature	5/9 (after subtracting 32)	Celsius temperature	°C

*1 in = 2.54 (exactly). For other exact conversions and more detailed tables, see NBS Misc. Publ. 286, Units of Weights and Measures, Price $2.25, SD Catalog No. C13.10:286.

Approximate Conversions from Metric Measures

Symbol	When You Know	Multiply by	To Find	Symbol
		LENGTH		
mm	millimeters	0.04	inches	in
cm	centimeters	0.4	inches	in
m	meters	3.3	feet	ft
m	meters	1.1	yards	yd
km	kilometers	0.6	miles	mi
		AREA		
cm^2	square centimeters	0.16	square inches	in^2
m^2	square meters	1.2	square yards	yd^2
km^2	square kilometers	0.4	square miles	mi^2
ha	hectares (10,000 m^2)	2.5	acres	
		MASS (weight)		
g	grams	0.035	ounces	oz
kg	kilograms	2.2	pounds	lb
t	tonnes (1000 kg)	1.1	short tons	
		VOLUME		
ml	milliliters	0.03	fluid ounces	fl oz
l	liters	2.1	pints	pt
l	liters	1.06	quarts	qt
l	liters	0.26	gallons	gal
m^3	cubic meters	35	cubic feet	ft^3
m^3	cubic meters	1.3	cubic yards	yd^3
		TEMPERATURE (exact)		
°C	Celsius temperature	9/5 (then add 32)	Fahrenheit temperature	°F

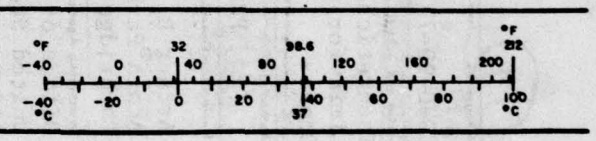

ACKNOWLEDGEMENT

This study was performed by Arthur D. Little, Inc., for the Environmental Technology Branch, Office of Research and Development, United States Coast Guard.

The project was initiated under the guidance of LCDR D. S. Jensen and was monitored by Mr. Richard Griffiths. The project team at Arthur D. Little was headed by Dr. P. K. Raj and included Drs. E. C. Kern (Jr.), G. Pollak, D. B. Rosenfield, Mr. J. H. Cawley (Jr.) and Ms. Dana Dietz. Professors J. H. Milgram and R. C. Reid of MIT were consultants on the project. The guidance, support and cooperation of Mr. Griffiths is gratefully acknowledged. Technical assistance and critique rendered by Professors Milgram and Reid are also thankfully acknowledged.

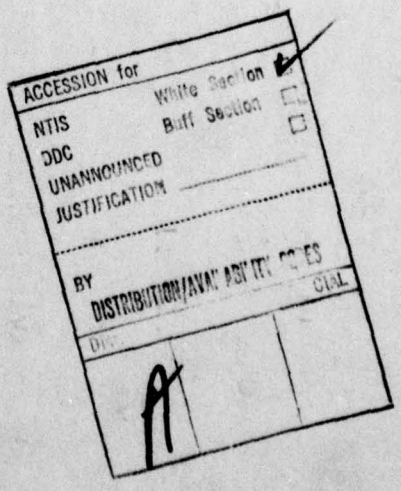

TABLE OF CONTENTS

TABLE OF CONTENTS (continued)

TABLE OF CONTENTS (continued)

TABLE OF CONTENTS (continued)

TABLE OF FIGURES

TABLE OF FIGURES (continued)

TABLE OF FIGURES

TABLE OF TABLES

CHAPTER 1

INTRODUCTION

1.1 Background

In 1967, the Torrey Canyon disaster focused the world's attention on the problem of large-scale oil pollution and alerted the public to the chronic oil spill problem plaguing the world. Subsequent major oil spills on the ocean and on inland waters have further raised the level of public concern. The growing appetite of the world for petroleum and the economics of ocean transportation of crude oil in very large crude carriers (VLCC) portend the occurrence of spills which will be several times larger than the Torrey Canyon spill, with their disastrous ecological and economic consequences. Accidental spills caused by damage to oil tankers are one of the major polluting sources. The quantities of oil discharged intentionally by tankers, either in lightening it in an emergency or in routine ballasting and tank-cleaning operations, are by no means inconsiderable, though the discharges are not so dramatic or in as large a quantity as in a severe accident. Very little information is currently available on what happens to the oil spilled on the oceans. The effect of spills occurring near shore has been to pollute the coastal areas and beaches. Even in these cases it is not certain how much of the oil is washed ashore, evaporates or remains in suspension. Therefore, there exists an urgent need to understand the behavior of oil and its ultimate fate when spilled on the high seas.

In order to meet the growing demands for energy and petroleum products, the United States will be importing ever increasing quantities of crude oil, at least for the next two decades. Large off-shore terminals called "deepwater ports" are to be built 25 to 50 miles off the coasts; they are intended to accommodate ships of the VLCC class (these need water depths of over 90 feet, but no port within the United States has adequate water depths to berth these vessels). Applications have already been filed by two consortia to build two deepwater ports, one off the Texas coast and the other off Louisiana. The National Climatic Center predicts that within the general area of these ports, the seas will be greater than five feet for 33% of the fall and winter seasons and greater than eight feet for 10% of these seasons. Very high sea states with waves of 30 feet have also been observed during storms. Due to the high cost associated with the closing of these ports, considerable incentive exists to continue to transfer the oil from the ship to the receiving terminal even in bad weather. However, the probability of a spill is higher under adverse weather conditions. The Deepwater Port Act of 1974 (PL 93-627) has recognized this aspect and has stipulated the use of the best technology available to protect the marine and coastal environments from oil spills.

Under the Deepwater Port Act of 1974, the United States Coast Guard (USCG) is responsible for the regulation of the deepwater ports. Their involvement in the development and regulation of these ports will include oil transfer systems, structures, casualty response systems, navigation, inspection, and other areas. One of the prime considerations given by the Coast Guard in this regard is the study of spill-response technology applicable to rough sea conditions. The Coast Guard is conducting and supporting research efforts in this area. The Coast Guard has recognized that before a new technology can be developed, several complementary efforts have to be conducted. One such effort is the identification of the sea-wave threshold limit beyond which containment and recovery of oil are impractical due to the dispersion of oil slicks. At present there is no comprehensive theory

describing the break-up of uncontained oil slicks in severe sea states. The Coast Guard has embarked on a research program to obtain a better understanding of the interaction between the sea and weather conditions and the spilled oil. The principal purpose of the research program is to make possible the prediction of the ultimate fate of the spilled oil and its dispersion.

In pursuit of the goals of the above research program, Arthur D. Little, Inc. was awarded a contract in March 1976 (DOT-CG-61,505-A) to perform a "Theoretical Study on the Dispersion of Oil Slicks Under Severe Sea and Weather Conditions". The study forms the first step in a larger overall effort undertaken by the Coast Guard. Related experiments in the laboratory and at sea will be performed as separate efforts. These may be followed by an additional theoretical study which will take advantage of the knowledge and expertise gained in the previous studies and attempt to develop a predictive model for determining the behavior of an oil slick on the sea.

1.2 Objective

The objective of the study undertaken by Arthur D. Little, Inc., was to develop theoretical and physical models to describe the dispersion of an oil slick subjected to waves on the open ocean. Such a study would aid the design of experiments to study the oil dispersion problem and delineate the important phenomena and parameters to be studied in the experiments.

The objective of the program did not include the determination of the effectiveness of the existing oil cleanup technology in open, rough sea conditions nor did it include the determination of the limit up to which the currently available spill-fighting equipment could be used in the sea.

1.3 Scope of Work

In order to achieve the above objective, the project work was divided into five major tasks.

- Background study and literature search;
- Determination of important factors, parameters and unknown phenomena;
- Estimation of the limiting sea state for incipient dispersion, using order of magnitude analysis and fundamental principles;
- Development of analytical models; and
- Identification of minimum number of measurements and observations to define the state of the sea.

In Chapter 2 of this report, the literature pertaining to the problem of oil on the ocean in general is reviewed. The review includes briefly the literature on the interaction between the wind and the ocean and the characterization of the sea by the energy density spectrum. What little information exists on the upper ocean turbulence and on breaking waves is also discussed. The scant information available to quantify the effect of the presence of oil on wave dynamics is also indicated. The data available on the variation of the oil properties during its weathering on the ocean are also reviewed.

In a subsequent section of Chapter 2, the important physical parameters and factors that affect oil dispersion are analyzed and in many cases, their range of values, or uncertainties in the values, are identified. The effects of the uncertainties on the predictive capability of the models given in the literature are also discussed. the parameters reviewed include the ocean breaking wave characteristics, the parameters in the definition of wave spectra, the turbulence parameters and ocean current effects. Also a brief review is made of oil globular dispersion models published in the literature.

The determination of the limiting sea state for the incipient dispersion by order of magnitude calculations is presented in Chapter 3.

In the initial part of this chapter, overall estimates are made of the energy budget of various physical phenomena occurring in the ocean. Also the basic calculations have been performed to obtain the surface energy and gravitational energy required to sink oil globules into water. A thermodynamic stability approach is considered for obtaining limiting conditions for oil-slick breakup. A slick-breakup criterion has been obtained, but it has not been possible to relate this to a sea state because of the lack of some important oil property data. The minimum sea state for dispersion is predicted using the spectral description of a fully developed sea. In this calculation the relationship between water particle velocities and their effect on the turbulence phenomena in the upper ocean have been assumed. This calculation has been made after deriving a criterion for the globulation of oil from the slick due to the turbulent pressure fluctuations in the upper ocean. Estimates have also been made for the turbulent intensity generated in the sea due to wind above water. The sea-state limits predicted and their sensitivity to assumptions in the values of both the environmental parameters and oil properties are discussed. However, in making these calculations the "oil" is considered to be a single component fluid with non-varying properties. It is recognized that the oil properties may vary due to differential evaporation and dissolution of the slick, temperature gradients in water, and other factors. Such fine details are not included in the overall estimates made in Chapter 3. Similarly, the possibility that the characteristics of the upper ocean turbulence underneath an oil slick may be significantly altered by the presence of the oil slick has not been taken into account.

A large part of the theoretical work performed in this project is developed in Chapter 4. Calculations show that oil slicks will not be affected by simple swell waves. The possibility that wind generated Langmuir circulations may herd oil into windrows and thus fracture the slick has been considered and modeled.

The emphasis of the models in Chapter 4 has been on the effect of breaking waves on the dispersion of oil slicks. Two types of oil dispersions have been considered. These are surface dispersion and globular dispersion into the water column. Surface dispersion is assumed to result when a large oil slick is broken up into smaller puddles ("slicklets") by a train of breaking waves. A stochastic model is developed which gives a time for initiating a slick fracture by breaking waves. The dependence of this time on various wave parameters and slick size is explicitly given. This model may be appropriate for the dispersion (by breaking waves on a shoal) of a large oil slick caused by the instantaneous release of a large quantity of oil. No attempt has been made in this particular model to investigate the effects of variation in oil properties on slicklet dispersion.

The globular dispersion is also modeled as being caused by breaking waves. The turbulence associated with the breaking action is assumed to be sufficiently strong to tear the oil slick into globules and drive them under water. To characterize this phenomenon, models have been developed to obtain, for a given sea state, the probability of occurrence of breaking waves in a given region, their average energy loss, the maximum depth of penetration of oil globules into water, the characterization of upper ocean turbulence generated under the breaking wave, and the distribution of oil globules subjected to turbulence. Also considered is the effect of Langmuir circulations on globules of oil.

A schematic view of the phenomena considered and the models developed is shown in Figure 1.1. The path indicating "macro-turbulence" has not been discussed because of the lack of information on the sizes of turbulent eddies and the turbulent energy density spectrum in the upper ocean. Similarly, the dispersion of oil globules under a steady-state turbulence condition has not been considered because of the availability of this model in the literature.

In developing the models for the globular dispersion, the oil globule diameter is used as a known parameter. No model has been developed to characterize the distribution of oil drop sizes formed when an oil slick is subjected to breaking waves. These data can be obtained only by experiments. The globule size distribution is likely to be a strong function of wave characteristics and the type of oil.

In Chapter 5, the parameters used in the definition of sea state (considered in the models in Chapter 4) are identified and discussion provided on the types of measurements to be made. The Joint North Sea Wave Project (JONSWAP) spectral description of the sea state is considered in detail. The minimum number, type and duration of measurements that are necessary to obtain statistically meaningful values for the parameters are indicated. These parameters include the wind velocity, surface elevation, fetch, modal (spectral) frequency, current velocity, and other on-site measurements. Also discussed are measurements of some parameters that are neither directly related to the sea state definition nor are used in the models developed in this project, but which may be incorporated into a second generation of physical models. The discussion in Chapter 5 has been limited to identifying the parameters. The scope of the work under this project does not include discussion of either the measuring instruments or the techniques of measurement.

1.4 Program Results and Conclusions

The results from this program are discussed under two broad classifications, viz., those obtained from the background study -- literature search and those resulting from the physical models developed.

The literature review indicates that many phenomena associated with the oil-on-the-ocean problem are not well understood and that no known analysis exists. Some of the poorly understood phenomena include:

- The effect of the presence of oil on the air-sea interaction, the attenuation of wave energy, the alteration of the breaking

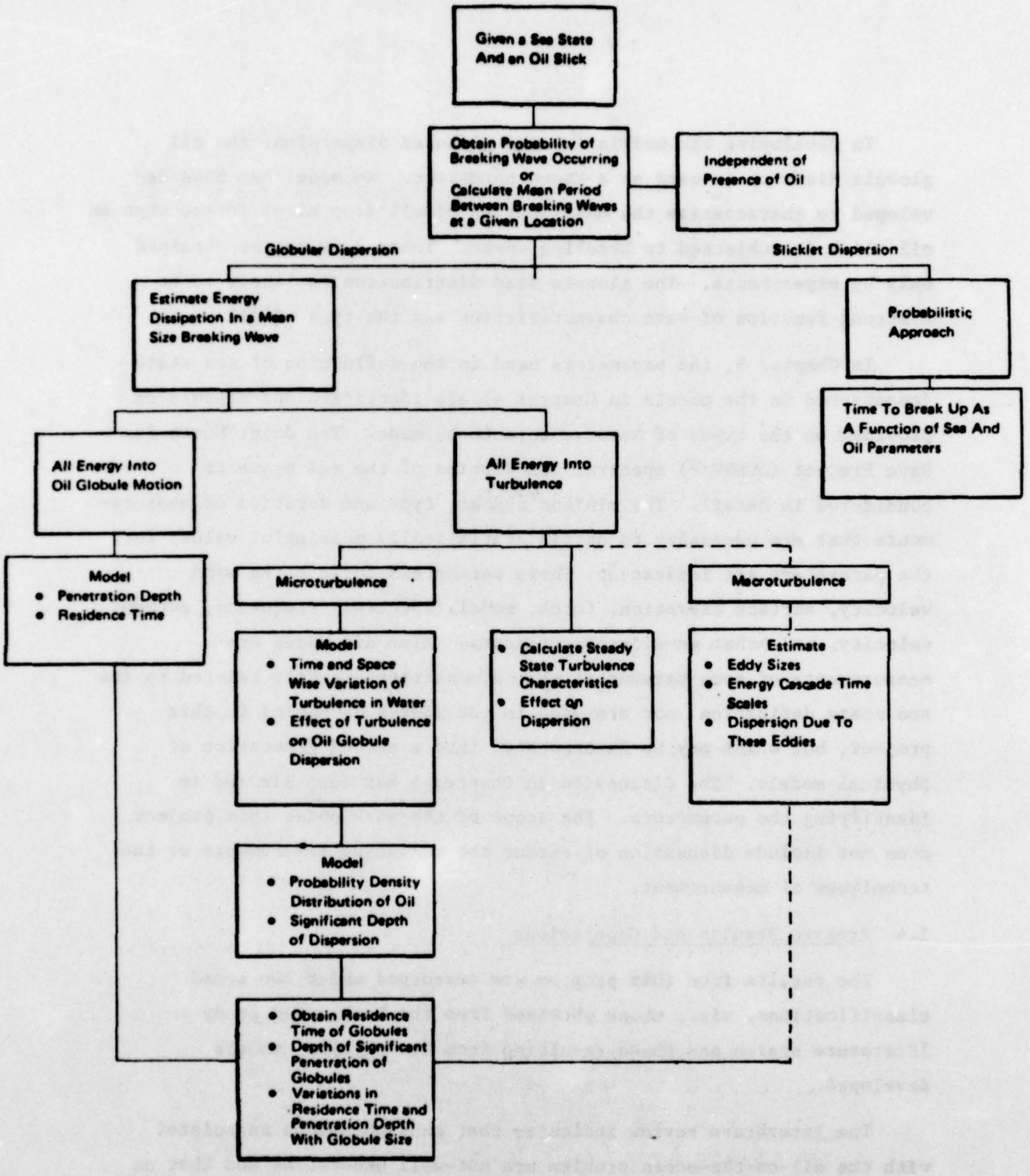

FIGURE 1.1 SCHEMATIC DIAGRAM OF THE VARIOUS PHENOMENA CONSIDERED IN THIS PROJECT ON MODELING THE DISPERSION OF OIL ON OPEN OCEAN

probability and size of breaking waves, etc.;

- The characteristics of the breaking waves (number density and crest-length distributions, mean period between occurrence), as function of sea state in the absence of an oil film;
- The characteristics of upper ocean turbulence, its generation mechanism, time and eddy size scales, energy dissipation rates;
- The variation of the properties of different kinds of oil (crude oil, refined oil, industrial grade oil, etc.), with aging on the ocean under varying environmental conditions of temperature, wind, and of sunlight.

The main achievements in this project have been the development of models to describe several of the phenomena that affect the dispersion of oil on the open ocean. The entire effort has been based on theoretical modeling. The numerical results have been based on the use of best available information or, where data are lacking, use of values which are, at best, educated guesses.

The principal results obtained from the models developed in the program indicate that:

- The significant wave height (indicating the sea state) of a fully developed sea at which oil of specific gravity 0.9 will undergo incipient globular dispersion is 3 m. This result is based on several assumptions regarding the spectral description of the sea, the interrelationship between the turbulent velocity fluctuations and the wave motion and the criterion for globulation. A change in any of the relationships will drastically change the value of the above sea state. The use of a different relationship between two parameters, viz. wind velocity and turbulent intensity results in 1.2 m significant wave height for the minimum sea state for oil to start dispersing in the form of globules.

- The fraction of the oil slick that undergoes globulation is about 12% for 3 m high ($H_{1/3}$) seas. This fraction increases for increasing sea states, but is still small (30%) at 5 m sea state.
- The fracture of an oil slick by simple, non-breaking swell waves is improbable, even though these waves contain enough energy to produce globules of oil and drive them into the water. Strain rates (stretching and compression) of the oil film developed during the passage of a swell are too small to affect the structure of the oil film and, also, the wave frequency needed to tear the oil film is high.
- Horizontal fracturing of an oil slick can be effected by breaking waves provided their average period of occurrence and their crest lengths have the proper values. However, if the ratio of the mean square crest length of the breaking waves to the principal dimension of the slick is smaller than about 1/3, it is highly unlikely that a continuous fracture of the slick by breaking waves can be sustained.
- A model has been developed to predict the probability of a breaking wave occurring at a given location (unit area), the mean energy dissipated in wave breaking and the mean time between the occurrence of breaking waves. These values are functions of the wind velocity and the fetch. Typical values for fetch limited seas indicate that the average wave energy loss during the wave breaking phase is between 1 and 5 kJ/m^2. Wave breaking probability ranges between 1/200 and 1/4000.
- The depth of penetration of oil globules into water is a strong function of the oil density and globule size. The model derived for the vertical motion of globules (in the absence of large-scale circulation) indicates that depth of penetration is of the order of a fraction of a meter. Larger globules

penetrate to greater depths than smaller ones. The ratio of penetration depth to the diameter of globules seems to be somewhat insensitive to the initial velocity with which the globules are projected into water.

- The motion of the oil globules, when subjected to a non-stationary (decaying) turbulence in water, is developed in a Stochastic model. Based on the example considered (turbulence characteristics assumed) it is seen that all of the oil globules will reach the surface and probably recoalesce to form a film of oil. The duration of time for this recoalescence to occur would be about twice the time of the globules to resurface in the absence of turbulence. It is likely that if the turbulence is totally different from the assumed characteristics, the above residence time estimates will be different. In any case, the total residence time seems to be of the order of 10 sec.

- Langmuir circulations caused by steady winds generate sufficiently large downwelling currents to carry oil globules. The oil globules may be carried down to much larger depths (order of several meters), and the residence time of the globules in the water will increase. In a steady wind of 10 m/s, the downwelling currents in Langmuir cells are sufficiently strong to drag down oil globules of 4 mm diameter and smaller (oil density:900 kg/m^3). At a 20 m/s wind speed, 1 cm diameter globules would be dispersed.

1.5 Limitations

In a completely theoretical approach, as has been the case with the present project, an important limitation of the models developed is the lack of experimental proof to buttress the results. We have made, wherever necessary, appropriate assumptions regarding the behavior of the physical phenomena. These have been based on our best scientific judgment and experience. However, nature in its infinite variety of behavior may present phenomena which have not been

considered in this study. Experimental confirmation of each of the models is therefore essential before the models can be accepted to be correct.

In addition, there are other important limitations:

1. Air-sea interaction in the presence of oil.

   In accounting for the air/sea interaction and in defining sea states, the changes that occur due to the presence of the oil on the water surface have not been fully considered. While the effects of the presence of the oil are known qualitatively, complete quantitative effects are not available.

2. Partially developed sea-state.

   All of the analyses assume fully developed sea-state conditions. It is entirely possible that certain processes (example: wave breaking frequency) which influence oil dispersion may be more severe in a developing sea than in a fully developed sea.

3. Variations in oil properties and aging of oil.

   Even though the physical properties of the oil are considered in the modeling, their complete effect is not included. Examples of this include the variations in density, viscosity and interfacial tension within a large slick. Models for slick dispersion and breakage that include these property variations will necessarily have to consider the types of oil, the initial composition, and effects of sunlight, sea water temperature, and winds and waves on evaporation and dissolution. Such exhaustive property information is currently not available and, therefore, has not been included in the theoretical models developed in this project.

1.6 Recommendations

Based on the analyses performed in this project and on the understanding of the difficulties in predicting the "fate" of the oil (in a sea invironment) with the available knowledge, we recommend that further research be directed towards the following three areas:

1. Controlled Experimental Investigations

Specifically we recommend that experiments be performed to

- Quantify the characteristics of turbulence in the upper ocean.
- Determine the energy transfer rates between wind and water with and without the presence of an oil slick. The thickness and type of oil should be varied.
- Measure the critical wind, wave and turbulence conditions at which oil globulation occurs under non-wave breaking conditions.
- Determine the rate and magnitude of energy loss during the breaking of a wave, the characteristics of the resulting turbulence field (eddy sizes, dissipation time scales, intensity, etc.) in water. Experiments should be conducted with and without the presence of an oil slick. Also in the experiments with an oil slick present, data should be obtained for the critical conditions under which breaking of a wave occurs.
- Ascertain the effect of wave breaking on the size distribution of oil globules formed and the depths to which they are driven. Experiments may be carried out initially with "simulated oil" consisting of uniform size glass or polystyrene beads of density equal to that of a "typical" oil to determine the penetration depth of globules.
- Conduct experiments to determine the physical and chemical properties of oil relevent to the problem of spread and dispersion.

- Gather data from the ocean on the statistics of breaking waves, such as the number density, crest length distribution, mean distance between breakers, and sizes -- all data to be gathered for a variety of sea state consitions. These may be obtained by aerial photographs.

It is recommended that, where feasible, the above experiments be carried out initially in the laboratory, with final tests on the ocean itself.

2. Development of Technology to Gather Data from Large Accidental Oil Spills

Some of the accidental spills of oil on the oceans have resulted in the release of tens of thousands of tons of oil in a variety of ocean conditions. Since controlled experiments of such magnitude are neither economically feasible nor ecologically acceptable, we recommend that the "spills of opportunity" be utilized to gather as much data as possible. Our specific recommendations in this regard call for

- Developing an overall oil response program plan by the Coast Guard that is designed exclusively for data gathering. The plan should take into account the type, nature and number of data to be gathered when a large scale spill occurs on the ocean.
- Research into and development of instruments and equipment that are simple, readily transportable and deployable on or into the oil slick from, say, a helicopter.

For example, at present it is not known what fraction of the oil in a large slick dissolves in water, is dispersed as globules under the slick or sinks. There is an immediate need to develop a simple sequential sampling device that will sink, in stages, to predetermined depths, take water samples at each stage, and finally resurface to be recovered by helicopters.

3. Further Theoretical Modeling Efforts

We recommend that further theoretical efforts be closely integrated with the experimental investigations. These efforts should be directed towards

- Developing a method for predicting the total mass of oil that may sink to the bottom, either because of sediment coagulation with oil drops, or because of turbulence transport and capture at the bottom.
- Analyzing the effects of oil aging and the effects of water temperature on the dispersion.
- Understanding the conditions and developing the criteria for the different and as yet inexplicable ways in which oil tends to spread on a water surface.
- Improving and refining existing models in the light of experimental data.

CHAPTER 2

LITERATURE SURVEY AND IDENTIFICATION OF IMPORTANT PARAMETERS

2.1 Introduction

In this chapter we review the technical literature pertinent to the prediction of the survivability of an oil slick on the ocean. A list of the referenced articles, papers, monographs and reports is given in the bibliography.

In Section 2.2, we present a general description of the ocean with particular emphasis on wind-wave interactions and turbulence. We then review the literature on the interaction between oil spilled on the ocean and the ocean itself. This includes an examination of the existing information on the spreading of oil on the ocean, the effect of oil on the ocean waves, the movement of the slick, and slick stability in oil recovery systems (with emphasis on the physical models). Finally, a brief review of the oil properties and their variation on the sea due to aging is also provided.

In Section 2.3, a review is made of the important parameters that may have a significant effect on the dispersion of unconfined oil slicks in the open ocean. The parameters include those that determine the behavior of the sea, the wind effects, ocean waves, oil properties, etc. Where pertinent correlations or theoretical formula exist, the important range of parameters are identified and the uncertainites in the predictive nature of the correlations are discussed.

Existing physical models describing the fate of oil on the sea are also examined, but we limit our review to unconfined oil spills. The behavior and fate of boomed oil is not considered.

2.2 Survey of Literature Relevant to the Dispersion of Oil on the Sea

General Description of the Sea

The book by Van Dorn (1974) is an excellent starting point for understanding the origin of the sea, atmospheric dynamics and its effects on the sea, and waves in particular, how they are formed and how they they may be categorized. The book illustrates and explains the basic principles with little mathematics. While it is instructive to read the book from the point of view of understanding the ocean, it is not meant to be a reference on ocean research.

Several books are devoted primarily to ocean waves. For example, Bigelow and Edmondson (1952) have described well the physical nature of wind waves and provide extensive data (contour plots) of high and low sea swells for different regions of the earth. The book, however, does not provide a detailed mathematical description of wave motion. Wave motions in inviscid fluids have been treated exhaustively by Lamb (1932), and this is an important reference in examining ocean stability and in analyzing various types of waves. Kinsman (1965) deals with wave phenomena in considerable mathematical detail. He has discussed methods of specifying a random sea and the determination of wave spectra from measurements in the sea. For a mathematical analysis of the wave phenomena, this is an excellent reference.

In this study the relationships among various wave parameters are often used. In order to facilitate easy reference to these relationships Table 2.1 is provided. The table is developed using the results derived in Lamb (1932). Relationships amongst wave parameters such as the wave phase velocity, wave length (or equivalently wave number), wave frequency, wave energy, etc. are indicated. Also given are the relationships that involve the physical properties of the medium in which the waves occur. The symbols are defined in the nomenclature.

TABLE 2.1

Important Relationships Among Water Wave parameters
(water-air interphase)

General Relationships $c = \frac{\omega}{\kappa}$; $\kappa = \frac{2\pi}{\lambda}$

Parameter	Gravity Waves	Capillary Waves	Combined Gravity-Capillary Waves
Phase velocity (c)	$c^2 = \frac{g}{\kappa}(1-s)\tanh(\kappa h)$ where h = water depth For deep-water waves ($\kappa h > \pi$) $c^2 = \frac{(1-s)\,g}{\kappa}$ For shallow water waves ($\kappa h < \frac{1}{4}$) $c^2 = (1-s)\,gh$	$c^2 = \frac{\sigma \kappa}{\rho_w}$	$c^2 = \left[\frac{g(1-s)}{\kappa} + \frac{\kappa \sigma}{\rho_w}\right]$
Group velocity (U)	Deep-water waves $U = \frac{1}{2}c$ Shallow water waves $U = c$	$U = \frac{3}{2}c$	$U = \left[1 - \frac{1}{2}\frac{(\kappa_m^2 - \kappa^2)}{(\kappa_m^2 + \kappa^2)}\right]c$ where $\kappa_m^2 = \frac{g(1-s)}{\sigma}$
Energy per unit area in the wave system (E")	$E'' = \frac{1}{4}\rho_w g a^2$	$E'' = \frac{1}{2}\sigma \kappa^2 a^2$	—

Wave Spectra

The energy in a wave is dependent on the amplitude of the wave in the case of gravity waves and on both amplitude and wave length for capillary waves. Typically the sea contains a myriad of waves, of all different sizes, lengths, and directions jumbled together usually as a result of wind generated disturbances of different intensities, locations and directions. The energy contained in such a confused sea motion is generally represented by a spectral diagram-essentially a representation of energy density as a function of the wave number (or frequency).

The characterization of a sea by its spectrum has been studied by a number of investigators, for example Michel (1968), Van Dorn (1974); also, Kinsman (1965) provides a detailed mathematical analysis of the various theories involved in the spectral analysis.

A histogram of the wave height, H, (vertical distance between the observed crest and trough of waves) can, in most cases, be represented by a Rayleigh distribution of the following type:

$$p = \frac{2H}{\overline{H^2}} \exp\left(-\frac{H^2}{\overline{H^2}}\right) \qquad 2.1$$

where p dH represents the probability of occurrence of a wave of height between H and H + dH. $\overline{H^2}$ is the mean square-wave height. It is more customary to express the height of waves by specifying the <u>significant wave height</u>. This is the mean height of the highest one-third of the waves present. This height, represented by $H_{1/3}$, is related to the root mean-square height; for the Rayleigh distribution this is given by (see Longuet-Higgins 1952):

$$H_s = H_{1/3} = 1.41 \left[\left(\overline{H^2}\right)\right]^{1/2} \qquad 2.2$$

Longuet-Higgins (1952) has derived the statistical distribution of wave heights when the total number of wave height observations is finite and the frequency separation of the waves is small compared to the central frequency.

Several researchers have proposed mathematical formulas to describe the observed sea spectra. A detailed analysis of the differences in the spectral distribution predicted by different correlations is given by Michel (1968), and it is probably the best paper for a comprehensive review of the subject of wave spectra. The correlation most often accepted for a fully developed sea is that of Pierson-Moskowitz. This correlation given by Michel (1968) is of the following dimensional form:

$$e(\omega) = \frac{135}{\omega^5} \exp\left[-\frac{9.7 \times 10^4}{U^4 \omega^4}\right] \qquad 2.3$$

where $e(\omega)$ = the energy spectral density (ft^2-sec) at frequency ω,

ω = radian frequency, s^{-1}

U = wind speed (knots) measured at 64 feet above "mean sea" level.

Defining E" as its average wave energy (ft lb/ft^2) per unit area of sea, it is seen that the relationship between $e(\omega)$ as given above and E" is given by *

$$E'' = \frac{1}{16} \rho_w g \int_0^\infty e(\omega) d\omega$$

The significant wave height (H_s) for the above correlation is given by:

$$H_s^2 = \frac{3.5\, U^4}{10^4} \qquad 2.4$$

where H_s is in feet and U is in knots.

Other correlations such as the Bretschneider's, International Snip Structures Congress' (ISSC) have been proposed where, instead of wind velocity, a term called the "significant period" (average period of the significant waves) is used. The ISSC spectrum is of the form:

$$e(\omega) = \frac{2760\, H_s^2}{T_s^4 \omega^5} \exp\left(-\frac{1050}{T_s^4 \omega^4}\right) \qquad 2.5$$

where T_s = significant period (s)

---

* ρ_w should be in the units of slugs/ft^3 when FPS units are used.

In a fully developed sea, the significant wave period T_s and wind velocity U are related (Bretshneider gives a correlation connecting U and T_s). However, for a partially developed sea there is no such interrelationship, and, therefore, two independent quantities (H_s and T_s) have to be specified to define the spectrum. That is, a two-parameter spectrum is necessary to specify a partially developed sea. Van Dorn (1974) discusses the meaning of the two terms--fully developed and partially developed sea.

Wind Wave Interaction

The generation of waves by wind blowing on top of water is a familiar phenomenon and, in spite of concentrated research over many years, a complete theory for the generation and growth of wind waves is still lacking. The ruffling of a water surface by wind was studied by Rayleigh, Stokes and other researchers in the last century (see Lamb, 1932). The threshold wind speed at which waves appear on a water surface depends on the purity of the water and varies from a low of 1.07 m/s (see Lamb, Chapter XI, 348) for pure water to about 1.5 m/s for sea water (Van Dorn, 1974). At wind speeds greater than 3 m/s, the sea surface becomes rough and wave growth is accelerated, due to both a decrease in the ripple angle (of propagation) and the onset of instability from the amplitude selective process. Waves with the shortest wave length and the steepest form grow fastest because they perturb the air flow significantly.

Efforts to understand the air-water energy transfer process began in the 1880's with Kelvin, Helmoltz and others who studied the oscillations set up at the interface between two fluids. More recent theoretical investigations by Jeffreys (1924) and Svedrup and Munk (1947) have been concerned with the tangential and normal stress energy transfer mechanisms between wind and water. Other theories, which include the mechanisms of wind turbulence and nonlinear interactions between wave groups have been thoroughly examined by Kinsman (1965).

Experimental investigations of the interaction between wind and waves have been primarily concerned with predicting the roughness

parameter of the sea and the drag coefficient. The Karman-Prandtl equation for the distribution of air velocity with height in turbulent flow over a rough surface (universal velocity distribution law) has been widely applied as a method of determining the dependence of the wind shear stress on the water as a function of wind velocity. Wilson (1960) has reviewed all of the available laboratory and field experimental correlations on wind stress measurements and has presented a table of derived drag coefficients. The drag coefficient is derived by using an equation of the form:

$$\tau_o = C_D \rho_{air} U^2 \qquad 2.6$$

where τ_o is the mean shear stress on the water surface, ρ_{air} is the density of the air, U is the mean wind speed measured 10 m above the (undisturbed) water level, and C_D is the drag coefficient. From a review of the data and using the Karman-Prandtl equation to scale the laboratory scale experimental results, Wilson (1960) has estimated that:

$$C_D \simeq 0.0024 \pm 0.0005 \text{ for strong winds}$$

and

$$C_D \simeq 0.0015 \pm 0.0008 \text{ for light winds}$$

More recent data from the experiments by Ruggles (1970) indicate that the airflow regime over the ocean in the wind speed range 2 to 10 m/s (at 10 m height) is best described as a region of constant drag coefficient with $C_D = 1.6 \times 10^{-3}$. This value is modified by the superposition of almost singular departures at a number of discrete wind speeds which are apparently caused by the onset of distinct peaks at wind speeds of 2 m/s, 4 m/s and 8 m/s. The 2 m/s speed is related to Jeffrey's minimum wind speed for wave generation (Lamb, 1932, p. 625) and the phenomenon at 8 m/s to classical Kelvin-Helholtz instability. Based on the measured data, Ruggles suggests the following empirical correlation between friction velocity u* and wind speed at 10 m height, U.

$$u^* = 0.04\ U \qquad 2.7$$

Falvey (1974) also has developed correlations between wind speed and friction velocity and wind speed and wave heights. His correlations for friction velocity are more involved than those above and different correlations apply to different regions depending on whether the sea surface is hydrodynamically smooth or rough. In addition Falvey indicates that his correlations are applicable to cases where the storm width is larger than the fetch.

The development of the sea state (expressed as the total energy content of waves) due to the presence of wind has been discussed by Van Dorn (1974). He has presented a cumulative sea-state diagram which is extremely useful in determining such sea-state parameters as the sea-state index (square root of energy), significant wave height and period, all quantities being shown as functions of wind speed and duration of wind action. Also, the fetch distances for development of a fully developed sea are presented. However, spectral distribution data are not presented as functions of the sea state.

The energy supplied by the wind to the sea after the sea is "fully developed" is lost by a variety of dissipative phenomena. The main energy dissipating mechanism is the breaking of waves. In addition, turbulence in the upper layers of the ocean and surface film effects do dissipate energy but not at a sufficiently large rate. Another important mechanism of energy removal from the waves in the sea is the geometric spreading of the waves.

The phenomenon of wave breaking has been studied by a number of workers from the middle of the last century. Several mechanisms which cause a wave to break have been propounded. Van Dorn (1974) has reviewed the salient features of breaking waves and concludes that:

(i) Waves of steepness ratio H/L will break when they reach a beach of slope S where $S^2 < 2\pi H/L$. H is the observed wave height and L the distance between crests.

(ii) Offshore wave breaking is dependent on the absolute wave height. Higher waves of same steepness will break farther offshore.

(iii) The angle at the wave crest in a spilling breaker is 120°.

Other workers such as Price (1970, 1971), Banner and Phillips (1974), Longuet-Higgins and Turner (1974), have all considered the detailed structure of breaking waves and have determined criteria under which waves break. A correlation for the height of the breakers (that occur near shore) as a function of the deep water wave steepness is presented by Van Dorn (1974) for different beach slope values. The correlation indicates that as the wave steepness increases the relative height of breaking (i.e., ratio of the height of the breaking wave to the deepwater wave height) decreases. The distribution of breaking waves in a sea is quite random. The frequency and the intensity of breaking are known to increase with increased wind speed, but there are no models to predict how many waves break at any given instant (within, say, a specified area) or what their height, length, and width relationships are to the sea state. Van Dorn (1974) presents a correlation for the probability of breaking - which he calls a "guesstimate" based on observing aerial photographs of breaking waves - as a function of wind speed. The correlation is given by:

$$P = 2U - 20 \text{ for } 10 < U \text{ (knots)} < 60 \qquad 2.8$$

where P is the percent of the high waves that break in a sea with a given wind speed U. It is emphasized by Van Dorn that the above relationship, having been developed by photographic observations and not having any sea-state information, is applicable to any sea-state condition rather than being restricted to fully developed states. He further defines "larger waves" as being the highest 10% waves in any sea state and relates the average height of the breaking waves to the average height of the highest 10% waves. Using this "guestimate," it is possible to calculate the average height of the breaking waves and the number

density per unit sea surface area. However, there are no data on the transverse length distribution of breaking waves. This is an important parameter for the "splitting" of an oil slick by breaking waves.

The energy loss due to wave breaking has been analyzed by Barnett (1968) and he gives a relationship between spectral form and frequency in the frequency range dominated by wave breaking. Longuet-Higgins (1969) has derived an expression for the fraction of wave energy "lost" in a wave cycle due to breaking of waves. This derivation is based on the assumption that waves of an amplitude above a critical value will break and that the wave amplitudes are distributed according to a Rayleigh distribution. The critical amplitude value is determined by the condition that the acceleration of water particles at the wave crest is equal to one-half of the acceleration due to gravity. Based on these criteria, Longuet-Higgins has shown that the fraction $\tilde{\omega}$ of the wave energy that is lost by breaking in one mean wave cycle is essentially a constant and is given by:

$$\tilde{\omega} = \exp\left(-\frac{1}{8\alpha}\right) \qquad 2.9$$

where α is a dimensionless constant appearing in the spectral density function describing the energy density in the wave. Using the value of $\alpha = 1.35 \times 10^{-2}$ which is typical of the equilibrium spectrum (see Phillips, 1958) with a sharp low frequency cutoff, it is seen that $\tilde{\omega} \simeq 10^{-4}$. It is suggested by Longuet-Higgins that a significant part of the energy lost by wave breaking goes directly into turbulence. A small part is also transferred to capillary waves (high frequency) and also to the gravity waves. Longuet-Higgins has also related η with the wind-wave drag coefficient C_D (see Ruggles, 1970) by the formula:

$$\tilde{\omega} \simeq 1600 \left(\frac{\rho_a}{\rho_w}\right) C_D^{3/2} \qquad 2.10$$

Ocean Turbulence

The phenomenon of turbulence in the ocean has not been studied in any great detail because of the difficulties in measurement. However, some important characteristics of ocean turbulence are reasonably well established. For example, it is known that the turbulent dissipation of energy in unit time in non breaking waves is small compared both to wave energy flow and to the energy input rate from wind. In addition the dissipation is confined to the upper levels of the ocean, essentially in regions above the trough of waves. Stewart and Grant (1962) have estimated from the data obtained in a tidal channel near Vancouver Island (under 6 m/s wind, 0.4 m wave height and 5 m wave length) that the turbulent dissipation function ε was essentially a constant at 0.03 erg/cm^{3}s over depths of 1 to 2 m. At a 15 m depth ε is an order of magnitude smaller than the above value. Stewart and Grant concluded that their measured turbulence is associated with the wind driven drift current rather than with the waves.

A more recent paper by Belyaev et al. (1975) indicates that, based on data obtained from measurements in the Atlantic and Indian Oceans, the value of the dissipation function varies between 0.15 erg/cm^{3}s at 36 m depth to 0.037 erg/cm^{3}s at 140 m depth. This clearly indicates that ocean turbulence is of a higher intensity. Unfortunately no other quantitative remarks can be made, because the paper does not give data or sea conditions or on turbulence closer to the ocean surface.

The energy to sustain turbulence in the ocean is derived from a variety of sources such as ocean currents, wind stresses and atmospheric turbulence, and the flow of water into oceans from rivers and rain. From the data provided by Belyaev et al., it can be argued that the turbulence measured by these workers is not representative of that generated by wave breaking but, instead, is generated by a thermal current at about 100 meter depth. Faller (1971) has given order-of-magnitude estimates of the energies involved in several identifiable phenomena associated with fluid motions in the ocean. He concludes that waves probably contribute about an order of magnitude more energy

than any other source to maintaining ocean turbulence in the surface (mixed) layer.

The literature on ocean turbulence is singularly lacking in information or analysis of the relationship between sea conditions ("sea state") and the characteristics of turbulence. Those researchers who have investigated the turbulence phenomenon in the ocean seemed to be more concerned with the structure of turbulence and its spectrum rather than either identifying the nature of its production or the relation of turbulent intensity to sea state (see Osborn, 1970). It stands to reason that the turbulent intensity and energy would increase with an increase in the sea roughness generated by, say, a storm. Several questions remain unanswered. For example, how does turbulent intensity in upper layers vary in a developing sea state, in a fully developed sea, and in zones outside the storm zone where there is still considerable energy in the waves? What is the relationship between breaking wave frequency and turbulent spectrum? Is the turbulence under a breaking wave characterized by scales comparable to the wave height? In our opinion these are extremely important questions that have to be considered in the study of oil dispersion by rough seas. Longuet-Higgins (1969) has derived expressions for energy loss in wave breaking -- but it is not clear whether all this energy ends up as turbulence in the ocean surface or a part of it is fed to other wave modes.

No review of turbulence phenomena in the ocean would be complete without a reference to the literature on turbulence in general. Probably the best starting point for understanding the basics of turbulence and the terminology is a book by Tennekes and Lumley (1974). The book by Hinze (1959) is a classical treatise on the subject but it is a difficult book to understand.

Oil on the Ocean

Ocean Dynamics in the Presence of an Oil Slick

The concept that the fury of the sea can be minimized (and sometimes eliminated) by a film of oil on the water surface seems to be

well entrenched in nautical literature since Ben Franklin's days. Van Dorn (1974, Chapter 27) in his book has dealt with this subject very elegantly and concludes that while oil and other films do indeed damp out small waves of less than 1 ft in height (essentially capillary waves) they have no effect whatsoever on larger waves and certainly no effect on breaking waves. He has also provided the following formula for the wave energy dissipation by monomolecular films (in which stretching energy is dissipated as heat):

$$\begin{pmatrix}\text{fraction of wave energy dissipated per second by film stretching relative to the average energy of wave motion}\end{pmatrix} = \frac{7 \times 10^{-5}}{T^{0.25}} \qquad 2.11$$

where T is the wave period in seconds.

This indicates that, for a 10 second wave, only 2×10^{-5} of the wave energy is lost per second by a film if it were present on the water surface.

Some theoretical work is being presently undertaken (Milgram, 1976) to evaluate the wave energy dissipation by a relatively thick (2 to 3 cm) oil slick spread over a large area on the sea. In this case, even long period waves may be attenuated to a considerable degree. What this may do to the frequency and number of breaking waves in a given sea state is a question that remains unanswered. There is, however, a possibility that at the perimeter of a thick oil slick the breaking waves may be amplified due to the obstruction provided by the oil in the wave path.

An experiment to determine the effect of wave height attenuation by the presence of oil film has been reported by Kolesnichenko et al. (?) With a 3 mm thick spindle oil layer in a wave tank, the wave height decreases parabolically with distance. Also, at a given location, the wave height decreases with an increase with oil thickness. While the data represent the first known quantitative information on the rate of attenuation of wave heights by an oil film, it is not clear how the results from the reported scale tests (1:25) can be extrapolated

to sea conditions. For example, it is uncertain how the results obtained in these experiments with single wavelength waves (though several wavelengths were investigated in different experiments) can be applied to a sea containing a spectrum of wavelengths. Besides, how to relate this information to a breaking wave remains in doubt.

The full-scale experiments of Barger et al. (1970) employed a 1 km by 0.5 km oleyl alcohol film in the sea off the coast of Massachusetts. The results indicate that the presence of monomolecular films on the sea surface affects not only the wave generation in the sea but also the turbulence in the lower layers of the atmosphere above the "slick." They report observing no breaking waves within the slick whereas outside of the slick many were present. Since no data on the sea states are given (other than that the average wind speed was about 8 m/s and 5 m/s on the respective measurement days) it is hard to evaluate the severity of the sea and draw any conclusions about the effect of the film on the breaking waves under other sea conditions.

The few studies reviewed above have added considerable information on the effect of oil on water as it relates to the dynamics and waves. However, a complete understanding is far from achieved. Several important questions remain to be answered, such as the effect of oil slicks on waves in a fully developed sea as against in a developing sea, whether the water turbulence is different underneath an oil slick, and how the wind energy is transferred to water (if at all) through the slick.

Behavior of Oil on the Ocean - Spreading and Movement

The spreading of oil on the ocean and its movement by wind, waves and other natural forces have been investigated by a number of people. Fallah and Stark (1976) reviewed the current literature on the movement of oil on the sea. In their article they considered spreading (gravitational and surface tension driven), slick drifts by wind, waves and currents and spreading of continuously released oil by oceanic turbulence (diffusion). The review is comprehensive, but it does not discuss the merits of one model against the other, nor does the review

recommend the best model to use in a given situation. The review, however, contains an exhaustive bibliography on the problem of oil on the sea. Another comprehensive review which includes mechanisms of oil spread not considered by Fallah and Stark has been given by Waldman et al. (1973). In the latter work, models have been developed to predict the spread of continuously released oil on calm water. Between these two principal review papers most of the literature currently available concerning the movement and spreading of oil on the ocean has been covered, and there seems to be no justification to repeat them in this survey. However, for the purposes of continuity, the physical mechanisms that are believed to cause oil spread and movement are catalogued below.

The principal forces that tend to spread oil on calm water are buoyancy and the interfacial tension. On the ocean, the surface movement of the oil caused by the waves is relatively small compared with the wind-induced motion. In very turbulent oceans and for small thickness slicks, the turbulent dispersion of oil can be important. One other phenomenon that has been noticed in large oil spills on the ocean is the development of the slicks into long thin streaks aligned in the direction of the wind. These are apparently associated with the formation of regular helical convection cells in water known as Langmuir vortices.

Another important factor in the spreading of oil on the ocean (especially large spills) is the change in oil properties due to weathering and fractionation. The naphtha fractions in the oil are known to evaporate within three days after the spill (Brunnock et al., 1968). The solubility of oil in water also affects the spreading due to the changes in the interfacial tension. Fay (1970) has considered this dissolution aspect and has presented a correlation for calculating the maximum slick size. The literature is particularly deficient in models of spread and movement of oil that have considered the time-wise change of oil properties due to environmental effects.

Stability of Oil Slicks on the Ocean

Perhaps the most important phenomenon that is of interest to the present study is the stability of an unconfined oil slick subjected to the various forces in the sea; yet it is precisely in this area that the literature has almost no information. We do, however, find numerous studies, both experimental and theoretical, dealing with the problem of oil-film stability when it is contained by a boom and subjected to a relative water current.

The only work that deals with an associated problem is that published by Leibovich (1975,ii) on the limitations to containment of oil in the open sea. Leibovich obtains expressions for the probability density of finding oil globules as a function of the depth in the sea. This probability density is related to the terminal velocity of the drop in calm water and to a turbulent diffusion coefficient related to the wind speed. While the analysis presented is elegant, Leibovich has not addressed the question of the conditions under which oil droplets can be formed (if at all) and how the droplet size and distribution is related to the sea conditions.

Stability of Contained Oil Slicks

While the problem of interest to the present study is the dispersion of unconfined oil slicks and how they break up, it is worthwhile reviewing in brief the conditions under which the booming of oil fails. Several physical phenomena that cause oil to flow underneath the boom skirt may also cause dispersion of an unconfined oil slick. It should, however, be kept in mind that a fundamental difference in the physical situation exists; in the booming of the oil there is always a relative current between oil and water. This need not be the case in an open sea condition.

The "failure" of boomed oil is said to occur when oil droplets are torn off from the slick, entrained in the water stream and pass under the barrier of the boom. Wicks (1969) gave a relationship between size of droplets formed and the water speed and also the critical water speed at which droplets are formed. This droplet

formation pehnomenon has been explained as being a consequence of interfacial wave amplification, behind the head wave, by a Kelvin-Helmholtz type of instability (see Jones 1972; Leibovich, 1975, (i); Milgram and Van Houten, 1974). Certain other experimental observations have indicated that droplet formation occurs first at the head wave and in the turbulent wave region behind the head wave. Such a failure has been considered by Leibovich (1975) and Zalosh and Jensen (1975). In all these analyses the primary aim is to predict the water-current speed at which droplets escape from the barrier. All consider the flow to be essentially laminar with instabilities occurring at the oil-water interface. No consideration is given to the effects of possible turbulence in the water. While the theories presented and the analyses in the above references are correct, they are of little use in the present study because of the omission of the effects of turbulence. In the case of an unconstrained oil slick on the ocean, the important phenomena are the presence of waves and turbulence in water and generally the absence of (high-speed) relative currents between oil and water.

Change of Oil Properties During Spreading

When oil is spilled on the ocean, its composition changes with time due to weathering. Processes which contribute to weathering are evaporation, photochemical and oxidation reactions, dissolution of individual components in water, emulsification and the action of microorganisms. The physical properties of the oil such as the density, viscosity, and surface tension change are affected. It is known that the principal mechanism that causes the greatest initial change in crude oil composition is the evaporation of light hydrocarbons.

The evaporation loss rate from a slick depends not only on the volatile fractions contained in the slick at any given time, but also on the area of the slick and environmental factors such as wind speed and wave agitation. This problem has not been considered in its completeness in the literature. Even the change of properties (with time) in an

actual slick on the sea has not been determined. The experiments of Harrison et al. (1975) were the first scale experiments under sea conditions to study the oil property changes. These experiments (using 275 gallons of crude oil) indicate that fractions whose boiling points are below 220°C should evaporate completely in three to eight hours in a typical oil spill under normal wind conditions. Harrison et al. also state that during their experiments they noticed a sudden and dramatic increase in evaporation rates when the sea was rough and had extensive whitecapping. This paper does not indicate whether property measurements were made during the aging of the slick. Regnier and Scott (1975) reported another series of oil evaporation experiments under the controlled conditions of a laboratory environmental chamber. They have provided extensive tables of evaporation rate constants for various n-alkane components as functions of temperature.

The measurement of the physical and chemical property changes of oil spilled from a large accident have been reported by McLean and Betancourt (1973). The oil deposited on the shore after the "ARROW" spill in Chedabucto Bay, Nova Scotia was studied to determine the property changes due to weathering. The data reported indicated that specific gravity rises fairly rapidly (from 0.95 to 0.98) up to about 18 months, after which time the rate drops. The asphaltene composition varied from 5% to about 25% by weight in a period of about 22 months. It is mentioned by these authors that the viscosity of the samples collected showed wide scatter, but that a trend of rapid increases in viscosity values could be discerned. The experiments of Davis and Gibbs (1975) give direct quantitative information on the changes in physical property values (and compositions) of oil exposed to sea conditions. The results obtained over a period of two years by exposing a 1.4 cm thick water in an oil-emulsion (chocolate mousee) layer of Kuwait crude in a tank exposed to tidal flushing indicate that both viscosity and specific gravity increase with time as did the percent asphaltenes. The specific gravity increased from 0.955 to 0.985 almost linearly over the two year period. The increase in kinematic

viscosity increases proportionately to the square of the elapsed time. It is concluded by the above authors that the experimental results are representative of the behavior of lumps of "mousse" in moderately calm sea conditions.

The results reported by McLean and Betancourt (1973) and Davis and Gibbs (1975) relate to the variation of physical properties of oil due to weathering under actual sea conditions, but no data are presented on the variation of surface tension with either composition or time. It is recalled that one of the driving forces for spreading oil, especially when the film thickness is small, is the interfacial tension at the air, oil, water interface. Besides spreading, interfacial tension between water and oil may have a profound effect on the ability of a slick to remain in one piece under the actions of waves and wind in the sea.

It is clear from the above brief review of oil physical property changes that, in any physical modeling of the slick behavior under perturbing forces, temporal changes of properties need not be considered if the periods of interest are of the order of days or a few weeks after the evaporation of light hydrocarbons. The properties that have to be used in the analysis of course should be appropriate to the oil remaining at the instant of concern. However, in the context of the present study, the period of interest would be the initial 24 hours to 72 hours after the occurrence of a spill. As such the variation of the properties of oil during this period is of concern.

2 3 Important and Unknown Parameters Affecting the Dispersion of Unconfined Oil Slicks on the Ocean

The behavior of oil on the open ocean is primarily influenced by the phenomena that occur in the oceans. These include the air-sea interaction, the wave effects and the oceanic turbulence. Any analysis of oil dispersion cannot be discussed independently of the above features of the oceans and their influence on the fate of the oil.

The word "dispersion" is used rather loosely in the literature. Many times it represents the movement of the oil slick as a whole on the water surface by wind, current, and wave action. It is also used to imply the breakage of the oil film and the scattering of smaller volumes of oil into or on the water. Under the purview of the present project, "dispersed" should be construed to be that state of the oil from which essentially none can be recovered by mechanical means from the ocean because either the oil is in suspension in the upper ocean water in the form of globules (maintained by ocean mixing forces) or the main slick has split up into a number of smaller slicklets which have floated away from each other.

The problem of oil dispersion in the open ocean has received very limited attention in the literature, and, therefore, only scant information is available on the types of forces (parameters) that affect dispersion. However, there exists a considerable body of literature dealing with the wind-sea interaction, wave spectra, and other ocean dynamics problems. We have reviewed below the importance of some of the physical parameters which influence the ocean dynamics and which have direct bearing on the dispersion of oil slicks. We analyze first the parameters relevant to the description of the sea state, i.e., the parameters that may influence oil dispersion.

2.3.1 Description of Sea State

- Known parameters and relationships.

A sea state is generally defined by the spectral distribution of energy in waves and by a parameter called the significant wave height (H_s). The fully developed sea (FDS) parameters can be completely described in terms of a single parameter, viz., the wind speed. These are given in Table 2.2. However, in the case of a developing sea, the specification of significant wave height is insufficient to describe the sea. Wind speed, fetch distance and duration of wind action should also be specified. Alternatively, the specification

Table 2-2: Values of the Parameters for a Fully Developed Sea (FDS) in terms of the Wind Speed at 10m Height above the Sea Surface

Symbol	Parameter	Unit	Formula
U	Wind speed at 10m above mean sea level	m/s	-
a^*	Root mean square wave amplitude, i.e., average energy per unit area in the wave field is $E'' = 1/2\ \rho g a^{*2}$	m	$7.83 \times 10^{-3}\ U^2$
F_m	Minimum fetch distance to establish an FDS	km	$14.25\ U^{4/3}$
t_m	Minimum wind duration to establish FDS	hrs	$8.03\ U^{1/3}$
T_m	Period associated with highest waves in the spectrum	s	$0.74\ U$
T_a^*	Average observable wave period	s	$0.564\ U$
L_a^*	Average length between wave crests	m	$1.06\ U^2$
H_s	Significant wave height	m	$2.83\ a^*$
H_f	Most probable (or frequent) wave height	m	$1.41\ a^*$
H_a	Average height of all waves	m	$1.77\ a^*$
H_{10}	Average height of highest 10% waves	m	$3.6\ a^*$

of a developing sea can be made complete, provided the wave energy and the wind speed are specified.

The energy spectrum of a partially developed sea is calculated by using some parts of the fully developed sea spectrum. A sharp cut-off is introduced at an appropriate low frequency so that the total wave energy is equal to the partially developed sea energy. For example, if the Pierson-Moskowitz spectrum is used [Michel 1968] we have for the spectral energy density,*

$$e(\omega) = \alpha \frac{g^2}{\omega^5} \exp\left[-\beta \left(\frac{g}{U\omega}\right)^4\right] \qquad 2.12$$

where

$$\alpha = 8.1 \times 10^{-3}$$

$$\beta = 0.74$$

Also the significant wave height is given by

$$H_S^2 = \left(\frac{4\alpha}{\beta}\right) \frac{U^4}{g^2} \left\{1 - \exp\left(-\beta \left(\frac{g}{U\omega_c}\right)^4\right)\right\} \qquad 2.13$$

where ω_c is the lowest frequency ("cut-off frequency") of the waves with any measurable energy content.

While the above equation provides a spectral description of the partially developed or fully developed sea state, it provides no information on either the fetch length or the wind duration needed to attain the given sea condition. A parametric chart involving the sea state energy (i.e., the significant wave height), fetch distance, wind duration and wind speed has been given by Van Dorn (1974). The chart,

---

*The total wave energy per unit nominal area of the sea is defined by

$$E'' = \rho_w g \int_{\omega_c}^{\infty} e(\omega)\, d\omega$$

called the cumulative sea state diagram (CSS diagram), is reproduced in Figure 2.1. This figure clearly illustrates the effect of wind duration and fetch on the development of the sea state. For a detailed description of how this chart may be used in predicting the sea state for various conditions, reference has to be made to Van Dorn's (1974) book.

2.3.2 Influence of Different Parameters on Sea Conditions

Table 2.2 illustrates comprehensively the effect of the single most important parameter, the wind speed U, on the characteristics of a fully developed sea. It is seen in this case that the energy in the wave field increases as the 4th power of the wind speed (and, therefore, all wave-height parameters increase as the speed squared). The minimum duration for which wind has to blow to obtain a fully developed sea is somewhat insensitive to the speed of the wind. From a spectral point of view, as the total wave energy increases, (representing a higher sea state), the frequency at which the energy spectral density ($e(\omega)$) is a maximum tends to shift towards lower frequency values.* However, the numerical value of this modal frequency depends on the particular spectral formula used to describe the sea. It is recalled that, while there exist several correlations for the sea state spectrum, no one is universally accurate for all sea conditions.

In the case of developing seas, the two important parameters of influence are the wind speed and the duration of wind action (or alternatively the fetch). The CSS diagram indicates that the sea state index grows very rapidly with wind duration at first, but, as the fully developed sea (FDS) is approached, the rate of rise of the index becomes small. In the case of limited fetch and high winds (as generally is the case in most seas), the spectrum would have a narrower range

---

*For example, in a 20 knot wind, the modal frequency is about 0.11 Hz and, in a 40 knot wind, the modal frequency is 0.056 Hz.

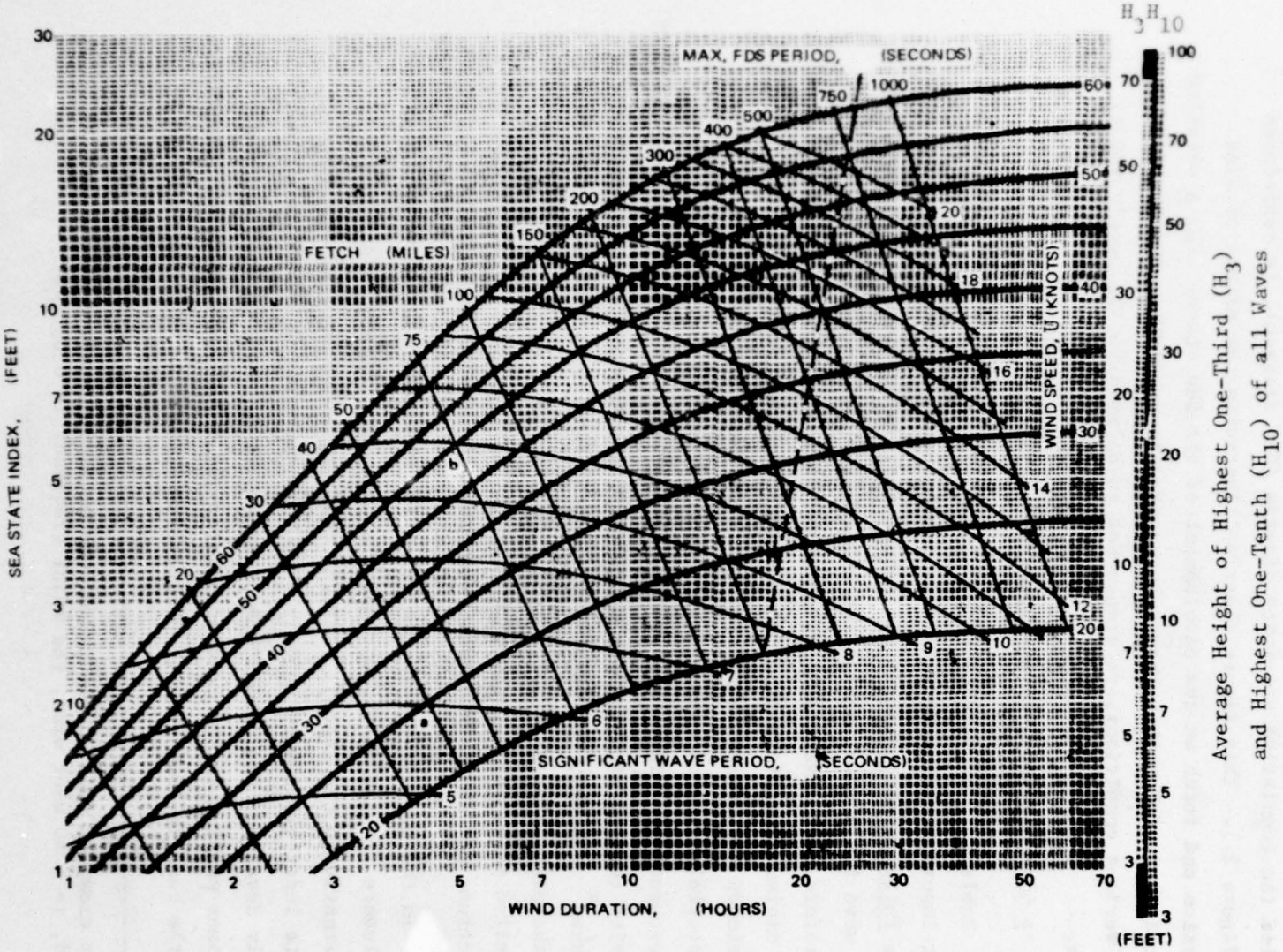

FIGURE 2.1 : CUMULATIVE SEA STATE DIAGRAM
[Reproduced with Permission From Van Dorn (1974)]

of ideal wave periods. Hence the waves would be steeper and more likely to form whitecaps or break. In other words, the wave heights measured by the significant wave height in a fetch limited and non-fully developed sea generated by high winds would be as large as those that would be produced by an unlimited fetch, lower wind speed, fully developed sea. This may be understood on the basis that in fetch limited seas the energy is transferred from the wind over limited distances, but at a much higher rate (because of high wind speeds) whereas in FDS the wind action takes place for long distances, but at a low energy input rate for low winds.

2.3.3 Unknown Parameters in the Definition of Sea Conditions Relevant to the Oil Dispersion Problems

2.3.3.1 Energy Dissipation

When the sea is fully developed, any additional energy input from the wind is dissipated in the sea due to the breaking action of the waves. This energy goes into creating turbulence in water which is ultimately dissipated by viscous friction into thermal energy. An attempt has been made to quantify energy dissipation in breaking waves (Longuet-Higgins, 1969) but the quantitative understanding of the problem in its entirety is far from complete. Longuet-Higgins (1969) has theoretically predicted the expected values or the fraction of total wave energy lost due to wave breaking. The value of this fraction is not only dependent on a dimensionless constant (called the equilibrium spectrum constant α), but also on what form of spectrum one chooses. Longuet-Higgins has shown that α is related to the wind drag coefficient which, in turn, is a function of the wind speed (Ruggles, 1970). The energy loss fraction ($\tilde{\omega}$) is proportional to the exponential of $(-1/\alpha)$, and, therefore, small changes in the value of α tend to result in large changes in $\tilde{\omega}$. The value of α is in the range (Longuet-Higgins, 1969):

$$0.8 \times 10^{-2} < \alpha < 1.48 \times 10^{-2}$$

which results in the following range of values for the estimated fractional energy loss in a single wave cycle:

$$1.637 \times 10^{-7} < \tilde{\omega} = e^{\left(-\frac{1}{8\alpha}\right)} < 2.148 \times 10^{-4}$$

It is seen therefore that a factor of two uncertainty in the value of α results in approximately a 3-order of magnitude variation in the prediction of the energy loss rate from wave breaking. Therefore, Longuet-Higgins' formula is applicable when a very approximate order of magnitude type of calculation of wave energy loss is being made; it cannot be used for any type of accurate calculations. However, a better correlation or formula is not available at the present time.

There are several important ocean parameters which may have a direct bearing on the oil dispersion but whose relationship to the sea state are not known at present. These parameters are discussed below:

2.3.3.2 Number Density, Size and Frequency of Breaking Waves

It is a fair assumption that breaking waves will be able to disperse an oil slick vertically into the ocean in the form of globules. Their size distribution, frequency of occurrence, number per unit area, and the length over which breaking action occurs are all unknown functions of the sea state. Another parameter that is not known is the fraction of energy in a single breaking wave that is dissipated under the wave. For example, it is not known whether the rate of energy dissipation of energy is uniform over the travel length of waves or whether it is non-uniform. Also, it is not known how this energy loss rate is related to the size of the breaking waves.

Another feature that is not known quantitatively at present is the behavior of breaking waves when they encounter an oil slick. Since the oil slick interferes with the wind-water interaction, its presence should have an effect on waves. It is reasonable to assume that large

breaking waves will not be affected by oil slicks because of the enormous energy they carry. On the other hand small amplitude breaking waves may very well be attenuated by oil slicks. The value of the critical height of breaking waves that would be influenced by an oil slick is not known at present. Another phenomenon that may occur is the initiation of breaking at the edge of the oil slick. This may be brought about by the kinetic energy of a wave being arrested by the oil slick with wave breaking. In short, the effects of an oil slick on the behavior of breaking waves and vice versa are not understood to any substantial degree, and no quantitative data exist at present.

2.3.4 Turbulence in the Upper Ocean Layers

The ultimate agents in the ocean that influence vertical dispersion of oil are the turbulent velocity fluctuations in the upper few meters depth of water. Turbulence within the ocean is generated from a variety of energy sources, such as the wind, the water current, the thermal instability motions and breaking waves. It is not known at present whether it is the small-scale turbulent motions that are important for the vertical dispersion of oil or whether large-scale eddies have considerable influence. These latter eddies may be generated by wave motion as well as by water currents. Only experiments can provide definitive answers.

The interest and the research in ocean turbulence phenomena are of very recent origin, and therefore not much information is available in the published literature. Besides, researchers are primarily interested in different scales of turbulence—oceanographers and meteorologists concentrate on large-scale eddies and the hydrodynamicists on the small-scale eddies. Unfortunately however, there has been almost no research into the characteristics of the turbulence in the top few meters of ocean water and their variations in different sea conditions.

The parameters of turbulence that influence oil dispersion include the mean square velocity fluctuations, the integral scale of turbulence, and the turbulent energy spectrum. In addition, the spatial and temporal variations of these quantities in different sea states are essential to describe the turbulent field completely.

Very little quantitative data are available in the literature on the above parameters. Stewart and Grant (1962) report measurements at various depths of velocity fluctuations in water under non-breaking waves at relatively low wind speeds (6 m/s). Their data indicate that the intensity of turbulence is low under non-breaking sea conditions and that the energy dissipation function (ε) is reasonably constant within the first 2 m depth. The possibility that the turbulence characteristics measured by Stewart et al. were not representative of wave-generated turbulence (but of turbulence generated by a current) has been alluded to by these authors. Belyaev et al. (1975) have also reported similar findings but with higher values for ε, which extend to larger depths. The data seem to indicate that the turbulence was generated by a large ocean current at about 100 m depth. The range of values of ε reported by Stewart and Grant (1962) is

$$0.003 \text{ erg/cm}^3 \text{ s} \quad (\text{at 15 m depth}) \quad < \quad \varepsilon \quad < \quad 0.03 \text{ erg/cm}^2 \text{ s} \quad (\text{at depths less than 2 m})$$

and the range given by Belyaev et al. (1975) is

$$0.037 \text{ erg/cm}^2 \text{ s} \quad (\text{140 m depth}) \quad < \quad \varepsilon \quad < \quad 0.15 \text{ erg/cm}^2 \text{ s} \quad (\text{36 m depth})$$

Kinsman (1965) indicates that energy associated with turbulence in non-breaking waves is orders of magnitude smaller than the energy in breaking waves.

Some crucial information regarding the upper ocean turbulence is not available at the present time. For example, it is not known what fraction of energy dissipated by a breaking wave results in

generating turbulent eddies. Also, the size of the eddies formed under the breaker, the spectral distribution, the spatial variation with depth of turbulent intensity under a breaker and the energy feed rate into turbulence from the breaking are some of the parameters whose values are unknown.

It is generally assumed that the characteristics of turbulence under a spilling wave would depend on the height of the wave and, therefore, indirectly on the sea state. It is not certain, however, whether turbulence also depends on the presence of oil in suspension. It is very likely that eddies of a size much larger than an oil globule would not be affected, but smaller size eddies certainly should be influenced by the presence of oil particles in water.

Lastly, the exact mechanism by which a spilling wave may tear an oil film and produce globules of oil and maintain them in suspension is unclear. It is reasonable to assume that the size distribution of globules will to some extent depend on the spectral distribution of turbulence in the ocean water surface during the time of wave breaking.

The magnitude of many of the unknown parameters or their effects can be discerned only by experimental measurements. Some experiments can be performed on a small-scale and results extrapolated to sea conditions. Some others may be obtainable only by measurements at sea.

2.3.5 Ocean Currents

The effect of upper ocean currents on the movement of oil is reasonably well understood. Unconfined slicks tend to move with the current at the water surface if there is no wind. The presence of wind and the earth's rotation, to a lesser extent, seem to affect the general direction of motion of slicks.

The interaction between an ocean current and an unconfined oil slick, from the point of view of slick stability and breakup is not known. It is likely that the effect of the current is indirect (through turbulence) rather than direct as in the case of a confined

slick. The current, on the other hand, may have a profound effect on the dissolution rates of various water-soluble fractions of the oil. No controlled experiments which have specifically addressed this question have been reported in the literature.

2.3.6 Oil Property Parameters and their Known Influence

The breaking of a slick and its subsequent dispersion will be dependent to a considerable extent upon the physical properties of the oil. It is not clear, however, which of the properties have significant roles in the dispersion process. In fact a recent demonstration experiment performed by Donnelly (1976) indicated that, depending on the type of oil (crude, refined, linseed oil, etc.), the sizes of oil globules formed are quite different. No quantitative data on oil breakup and dispersion are available. However, based on the analysis of the behavior of the oil under similar physical circumstances (contained, spreading), it may be argued that the oil density and surface tension (including any surfactants in the oil) play important roles.

The density of crude oil (ρ_o) varies depending on the source and the age (of the slick). The range of density values given by Dean (1968) for crude oil is:

$$0.829 \text{ gm/cm}^3 < \rho_o < 0.869$$

(Libyan oil) (Kuwait crude)

The densities of the heavies remaining after the evaporation of the light oil fractions in crudes of Kuwaiti or Iranian origin are in the range of

$$1.023 \text{ gm/cm}^3 < \rho_{\text{heavies}} < 1.027$$

Detailed physical properties and compositions of crude oils from different sources in the world have been given in crude evaluation charts published by Oil and Gas Journal (1963).

The oil density has a profound influence not only on the rate of the spreading of oil film during the initial regimes of spread, but also on the terminal velocity of rise of oil globules.

While the effect of density change on spreading and globulation is well understood, the rate of change of density with age in an oil slick is not that well-known. It is qualitatively known (and in a few controlled experiments quantitative information is available) that the higher fractions of the oil evaporate within 48 to 72 hours after a spill, leaving behind the heavies in the slick. It has been argued by Dean (1968) that the heavies may behave more as solids than as a continuous liquid, and hence probably aggregate in the form of large "droplets" and sink (or remain in neutral suspension).

The quantitative description of the effect of ambient temperature on the density variation of oils and the consequent behavior of oil slicks on ocean waters of different temperatures has not been fully documented. However, several instances are known in which oil slicks were barely visible, but ultimately considerable quantities of oil were washed ashore.

Surface tension (or more accurately the interfacial tension) is another important oil property parameter that influences the dispersion behavior of slicks. It is likely that the surface tension determines not only the maximum size of the oil drops that can be formed when the slick breaks up into globules, but it may also influence the thickness at which the slick may breakup. The maximum size of oil globules formed depends on the square root of the surface tension (Levich, 1962); that is:

$$d = f\left[\left\{\frac{\sigma}{g\rho_w\left(1-\frac{\rho_o}{\rho_w}\right)}\right\}^{\frac{1}{2}}\right] \qquad 2.14$$

where

d = diameter of oil drop formed

f = function

σ = surface tension of oil

ρ_w and ρ_o = water and oil densities, respectively.

The value of surface tension varies with the composition of the crude and probably is dependent also on the local temperature. It is certainly very sensitive to the presence of any surfactants in oil. A generally accepted value for σ is 30 dynes/cm. However, no information is available on the variation of this value with different crude oils or its variation with time (due to aging) for a given crude. Fay (1970) has assumed that σ goes to zero because of evaporation and dissolution of a considerable fraction of the slick. Based on this assumption Fay derives the following expression for the maximum area of slick spread in calm water:

$$\begin{matrix}A = \\ (\text{max area of} \\ \text{slick spread})\end{matrix} \left[\frac{\sigma^2 V^6}{\rho_w^2 \nu_w D^3 S^6} \right]^{\frac{1}{8}} \qquad 2.15$$

where σ is the interfacial tension of the crude before aging and S the solubility (order of magnitude 10^{-3}). The above formula does not take into account the possible slick breakup and oil dispersion by waves and ocean turbulence. Because of the 1/4th power dependence on surface tension, the final area of spread is insensitive to the errors or variations in the value of σ.

The viscosity of crude oils is, in general, two to three orders of magnitude higher than that of water. Therefore, in the spreading of oil on calm water it is the viscosity of water that determines the rate of spreading. To a large degree the oil viscosity has no effect

on the spread behavior. Similarly, it is expected that viscosity of oil will not play any role in either the formation of or the subsequent dispersion of oil globules in water.

2.3.7 Emulsification

Most of the earlier discussion has been based on the assumption that the vertical dispersion of oil will be in the form of oil globules in water. The Torrey Canyon spill has, however, demonstrated that the formation of water-in-oil emulsion occurs quite rapidly at sea. The emulsion manifests itself in the form of very stable "mousse" containing 70 to 80% water and which resembles more a gel than an oil (Dean 1968). This mousse floats around in blobs and seems to be less affected by wind and sun than are oil slicks.

While the mousse formation is an important factor in the dispersion of oil, quantitative information on the conditions under which such emulsions are formed are not available.

The effect of breaking waves, the physical properties of oil, and upper-ocean turbulence in forming, mixing and breaking up mousse is not at all understood. The extreme stability of the mousse may be due to the agglomeration of sea surface plankton. Considerable experimental work needs to be performed before a clearer understanding of the emulsification phenomenon at sea can be quantitatively understood.

2.4 Analysis of Existing Dispersion Models and Identification of Important Parameters

A beginning has been made by Leibovich (1975, (ii)) to model the vertical dispersion of oil globules in an open sea. The model provides an expression for the probability density distribution of oil particles with depths as a function of the wind speed. The following are the important results from this model:

Important Parameters Considered:

(1) Mean square turbulent velocity fluctuations ($\overline{u'^2}$);

(2) Terminal velocity of oil drops (U_T) which includes oil density and size;

(3) Wind speed over the ocean (U_{wind});

Major Unknowns

(1) Relationship between velocity fluctuations and sea state;

(2) Droplet size distribution and its relationship to the sea state;

Major Assumptions:

(1) Scale of turbulence (eddy size) much larger than the oil drops;

(2) Steady state (stationary) turbulent field which does not vary with depth or laterally;

(3) The motion of the oil drops relative to the local water environment is always at the appropriate terminal velocity (size dependent).

Results

The model indicates that, with constant "turbulent diffusion coefficient," the concentration distribution with depth is exponential, i.e.,

$$C = C_0 \, e^{-z/z_0} \qquad 2.16$$

where

z is the depth, z_0 is a "mixing depth." C and C_0 are respectively oil volume concentrations in water at depth z and at the water surface. z_0 is related to the turbulent diffusion coefficient and the terminal velocity by:

$$z_0 = \frac{2K}{u_t} \qquad 2.17$$

where

K = turbulent diffusion coefficient (assumed by Leibovich to be proportional to the square of the mean wind speed)

u_t = terminal velocity of oil globules.

There are some limitations to the model proposed by Leibovich. His model assumes that all of the oil is in suspension at any given time. This is equivalent to assuming that the surface is a perfect reflector. In effect the model disallows the possibility of formation of a partial film of oil on water. The second limitation in his model is the assumption of stationary (non-time dependent) turbulence. Leibovich has argued that most of the turbulence is produced by breaker waves. In such a case the turbulence is highly non-stationary and is spatially varying. This non-stationary and intermittent character of turbulence causes the oil globules to behave in a different way than has been suggested by Leibovich.

The use of turbulent diffusion coefficients which have been correlated from dye dispersion studies is questionable. The dye dispersion gives only gross estimates of the average conditions in the sea. The fundamental difference between oil and dye is that the former is buoyant while the latter is not; therefore, whenever the perturbation subsides, oil tends to collect up at the surface. Laboratory studies on turbulent diffusion coefficients in the presence of waves indicate that variations by orders of magnitudes are possible in the value of the diffusion coefficient. Therefore, the use of a single correlating equation to obtain a diffusion coefficient from speed is to be questioned.

While the statistical approach to establishing the oil concentration distribution is somewhat novel, the ultimate result obtained by Leibovich has been obtained for sediment distributions in a river by using more direct physical concepts (see Yalin, 1972). As such the model is not new, only its application to oil recovery in sea is new. However, some fundamental differences between a sediment transport phenomenon and the oil dispersion in breaking wave conditions seem to have been ignored.

Other Models:

There do not seem to be any other "globular dispersion" models available in the literature. Other stability models reported in the literature deal almost exclusively with the stability of oil slicks when contained by booms. These models are not reviewed in this report, because of the considerable differences in the physical situations, viz., boomed as against unconfined oil dispersion. Other models on "dispersion" are of only marginal interest inasmuch as these models consider the "movement" of oil slicks en masse on the water body.

2.5 Conclusions

The review of the literature and analysis of one of the relevant physical models on the dispersion of oil on the ocean lead to the following conclusions:

- Even though the wind-wave interaction and the characterization of the sea for given conditions of the sea are reasonably well understood, there are many questions that remain unanswered. These have to do with the probability of breaking, energy loss in breaking, and the number of breaking waves per unit area of the sea, all as functions of the sea state.
- Very little is known about the upper-ocean turbulence, its generation, and characteristics.

- The interaction between wind and waves in the presence of a large oil slick is unknown and has not been studied.
- The weathering of an oil slick on the ocean and consequently its property changes are not known to any degree of accuracy.
- The variation of the physical properties of crude with the components has not been measured.
- To understand the dispersion of oil into the water column in the form of oil globules held in suspension, it is essential to have data on the size distribution of oil globules (this distribution may be a function of the phenomena which create the globules--such as a breaking wave) and the details of the upper-ocean dynamics.

CHAPTER 3

ORDER-OF-MAGNITUDE ESTIMATES OF LIMITING SEA STATE FOR DISPERSION

3.0 Summary

In this chapter several analyses are performed to delineate the minimum sea state in which crude oil tends to disperse. In the calculations presented, the emphasis has been on using basic physical laws and obtaining order of magnitude estimates for the sea conditions.

The chapter has three main parts. In the first part, estimates are made for the energy in various systems having a bearing on the oil dispersion in the sea. Subsequently an analysis based on the intrinsic thermodynamic stability of films is given. Finally, the globular dispersion of oil in the sea is analyzed and order of magnitude estimates are obtained for the minimum sea state for such a dispersion.

3.1 Introduction

It is a common observation that when large quantities of crude oil are spilled accidentally into calm oceans, the oil slick formed persists for several days. However, the slick undergoes mass loss due to the evaporation of the more volatile components of the crude and the dissolution of the water soluble compounds. As the slick spreads and thins out, it becomes less and less stable and may ultimately break up. This is probably due to the fact that even the "calm" sea consists of waves and other disturbances to which the thin oil film is subjected. The thickness of the oil film which tears under such "calm" conditions is about 50 to 100 microns.

It is also possible that the slick breakup is a phenomenon brought about by the variation of oil properties (especially the surface tension) over the slick caused by the difference in the volatilization and evaporation rates from different parts of the slick. The oil slick breakup seems to occur by the selective thinning out of certain regions around a nucleus (which is thick) and ultimately forming smaller slicks independent of the "mother" slick. Such a dispersion could be termed the "slicklet" dispersion. Under rough sea conditions such a slicklet dispersion may be accelerated by the action of waves, particularly by breaking waves.

While the above observations are well known and are documented in the literature, it is not known how the same oil slick would behave under more severe sea conditions. It is very likely that the response of the oil slick to a severe sea state would depend, to a larger extent, on the type of crude oil, the age of the slick following the spill, and of course the severity of the sea itself. There are no known observational data on which to infer how an oil slick would disperse. It is possible that the oil slick would be torn apart into fine globules of oil which might remain in suspension under water, or the slick might simply break up into several smaller pieces, or both types of dispersions might coexist. In a severe sea, the condition (of agitation) at a given location would be a strong function of time, and therefore there may be strong interflow between the oil in suspension and that in the form of small slicks.

With this background picture of oil dispersion in severe sea conditions in mind, we made several analyses using only basic principles and estimates of order of magnitude. This chapter contains the principles of the analyses and the main results and conclusions therefrom. Detailed derivations, calculations, etc. have also been indicated.

The analyses begin in Section 3.2 with consideration of the energy involved in various physical phenomena, such as the wave, the wind, and gravitational energy in keeping an oil globule in suspension, etc. The primary purpose of this analysis is to obtain an understanding of the magnitudes of the energies involved and to determine the fraction of wave energy needed to break oil slicks.

In Section 3.3, a thermodynamic stability analysis is developed to calculate a criterion for the breakup of an oil film. The results of this analysis will give an upper bound (most severe) on the minimum conditions in which an oil slick may break up. Several unknowns are identified. In this analysis several "technical liberties" are taken to "stretch" the applicability of the analysis from monomolecular layers to oil slicks of finite thickness.

Section 3.4 deals with the characterization of the globular dispersion. In Section 3.4.1, a globulation criterion is derived which gives the minimum conditions necessary for "pulling" into water a globule of oil from the floating slick. This analysis is based on the assumption that the turbulent pressure fluctuations in water cause an instability in the slick and produce oil globules. In Section 3.4.2 another approach, using the Kelvin-Helmholtz instability criterion, is indicated.

The effect of wind in generating turbulent velocity fluctuations in water is analyzed in Section 3.5. This is an order of magnitude estimate. The result obtained from this analysis provides a link between the water velocities generated by waves and the turbulent velocities.

Finally, in Section 3.6, an estimation is made to determine the minimum sea state in which oil globulation may begin, i.e., when there is "incipient globulation." This sea state is characterized in terms of the significant wave height of a fully developed sea.

3.2 Energy Estimates

In this section we consider the energies of various states on an order of magnitude basis. The energies of importance are:

- Surface energy stored in the oil globules,
- Gravitational energy required to keep the globules in suspension,
- Rate of energy transfer from wind, and
- Energy in wave motion.

3.2.1 Surface Energy and Gravitational Energy

Consider a unit surface area (plan area) in the sea in which:

the mean oil film thickness = b,

the mean diameter of oil globules formed = d,

the surface tension of oil = σ,

the mean depth at which the globules are held suspended = h, and

the density of oil = ρ_o

Hence:

the surface energy stored in one globule = $\sigma \pi d^2$,

the gravitational energy stored in one globule = $\frac{\pi d^3}{6} (\rho_w - \rho_o)$ gh, and

the total number of oil globules of diameter d that can be formed in a unit area and thickness b = $N = \frac{6b}{\pi d^3}$

Therefore,

the surface energy required to form globules of diameter d from an oil film of thickness b in a unit nominal area = $\frac{6b\sigma}{d}$, and 3.1

the gravitational energy required to keep these globules in suspension = $b(\rho_w - \rho_o)$ gh. 3.2

Numerical Values

For the sake of estimating the magnitudes of the energy terms, we assume the following values.

$b = 5 \text{ mm} = 5 \times 10^{-3} \text{ m}$

$d = 1 \text{ mm} = 10^{-3} \text{ m}$

$h = 2 \text{ m}$

$\sigma = 30 \text{ dynes/cm} = 3 \times 10^{-2} \text{ J/m}^2$

$\rho_o = 0.9 \text{ gm/cm}^3 = 900 \text{ kg/m}^3$

ρ_w = density of water = 1000 kg/m^3

Substituting in Equations 3.1 and 3.2, we get:

The surface energy stored in oil/unit area of sea

$$= \frac{6 \times 5 \times 10^{-3}}{10^{-3}} \times 3 \times 10^{-2}$$

$$= 0.9 \text{ J/m}^2$$

The gravitational energy stored in oil/unit area of sea surface

$$= 5 \times 10^{-3} (1000-900)\ 9.8 \times 2$$

$$= 9.8 \text{ J/m}^2$$

From the above calculation, it is readily seen that the gravitational energy required to keep the oil drops in suspension (at a 2-meter depth) far exceeds the energy required to make the drops out of a horizontal oil film.

3.2.2 Energy Transfer from Wind

We assume the following typical values to estimate the order of magnitude of energy transfer from the wind:

wind speed = $U = 5 \text{ m/s}$

wind friction velocity = $u^* = 0.04\ U = 0.2 \text{ m/s}$

surface drag coefficient between wind and wavy water $= \alpha C_D = 0.01$

density of air $= \rho_a = 1.2 \text{ kg/m}^3$

Hence, the rate of energy transfer to a unit area of sea surface

$$= \dot{E}''_{wind} = \frac{1}{2} \rho_a U^2 C_D u^*$$

$$= \frac{1}{2} \times 1.2 \times 5^2 \times 0.01 \times 0.2$$

$$= 0.03 \text{ J/m}^2 \text{ s}$$

3.2.3 Energy Contained in a Wave

The following typical values of wave parameters are assumed:

wave amplitude $= a = 1$ m

wave phase speed $= c = 6$ m/s

(corresponding to about a 25 m wave length in deep water.)

Hence, the wave energy contained in a unit surface area E''

$$= \frac{1}{2} \rho_w g a^2$$

$$= \frac{1}{2} \times 1000 \times 9.8 \times 1 = 4900 \text{ J/m}^2$$

Rate of energy flow across an area of 1 m width normal to wave propagation direction with infinite depth $= \dot{E}'' \frac{c}{2}$

$$= 4900 \times 3$$

$$= 14{,}700 \text{ J/ms}$$

However, it should be noted that this enormous energy flow is contained in the wave system and only a small part of it may be dissipated in viscous dissipation by turbulent eddies.

3.2.4 Terminal Velocity and Globule Residence Time

Assuming that the oil globules penetrate the water to a depth of h, the residence time can be estimated as follows:

$$\text{residence time} = t_r = \frac{h}{u_t} \qquad 3.3$$

where

$$u_t \simeq 1.81 \sqrt{d} \quad \text{(m/s for d in meters)} \qquad 3.4$$

The above equation is applicable for oil density 0.9 gm/cm^3.

For a 1-mm diameter drop, $u_t \simeq 6$ cm/s

Hence, for h = 2 m, the residence time $t_r \simeq 35$ s.

The energy transferred by wind of 5 m/s in the duration t_r = 0.03 x 35 ≃ 1 J/m^2

It is seen from the calculations indicated in subsections 3.2.1 through 3.2.4 that:

- The energy required to form the drops is about an order of magnitude smaller than the energy required to keep the same drops in suspension.
- The energy content in a wave is enormous, and a very tiny fraction of wave energy, if tapped, would be sufficient not only to form oil drops but also to keep them in suspension in water.
- Energy supplied by wind of 5 m/s in 30 seconds is sufficient to provide for the surface energy to make the oil drops. Within the rise time of the 1 mm diameter globules from a depth of 2 m, the energy supplied by wind is 1 J/m^2, whereas about 10 J/m^2 are needed to provide the gravitational energy to push the globules to a 2 m depth. This indicates that if the wind is the only energy source for putting the globules in suspension a penetration depth of 2 m is impossible. However, since the energy transfer rate from wind is directly proportional to the cube of the wind velocity, a 12 m/s wind (25 knots) would be able to provide the necessary energy input to push 1 mm drops to a 2 m depth.

3.3 Thermodynamic Stability Analysis

The problem of predicting the conditions under which a liquid film breaks up has fascinated researchers in a variety of disciplines including thermodynamics. Slattery (1975) has derived thermodynamic criteria for the collapse of monomolecular films, based on the ideas of entropy maximization. Beegle et al. (1974) have derived general stability criteria for pure substances and mixtures using Legendre Transform techniques. Though no "criterion" exists for predicting the break up of thick oil films on the ocean, an attempt will be made here to derive a criterion based on the approach of Beegle et al. This will at least illustrate the areas of future work. The applicability of the stability criterion to an oil film can be transformed to a sea state index provided the relationship among various parameters is known.

For the surface phase (oil layer), let the internal energy $\underline{U}$ be a function given by

$$\underline{U} \equiv \underline{U} (\underline{S}, N_1 \text{ ----- } N_{n-1}, N_n, A) \qquad 3.5$$

where $\underline{U}$ is the total energy of the film, $\underline{S}$ the total entropy, A the area, and N_j the moles of j^{th} specie in the film.

From Beegle et al. (1974), the criterion for thermodynamic stability of the film is:

$$\left(\frac{\partial \xi_{n+1}}{\partial X_{n+1}}\right)_{\xi_1, \xi_2 \text{ ----} \xi_n, X_{n+2}} > 0 \qquad 3.6$$

where in a n-component system:

$$\xi_j = \left(\frac{\partial \underline{U}}{\partial X_j}\right)_{X_i\ (i \neq j)} \qquad 3.7$$

and X_j represents the j^{th} independent variable in Equation 3.5. With the ordering of variables indicated in Equation 3.5, we get, with $X_{n+1} = A$

$$\xi_{n+1} = \left(\frac{\partial \underline{U}}{\partial A}\right)_{\underline{S},\ N_1 \cdots N_{n-1},\ N_n} = \gamma \qquad 3.8$$

where γ, by definition, is the interfacial tension. Hence, from Equations 3.6 and 3.8, we have:

$$\left(\frac{\partial \gamma}{\partial A}\right)_{T,\ \mu_1, \mu_2 \cdots \mu_{n-1},\ N_n} > 0 \qquad 3.9$$

where μ_j is the chemical potential of j^{th} specie and N_n is the total moles of components in area A.

Now the molar area density ρ_n is

$$\rho_n = \frac{N_n}{A} \qquad 3.10$$

$$\therefore \quad \left(\frac{\partial \rho_n}{\partial A}\right)_{T, \mu_1, \cdots \mu_{n-1},\ N_n} = -\frac{N_n}{A^2} \qquad 3.11$$

Hence substituting Equation 3.11 in 3.9, we get the <u>stability criterion</u> as

$$\left(\frac{\partial \gamma}{\partial \rho_n}\right)_{T,\ p,\ \mu_1 \cdots \mu_{n-1}} < 0 \qquad 3.12$$

Equation 3.12 is a useful relation to determine the intrinsic stability criterion of oil films, provided one has an equation of state relating interfacial tension γ to composition; unfortunately, this is almost never possible to obtain.

If, however, we assume that the surface layer of oil is a pure component (or the mixture is composed of chemical compounds which are similar in physical behavior), then Equation 3.12 becomes for stability,

$$\left(\frac{\partial \gamma}{\partial \rho}\right)_T < 0 \qquad 3.13$$

where the restriction of constant pressure has been dropped since for the cases of interest here, the pressure is atmospheric.

Equation 3.13 states that for a stable, isothermal surface layer, *an increase in the surface density of the layer leads to a decrease in* the interfacial tension γ. Suppose we consider such a surface layer of oil in a sea with wave action. The oil film will be compressed and stretched alternatively, i.e., ρ will increase and then decrease. Expansion will lead to larger value of γ (as can be seen from Equation 3.13, and the film will become stronger whereas compression will reduce γ. However, in these cyclic variations there may result a point where the stability criterion (Equation 3.13) will be violated. At this point, the surface layer collapses and oil will be forced into the bulk water.

In order to determine the sea state at which this instability may result, it is essential to have the data on the variation of γ with ρ for oils of various fractions. With these data, the value of $\rho = \rho^*$ at which $\left(\frac{\partial \gamma}{\partial \rho}\right) = 0$ can be determined. In any sea state there will be the alternate stretching and compression of an oil film due to the waves. The maximum compression of a film of oil can be obtained in terms of wave parameters. (This may require solving the complete hydrodynamic equations for the oil-water system. However, a simpler, but an approximate analysis is shown in Section 4.2). Intrinsic

thermodynamic instability of the oil slick can then be determined by determining the sea state parameters that result in a surface density ρ^* for the slick.

Unfortunately, however, such a calculation cannot be made at the present time because of the nonavailability of the γ vs. ρ data for oil. Besides, the calculation of the variation in area density of an oil film (alternatively the thickness of an oil layer) with time and spatial position, when the film is subjected to even a simple sinusoidal wave, is an extremely complicated task.

3.4 Globulation Criterion

When a calm sea is subjected to the action of a wind, as in a storm, the waves build up, with predominantly long wavelength waves. In addition, the wind shear stress on the water surface, as well as breaking action of the waves, results in a turbulent upper ocean surface. If we now consider a situation in which there exists an oil slick of uniform thickness subjected to the action of increasing sea states (due to a storm), it is postulated that there results a situation in which globules of oil will be torn off the oil film. This tearing is accomplished primarily by the turbulence in the water. It is the purpose of the order-of-magnitude analysis developed below to derive a criterion for such an incipient globulation to occur.

3.4.1 Globulation Due to Turbulent Pressure Fluctuations in Water

Consider the situation, shown in Figure 3.1, in which an oil layer of a given thickness on water is being subjected to wave action. The domain is assumed to be infinite in a plane normal to the paper so that there are no effects on boundaries. We first derive the conditions under which a globule will be formed as a function of the intensity of turbulence. Subsequently, the intensity of turbulence will be related to the sea state parameters to obtain limiting sea state value.

Figure 3.2 is a schematic illustration of the forces on an oil drop attached to the oil slick subjected to wave action. It is assumed that the acceleration effects of water (subjected to wave motion) on the oil drop are negligible.

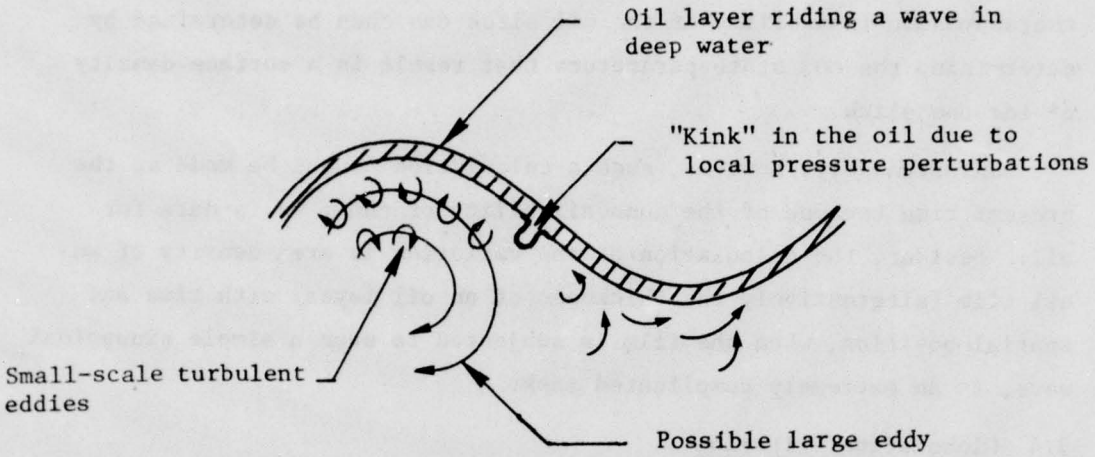

FIGURE 3.1: OIL LAYER RIDING A WAVE. ANALYSIS OF INCIPIENT GLOBULATION

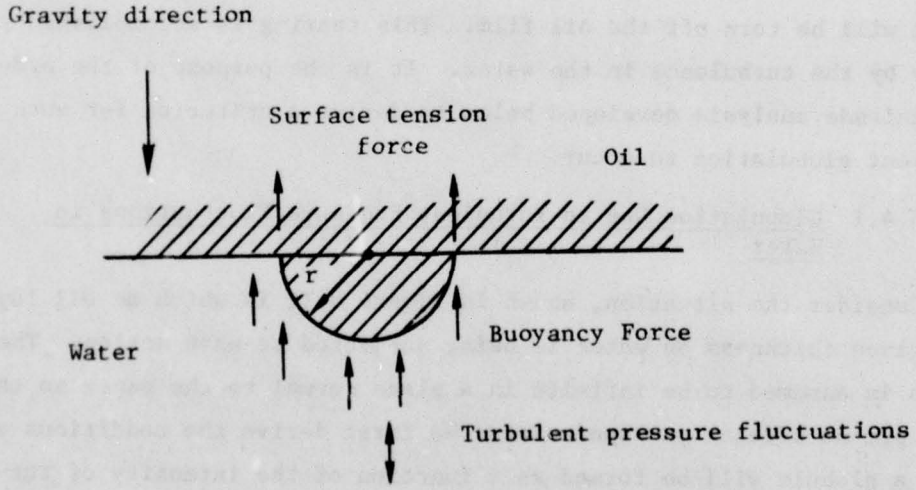

FIGURE 3.2: SCHEMATIC REPRESENTATION OF THE FORCES ON A PENDULAR GLOBULE OF OIL

Consider a hemispherical drop of oil of radius "r" (see Figure 3.2) protruding into water below the mean film level. The root mean square fluctuating pressure $p^* \left(= \sqrt{\overline{p'^2}}\right)$ that will be capable of separating the oil drop from the main oil film is obtained by

$$\underbrace{p^* \pi r^2}_{\text{"suction" force}} \sim \frac{2}{3} \underbrace{\pi r^3 \rho_w g \left(1 - \frac{\rho_o}{\rho_w}\right)}_{\text{buoyancy force}} + \underbrace{2 \pi r \sigma}_{\text{surface tension force}} \qquad 3.14$$

For turbulent pressure fluctuations in water we have

$$p^* \sim \frac{1}{2} \rho_w \overline{u'^2} \qquad 3.15$$

where $\overline{u'^2}$ is the mean square fluctuating velocity (a measure of intensity of turbulence).

Hence from Equations 3.14 and 3.15, we have:

$$\overline{u'^2} \sim \frac{4}{3} g \left(1 - \frac{\rho_o}{\rho_w}\right) r + \frac{4\sigma}{\rho_w} \frac{1}{r} \qquad 3.16$$

A plot of Equation 3.16 is shown in Figure 3.3. It can easily be shown from Equation 3.16 that oil drops are formed only if the turbulent fluctuation intensity exceeds a minimum value given by

$$\left(\overline{u'^2}\right)_{min} = \frac{8}{3} g \left(1 - \frac{\rho_o}{\rho_w}\right) r_c = \left[\frac{64}{3} \frac{g\sigma}{\rho_w} \left(1 - \frac{\rho_o}{\rho_w}\right)\right]^{\frac{1}{2}} \qquad 3.17$$

where the size of the drop formed at the above intensity is given by

$$r_c = \sqrt{\frac{3\sigma}{g(\rho_w - \rho_o)}} \qquad 3.18$$

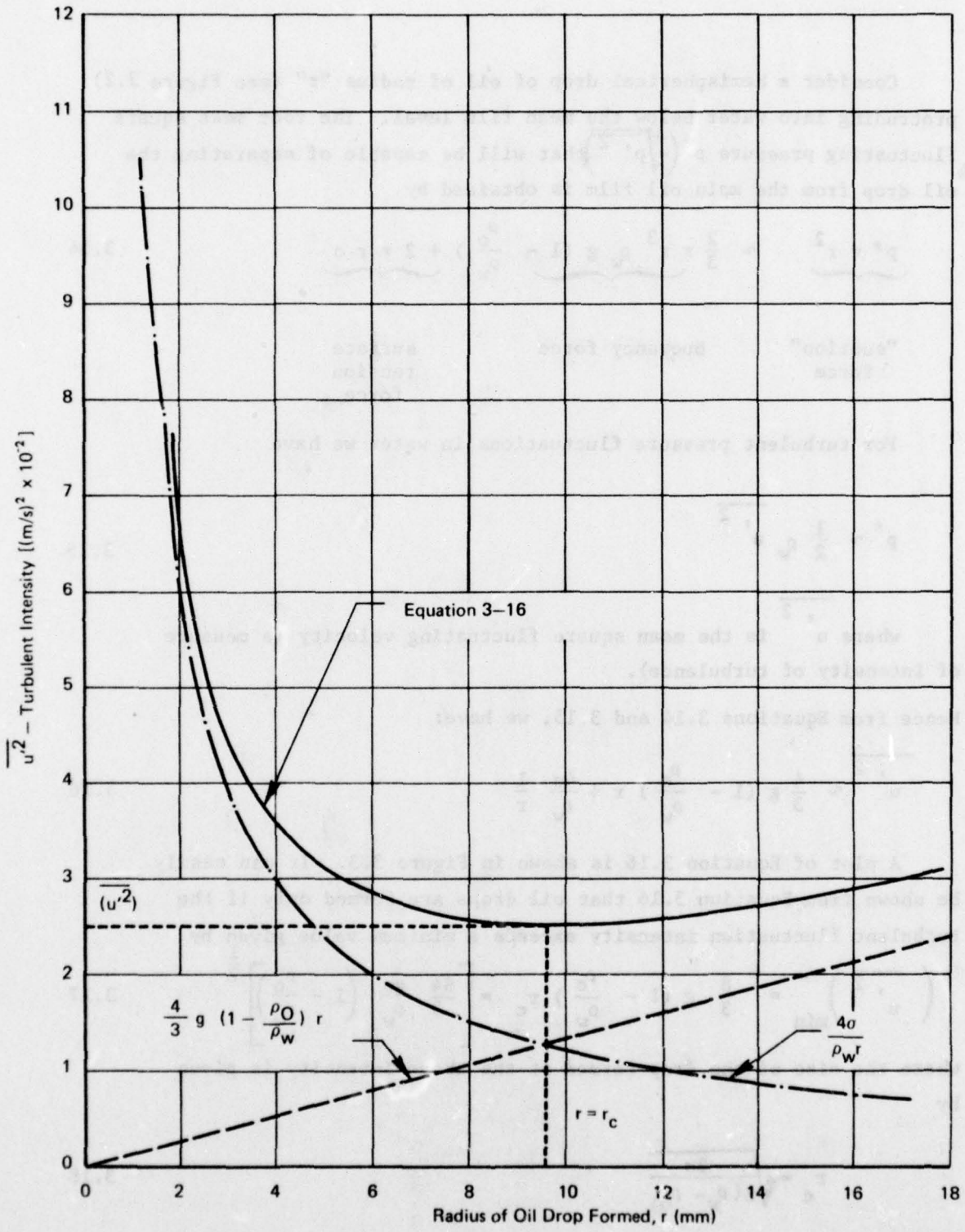

FIGURE 3–3 DROP SIZE FORMED AS A FUNCTION OF INTENSITY OF TURBULENCE

As can be seen from Figure 3.3, any increase in the turbulent intensity, over and above the minimum value predicted by Equation 3.17, results in globules of at least two sizes; which of the sizes is more abundant in a given situation cannot be predicted by the simple analysis given above.

To obtain a feel for the numerical magnitudes of the values of the parameters, we give below an illustrative calculation. We assume:

Surface tension of oil $\sigma = 3 \times 10^{-2}$ N/m

Density of oil $\rho_o = 900$ kg/m^3

Acceleration due to gravity $g = 9.8$ m/s^2

Hence, from Equation 3.17, the minimum turbulent intensity needed is:

$$\left(\overline{u'^2}\right)_{min} = 2.5 \times 10^{-2} \text{ m}^2/\text{s}^2$$

Hence, we have $\sqrt{\left(\overline{u'^2}\right)_{min}}$ = 0.15 m/s

Radius of oil drop formed at the above turbulent intensity (Equation 3.18) = $r_c = 9.58 \times 10^{-3}$ m

3.4.2 Globulation Criterion Based on a Kelvin-Helmholtz Type Instability

When there exists a relative velocity at the interface of two fluids of different density, the inviscid solution to the equation for the interfacial wave indicates that under certain conditions an instability may develop (see Lamb (1932), page 462). This instability is called the Kelvin-Helmholtz instability and occurs when the wavelength of the interfacial waves exceeds a certain minimum value. We utilize these ideas and obtain an estimate for the turbulent velocity fluctuations in water to cause such an instability at the oil-water interface.

Consider a situation in which the turbulent velocity fluctuation in water close to the oil water interface has a value $\sqrt{\overline{u'^2}}$. If we assume the turbulence to be isotropic and the velocity fluctuations to have

zero mean, then on the average, in a given duration, water will be moving in a given direction at a speed $\sqrt{\overline{u'^2}}$ for one-half of the duration and in the opposite direction with the same speed. We now analyze the situation in which water is moving parallel to the oil-water interface (at any instant) at a speed given by $\sqrt{\overline{u'^2}}$ and assume that there are no such speeds in oil (because of high viscosity). Then the relative speed between water and oil over this small time duration will be equal to $\sqrt{\overline{u'^2}}$. We also assume that because of this relative speed, a local interfacial wave occurs.

Lamb (1932) has shown that the interfacial instability grows when --

$$\text{relative speed magnitude} > \frac{1+s}{\sqrt{s}}\, c_{min} \qquad 3.19$$

$$\text{i.e., } \sqrt{\overline{u'^2}} > \frac{1+s}{\sqrt{s}}\, c_{min} \qquad 3.20$$

where $s = \rho_o / \rho_w$ = specific density of oil relative to water

c_{min} = minimum value of the phase speed of capillary waves.

$$c_{min}^2 = 2\left(\frac{1-s}{1+s}\right)\left[\frac{g\,\sigma}{\rho_w\,(1-s)}\right]^{\frac{1}{2}} \qquad 3.21$$

where σ = surface tension of oil.

This minimum speed occurs at a wavelength λ_m, given by

$$\lambda_{min} = 2\pi \sqrt{\frac{\sigma}{g(1-s)\rho_w}} \qquad 3.22$$

Substituting Equation 3.21 in 3.20, we can obtain an estimate of the minimum turbulent velocity fluctuations necessary for producing instability in the oil-water interface.

We now interpret the interfacial instability as a globulation phenomenon. Then the size of the globule formed can be estimated from the wavelength of the interfacial wave, assuming that the oil film within half of a wavelength breaks up to form a globule. That is:

$$r_c = 0\left(\frac{1}{4}\lambda_{min}\right) \qquad 3.23$$

Substituting Equations 3.21 in 3.20 and 3.22 in 3.23, we get, respectively:

$$\left(\overline{u'^2}\right)_{min} = 2\left(\frac{1+s}{s}\right)\left[\frac{g\sigma\,(1-s)}{\rho_w}\right]^{\frac{1}{2}} \qquad 3.24$$

$$\text{and} \quad r_c = 0\left(\frac{1}{4}\lambda_m\right) = \frac{\pi}{2}\sqrt{\frac{\sigma}{g(\rho_w-\rho_o)}} \qquad 3.25$$

If we use the numerical values assumed in Section 3.4.1, we get, from Equations 3.24 and 3.25, respectively:

$$\sqrt{\overline{(u'^2)}} = 0.1513 \text{ m/s}$$

$$\text{and} \quad r_c = 8.69 \times 10^{-3} \text{ m}$$

Comparisons of Equations 3.17 and 3.25 and Equations 3.18 and 3.25 indicate that the final results obtained by two completely independent approaches have the same forms (differing in only constant factors for a given oil density). The analyses therefore give a reasonable estimate for the minimum velocity of turbulence necessary for globulation and also indicate the expected size of the globule (which is about 1 cm in radius).

3.5 Turbulent Velocity Fluctuations in Water Due to Wind

A wind blowing over an ocean transfers momentum to water in the form of both shear stresses and normal forces. In addition, the scale of motion of wind in the atmosphere is such that the flow is always turbulent. In effect, a significant part of the stress on the water is caused by turbulent fluctuations (Reynolds stresses).

It may be argued that the fluid motions on the water side are also turbulent -- at least for describing the water-air interface stress effects. Turbulent motion is synonymous with the distortion of vorticity. Hence, in estimating turbulent velocity fluctuations in water, it is preferable to estimate first the vorticity fluctuations. The method described below is based on the above physical ideas.

The objective of the analysis performed in this section is to obtain an order of magnitude relationship between wind speed and the turbulent intensity in water in an ocean. Knowing such a relationship and the nature of the sea state induced by the wind, one can develop a relationship between turbulent velocities in water and sea state. An inherent assumption in such an analysis is that the turbulence in the upper ocean waters is generated only by the wind. This may not always be the case.

Analysis

Since the Reynolds number of flow both in air and in water is very high* (Reynolds number is based on mean flow velocity and scale of motion), it may be assumed that the stresses are entirely due to turbulence. In addition, Falvey (1974) has shown that a large fraction of the momentum loss (rate) suffered by the wind manifests itself as a shear stress at the air-water interface.

---

* See the discussion under Equation 3.28.

Hence, the turbulent shear stress on the air-water interface is

$$\tau = \frac{1}{2} \rho_a C_D U^2 \qquad 3.26$$

Since there is a shear stress continuity across the air-water interface, we can calculate the shear strain rate at the interface as:

Turbulent shear strain rate on the water side

$$s \sim 0 \left(\frac{\tau}{\mu_w}\right) \qquad 3.27$$

It is shown by Tennekes and Lumley (1972, p. 88) that, in flows with very high turbulent Reynolds number $\left(\frac{\sqrt{\overline{u'^2}}\,\ell}{\nu_w}\right) >> 1$, the root mean square fluctuations of vorticity are of the same order of magnitude as the turbulent shear strain rate; i.e.,

$$\sqrt{\overline{\Omega'^2}} \sim O(s) \qquad 3.28$$

That the turbulent Reynolds number for wind-water flows is indeed very large is proved *a posteriori*.

In a steady state (i.e., fully developed sea) the energy input by the wind is completely dissipated in water by turbulent friction. Therefore, the vorticity production rate is equal to dissipation rate at small scales. Hence, from Tennekes and Lumley (1972, Equations 3.3.46 and 3.3.20), we have:

$$\underbrace{\varepsilon \sim O\left(\nu_w \overline{\Omega'^2}\right)}_{\text{Turbulent Energy dissipation rate per unit mass of water}} \simeq O\left(\frac{\left[\overline{u'^2}\right]^{3/2}}{\ell}\right) \qquad 3.29$$

where $\overline{u'^2}$ is the mean square velocity fluctuation (intensity of turbulence) and ℓ the integral scale of turbulent motions in water.

Hence combining Equations 3.28 and 3.29 and re-arranging, we get:

$$\left[\overline{u'^2}\right]^{1/2} \sim O\left[(\nu_w \ell \overline{\Omega'^2})^{1/3}\right] \qquad 3.30$$

Substituting Equation 3.27, we have:

$$\overline{(u'^2)}^{1/2} \sim O\left[(\nu_w \ell \frac{\tau^2}{\mu_w^2})^{1/3}\right] \qquad 3.31$$

$$\left[\overline{u'^2}\right]^{1/2} \sim O\left[\left\{\ell \left(\frac{\rho_a}{\rho_w}\right)^2 C_D^2 \frac{U^4}{\nu_w}\right\}^{1/3}\right] \qquad 3.32$$

The parameter ℓ in Equation 3.32 is the scale of eddies in water. This is, however, unknown *a priori*, and we have to make reasonable assumptions. Kinsman (1965, p. 511) assumes that ℓ is the order of the inverse of the wave number (κ) of the waves developed in water. However, Levich (1962) has argued, based on physical reasoning, that the wavelength of waves cannot be used as a measure of the scale of turbulence. Instead he uses the "amplitude of the wave" as the integral scale of turbulence.

In a given sea state there is neither a single wavelength nor is there a single amplitude. This makes the estimation of the scale of the eddies difficult. However, to obtain a reasonable estimate of the turbulent intensity in water, we assume that the parameter ℓ can be characterized by either:

- the expected wave number in a given sea state, or
- the most frequently appearing wave amplitude.

Given below is such an estimate based on assuming a specific spectral description of the sea.

To calculate a relationship between a sea state and the turbulent fluctuating velocity, we assume the Pierson-Moskowitz (P.M.) spectrum and fully developed sea condition.

Therefore, the "expected" frequency of waves formed by a wind of speed U (see note below) is:

$$\omega_e = (\Pi\beta)^{1/4} \frac{g}{U}$$

For gravity waves, we have:

$$\omega_e^2 = g\,\kappa_e .$$

Hence
$$\kappa_e = \frac{\omega_e^2}{g} = \frac{(\Pi\beta)^{1/2}\, g}{U^2} \qquad 3.33$$

Substituting the values of β in Equation 3.33, we have:

$$\frac{1}{\kappa_e} = 0.656 \frac{U^2}{g} . \qquad 3.34$$

If we assume that the wave height record can be described by a Rayleigh distribution, i.e.:

$$p(a) = \frac{2a}{\overline{a^2}} \exp\left(-\frac{a^2}{\overline{a^2}}\right) \qquad 3.35$$

where $\overline{a^2}$ is the variance of the amplitude record, then the most frequently occurring amplitude (at which p(a) is a maximum) is given by

$$a^2_{\text{most frequent}} = \frac{\overline{a^2}}{2} \qquad 3.36$$

β = 0.74 for P.M. spectrum.

From the P.M. spectrum, we have:*

$$\overline{a^2} = 2\int_{\omega=0}^{\infty} S(\omega)\, d\omega = \frac{\alpha}{4\beta}\,\frac{U^4}{g^2} \qquad 3.37$$

Therefore,

$$a_{\text{most frequent}} = \sqrt{\frac{\alpha}{8\beta}}\,\frac{U^2}{g} \qquad 3.38$$

Substituting α and β values

$$a_{\text{most frequent}} = 0.052\,\frac{U^2}{g} \qquad 3.39$$

Comparing Equations 3.34 and 3.39, we find that the scale lengths (that may be used to characterize the scale of the turbulent eddy generated by wind) differ by an order of magnitude.

Table 3.1 summarizes the numerical results obtained, based on the analysis in this section. Basically the table gives the calculated values of the mean square velocity fluctuations in water, generated by a wind, assuming that the sea is fully developed. Also the variations in the calculated results obtained by making the two different assumptions regarding the scale of eddies are shown. The results in Table 3.1 are plotted in Figure 3.4.

---

*α for P.M. spectrum for the way in which $S(\omega)$ is defined is $\alpha = 1.62 \times 10^{-2}$.

Table 3.1: Calculations of the root mean square turbulent velocity fluctuations in water resulting from a wind over an ocean

Wind speed U (m/s)	Significant wave height H_s (m)	(Values based on Pierson-Moskowitz spectrum for fully developed sea) Expected value of circular frequency (ω_e) (rad/s)	Significant water speed $U_s = H_s \frac{\omega_e}{2}$ (m/s)	Inverse of expected wave number $= 1/\kappa_e$ (m)	Most frequently occurring amplitude a_F (m)	r.m.s. vorticity $\sqrt{\overline{\Omega'^2}}$	rms velocity (m/s) fluctuations using the following integral length scales $\ell = \frac{1}{\kappa_e}$	$\ell = a_F$	$\left(\sqrt{\overline{u'^2}}\right)_{a_F} / U_s$
5	0.334	2.42	0.646	1.67	0.133	45.0	0.15	0.065	0.100
8	1.367	1.513	1.034	4.28	0.342	115.2	0.384	0.166	0.161
10	2.14	1.21	1.292	6.73	0.535	180.0	0.604	0.259	0.20
15	4.8	0.807	1.938	15.04	1.2	405.0	1.35	0.582	0.3
20	8.54	0.605	2.584	26.81	2.135	720.0	2.4	1.034	0.4

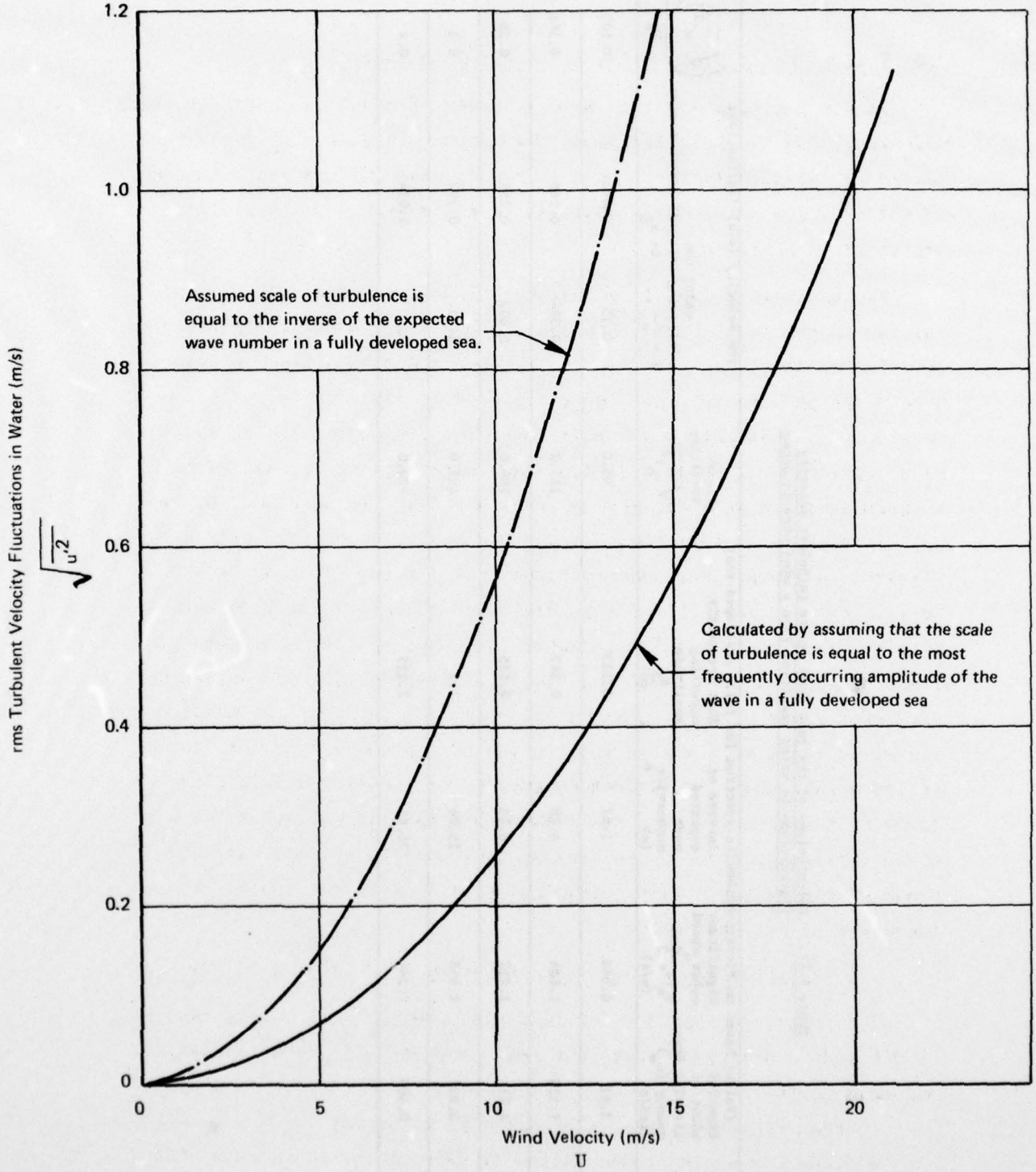

FIGURE 3–4 CALCULATED RELATIONSHIP BETWEEN WIND SPEED AND rms TURBULENT VELOCITY FLUCTUATIONS IN WATER IN A FULLY DEVELOPED SEA

3.6 Estimation of Minimum Sea State for Globulation

In the previous sections several order of magnitude estimates were made including the calculation of the minimum intensity of turbulence necessary for globulation. In this section the information obtained in the previous sections is utilized in estimating a sea state for incipient globulation.

The key result that is necessary before a sea state can be calculated is the relationship between the sea state and turbulent velocity fluctuations. In Section 3.5, we obtained a relationship between wind speed and the intensity of turbulence in water. The fully developed sea parameters are related to the wind speed and these could be utilized in estimating the sea state necessary for globulation. Such an approach is indicated in Section 3.6.1. In Section 3.6.2 we calculate the sea state based on the assumption that there exists a linear relationship between the turbulent velocity in water and "significant" velocity of water particles induced by the wave motion. Finally, in Section 3.6.3 a somewhat different approach is taken by assuming (1) that the turbulent fluctuations induced under a wave depend on the water velocity under the wave, and (2) that in any given sea state there will always exist waves that produce turbulent intensities higher than the minimum necessary for inducing globulation. However, the occurrence of these waves becomes infrequent as the sea state (index) decreases. Therefore, in this context, one can only speak of the probability of globulation in a given sea state. These ideas are elaborated below.

3.6.1 Estimation of Sea State Based on Wind Induced Turbulence

The results of Section 3.2 indicate that for oil with a density of 900 kg/m^3 a minimum turbulent rms value of 0.15 m/s is needed. Assuming further

- that the turbulence is produced by wind only, and
- that the scale of the eddies in water is of the size of the most frequently occurring wave amplitude in the sea,

we see from Figure 3.4 that the steady wind speed necessary for generating the above turbulence is U = 7.5 m/s.

In Appendix B, the relationships among various sea parameters are developed for a fully developed sea described by the Pierson-Moskowitz spectrum. Using these results (Equation B.9 of Appendix B, in particular), we see that at the wind speed of U = 7.5 m/s the significant wave height is:

$$H_s = \sqrt{\frac{2 \times 1.62 \times 10^{-3}}{0.74}} \times \frac{7.5^2}{9.8} = 1.2 \text{ m}$$

This result shows that when the sea state is such that the significant wave height is about 1 m globulation of oil should begin.

3.6.2 Estimation of Sea State Based on Linear Relationship between Water Speed and rms Turbulent Velocity

We assume that the rms turbulent velocity and the significant speed (wave induced) of water are related by:

$$\sqrt{\overline{u'^2}} = f\, U_s \qquad 3.40$$

where the factor f is unknown and has to be obtained from experimental data. Based on the results with other similar flows*, we can assume a reasonable value for f to be:

$f \simeq 0.1$

Hence, for $\sqrt{\overline{u'^2}} \simeq 0.15$ m/s

the significant water velocity $U_s = \frac{0.15}{0.1} = 1.5$ m/s

---

* In general, for turbulent flows (wind tunnels, boundary layer flow, etc.) and rms turbulent velocity fluctuations are between 1% and a maximum of 10% of the mean flow velocities, i.e., in the terminology of Equation 3.40, $0.01 < f < 0.1$.

Referring to Equations B.6 and B.10 of Appendix B, we get (for a fully developed sea described by P-M spectrum).

$$\text{Significant wave height } H_s = 12.54 \frac{U_s^2}{g} = \frac{12.54 \times 1.5^2}{9.8}$$

$$= 2.88 \text{ m} \simeq 3 \text{ m}$$

and the wind corresponding to this significant wave height (Equation B.7, Appendix B)

$$= \frac{1.5}{0.129} = 11.6 \text{ m/s}$$

A sensitivity analysis is performed to ascertain the differences in the predicted sea state for the different assumptions regarding the parameter f and the type of spectral description of the sea. These results are shown in Table 3.2. The results indicate that the value of the parameter f and the type of spectrum used to describe sea state are important. These have to be known reasonably well before definitive predictions of the minimum sea state can be made.

3.6.3 Estimation of Sea State for Globulation Considering the Distribution of Water Particle Velocities

It was shown earlier in Sections 3.4.1 and 3.4.2 that, when the rms value of the turbulent velocities in water exceeds a certain minimum, globulation of oil can be expected. In a given sea, the water particle velocity amplitudes are not uniform, but vary depending on the wave size. In effect there exists a probability distribution for water velocities similar to the wave height probability distribution. Because of the assumed relationship between water particle speeds and the turbulent velocity rms values (Equation 3.40), there will exist a probability distribution of rms velocities. Therefore, in a given area (considering a specific sea state given by a significant wave height), only a fraction of the sea will contain turbulent velocities greater than the minimum necessary to initiate oil globulation. This fractional area (or probability) of globulation can be determined as a function of sea state as follows:

Table 3.2: Estimates of Minimum Sea Limit for Incipient Globulation of Oil

[The numbers in the table represent significant wave heights for the sea state calculated.]

Spectrum† \ $f = \frac{\overline{(u'^2)}^{\frac{1}{2}}}{U_s}$	f = 0.1	f = 0.03	Oil Parameters
Pierson-Moskowitz $\alpha = 1.62 \times 10^{-2}$ $\beta = 0.74$	3	30	$\rho_w = 1000$ kg/m^3 $\rho_o = 900$ kg/m^3 $\sigma = 3 \times 10^{-2}$ J/m^2
International Ship Structures Congress (ISSC) $\alpha = 1.24 \times 10^{-3}$ $\beta = 0.031$	11	110	

†The spectrum is defined by

$$e(\omega) = \frac{\alpha g^2}{\omega^5} \quad \text{Exp} \left[- \beta \left(\frac{g}{U\omega} \right)^4 \right]$$

with $E'' = \frac{1}{2} \rho_w g \int_0^\infty e(\omega)\, d\omega$ = average energy per unit area of sea.

α, β are dimensionless constants

Significant wave height $H_s = \left(\frac{2\alpha}{\beta} \right)^{0.5} \frac{U^2}{g}$

Modal frequency in the spectrum $\omega_0 = (0.8\beta)^{0.25} \frac{g}{U}$

Using an equation similar to Equation 3.40, we get

$$\overline{u'^2} = f^2 \, U_w^2 \qquad 3.41$$

where U_w is the water particle velocity amplitude and $\sqrt{\overline{u'^2}}$ is the turbulent velocity fluctuation generated by the water velocity U_w. The minimum rms value for initiating globulation is given in Equations 3.17 or 3.24.

Also we assume that the water particle velocity amplitudes are Rayleigh distributed; that is:

$$P\left(U_w > U_{min} \right) = \exp\left(- \frac{U_{min}^2}{\overline{U_w^2}} \right) \qquad 3.42$$

where P is the cumulative probability that, in a given measurement, the water particle velocity exceeds a given minimum value U_{min}. P can also be interpreted as the fractional area of the fully developed sea in which the water velocity amplitude exceeds U_{min}. In the above equation, $\overline{U_w^2}$ is the mean square velocity amplitude which is related to sea state by (see Equation B.10, Appendix B).

$$\overline{U_w^2} = \sqrt{\frac{\alpha\pi}{32}} \; g \, H_s. \qquad 3.43$$

Substituting Equation 3.43 into 3.42, we get:

$$P \left(U_w > U_{min} \right) = \exp\left(- \sqrt{\frac{32}{\alpha\pi}} \; \frac{U_{min}^2}{g \, H_s} \right). \qquad 3.44$$

The above equation indicates that in any given sea state (characterized by a significant wave height H_s), there exists a finite probability P with which globulation would occur. Of course, this globulation occurs in only selected locations in the oil slick (provided it covers a "large area"). The above probability should therefore be interpreted as a fraction of the oil slick that is undergoing globulation at any given time, when the sea is fully developed and is of height, H_s.

In Figure 3.5, a plot of the Equation 3.44 is indicated for the following conditions

$$\sqrt{\left(\overline{u'^2}\right)_{min}} = 0.15 \text{ m/s}$$

$$f = 0.1$$

$$U_{min} = \frac{0.15}{0.1} = 1.5 \text{ m/s}$$

and the spectrum used is the P-M spectrum. It is seen from the figure that the probability of globulation (alternatively the fractional area of slick undergoing globulation) increases as the sea state index (H_s) increases. For just 30% of the slick to be globulated, the sea has to be quite rough ($H_s \simeq 5$ m).

3.7 Discussion

In this chapter we have approached the problem of estimating the sea state for oil dispersion by first considering several allied problems. The results of these analyses are all accurate only to within an order of magnitude. First the energies involved in various phenomena are calculated. This study indicates that the energy in the wave system (per unit area) in the ocean is enormous and a small fraction of this energy is enough to break up an oil slick and drive oil into water. The calculations also show that for oil globules of about 1 cm diameter the gravitational energy necessary to push them to any reasonable depth (2 m) in water is significantly larger than the surface energy required to form them. However, for very small oil globules (of sizes 1 mm or less) the energy stored as surface energy is significant. The upshot of these calculations is that if an extremely small part of the ocean energy is transferred to oil, the oil globules formed can be expected to be carried very deeply into water. The key question, therefore, to answer is: "What part of the ocean's wave energy is fed into an oil slick, and what is this energy feed mechanism?" Our assumption is that this "feed mechanism" is indirect and the principal agency in the sea which would be responsible for the vertical dispersion of the oil is the upper ocean turbulence. It is, of course, not known at present whether this upper ocean turbulence gets its energy from the ocean wave field alone (by, say, breaking action and other

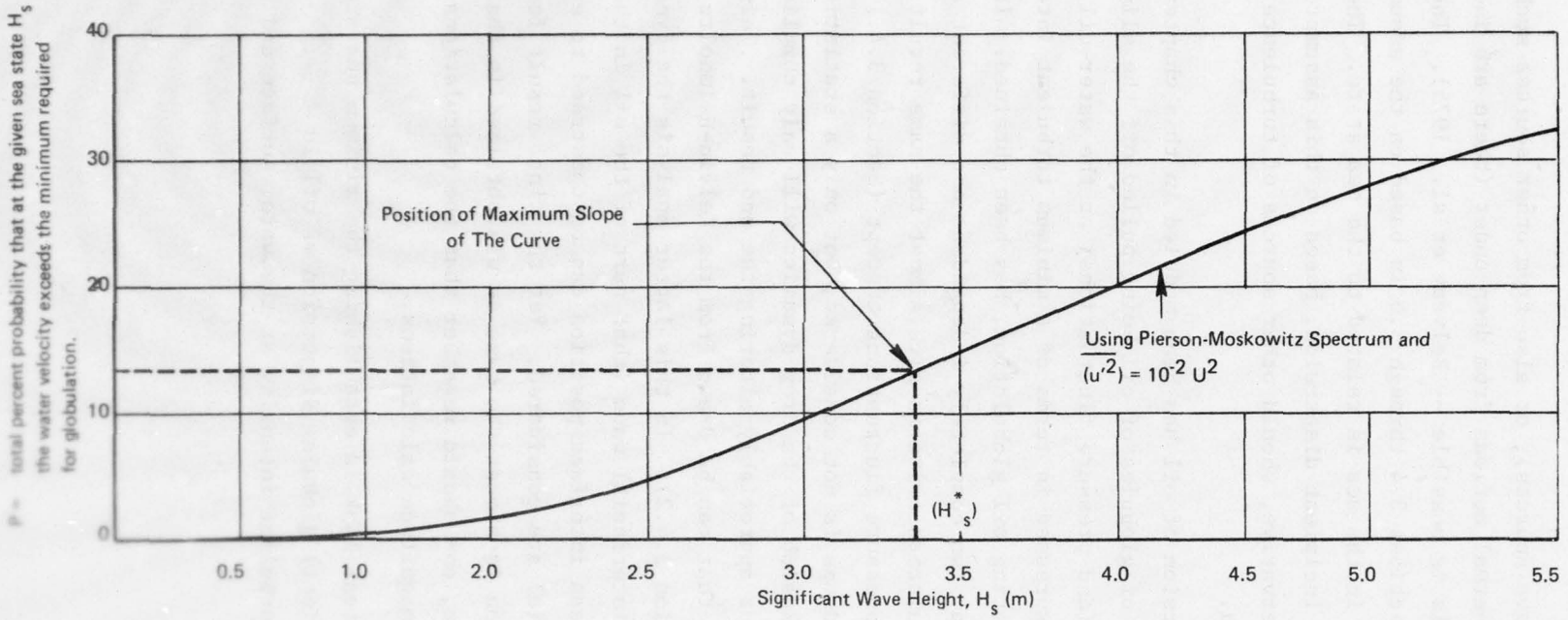

FIGURE 3–5 PROBABILITY OF GLOBULATION VERSUS SEA STATE

AD-A049 794 LITTLE (ARTHUR D) INC CAMBRIDGE MASS F/G 6/6
THEORETICAL STUDY TO DETERMINE THE SEA STATE LIMIT FOR THE SURV--ETC(U)
JUN 77 P P RAJ DOT-CG-61505-A
UNCLASSIFIED ADL-79299-F USCG-D-90-77 NL

2 OF 3
AD
A049794

unidentified wave sources), or also from other sources such as currents and thermal motions from deep under (there are indications that indeed this is possible -- Belyeav et al., 1975). The analysis performed in Sections 3.4 through 3.6 is based on the assumption that the turbulence in the sea is related to the sea state. The sea state calculated for incipient dispersion, based on this assumption may not always be conservative, should other sources of turbulence dominate the upper ocean.

The dispersion of oil has been modeled in this chapter based on the assumption of globules of oil being pulled off the slick by the instabilities (and pressure fluctuations) at the water-oil interface. A criterion, expressed in terms of a minimum turbulent intensity necessary for initiating oil globulation, has been obtained. It is interesting to see that two completely independent and different approaches to obtaining globulation criteria give almost the same result. In using the turbulent pressure fluctuations concept (Section 3.4.1) the dynamic motion of the drops is not considered, but only a statistical approach is taken. Inclusion of the drop dynamics will only complicate the problem, without appreciably altering the end result. This is precisely the conclusion that can be drawn from the Kelvin-Helmholtz instability analysis (Section 3.4.2). In this latter analysis the dynamics of motion of the interfacial wave (that part of the oil in the wave which is below the mean interface position can be construed to eventually form the globule) are considered. Yet the final result for the globulation criterion is almost the same as was obtained in the static analysis. Of course, one should remember that the calculations per se are only order of magnitude calculations.

The important link in establishing the minimum sea state required for the (incipient) globular dispersion of oil is a relationship between turbulent intensity at the water surface and the sea state.

This has been attempted in Section 3.5 by considering the turbulent velocity flucations induced in water by wind; the relationship between a fully developed sea state and the wind speed is well known and has been reviewed in Chapter 2. In performing the calculations indicated in Section 3.5, it has been tacitly assumed that the presence of the oil does not interfere with the wind shear process. In addition, it is assumed that the presence of an oil layer does not materially alter the distribution of the intensity of turbulence in the water. It can certainly be argued that the presence of oil will indeed affect the energy transfer and also damp out turbulence (at the water-oil interface). If one had information on the extent of this effect and were to include it in an analysis, one would predict, in fact, a higher wind speed (and consequently a higher sea state) for incipient dispersion. Therefore, the analysis proposed is conservative in that dispersion would be predicted to occur at a sea state lower than what may actually be needed.

In the estimation of turbulent intensity generated in water by a wind (Section 3.5), we find that the results are sensitive to the nature of the assumption that one makes regarding the size of the energy containing eddies genrated by wind in the ocean. Two possible length scales are used for these eddies and considerably different results are calculated (see Table 3.1). The estimate of minimum sea state is, therefore, very sensitive to the above assumption on eddy sizes. However, since no data exist on the eddy sizes, the results obtained for the sea states should be considered as approximate.

Another possible approach to relating the turbulent intensity to the waves in the sea is considered in Sections 3.6.2 and 3.6.3. In this approach the orbital speed of water particles due to the wave motion and the rms turbulent velocity are assumed to have a linear relationship. (This idea is taken from turbulent flow literature. In turbulent flows, where the turbulence is generated by the mean flows, it is known that the rms velocities are about 10% of the mean flow velocity.) Because of the difficulty of establishing a single

water speed in a random sea, we have related the significant water speed (for a definition, see Equation B.6 of Appendix B) and the turbulent velocity. In this case, a unique sea state, represented by a significant wave height value, can be calculated for initiating globulation. In the second approach, we have retained the linear relationship between water particle (orbital) speed and the rms turbulent velocity, but have considered the distribution of water speeds. This leads to the prediction that globulation is possible in all sea states, but the probability varies as a function of the sea state. The probability of globulation in sea states below 3 m significant wave height is less than about 12% (see Figure 3.5).

The actual calculation of the minimum sea state is illustrated in Section 3.6, using the known relationships among wind, waves, and sea states. In the examples shown, we have assumed that the fully developed sea can be represented by the (widely used) Pierson-Moskowitz spectrum. Use of other spectra will give substantially different results for the sea state as can be seen from Table 3.2.

One other approach that was considered in this chapter--to establish a criterion for slick breakage and dispersion--has been indicated in Section 3.3. In this section an attempt has been made to derive the slick instability criterion, based on a thermodynamic approach. To the extent that the methodology has not yielded a numerical result for a minimum sea state for oil dispersion, the methods can be termed unsuccessful. However, we feel that significant progress has been made in applying to the study of oil slick dispersion some newly formed ideas from the thermodynamic literature on thin silm stability. In addition important physical property data needed for a cursory application of the theory have been identified. Of course, several questions on the appropriateness of applying an analysis that is valid for thin films (monomolecular layer) have been left unanswered. The section on thermodynamic stability analysis should, therefore, be interpreted as a first attempt at using purely fundamental principles to arrive at criteria for oil slick breakup. Much more research and experimental data are required before this method can be established on a solid footing.

3.8 Conclusions

In this chapter several possible methods have been explored, using basic physical laws (such as satisfying kinematical conditions), to obtain an estimate of the minimum sea state necessary to cause an oil slick on the open ocean to be dispersed. Energies associated with various phenomena have been estimated. Mechanisms of ocean turbulence and intrinsic thermodynamic instabilities have been considered in terms of their effects on the oil slick. From these analyses the following conclusions are drawn:

- Estimates of various energy quantities indicate that a small fraction of wave energy is sufficient to maintain oil in suspension.
- A 12 m/s wind can supply energy sufficient to maintain oil globules at depths up to 2 m.
- The thermodynamic stability criterion derived here cannot be applied at present to determine the minimum sea state for oil dispersion because of unavailability of the data on the variation of surface tension with area density of oil.
- Incipient globulation may occur in seas of 3 m significant height. This is based on the assumption that wave generated water speeds and turbulent intensities in the upper ocean are closely correlated. Only experiments, both lab scale and on the ocean, can indicate whether this is indeed true. In addition, the type of spectral description also has influence on the above estimate.
- Assumption of a linear relationship between instantaneous water particle velocity and the local turbulent intensity leads to the result that globulation is possible in all sea states, but that the fraction of slick area undergoing globulation is very small. In a 3-m significant wave height sea, only about 12% of the oil slick is predicted to be undergoing globulation at any given instant.

It may be concluded, based on the results of the above analyses, that the principal phenomenon that will rupture an oil film and form globules of oil is the breaking action of the waves.

CHAPTER 4

THEORETICAL MODELS FOR SLICK FRACTURE AND DISPERSION

4.0 Summary

Two main types of slick dispersion are considered in this chapter. These include the breakage of an oil slick into smaller sizes and their dispersion on the water surface. The second type is the globular dispersion into the water column. The theoretical model for the former type of dispersion gives the conditions under which a large slick will be fractured by the breaking waves in the ocean. The models for the second type of dispersion give the depth of penetration of the globules, their residence time, and the depth-wise distribution of the globules as a function of time. These results are useful in estimating the total mass of oil that may be present in the water column in the form of globules at any given time for a given sea state.

4.1 Introduction

The technology of cleaning up oil spills on the open ocean is still in its infancy. Skimmers and oil booms that work effectively on calm waters seem to have limited effectiveness when the waves are larger than about 1 foot. A necessary requirement for the efficient working of booms seems to be the presence of a film of oil on water, in addition to the need for reasonably calm water. Should oil occur in patches scattered over a large area or be dispersed into the water as globules, skimmers and booms may become ineffective. Therefore, there exists a need to develop better methods of cleaning up (physically) the oil spilled on the oceans. However, before this can be achieved, it is imperative to understand how an oil slick behaves on the open ocean and how the natural forces of wind, waves, and currents interact with the oil slick, and to answer questions as to whether indeed the oil slick

remains as a single entity or is dispersed horizontally as in the form of many slicklets or is dispersed vertically in either globular form or in the form of an emulsion. There are many such unanswered questions about the behavior of oil on the open ocean and its relationship to the sea state. A modest beginning is made in this chapter by proposing two principal ways in which "oil" may behave on the ocean. Based on these concepts, theoretical models have been developed in this chapter, and the relationships among various sea and oil parameters have been developed. It is needless to say that several important assumptions have been made (which are inevitable in a theoretical approach based purely on speculation, without much of an experimental backing) both as to the behavior of oil under certain circumstances as well as on the behavior of the sea. It is hoped that these theoretical models will provide the necessary basis on which to design and conduct both small-scale and large-scale experiments.

The models developed in this chapter are based on the two broad classifications of slick behavior, viz, the breakdown of continuous oil slicks into smaller slicks ("slicklets") and their surface dispersion and, secondly, the dispersion in the form of droplets, globules, and emulsions suspended vertically in the water column.

In Section 4.2 the effect of the nonbreaking (swells) and breaking waves on the slick fracture are considered. The objective of the models presented in this section is to determine the criteria for slick film breakage and its subsequent dispersion in the form of slicklets. Section 4.2.1 deals with the film breakage caused by the stretching and compression of the film due to the passage of swells. A criterion for the breakage in terms of the wave frequency is derived. In Section 4.2.2, the fracturing of an oil slick by breaking waves is modeled and discussed. Because of the very nature of random behavior of the breaking waves, the model developed is probabilistic. The ultimate result from this model is the characteristic time for slick breakage and its relationship to the various sea and wave parameters. Once the relationship among the wave parameters used in the model and the sea state is obtained experimentally (as of now these data do not seem to be available), the time for fracture

in any sea state can easily be determined. Another mechanism by which a slick may be broken up on the surface is considered in Section 4.2.3. Langmuir circulations are reported to occur whenever there is a strong, sustained wind. The eddy circulations created by the Langmuir cells could conceivably break up a slick. A model, which is very simplistic in its approach (because of the lack of complete understanding of the phenomenon of Langmuir circulations), is discussed in Section 4.2.3. The result of the model is a critical wind speed above which the slick can be expected to fracture.

The globular dispersion of oil into the water column is discussed in Section 4.3. Several models describing and quantifying the effects of the sea and the motion of oil globules are discussed in several subsections. In Section 4.3.1 a general overview of the phenomenon of globular dispersion is discussed and the philosophy of modeling is described. In Section 4.3.2 the dynamics of oil globules in quiescent water is discussed, and the model leads to quantifying the terminal velocity of globules as a function of drop size and oil density. A further extension of the model to solving the exact motion is given in Section 4.3.5. The results obtained in Section 4.3.2 are used in the model on vertical dispersion by Langmuir circulation given in Section 4.3.3. This model is a logical extension of the slick fracture by Langmuir circulation discussed in Section 4.2.3. The results from the model in Section 4.3.3 also give a critical wind speed for "sinking" oil droplets of a given size due to the downwelling generated by the Langmuir circulation.

In order to maintain the naturally buoyant oil globules suspended in water, the water has to be in a state of continuous agitation. This agitation, also referred to as turbulent mixing, is brought about by the upper ocean turbulence, which is assumed to be generated principally by the breaking action of the waves. In Section 4.3.4 a model is developed to calculate the probability of wave breaking and the energy dissipated in the breaking action. This model is an extension of Longuet-Higgins Model (1956, 1975) but uses more recent JONSWAP data. The model provides a quantitative estimate for the mechanical energy imparted to the ocean water by the breaking waves. A major fraction

of this energy finally ends up as turbulent energy. In Section 4.3.5 a simple turbulence model is derived to characterize the turbulent intensity as a function of time and depth-wise position. This model uses the calculation of energy dissipated by a breaking wave, modeled in the earlier section. Finally in Section 4.3.6 the vertical motion of the oil globules subjected to the breaking action of the waves and the subsequent nonstationary turbulence is modeled. The motion of the globules is analyzed partly with a deterministic model and partly by a stochastic approach. The ultimate result from this analysis is the probability density distribution of oil globules with depth at each instant of time. From the results the fractional mass of oil that is present within the water column as a function of time is obtained in a probabilistic sense.

Each of the models derived in the following chapter is illustrated with a numerical example so that the use of the derived results becomes clear. The assumptions made and their effects on the results are also discussed. Wherever possible, the symbols used in a model are defined. However, because of the completely different physical concepts treated in each model, a certain amount of duplication in notations has become unavoidable. A general nomenclature is provided in Appendix A.

4.2 Horizontal Fracture and Dispersion of Oil Slicks

In this section two separate mechanisms of slick fracture are considered. In Section 4.2.1, the failure of the film of oil by non-breaking waves is analyzed. In the following Section 4.2.2, a model is developed for the surface fracture of the slick by a train of breaking waves. The objective of these analyses is to obtain criteria for slick breakage (and therefore surface dispersal). Once such criteria are obtained, they can be related to sea state. This will finally result, it is hoped, in establishing a sea state for surface dispersal of oil slicks.

In the models discussed below the effects of variation in oil properties, either due to composition variations or due to the differences in oil temperature and water temperature, have not been considered.

4.2.1 Oil Slick Breakage by Film Stretching Caused by Nonbreaking Waves

The passage of crests and troughs of waves through oil at sea results in the alternate stretching and compression of the film; this causes the film to be subjected to stresses. When these stresses exceed a critical value, the film of oil will fail, essentially because of tension. The rate of strain of the film is the important quantity to be determined, because the stresses in a fluid depend on the rates of strain rather than on the strain (as in the case of solids).

In this section, we first obtain the rates of strain of a film of oil subjected to a given sinusoidal wave. Then, using two different film breakage criteria, we obtain an estimate for the sea state at which the oil may break by film fracture. In performing such a calculation certain important assumptions are made which reduce the complexity of the analysis without compromising the physics of the problem. These assumptions include:

- neglecting the flow in the oil layer generated by the dynamic forces (wave motion); that is, we assume the oil thickness to be uniform and neglect any stresses that may be generated as a result of the flow of oil. In effect the dynamic effects are neglected and calculations satisfy only the kinematical conditions;
- calculating the water (surface) particle velocities and motions using the results of small amplitude wave theory.

While the second assumption is adequate when the wave steepness, $\frac{2a}{\lambda}$ is small, its applicability to very steep waves remains questionable. Since the objective of the analysis is to obtain estimates for the wavelength of waves that may fracture the oil film (due to high strain rates), we propose to retain the above assumption.

Consider an oil slick of uniform thickness subjected to a travelling sinusoidal wave of wavelength λ. The location of the particles of oil on the wave are indicated schematically in Figures C.1a and C.1b. The oil film is stretched in some places and compressed in other locations. Because of the wave motion, the oil particles that are elongated at one instant would be compressed half of a wave period later. This alternate stretching and compressing induces stresses in the film. The stresses are proportional to the rate of strain. Therefore the strain rates are calculated initially.

Rate of Strain Calculations

The strain rate of any portion of a thin film subjected to a travelling wave of length λ (and of circular frequency ω) is defined by

$$\text{Strain rate at point "a" on the oil film} = \Gamma = \lim_{\substack{\Delta t \to 0 \\ L_{a,b} \to 0}} \frac{1}{\Delta t} \left[\frac{L_{a,b}(\Delta t)}{L_{a,b}(0)} - 1 \right] \qquad 4.1$$

where $L_{a,b}$ is the length of oil film between points a and b. In Appendix C, expressions are derived for the lengths of curved elements and the strain rates. From Equation C.28 of Appendix C, we see that the maximum tensile strain rate is given by

$$\Gamma_{max} = \frac{\omega}{2} \frac{1}{\sqrt{A^2 - 1}} \qquad 4.2$$

where A is a geometric parameter describing the wave steepness, defined by

$$A = \frac{1 + (\pi S)^2}{2\pi S} \qquad 4.3$$

$$\text{with } S = \frac{2a}{\lambda} = \text{wave steepness} \qquad 4.4$$

The maximum normal tensile stress ψ_s that develops in the oil film due to the above strain rate is given by (see Schlichting, 1962, page 50).

$$\psi_s = 2\mu_o \Gamma_{max} \qquad 4.5$$

Hence the total tensile stress in the oil layer at the location of maximum strain rate is*

$$\psi = -p_{atm} + \psi_s \equiv -p_{atm} + 2\mu_o \Gamma_{max} \qquad 4.6$$

Criteria for the Slick Breakage

The above derived stress has to be interpreted in terms of a film breakage condition to relate the wave parameters (and hence sea state) to slick stability. Two breakage criteria are considered below, one involving the cavitation of liquids and the other based on the fracture of the slick when the stress exceeds the intermolecular force (surface tension).

When a single-component liquid is subjected to decreasing pressures at a constant temperature, ordinarily the liquid boils when the pressure is equal to the vapor pressure corresponding to the temperature (super pure liquids with no dust, dirt or other nucleating sites, however, are known not to boil, even when subjected to pressures far below the vapor pressure — sometimes even when under tension). Crude oil is a mixture of several hydrocarbons and, therefore, a single boiling temperature / pressure relationship cannot be formulated. However, it is known that cumene and n-nonane form the most volatile fractions of crude. Hence, when crude oil is subjected to a rapid decrease in pressure (as happens when a film of crude is stretched at high strain rates), local boiling may take place with the liberation of bubbles of cumene and n-nonane.

Therefore, the first criterion for oil film breakage that we propose to use is the condition at which local boiling takes place.

---

* In writing equation 4.6, an implicit assumption as to the smallness of oil thickness is made. Therefore, the pressure increase at the bottom layer of the oil due to the hydrostatic head is small compared to the atmospheric pressure.

Harrison et al. (1975) have used a value of 537 N/m^2 for the vapor pressure (p_{vap}) of cumene and n-nonane at 297 K. Hence based on the cavitation criterion, the oil slick can be said to be stable when

$$(p_{atm} - p_{vap}) > 2\mu_o\Gamma_{max} \qquad 4.7$$

The second possible criterion that may be postulated for oil film breakup (for order of magnitude estimation of sea conditions) is based on comparing the tensile normal stress developed due to the stretching with the molecular cohesive stress between liquid particles. The latter may be approximated by dividing the surface tension by the film thickness. Hence the stability criterion can be expressed by

$$\frac{\sigma}{b} > 2\mu_o\Gamma_{max} \qquad 4.8$$

Equations 4.7 and 4.8 represent two criteria for the non-breakage of an oil slick. However, to understand the type of wave necessary to cause slick breakage by either of the above criteria, numerical values have to be used. We have therefore worked out an example below using reasonable property and other values.

Numerical Example

Consider a wave of steepness	$S = 1/10$
Hence, from Table C.1 of Appendix C the steepness parameter	$A = 1.749$
Surface tension of oil	$\sigma = 3 \times 10^{-2}$ N/m
Viscosity of oil (assumed to be 100 times that of water)	$\mu = 10^{-1}$ N s/m^2
Oil film thickness	$b = 10^{-2}$ m
Atmospheric pressure	$P_{atm} = 101.33 \times 10^3$ N/m^2
Vapor pressure at which boiling ensues in crude oil at 279 K (from Harrison, et al. [1975])	$P_{vap} = 0.537 \times 10^3$ N/m^2

Substituting the above values in Equation 4.7 yields the strain rate necessary for the cavitation failure of the slick:

$$\Gamma_{max} = \frac{(101.33 - 0.537) \times 10^3}{2 \times 10^{-1}} = 50.4 \times 10^4 \ s^{-1}$$

Hence, from Equation 4.2, the frequency of waves necessary to induce cavitation in crude oil is given by

$$\omega = 2 \times 50.4 \times 10^4 \sqrt{1.749^2 - 1} = 1.44 \times 10^6 \text{ rad/s} = 2.3 \times 10^5 \text{ Hz}$$

Any wave of frequency lower than the above value would not produce strain rates high enough to cause cavitation and, therefore, would not rupture the slick. In any real sea, waves of significant size having the above frequency will not be found. This leads, therefore, to the conclusion that slick breakup by cavitation effects will not occur.

Using the second break criterion, equation 4.8, and the values of properties assumed, we get

$$\left(\Gamma_{max}\right)_{\text{for slick rupture}} = \frac{3 \times 10^{-2}}{10^{-2} \times 2 \times 10^{-1}} = 15 \text{ s}^{-1}$$

Substituting this in Equation 4.2, we get

$$(\omega)_{\text{for slick rupture}} = 1.5 \times 2 \sqrt{1.749^2 - 1} = 43 \text{ rad/s} = 6.8 \text{ Hz}$$

which corresponds to a gravity wave of

$$\lambda = 3.3 \times 10^{-2} \text{ m}$$

This indicates that waves with lengths less than about 3 cm would break the film by stretching, if indeed the second criterion is valid.

There are two problems in using the criterion of Equation 4.8. First of all, the equation indicates that the strain rate needed to break an oil film decreases with an increase in film thickness. This conclusion is contrary to judgment which would indicate that the thicker the film the harder it is to rupture (with the same strain rate). Secondly, this criterion does not take into account the dynamics of the oil film motion due to the wave action. This may be a serious limitation to the analysis considered.

From the results of the analysis presented and discussed, we conclude that simple stretching and compression of an oil slick by a swell-type wave in the ocean would not rupture the slick. As a complementary conclusion it may be stated that only breaking waves will have any influence on the breakage and dispersion of oil slicks on the ocean.

4.2.2 Fracturing of an Oil Slick Due to Breaking Waves

When a large oil slick is subjected to the action of breaking waves (of length smaller than the width of the oil slick), conceivably a slot will be opened up in the oil slick under such a breaking wave. This would result from the intense turbulence created at the crest of a breaking wave, and also by the spilling action of the water. It is not certain whether the breaking wave will continue to exist over large distances through the oil slick. However, if we assume that the breaking wave opens up a slit (not very much greater than the wave height) and then ceases breaking, the slit tends to close up due to the gravity flow of oil. If before the closing up of the slit another breaker wave hits the same spot, the opening in the oil film is sustained. Also, if the second slit is overlapping and contiguous with the first, then a wider length of slick is fractured. Therefore, a series of breaker waves occurring sequentially and opening up slits in an oil film may be able to fracture an entire oil slick.

The objective of the analysis given below is to obtain the conditions under which an oil slick fracture is possible and to determine the relationship among the parameters that influence the occurrence of a fracture.

(a) Analysis:

The problem as stated above is two-dimensional. The fracture in the slick can occur, at least in principle, in any direction relative to the direction of propagation of the waves. However, the probability of slick fracture normal to the wave travel direction is very high. In analyzing the above problem, we made the following assumptions:

1. The breaking waves occurred at random intervals, but all of them have their crest lengths oriented in a given direction.
2. The breaking waves open up rectangular "slots" in the oil slick of length equal to crest length and widths.
3. The slot tends to close up at a constant rate determined by the oil density and film thickness.

Assumption 1 is probably reasonable when breaking waves occur due to shoaling. In this case the crests of waves are essentially parallel to each other. However, if breaking waves occur due to the nonlinear 3-D interaction of waves, as would occur in deep water, then the above assumption has serious limitations. In fact, in the latter case even the second assumption on the formation of "slots" may be incorrect. In making the second assumption, we have taken for granted that a spilling wave in an oil slick will "cut open" a slot. This needs to be verified experimentally. Even in such a case, the oil slick may be closed by the resurfacing of the oil that is driven under the water, rather than by the movement of the oil from the sides, as has been implied by assumption 3. The third assumption will indeed be true if the oil is simply pushed to the side by the breaking wave (in opening up a slot), or if the oil driven under by the wave resurfaces under an unopened slick. It suffices, therefore, to say that many questions remain to be answered. However, based on the above assumptions, one can formulate a slick (surface) breakup model and, for obvious reasons, its validity or otherwise can be proved only by large-scale experiments.

(b) Formulation of the Model:

For the purpose of mathematical modeling, we consider the slick to be a square of side L such that its total area is the same as the area of the actual slick. A breaking wave is assumed to cause a slot of width W(0), as shown in Figure 4.1. It is assumed that the slot will close up by the gravitational flow of oil (in the width-wise direction) in time T_c.

A slick that has been fractured in calm water will close itself as the two edges move together, the speed of the edges being given approximately by

$$V = \sqrt{gh(1-\rho_o/\rho_w)} \qquad 4.9$$

where V = speed of the edges, and

h = thickness of the oil layer.

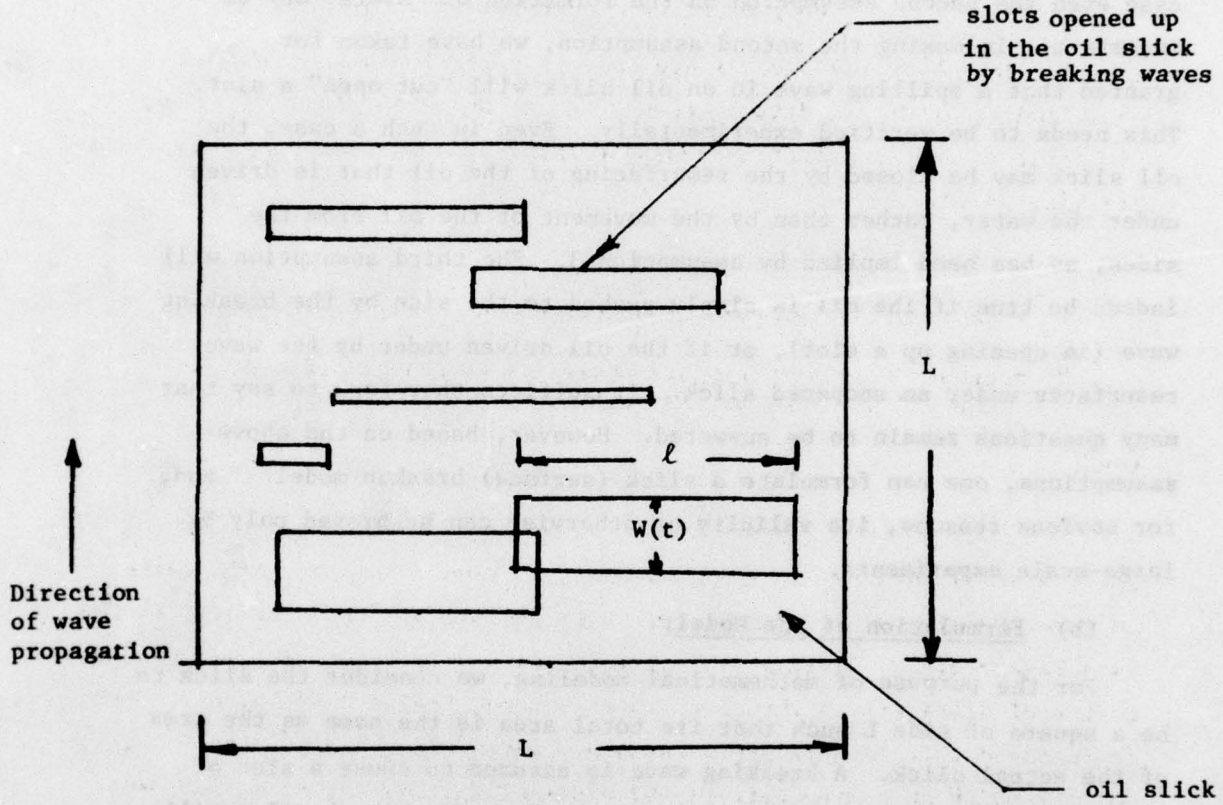

Figure 4.1 Schematic Representation of the Creation of Different Size Slots of an Oil Slick Due to Breaking Wave Action

The above expression applies to the oil front when its dynamics depend on the balance of inertial and gravitational forces generally associated with the initial phases of the spreading of a spill. Hence, the "closing-up" time can be approximated by

$$T_c = \frac{0.5\ W(0)}{V} = \text{average closing time for an oil slot of } W(0) \text{ where both edges are moving.} \qquad 4.10$$

The length of the slots ℓ are assumed to follow a general (but specified) statistical distribution function which is identical to the distribution function that is characteristic of the crest length of breaking waves.

If

T_w = mean period between the occurrence of breaking waves, and

N = number of distinct slots (breaking waves) present within the oil slick at any instant of time,

then,

$$N = T_c/T_w. \qquad 4.11$$

These N slots have random widths as well as random lengths (transverse to wave propagation direction) and their centers are randomly distributed (see Figure 4.1). An important desired result is the probability that a series of slots exists that forms a continuous fracture of the oil slick. It is noted that as time progresses, new slots will be appearing within the oil slick at a mean rate of one slot per T_w time units; at the same time, the existing slots will be closing up.

Figure 4.2 illustrates schematically the time-wise development of the slick state in time. Suppose one considers an unfractured state ("Uf") of the slick at any instant and the state of the same slick after a time interval Δt. There are two possibilities. First, there is a finite probability (P_{uu}) that the slick would remain in the unfractured state. There is also a probability (P_{uf}) that the slick would be in a fractured state. Therefore,

$$P_{uf} + P_{uu} = 1 \qquad 4.12$$

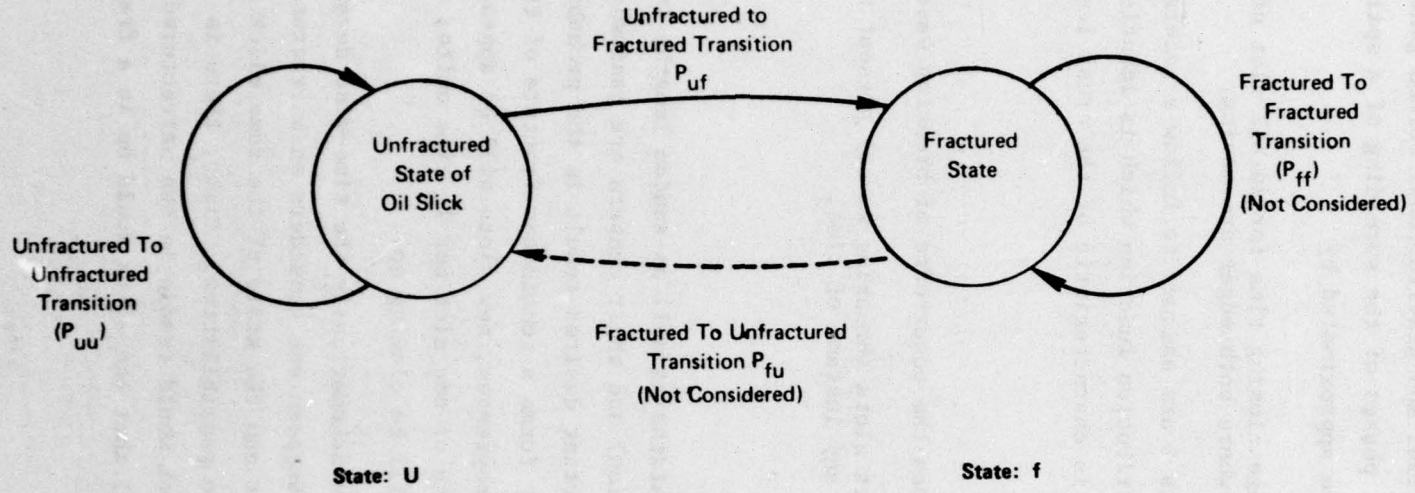

FIGURE 4–2 POSSIBLE STATE TRANSITIONS OF AN OIL SLICK SUBJECTED TO BREAKING WAVES

Similarly, a fractured slick (in a state "f") has a finite possibility (P_{ff}) of continuing to be in a fractured state or reverting back to unfractured state with a probability (P_{fu}).

In this case also

$$P_{ff} + P_{fu} = 1 \qquad 4.12$$

In our analysis we choose to ignore the probable transitions from fractured state to unfractured state (f → uf). This is because we start the problem from an unfractured slick and seek to find out the minimum sea conditions under which the slick may undergo transition to fracture due to breaking waves.

A "transition of oil state" is defined to occur every time a new breaking wave enters the oil layer.

If a slick begins in the state "U", the probability that it has not passed into the fractured state "f" after K transitions is given by

$$P_{U \not\rightarrow f} = (1 - P_{uf})^K \qquad 4.13$$

Therefore, the probability (P) for the existence of a fracture after K transitions is given by

$$\underline{P} = 1 - (1 - P_{uf})^K \qquad 4.14$$

Equation 4.14 is the important equation in that once P_{uf} is estimated the total probability can be easily established as a function of time. This is because

$$K = \text{number of transitions} = \frac{t}{T_w}$$

where t = total elapsed time

Substituting the above in Equation 4.14 we get:

$$\underline{P}(t) = 1 - (1 - P_{uf})^{t/T_w} \qquad 4.15$$

That is

$$\underline{P}(t) = 1 - e^{\frac{t}{T_w} \ln (1 - P_{uf})} \qquad 4.16$$

Hence, the characteristic time in which a fracture may occur is given by

$$t_c = \frac{T_w}{-\ell n\ (1 - P_{uf})} \qquad 4.18$$

or expressed in dimensionless way

$$\tau = \frac{t_c}{T_w} = \frac{1}{\ell n\ (\frac{1}{1 - P_{uf}})} \qquad 4.19$$

Note that since $P_{uf} < 1$, the natural logarithmic term in Equation 4.18 results in a negative value giving a positive value for t_c. Physically, t_c represents the time in which $\underline{P}(t) = 1$ if the probability increased with time at the same rate as at zero time. In fact, the value of $\underline{P}(t)$ at $t = t_c$ is equal to 0.632.

The important parameter that has to be calculated to obtain the time for fracture of the slick is the probability P_{uf} that the slick undergoes a transition from uncut to the fractured state in a given change of state. For the two-dimensional case, the evaluation of this parameter is an extremely complicated task. Therefore, we analyze an equivalent one-dimensional problem. It is expected that the one-dimensional problem will yield times for fracture which will be smaller than in the associated two-dimensional problem.

In formulating and solving the 1-D problem, we have considered three different approaches. Initially, a simple (but approximate) result is obtained. Subsequently, a more nearly exact formulation is provided and solutions obtained for P_{uf}. Finally, the Monte Carlo technique is utilized and the value for P_{uf} obtained for various values of the parameters that describe the physical situation.

Estimation of P_{uf} Using a Simple One-Dimensional Model:

We note that P_{uf} is simply the probability than an average number N of slots will form a complete cut. In one dimension, the problem of determining P_{uf} becomes simply an evaluation of whether a line of length L is covered by N slots having a length distribution given by $q(\ell)$, as shown in Figure 4.3.

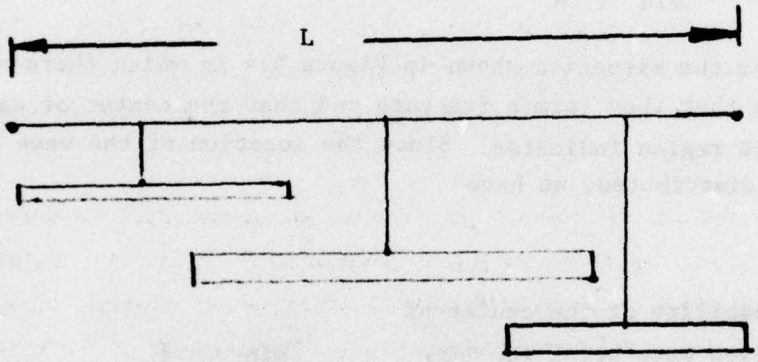

Figure 4.3: Fracturing of a One-Dimensional Slick by Waves of Length Distribution q_ℓ

Since the breaking waves are assumed to occur at random with their centers located randomly on the oil slick of length L, we assume a uniformly distributed set of centers of waves of total number N. This means that

$$\text{the average center-to-center spacing of slots with the 1-D slick of length L} = \frac{L}{N} \tag{4.20}$$

The criterion we use for the presence of a continuous fracture in this one-dimensional case is that the minimum length of slots be larger than the inter-slot center spacing, i.e.,

$$\text{i.e.,} \qquad \ell_{min} \geq \frac{L}{N} \tag{4.21}$$

Consider the situation shown in Figure 4.4 in which there are N slots present such that they form a fracture and that the center of each wave is within the region indicated. Since the location of the wave center is randomly distributed, we have

$$\text{Probability of the center of a given wave being in, say, region AB (See Figure 4.4) is} = \frac{\ell_{min}}{L} = \frac{1}{N} \tag{4.22}$$

Now the probability that each wave completely occupies its region (say AB) is given by (See Figure 4.5):

$$\text{Probability of one wave covering completely a region AB} \quad P^* = 2 \sum \text{Probability that the wave center lies between } x + dx \text{ and } x \text{ and its semi length is greater than } (\ell_{min} - x) \tag{4.23}$$

Assuming that the wave crest lengths are Rayleigh-distributed, we have,

$$P^* = 2 \int_{x=0}^{\frac{\ell_{min}}{2}} \frac{dx}{\ell_{min}} \, e^{-\frac{\left[2(\ell_{min}-x)\right]^2}{\ell^2}} \tag{4.24}$$

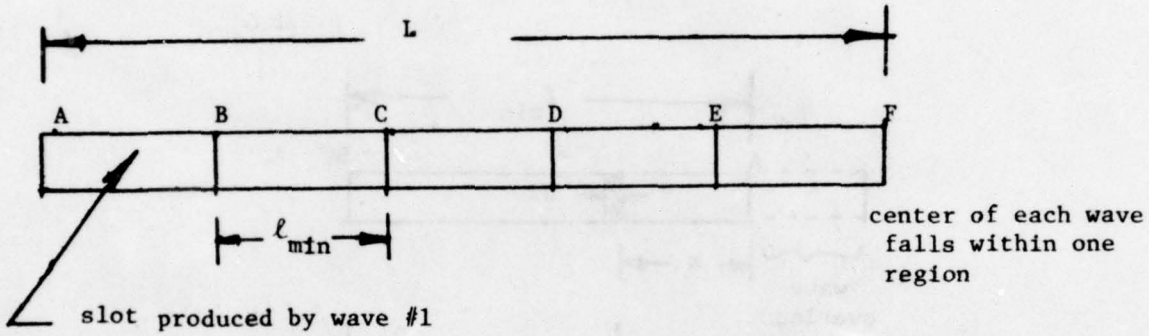

Figure 4.4 Location of Waves Arranged Contiguously to Form a Fracture

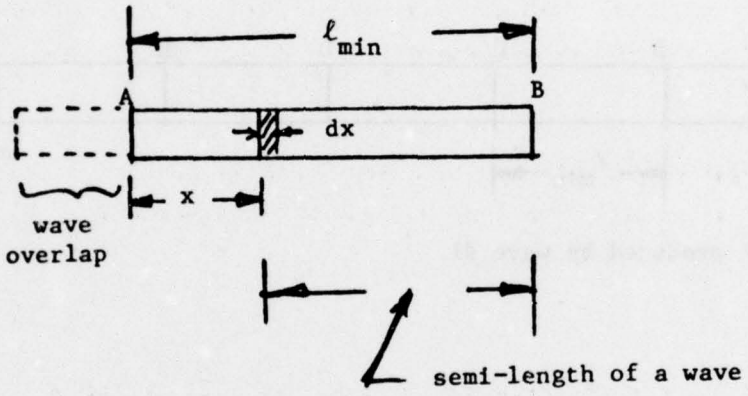

Figure 4.5: Arrangement of a Wave Centered at x from One End of a Region AB

In Equation 4.24,

$$P^* = \text{probability of wave covering completely a typical region AB} = \sqrt{\frac{\pi}{2}}\ \frac{(\text{erf } 2\Gamma - \text{erf } \Gamma)}{\Gamma} \qquad 4.25$$

$$\text{where } \Gamma = \frac{\ell_{min}}{\sqrt{\bar{\ell}^2}} = \frac{L}{N\sqrt{\bar{\ell}^2}} \qquad 4.26$$

Probability that a wave with center within region AB does not cover the region therefore $= (1 - P^*)$

Hence the probability that any one wave occurs within a given region AB but does not cover the region $= \frac{1}{N}(1 - P^*)$.

The total number of ways in which N spaces can be filled with N waves, of which only one does not cover its space $= {}_{N}C_{1}$.

Therefore, the weighted probability that all spaces are occupied except one is given by

$${}_{N}C_{1}\ \frac{(1-P^*)}{N}$$

Similarly the joint weighted probability in which two waves do not occupy their respective spaces simultaneously while the rest of the spaces are occupied is :

$$= {}_{N}C_{2}\ \left[\frac{1}{N}(1-P^*)\right]^2$$

Therefore, the total probability in which N waves can be arranged by taking 1, 2, 3... at a time which will not produce a fracture is:

$$P_{u \not\to f} = \frac{{}_{N}C_{1}\left[\frac{(1-P^*)}{N}\right] + {}_{N}C_{2}\left[\frac{(1-P^*)}{N}\right] + \ldots + {}_{N}C_{N}\left[\frac{(1-P^*)}{N}\right]^N}{{}_{N}C_{1} + {}_{N}C_{2} + {}_{N}C_{3} + \ldots + {}_{N}C_{N}}$$

$$= \frac{\left[1 + \frac{(1-P^*)}{N}\right]^N - 1}{\left(2^N - 1\right)}$$

Hence the probability that there exists a cut by an N wave system is

$$P_{uf} = 1 - P_{u \not\to f} = \left[\frac{2^N - \left\{ 1 + \frac{(1-\bar{P})}{N} \right\}^N}{2^N - 1} \right] \qquad 4.27$$

The result of Equation 4.27 for various values of the ratio $L/\sqrt{\bar{\ell}^2}$ and number of waves N is shown in Table 4.1. The first of the numbers in the table represents the transition probability of fracture P_{uf} and the second number is the characteristic non dimensional time for cut (Equation 4.19). The results given in Table 4.1 are compared later with results obtained by a more precise theory.

Complete One-Dimensional Formulation of the Slick Fracture Problem:

If there are N waves present at any instant of time* within the 1-D oil slick (each with a length of a given probability of occurrence), then these N waves (or slots produced by them) can combine in several ways to result in a complete fracture of the oil slick. The larger the value of N, the larger is the number of ways of combination by which a fracture can be achieved. In fact, the principal difficulty in determining the probability of fracture of the oil slick arises in tabulating the number of wavs in which the slots can combine.

The explanation of the physics of the problem becomes clearer if we consider the case of a two-wave system. In this system, first of all there is the possibility that the length of each of the waves exceeds that of the oil slick, in which case a fracture is achieved by a single wave itself. That is, there are two such possibilities. In addition, there is the case of both waves together forming a cut with possible overlapping lengths.

---

*For the discussion in this section, N takes only integer values.

TABLE 4.1: Transition Probability (P_{uf}) and Dimensionless Time Constant (τ) Obtained from Approximate Analysis. Number of Waves (N) Present in the System and Root Mean Square Length of Waves ($\sqrt{\ell^2}$) are the Parameters.

N	$\frac{L}{\sqrt{\ell^2}}$	1.111	1.25	1.43	1.67	2.0	2.5
1	P_{uf} →	0.092276	0.054778	0.026984	0.009819	0.002075	0.000144
	τ →	10.3290	17.7507	36.5563	101.3414	481.4053	6932.7339
2		0.813335	0.780402	0.740887	0.695942	0.650432	0.610472
		0.5958	0.6596	0.7405	0.8400	0.9514	1.0606
3		0.958427	0.948166	0.934662	0.916395	0.891933	0.860337
		0.3154	0.3379	0.3665	0.4030	0.4494	0.5080
4		0.988458	0.985559	0.981463	0.975453	0.966090	0.952492
		0.2241	0.2360	0.2508	0.2697	0.2955	0.3282
5		0.996362	0.995424	0.994079	0.992064	0.988871	0.983390
		0.1761	0.1856	0.1950	0.2068	0.2223	0.2440
6		0.998746	0.998420	0.997948	0.997232	0.996079	0.994067
		0.1497	0.1550	0.1616	0.1698	0.1805	0.1950
7		0.999541	0.999421	0.999246	0.998980	0.998547	0.997778
		0.1301	0.1342	0.1391	0.1452	0.1530	0.1637
8		0.999825	0.999778	0.999711	0.999609	0.999441	0.999139
		0.1156	0.1188	0.1227	0.1275	0.1335	0.1417
9		0.999931	0.999912	0.999886	0.999845	0.999778	0.999657
		0.1044	0.1070	0.1102	0.1140	0.1189	0.1253
10		0.999972	0.999964	0.999954	0.999937	0.999910	0.999860
		0.0954	0.0976	0.1002	0.1034	0.1074	0.1127

Therefore, the probability of fracture by a two wave system is given by

$$P_2 = 1 - (1-P_1^\circ)^2 \quad (1 - P_2^\circ) \qquad 4.28$$

where

P_2 = probability of fracture with a <u>two</u> wave system ,

P_1° = probability that <u>a</u> single wave <u>alone</u> fractures the slick,

$(1-P_1^\circ)^2$ = probability that <u>neither</u> of the two waves <u>individually</u> cuts the slick, and

P_2° = probability that <u>both</u> waves <u>together</u> fracture the slick (but not individually).

The superscript "o" indicates the condition that <u>all waves</u> present are together necessary to form a fracture.

By a similar reasoning, Equation 4.28 can be extended to a N wave system,

$$P_N = 1 - (1-P_1^\circ)^N \; (1-P_2^\circ)^{\frac{N(N-1)}{2!}} \; (1-P_3^\circ)^{\frac{N(N-1)(N-2)}{3!}} \qquad 4.29$$

or

$$P_N = 1 - \prod_{r=1}^{r=N} \left[(1-P_r^\circ)\right]^{{}^{N}C_r} \qquad 4.30$$

where

P_N = probability of fracture by a N wave system = P_{uf}

$${}^{N}C_r = \frac{N!}{r!(N-r)!} = \text{Number of ways in which "N" things can be arranged, taken "r" at a time, and} \qquad 4.31$$

$\prod$ stands for product of terms.

The major problem in evaluating P_N arises in the evaluation of the various P° terms. In Appendix D, the values of P_1° and P_2° are calculated. Attempts to obtain some form of recurrence relationship to evaluate the various terms have not met with success. However, to obtain a reasonable value for the probability P_N we propose the following approximation to Equation 4.29.

We make the a priori assumption that:

$$P_N^\circ \ll 1 \quad \text{for all } N > 2 \tag{4.32}$$

The physical meaning of this assumption is that the probability of fracture of the slick by all N waves combining, but no fracture with less than N waves, is very small. This is because the achievement of fracture with all N waves participating requires that they be arranged in specific ways and that their lengths be larger than some minimum value. The occurrence of such situations has low probability. Therefore:

$$P_N \simeq 1 - (1-P_1^\circ)^N \, (1-P_2^\circ)^{\frac{N(N-1)}{2}} \tag{4.33}$$

Because of this approximation, the probability of fracture calculated by using Equation 4.33 will be smaller than that resulting from Equation 4.30 (if we knew all P° values). Therefore, the predicted oil breakup time using the result of approximate Equation 4.33 will be longer than that obtained from the results of an exact analysis. Alternatively, using Equation 4.33, the sea state at which an oil slick will be fractured by breaking waves within a specified time will be more severe than the one calculated by using the exact Equation 4.30. To this extent, the approximation does not lead to conservative estimates. The results obtained for a range of parameters by using the Equation 4.33 are given in Table 4.2. These results are discussed later.

Monte Carlo Method of Estimating the Transition Probability of Fracture of an Oil Slick Subjected to Breaking Waves

In this section calculations are performed using the Monte Carlo method to estimate the probability of fracture of a slick at length L subjected to N breaking waves. The method involves generating two random numbers on a computer for each wave. The first random number positions the wave center relative to the midpoint of the slick length. The second random number is utilized in estimating the crest length of the wave occurring. By generating two random numbers and testing whether the waves arrange themselves to form a fracture, the transition probability can be estimated. The random numbers generated are in the numerical range between zero and unity.

Table 4.2 Transition Probability (P_{uf}) and Dimensionless Time Constant (τ) as Functions of Wave Crest Length Parameter ($\sqrt{\overline{\ell^2}}$) and Average Number of Breaking Waves (N) Present in the Slick. (Equation 4.30)

$\frac{L_c}{\sqrt{\overline{\ell^2}}}$		1.1111		1.4706	1.8867	2.0000	2.5000
N							
1	P_{uf}	0.002276	0.054778	0.026984	0.009819	0.002075	0.000144
	τ	10.3298	17.7507	36.5563	101.3414	481.3984	6929.8701
2		0.289356	0.213186	0.139534	0.075602	0.029986	0.006737
		2.9275	4.1708	6.6542	12.7206	32.8467	147.9335
3		0.520163	0.423213	0.308422	0.186357	0.081581	0.019351
		1.3618	1.8173	2.7116	4.8489	11.7507	50.3973
4		0.720565	0.627639	0.494824	0.324791	0.152995	0.038538
		0.7843	1.0123	1.4645	2.5463	6.0223	25.3781
5		0.859651	0.788302	0.664619	0.471789	0.239124	0.063338
		0.5093	0.6441	0.9153	1.5671	3.6592	15.2828
6		0.930203	0.894007	0.797639	0.618294	0.334234	0.093290
		0.3571	0.4456	0.6259	1.0612	2.4581	10.2111
7		0.972286	0.953265	0.889029	0.728961	0.432564	0.127946
		0.2642	0.3264	0.4549	0.7669	1.7648	7.3344
8		0.992681	0.981853	0.944692	0.822272	0.528923	0.166687
		0.2034	0.2494	0.3454	0.5789	1.3255	5.4841
9		0.997096	0.993704	0.974937	0.890122	0.619067	0.208344
		0.1614	0.1968	0.2712	0.4528	1.0361	4.2838
10		0.999512	0.998131	0.989686	0.935953	0.699953	0.253712
		0.1311	0.1592	0.2186	0.3639	0.8307	3.4171
P10		0.002276	0.054778	0.026984	0.009819	0.002075	0.000144
P20		0.137530	0.119547	0.081156	0.057177	0.025947	0.006450

For several such sets of "throws" (each throw is the operation of generating 2N random numbers for an N wave system and testing for fracture), the probability of fracture is simply the ratio of the number of times a fracture is recorded to the number of throws.

With the first random number r_1, we associate a crest length of the wave. We arbitrarily impose the condition that when the value of the random number is zero, the crest length shall be zero; and when the value of r_1 is 1, the crest length shall be infinity. To relate the value of the random number to a wave crest length (X), we use the following formula.†

$$\frac{X}{L} = \frac{\sqrt{\ell^2}}{L} \sqrt{\ell n \frac{1}{(1 - r_1)}} \qquad 4.34$$

Similarly, the second random number r_2 generated is assumed to give the location X_c of the center of the above wave according to the equation

$$\frac{X_c}{L} = r_2, \qquad 4.35$$

where X_c is measured from one end of the slick.

To perceive the effects on the values of transition probability of fracture due to variations in crest length distributions, wave period, and the time for closing of the slot, a parametric study was undertaken. The root mean square length was varied between 0.9 through 0.4 of the slick length $\left(0.4 \leq \frac{\sqrt{\ell^2}}{L} \leq 0.9\right)$, and the ratio of slick closing time to wave time (N) was varied between 1 and 10. [This is also the average number of waves present in the system - see Equation 4.11].

The results obtained by using the Monte Carlo method (indicated in this section) are shown in Table 4.3. The table contains two numbers for each combination of N and $L/\sqrt{\ell^2}$. The first number printed gives the transition probability P_{uf} and the second gives the dimensionless characteristic time (τ) for slick fracture (see Equation 4.19).

---

† This formula is derived on the assumption that the crest lengths are Rayleigh distributed and that r is the cumulative probability associated with a maximum crest length X.

Table 4.3

Transition Probability P_{uf} Obtained From Monte Carlo Method

N ↓	$\frac{L}{\sqrt{\bar{\ell}^2}}$ →	1.1111	1.2500	1.4286	1.6667	2.0000	2.5000
1	P_{uf} →	.0895	.0285	-	-	-	-
	τ →	10.7000	34.6000	-	-	-	-
2		.2985	.1960	.1000	.0505	.0080	-
		2.8200	4.5800	9.4900	19.3000	124.0000	-
3		.5105	.4015	.2745	.1680	.0670	.0140
		1.4000	1.9500	3.1200	5.4400	14.400	70.9000
4		.6750	.5735	.4405	.3215	.1595	.0625
		.8900	1.1700	1.7200	2.5800	5.7600	15.5000
5		.7885	.7190	.5785	.4490	.2680	.1170
		.6440	.7880	1.1600	1.6800	3.2100	8.0400
6		.8695	.8200	.7125	.5830	.3840	.1865
		.4910	.5830	.8020	1.1400	2.0600	4.8400
7		.9180	.8830	.7940	.6760	.4895	.2660
		.4000	.4660	.6330	.8870	1.4900	3.2300
8		.9140	.8840	.8115	.7365	.5850	.3810
		.4080	.4640	.5990	.7500	1.1400	2.0800
9		.9715	.9495	.8885	.8060	.6560	.4500
		.2810	.3350	.4560	.6100	.9370	1.6700
10		.9850	.9685	.9240	.8585	.7250	.5255
		.2380	.2890	.3880	.5110	.7750	1.3400

Note: In generating the numbers in this table 2000 throws were simulated.

This table shows that, as the number of waves N increases for a given root mean square length of waves, the probability of cut increases and the time decreases. Similarly, as the mean square length of waves increases relative to the slick length L, the probability increases.

Results:

Tables 4.1, 4.2, and 4.3 contain results of the transition probability estimated by various methods. The only common feature of the results of these three methods is that the trend in the probability values is similar in each of the tables. However, the similarity between Table 4.1 results (obtained by approximate, analytical analysis) and that of either Table 4.2 or 4.3 ends here. Table 4.1 results give an over-estimate of the transition probability for given conditions. Hence, using Equation 4.27 to estimate the minimum conditions of the sea at which fracture may occur will lead to overly conservative (low sea state) values. The reason for getting such high transition probabilities, even for a two-wave system, can be attributed to the principal assumption about the way in which the wave centers occur in given regions. This may not occur in nature with such high probability.

The results of Table 4.2 and Table 4.3 agree better, at least for low values of $L/\sqrt{\ell^2}$. For example, for N = 10 and in the first column, Table 4.2 indicates a P_{uf} value of 0.995, whereas Table 4.3, for the same conditions, gives a P_{uf} value of 0.985. It has already been mentioned that the results in Table 4.2 are the lower bounds of the transition probability (i.e., actual values would be higher than Table 4.2 values). That Monte Carlo results in Table 4.3 give lower values indicates that a larger number of throws (than the present 2000) should be used. On the other hand, for N = 10 and $L/\sqrt{\ell^2} = 2.5$, Table 4.2 gives 0.2537, whereas Table 4.3 gives $P_{uf} = 0.5255$, the latter of which is a closer value to the correct value.

It can, therefore, be argued that for root mean square length values of the waves, which are not too different from the slick length (L) values, Equation 4.33 adequately describes the transition probability. For length ratios $L/\sqrt{\ell^2}$ larger than 2, use of Equation 4.33 will result in more than 100% error in the predicted transition probability value and correspondingly larger errors in τ. In such cases the only resort is to a Monte Carlo method with a larger number of tries.

Numerical Example

Consider the spill of crude oil of the following quantity and properties:

Spill Volume = 10^6 gallons = 24,000 bbls = $3.785 \times 10^3 m^3$

Density of oil (assumed) = $950\ kg/m^3$

Oil thickness (assumed) = 0.02 m

Diameter of oil slick (with no mass loss)

$$= \sqrt{\frac{4}{\pi} \times \frac{3.785 \times 10^3}{0.02}} = 490 \text{ m}$$

Based on gravity inertia spread theory for instantaneous release the above diameter is reached in about 40 minutes.

Height of breaking waves (assumed) = 3 m

Width of slot opened in oil (assumed) = 3 m

Time for closing up the slot (calculated using the maximum speed of spread of 2 cm thick oil, see Equations 4.9 and 4.10). T_c = 15 seconds

Assumed period of breaking waves T_w = 6 seconds

Assumed root mean square length of breaking wave $\sqrt{\bar{\ell}^2}$ = 200 m

Hence from Equation 4.11, we have:

N = average number of waves present = $\frac{15}{6} = 2.5$;

also

$$\frac{L}{\sqrt{\bar{\ell}^2}} = \frac{500}{200} = 2.5$$

If we refer to Table 4.2, we find that there are no data for N=2.5 Hence we interpolate (for the present purposes a linear interpolation); i.e.,

P_{uf} = transition probability = 0.01319 .

Hence, from Equation 4.19:

$$\tau = \frac{1}{\ell n \left(\frac{1}{1-P_{uf}}\right)} = 75.3$$

---

*This value may be too high. Since no correlation is available relating to the sea state and r.m.s. crest length of breaking waves in the oceans, we retain this value for illustration.

i.e.,

$$t_c = \tau \times T_w = 451.8 \text{ sec} \simeq 8 \text{ min}$$

This indicates that for the above assumed data the slick should be fractured with 63% probability in about 8 minutes, or with higher than 95% probability in 30 minutes.

Using the results obtained from the Monte Carlo simulation (Table 4.3), we get:

$$P_{uf} \simeq 0.007$$

$$\tau \simeq 142$$

i.e.,

$$t_c = 854 \text{ sec} \simeq 15 \text{ min.}$$

The calculations above indicate that there is a high probability that the slick will rupture within about 1 hour after the spill, if subjected to the above kinds of waves.

Discussion:

The model proposed in this section is for one of several ways in which the breaking waves may interact with oil slicks on the ocean. It is not certain whether, indeed, the scenario presented by this model will be duplicated by nature. The crucial assumption that has been made in developing the model is that "slots" are created in the slick by the action of the breakers. Sufficient experimental data do not exist at present either to support or to contradict the assumption. It is, therefore, to be assumed that the model is derived and analyzed to visualize what might happen should indeed the waves interact with the slick as proposed.

The other assumptions made in the model and their effects on the analysis have already been discussed. It suffices to state that the breaking wave field in the ocean has been described in very simple terms. The question of whether the idea of trains of breaking waves is an oversimplification of the actual conditions and, if so, what effect this may have on the predictions of the sea state for slick fracture has not been addressed in this model.

The underlying principle in formulating the slick-breakage problem is that, given a "long time" and exposure of the slick to a sequence of breaking waves, there exists a finite probability of slick fracture. This probability of fracture increases as the time or age increases. In effect, the process of slick fracture is assumed to be a Markov process with probability of transitions from "uncut" to "cut" events. Given this premise, then, the only parameter that describes whether a slick undergoes fracture in "reasonable time" is the characteristic time of the process. The formulation of the problem is aimed at calculating this characteristic transition time.

The model has been formulated for the two-dimensional case, but detailed solutions have been obtained only for the 1-D case. Even for the one-dimensional case the mathematics become extremely tedious and complicated. However, it was felt that solving the 1-D case would give insight into the conditions for break-up of a 2-D slick. The criterion for slick fracture obtained by a 1-D analysis will give a more conservative sea state estimate; that is, the sea state predicted by the 1-D analysis for slick fracture (in the sense of the above model) will be lower than the sea state predicted if the 2-D case had been solved in toto.

The results obtained for the 1-D model are indicated in Tables 4.1 through 4.3. The first table indicates the transition probabilities and the time constant for a range of values of the parameter $L\sqrt{\overline{\ell^2}}$ and for the slick breakage by different number of waves. The values in this table have been obtained by a very simple 1-D approximate model. The calculations indicate that, as the length ratio is nearer to unity, the probability for breakage increases and the time (characteristic) decreases. Needless to say, as the total number of waves (N) contributing to the fracture at any given instant decreases, the probability of fracture increases. However, Table 4.1 shows that high probability values (89% and above) are predicted by this approximate model, even when the number of waves is only three and the length ratio is 2.0. This is rather unlikely. Values in Tables 4.2 and 4.3 have been obtained by more exact formulation and by a Monte Carlo scheme, respectively. They indicate that as the length ratio $L\sqrt{\overline{\ell^2}}$ differs from unity significantly, the transition probability

decreases rapidly. The physical meaning of this is quite clear; it means that the probability of slick fracture by waves whose r.m.s. crest length is considerably less than (i.e., say, 1/2 or less) the slick width is very small. The interpretation of this result is that large oil slicks cannot be fractured by breaking waves whose crest lengths are small compared to the principal dimension of the slick, unless their frequency of occurrence is very high. In the latter case, there will be large number of waves (N) at any given instant within the oil slick and, therefore, slick fracture may result.

Finally, the assumption made regarding the way in which the "slot" in the oil slick will tend to close needs experimental verification. The problem of slot closing during the spreading of the oil slick is an extremely complicated problem to analyze. What we have done is merely an order of magnitude calculation for the time to recombine.

Conclusions:

A model has been proposed for the breakage of an oil slick due to the breaking action of the waves. Several crucial assumptions have been made in the formulation of the model which need experimental verification. The model formulated has been solved for a one-dimensional case only. The results indicate that large slicks cannot be broken up by breaking waves, unless their crest lengths are comparable to the size of the slick or their frequency of occurrence is very high.

In this model no consideration is given to the possible fracture of a slick by the combined action of breaking waves and the oil property variations in the oil slick.

4.2.3 Surface Dispersion of Oil Slicks by Langmuir Circulation

It is a common observation that when oil leaks continuously from a fixed source (such as from, say, a grounded and leaking tanker), an elongated slick develops when wind-driven or surface currents are present. Many times it is observed that in the presence of strong

winds, foam and debris on the ocean align themselves in long streaks parallel to the wind (windrows). It is a common belief that this phenomenon is brought about by the presence of circulations termed "Langmuir circulations," whose axes are aligned in the wind direction.

The Langmuir cells may concentrate oil slicks in longitudinal windrows parallel to the wind. Only in the recent few years has any analysis been made of the Langmuir circulation -- what little is known of these circulations concerns their downwelling speeds beneath lines of convergence. Scott et al. (1969) have performed experiments from which they estimate that the downwelling speed is about 0.85% of the wind speed. If it is assumed that the horizontal speeds of water at the surface are comparable, then an approximate estimate can be made of the thickest slick that can be fractured by Langmuir circulation. Such a calculation is given below.

The model proposed for slick breakage by Langmuir circulations is schematically illustrated in Figure 4.6. Consider an oil slick of uniform thickness subjected to a Langmuir circulation as shown in Figure 4.6. At the position of upwelling the slick is drawn apart by the diverging flow and at the position of the downwelling, the oil either may be carried down or may be thickened by the converging flow. However, because of the thickness variations the oil tends to spread against the water flow (due to the gravitational head). If the thickness is such that the gravitational spread speed (see equation 4.9) is higher than the speed of the diverging surface currents, then the slick will be stable and not break. Using this idea we calculate the critical slick thickness for slick breakage as follows:

(a) Thickness greater than critical

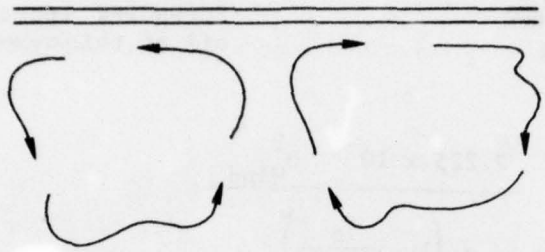

(b) Thickness critical

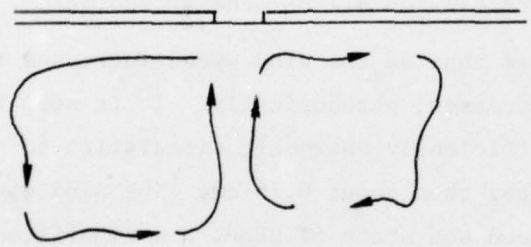

(c) Less than critical; thickness increases until patch attains critical thickness.

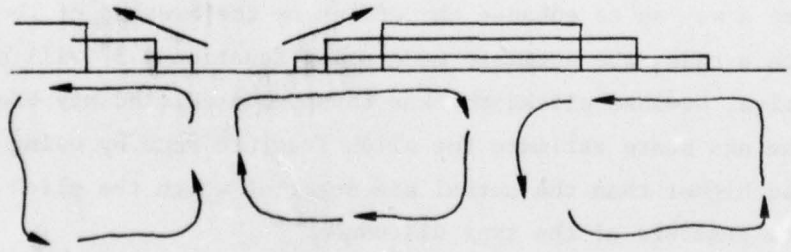

Figure 4.6: Oil slick breakage by wind-generated Langmuir circulations.

$$0.0085\, U_{Wind} = \sqrt{g\, h_c \left(1 - \frac{\rho_o}{\rho_w}\right)} \qquad 4.36$$

Langmuir cell speed generated by wind

Spreading speed oil of thickness h_c

Hence,

$$h_c = \frac{7.225 \times 10^{-5}\ U_{Wind}^2}{g \left(1 - \frac{\rho_o}{\rho_w}\right)} \qquad 4.37$$

Figures 4.6b and 4.6c illustrate schematically what the physical situation may be for critical thickness oil film and hypo-critical thickness when subjected to Langmuir circulation cells. Equation 4.37 is also plotted in Figure 4.7 for oil of density 900 kg/m^3.

Figure 4.7 indicates that as the wind speed increases the critical slick thickness also increases, parabolically. It is seen that a 10 m/s wind will not create sufficiently energetic circulation to fracture slicks of thickness larger than about 0.75 cm. The wind speed corresponds to a fully developed sea state of about 2 m significant wave height. It is recalled, however, that the wave effects were not considered in developing the estimate for the critical oil thickness that will be broken up by Lnagmuir circulation (Equation 4.37). In fact, the combined action of wind-generated Langmuir circulation, wave action, and other perturbations (non-circulating surface current) may all interact in such a way as to enhance the effect on the breakup of the oil slick. In such a case, the estimate made using Equation 4.37 will not be conservative, because slicks thicker than the predicted may break up. That is, the sea state estimate for slick fracture made by using Equation 4.37 will be higher than the actual sea state at which the slick may undergo surface fracture of the type discussed.

The effects of Langmuir circulations, breaking waves, and turbulence in the upper ocean in dispersing the oil vertically into the water column are discussed in the next section.

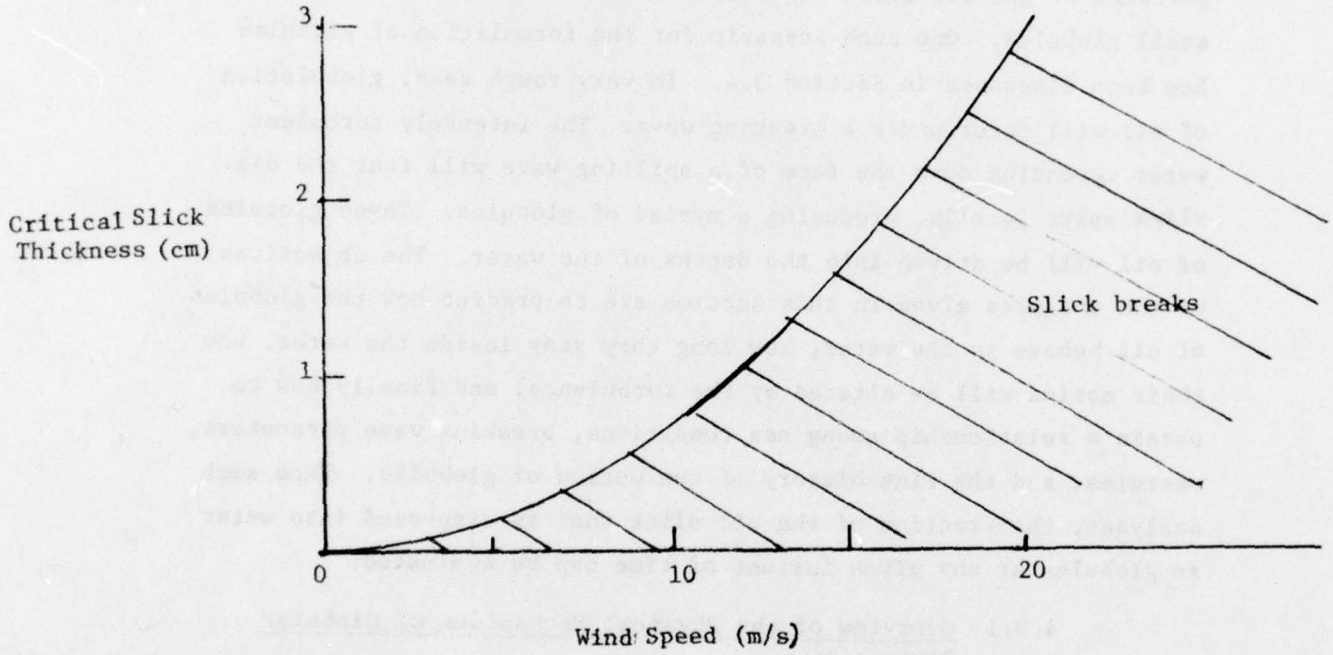

Figure 4.7: Relationship between Critical Thickness and Wind Speed for Fracture of a Slick by Wind-driven Langmuir Circulation

4.3 Depth-wise Dispersion of Oil in the Oceans

In Section 4.2 only the surface fracture and dispersion of oil slicks was considered. In this section the dispersion of oil in the form of globules into the water column is discussed.

Oil floating on an ocean is subjected to several forces, such as the wind, the waves, and water currents. Under suitable conditions, portions of the oil slick may become unstable and break up into small globules. One such scenario for the formulation of globules has been discussed in Section 3.4. In very rough seas, globulation of oil will occur under a breaking wave. The intensely turbulent water cascading down the face of a spilling wave will tear the oil slick apart locally, producing a myriad of globules. These globules of oil will be driven into the depths of the water. The objectives of the analyses given in this section are to predict how the globules of oil behave in the water, how long they stay inside the water, how their motion will be altered by the turbulence, and finally how to obtain a relationship among sea conditions, breaking wave parameters, energies, and the time history of the motion of globules. From such analyses, the fraction of the oil slick that is dispersed into water as globules at any given instant of time can be evaluated.

4.3.1 Overview of the Physical Mechanisms of Globular Dispersion.

Consider the event of a spilling wave occurring within an area of the sea covered by an oil slick. Depending upon the size of the wave and its principal frequency (or alternatively the length of the breaking wave), the wave loses the energy over a certain run, and the white capping ceases after this length. This loss in wave energy will be transferred to the water in the form of turbulent energy, and may also be manifest as mean kinetic energy of water motion. In the presence of oil a part of this wave energy will be utilized in tearing the oil film and producing the globules. It is not known, however, what the size distribution of the globules will be, and how this distribution will depend on the wave parameters, oil, and water properties.

The globules so formed underneath the breaking wave will be imparted a downward kinetic energy by the tumbling action of the water down the face of the wave. Again the fraction of the dissipated wave energy that is utilized in imparting initial motion of the globules of oil is not known and has to be determined by careful experimentation. The globules that are moving downward in water experience different magnitudes of buoyancy, drag, and fluctuating pressure forces depending mainly on their size. Even if one considers a single size of oil globules, each globule experiences a certain deterministic force (due to buoyancy and drag) and a random force due to the turbulence in the water, with the result that not all globules behave identically, even when their sizes are the same. Each globule, whatever its size, ultimately ceases its vertical downward motion (because of the hydrodynamic drag and the upward buoyancy force), stops and rises again, this time being forced up by the buoyancy force. However, the time and the depth at which the direction of motion changes depend on the size and initial downward speed imparted by the breaking wave.

During the entire downward and upward motion of the globules, the turbulence generated by the breaking wave in the water column is nonstationary and in many cases varies with depth. The analysis of the motion of oil globules subjected to the nonstationary, nonhomogenous turbulent fluctuations is extremely complicated.

The variation in globule sizes and their size-dependent motion dynamics, coupled with the effect of turbulence, results in a distribution of oil globules with depth at every instant of time. Because of the inherent randomness of the turbulent velocity fluctuations, one can only speak of the probability of finding a given oil globule at any specified depth at a specified instant of time. For the ensemble of oil globules as a whole (of a given size), one can speak of the number density distribution with depth at a given time.

The globules that are near the water surface may coalesce to form again an oil film. The subsequent globules that arrive at the water surface may be captured by the film or may bounce off the film back into the water column. As of now there does not exist a quantitative estimate for the "capture efficiency" of the films of oil. In our analysis presented in this section it is assumed that all of the globules that arrive at the water surface are captured and the film thickness steadily, therefore, increases.

The mass of oil on the water surface per unit sea area goes from 100% before the occurrence of the breaking wave to 0% immediately after the breaking wave occurs in the given location. Subsequently the mass of oil on the surface per unit area in the same location increases initially slowly from 0% to 100% (rapidly toward the end) when the globules rise up and coalesce to form a film. The turbulence in water tends to increase the time over which this phenomenon takes place.

The analytical models derived in the subsequent sections are based on the above physical picture of the dispersion of oil globules. The first part of the analysis is concerned with the evaluation of the energy dissipated by the breaking waves. Subsequent analyses deal with the dynamics of motion of oil globles under the influence of turbulence, buoyancy, and other forces.

4.3.2 Dynamics of Oil Globules in a Vertical Plane

In this section the motion of globules of oil in quiescent water is discusssed briefly. The results obtained are utilized in sections to follow.

The motion of liquid drops in another liquid, generated by the buoyancy force or weight, is an extremely complicated phenomenon because of the circulation generated in the drop by the motion. In addition, instabilities inherent in the motion result in the path of the drop being zig-zag and most of the time being somewhat helical. A comprehensive analysis of the motion with circulation included is given by Levich (Chapter VIII, 1962). It is contended that for very small drops, or for drops coated with a surface active agent, the drop motion can be represented analytically by the motion of an equivalent solid spherical drop. Since crude oil consists of various components, some of which drastically change the surface chemistry, we assume, for the analysis given below, that the motion of oil drops (irrespective of size) can be described by the motion of an equivalent solid sphere of the same density. Then, for evaluating the terminal velocity of the rise of an oil drop of diameter d, we write;

$$\underbrace{\frac{\pi}{6}\, g\, d^3\, (\rho_w - \rho_o)}_{\text{Upward buoyancy force}} = \underbrace{\frac{1}{2}\, \rho_w\, u_t^2\, C_D\, (\frac{\pi d^2}{4})}_{\text{Resisting drag force}} \qquad 4.38$$

where u_t is the terminal velocity.

The drag coefficient C_D in the above equation is dependent on the Reynolds number $u_t\, d/\nu_w$. C_D is substantially a constant at about 0.5 for spherical particles at Reynolds numbers beyond a value of 100. For Reynolds numbers below 10, C_D value is related by the formula (laminar regime):

$$C_D = \frac{24}{Re_t}\ ; \quad 0 < Re_t < 10 \qquad 4.39$$

where

$$Re_t = \frac{u_t d}{\nu_w} \qquad 4.40$$

The solution of Equation 4.38 is very simple for constant C_D and slightly more complicated when C_D is a function of the speed. In Figure 4.8 the terminal velocity (in the form of dimensionless terminal Reynolds number, Re_t) is plotted as a function of the diameter and density of the drop. Also shown in the figure are the velocities for two specific diameter oil drops of specific gravity 0.9, rising in water.

For example, consider a 1 cm and a 1 mm droplet of oil with specific gravity 0.9 in water of kinematic viscosity $\nu = 10^{-6}\ m^2\ s^{-1}$. The buoyancy terms (abscissa) are 6.12 and 3.12, respectively, corresponding to Reynolds numbers of $10^{3.22}$ and $10^{1.38}$. The terminal velocities are, therefore, $0.166\ m\ s^{-1}$ and $0.024\ m\ s^{-1}$. The smaller droplet's Reynolds number is less than that for which the drag coefficient is essentially constant which makes the use of Figure 4.8 important. For droplets 1-cm in diameter and larger, the drag coefficient is fairly uniform and one may use the expression:

$$u_t \approx \left[\frac{10}{3}\ g\ d\ (1-s)\right]^{1/2} \qquad 4.41$$

where u_t is the terminal velocity and s is the specific gravity of oil relative to water.

It is generally assumed in the literature that if the water itself is in motion (as is the case in the ocean because of wave effects and currents) the oil drops move at terminal velocities relative to the motion of the water in the immediate vicinity of the oil drop. This will be true only if the water itself is not accelerating. In an accelerating flow surrounding the drop, there occurs an additional force on the droplet due to the fluctuations of the pressure gradient from the hydrostatic. Hence, the actual buoyancy force on the drop is given by:

$$\vec{F}_B = -\frac{\pi}{6}\ \rho_o\ d^3\ (\vec{g} - \dot{\vec{v}}) \qquad 4.42$$

---

* The negative sign in Equation 4.42 indicates that force $\vec{F}_B$ is in a direction opposite to that of $\vec{g}$. The velocity $\vec{v}$ is assumed to be positive if it is in the direction of gravity.

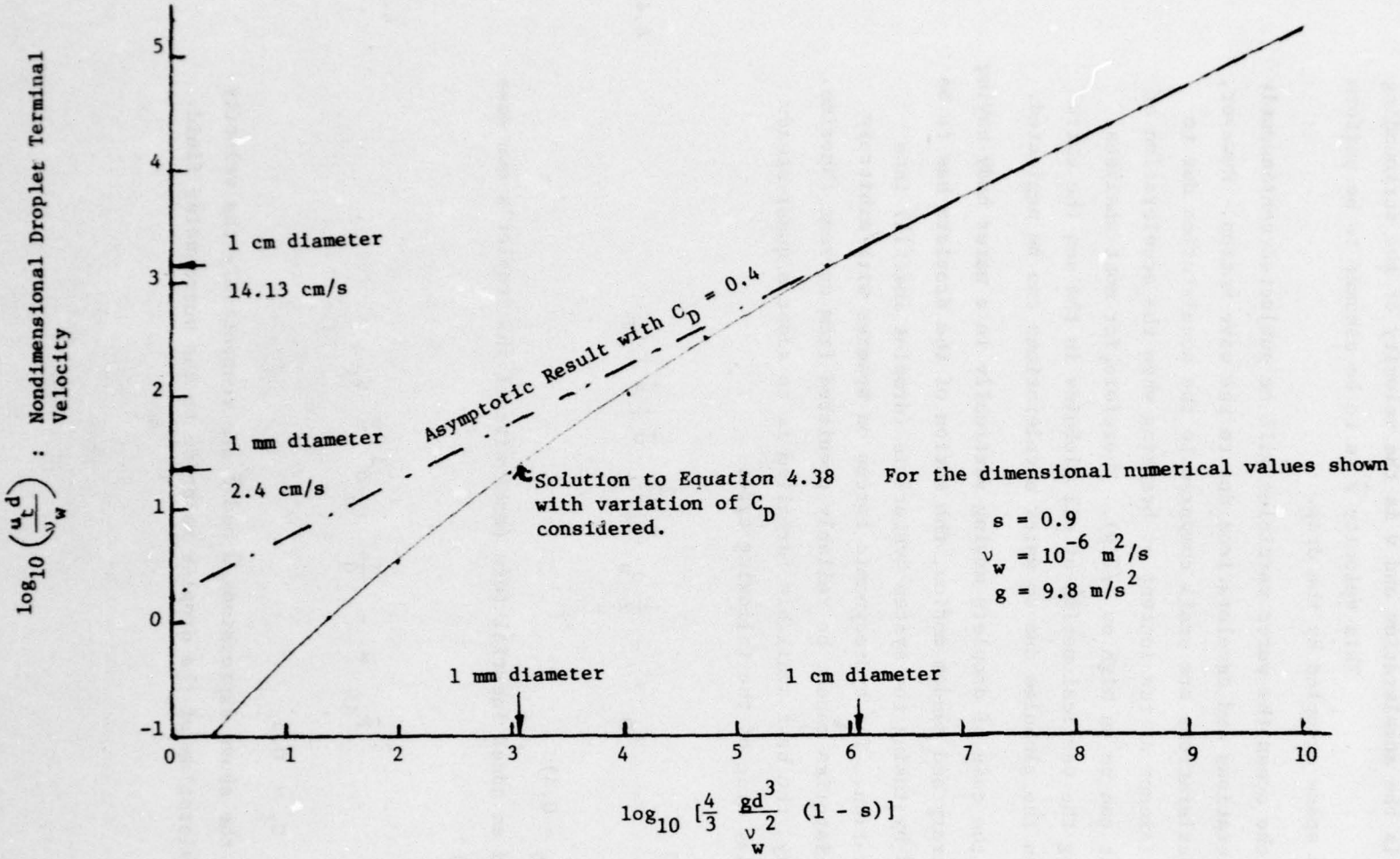

Figure 4.8: Variation of droplet terminal velocity with diameter.

where $\dot{\vec{v}}$ is the acceleration and $\vec{v}$ is the velocity of the surrounding fluid. This velocity $\vec{v}$ is to be assumed to be uniform over the space occupied by the drop.

In the ocean the water particles will be subjected continuously to accelerations and decelerations due to the wave motion. However, these accelerations are small compared to the acceleration due to gravity (except at the instant of breaking when the acceleration at the crest can be as high as 1/2 g). Therefore, for most analyses involving the vertical motion of oil globules in the sea the extra forces on the globules due to water accelerations can be neglected.

In the case of droplets moving vertically in a water body having an arbitrary and random motion, the motion of the droplets has to be analyzed by taking the system hysteresis (droplet inertia) into consideration. The hydrodynamic forces on spheres with arbitrary motion histories cannot be reliably predicted from current theories. Presently, the best available formalism is to adopt a quasi-steady square-law drag of the following type:

$$\vec{F}_D = - \frac{1}{2} \rho_w \left(\frac{\pi d^2}{4}\right) \vec{u} \mid \vec{u} \mid C_D \qquad 4.43$$

(with $C_D \simeq 0.4$)

and an added inertial term (exclusive of the droplet's own mass inertia)

$$\vec{F}_{AI} = - \frac{\pi}{6} \rho_w d^3 \dot{\vec{u}} C_I \qquad 4.44$$

where $C_I \simeq 0.5$.

In the above expressions $\vec{u}$ and $\dot{\vec{u}}$ are respectively the velocity and acceleration of the droplet relative to the surrounding fluid.

The transient motion of the droplets can then be analyzed by writing an equation for the balance of forces involving the inertia, added inertia, buoyancy, weight, and the drag. In Section 4.3.6.1, an analysis is performed using the above ideas to determine the vertical motion of the oil globules.

4.3.3 Vertical Dispersion by Langmuir Circulations

Langmuir circulation cells have been reported to have downwelling speeds of about 0.85% of the wind speed at and below their convergence lines. Such a circulation can pull certain oil droplets below the surface when the downwelling speed is greater than the droplets' terminal velocity. This mechanism will not, however, hold a particle below the surface indefinitely, since the water flow diverges with depth, the oil particles will return to the surface away from the convergence lines. Figure 4.9 illustrates the suggested flow pattern. If the strongest downwelling is assumed to occur at the convergence line, the biggest droplets will be concentrated in this region. Smaller droplets can be swept to greater depths and spread to greater horizontal extent. As particle diameters tend to zero, they will be swept around the cells as if they were water.

Assuming that the downwelling speed is 0.85% of wind speed, we have calculated the size of oil particles that may be swept into the circulating water. This calculation involves equating the water speed to the terminal velocity of the drop. All drops larger than this critical drop size will not be carried down by the downwelling current. Figure 4.10 illustrates the result obtained from such a calculation (the calculation of terminal velocity was treated in the previous Section). The critical size that may be in suspension is plotted as a function of the wind speed. It is seen that even a 20 m/s wind speed ($\simeq$ 40 knots), only 10 mm and smaller diameter oil globules would be carried down. Figure 4.8 shows that the terminal velocity of drops smaller than 1 cm cannot be adequately represented by a constant drag coefficient. The lines shown on Figure 4.10 illustrate this effect. The "exact theory" is the curve obtained by taking the proper value

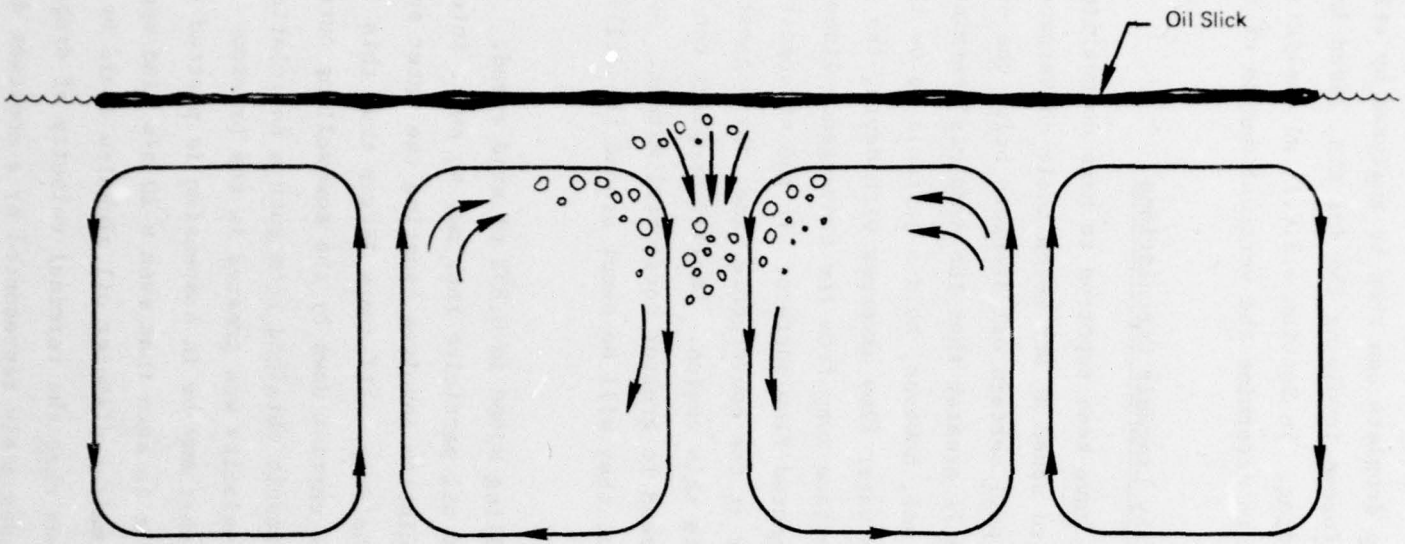

FIGURE 4–9 CROSSWIND SECTION OF LANGMUIR CELLS

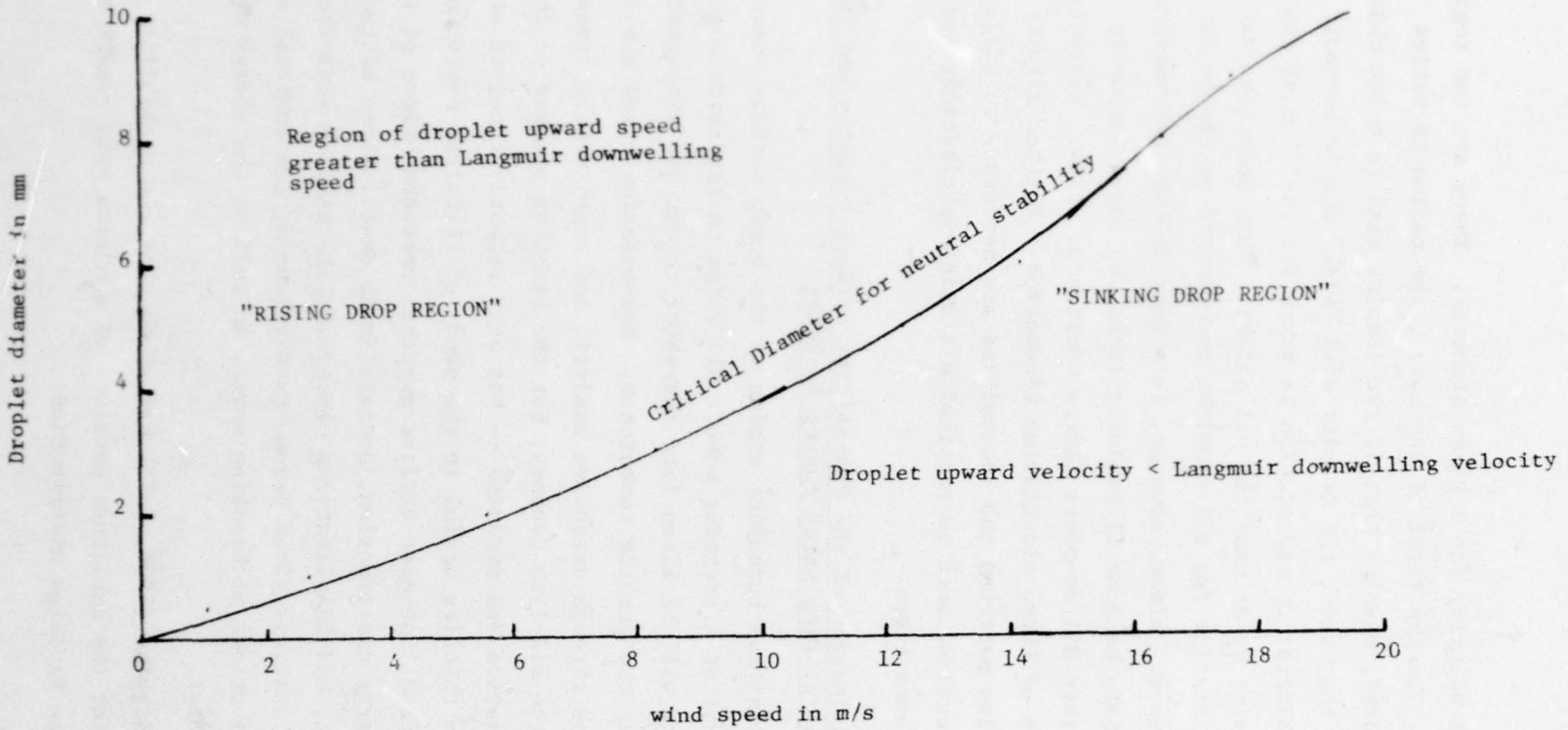

Figure 4.10: Oil droplet diameters affected by Langmuir circulations, as a function of wind speed

of the terminal velocity for a given diameter. There are two regions in Figure 4.10. To the right of the curve, the region is tabled "sinking droplets", meaning that if the droplet size is below that represented by the curve, the droplet will "sink" due to Langmuir circulation. Similar interpretation is given for the "rising droplets" (in that they stay at or near the oil slick). This mechanism may provide an explanation for oil droplets encountered at depths by some investigators. Alone, however, it cannot account for vertically dispersed droplets because it probably lacks the local intensity needed to generate oil droplets from a continuous slick. Regrettably little is known of these circulation kinematics. Further efforts to determine flow patterns and intensities are necessary to yield quantitative results, such as vertical oil mass distributions and particle residence times.

4.3.4 Estimation of the Probability of Wave Breaking and the Energy Dissipated during Breaking

The most intense turbulent mixing at the ocean surface occurs within the crest of a breaking wave. Oil lying on the surface prior to the breaking will be mixed into the water column and dispersed in droplet form by the ensuing turbulence. Non-breaking waves are rather well understood through extensive analytic and experimental research beginning in the mid-19th Century, but the breaking process -- the detailed kinematics and dynamics -- has only recently received attention. To render wave theories useful in the study of turbulent mixing on the ocean surface, one must utilize spectral representations of the ocean wave energy distribution, probabalistic descriptions of the wave elevation, and idealizations concerning the maximum wave steepness. In the analysis given below, predictions of the temporal and spatial distributions of breaking waves, as well as the energy dissipated, are made.

Longuet-Higgins (1956, 1975) has shown that the probability distribution for the amplitude envelope of a narrow band random sea is given by the Rayleigh distribution:

$$p(a) = \frac{a}{\eta^2} \exp\left\{-\frac{a^2}{2\eta^2}\right\} \qquad 4.45$$

Here a is the amplitude of a wave elevation record given by η, so that a sinusoidal wave of frequency ω would be given by

$$\eta(t) = a \sin(\omega t) \qquad 4.46$$

Linear wave theory quite accurately predicts the relation between wave frequency and length. This dispersion relation and related definitions are

$$\omega^2 = g\kappa, \quad \omega = \frac{2\pi}{T}, \quad \lambda = \frac{2\pi}{\kappa} \qquad 4.47$$

For single-frequency plane progressive waves, the limiting wave height is well established as a fraction of the wave length λ. The exact theory of Stokes gives the wave steepness $\delta = 2a\lambda^{-1}$ equal to 0.142. Using linear theory and the same physical criteria (one-half g downward acceleration at the crest), one sees that the steepness increases to $(2\pi)^{-1}$. Recent experimental work on the kinematics of wave breaking in deep water by Van Dorn and Pazan (1975) shows breaking to occur when δ is in the range 0.125 to 0.135. When the height is rapidly growing, they found the wave steepness attained the high end of the above range, whereas slowly varying wave crests broke when the steepness reached the lower limit.

The specification of a limiting maximum wave amplitude requires both a steepness criterion and a wavelength. Selecting a wavelength is rather difficult since the sea is perceived as being random. If one can assume that the randomness is narrow band, however, considerable progress can be made. This assumption is made somewhat less tenuous by the recent work -- ensuing from the JONSWAP experiments (Hasselmann et al., 1973) -- which has shown sea spectra to be narrower

in bandwidth than previously believed. The JONSWAP spectrum is adopted for this study since it has been shown (Hasselmann et al., 1976) to represent both developing and fully developed spectra. The JONSWAP spectrum is given by:

$$S(\omega) = \alpha\, g^2\, \omega^{-5} \exp\left\{-\frac{5}{4}\left(\frac{\omega_m}{\omega}\right)^4 + (\ln \gamma) \exp\left[-\frac{1}{2\sigma^2}\left(\frac{\omega}{\omega_m} - 1\right)^2\right]\right\} \qquad 4.48$$

This form is similar to the more familiar Pierson-Moskowitz spectrum, differing only in the unspecified Phillips' constant α, modal frequency ω_m and "peak enhancement" given by the second term in the exponent. The expected frequency of a zero-mean, narrow band random process ω_o is determined by the average rate of upcrossings of the mean (zero) level. Crandall (1963) gives:

$$\omega_o^2 = \frac{\overline{\dot{\eta}^2}}{\overline{\eta^2}} = \frac{\int_0^\infty \omega^2 S(\omega)\, d\omega}{\int_0^\infty S(\omega)\, d\omega} \qquad 4.49$$

Taking $\gamma = 3.3$, $\sigma = 0.07$ $(\omega \leq \omega_m)$ and $\sigma = 0.09$ $(\omega > \omega_m)$, the expected frequency of the JONSWAP spectrum has been found to be $1.2871\ \omega_m$.

Hasselman et al. (1976) show that the two JONSWAP spectrum parameters closely follow the relation

$$\alpha = 0.032 \left[\frac{\omega_m U}{2\pi g}\right]^{2/3} \qquad 4.50$$

among the energy in the sea state -- linearly proportional to the area under the spectrum and, therefore, to α, the modal frequency,—

the wind speed U (at 10 meters above mean sea level), and the acceleration of gravity. For a fully developed spectrum, the modal frequency is determined such that the wave phase speed roughly equals the wind speed. In developing spectra, the waves travel more slowly (higher frequency) and draw energy more rapidly from the wind to maintain their growth in height and length.

Breaking amplitude a_b is related to the wave length corresponding to the expected wave frequency by the steepness criterion. That is:

$$a_b = (1/2)\,\delta\,\lambda_{expected}$$

Using the relationship between the wavelength and frequency for deep water waves ($\omega^2 = \frac{2\pi g}{\lambda}$) we get:

$$a_b = \pi \delta g \omega_o^2 \qquad 4.51$$

where ω_o is the expected frequency (see equation 4.49).

For comparison, the mean square wave elevation $\overline{\eta^2}$, as calculated from the JONSWAP spectrum, is

$$\overline{\eta^2} = 3.046 \times 10^{-1}\ \alpha\, g^2\, \omega_m^{-4} \qquad 4.52$$

and the breaking amplitude can be expressed as

$$a_b = 1.087\ \pi\ \delta\ \alpha^{-1/2}\ (\overline{\eta^2})^{1/2} \qquad 4.53$$

The probability distribution for the wave elevation η is Gaussian.

$$p(\eta) = \frac{1}{\sqrt{2\pi\ \overline{\eta^2}}}\ \exp\left(-\frac{\eta^2}{\overline{\eta^2}}\right) \qquad 4.54$$

With the approximation of Equation 4.52, one can estimate both the fraction of time wave breaking takes place at a point and the fraction of space occupied by wave breaking. This probability of breaking is: (noting that breaking occurs only when the elevation is positive)

$$P_B = \int_{a_b}^{\infty} \frac{1}{2} p(\eta)\, d\eta = \frac{1}{2}\ \mathrm{erfc}\ [0.7686\ \pi\ \delta\ \alpha^{-1/2}] \qquad 4.55$$

where the argument of the complementary error function is expressed in terms of the steepness limit and Phillips constant. The probability of breaking for typical values of $\delta^2\ \alpha^{-1}$ is shown in Figure 4.11.

The frequency of wave breaking at a point is given by the rate of upcrossings of the level $\eta = a_b$. Crandall (1963) gives this rate for a narrow band Gaussian process as:

$$\nu^{+}_{a_b} = \frac{1}{2\pi}\ \omega_o\ \exp\left[\frac{-0.5909\ \pi^2\ \delta^2}{\alpha}\right] \qquad 4.56$$

The rate of breaking wave events together with the overall probability that a wave is breaking P_B establishes the average length of time during which a wave continues to break. This length of time, made dimensionless with the expected period, $2\pi\ \omega_o^{-1}$, is:

$$\frac{\omega_o\ T_B}{2\pi} = \frac{1}{2}\ \left\{\exp\left(0.5909\ \frac{\pi^2\ \delta^2}{\alpha}\right)\right\}\ erfc\ \left(\frac{0.7686\ \pi\ \delta}{\alpha^{1/2}}\right) \qquad 4.57$$

During the breaking process the crest of the wave will advance a distance equal to a fraction of the expected wavelength. This fraction is the same as the fractional period over which the wave breaks. The expression for the latter is given in equation 4.57. The number of breaking waves (N) per expected wavelength measured along a line in the direction of wave propagation can be estimated with the expected breaking length and probability of breaking P_B. That is:

$$N = e^{-0.5909\ \pi^2\delta^2\alpha^{-1}} \qquad 4.58$$

The above estimates of wave breaking frequency, the time and travel of a wave during breaking, and the spatial distribution of breaking waves are presented graphically in Figure 4.11 as a function of the quantity $\delta^2\ \alpha^{-1}$.

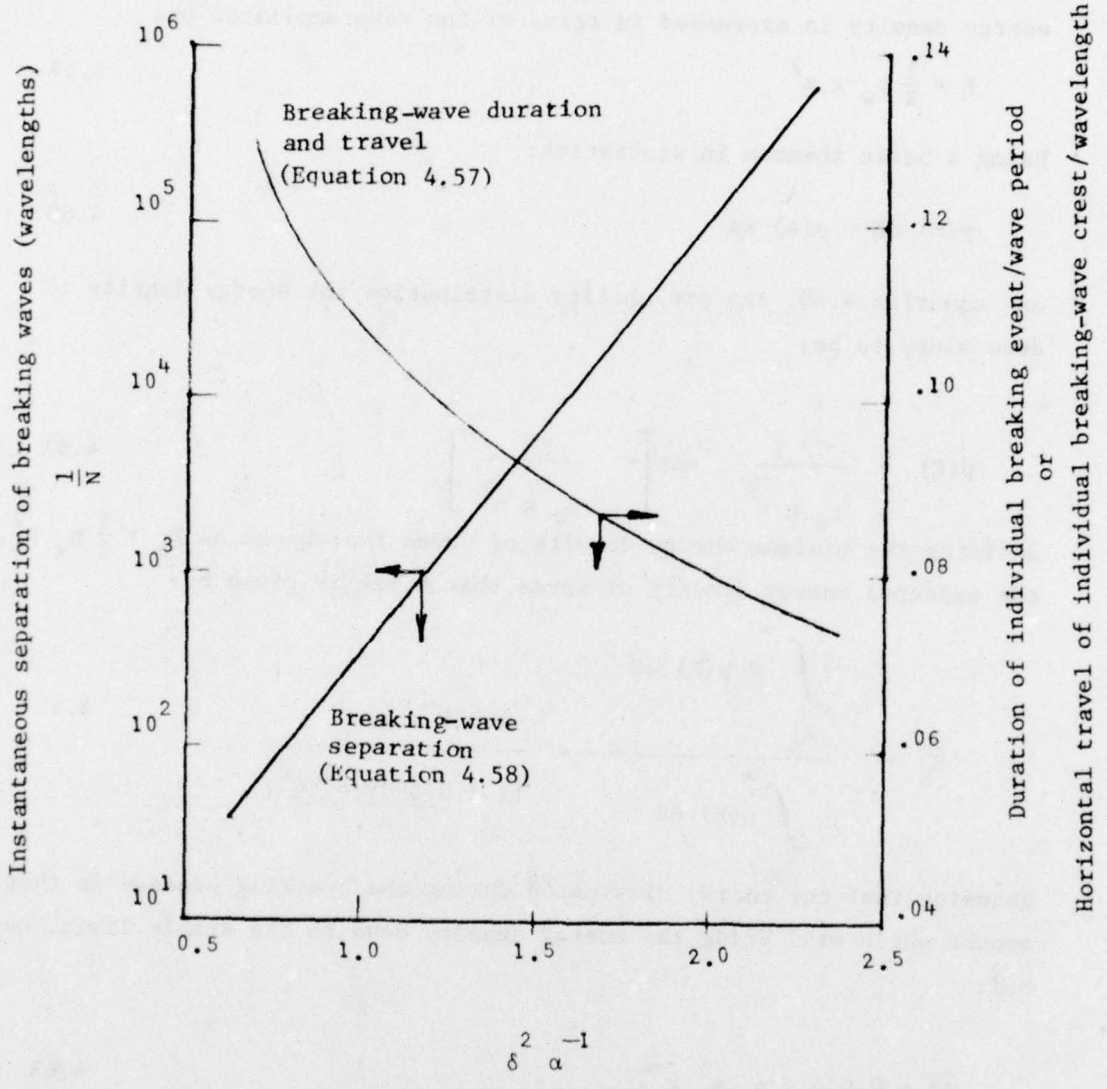

Figure 4.11: The downwind distribution of breaking waves and their characteristic breaking length and time.

The energy dissipated during these breaking events can be estimated from the probability distribution of wave energy density. The energy density is expressed in terms of the wave amplitude by:

$$E = \frac{1}{2} \rho_w \, g \, a^2 \qquad 4.59$$

Using a basic theorem in statistics:

$$p(E) \, dE = p(a) \, da \qquad 4.60$$

and equation 4.45, the probability distribution for energy density is determined to be:

$$p(E) = \frac{1}{\rho_w \, g \, \overline{\eta^2}} \exp\left[- \frac{E}{\rho_w \, g \, \overline{\eta^2}} \right] \qquad 4.61$$

Defining the minimum energy density of waves that break as $E_m = \frac{1}{2} \rho_w \, a_b^2$, the expected energy density of waves that break is given by:

$$\overline{E_b} = \frac{\int_{E_m}^{\infty} E \, p(E) \, dE}{\int_{E_m}^{\infty} p(E) \, dE} = \frac{0.836 \, \alpha \, g \, \rho_w^3}{\left[1 + \frac{0.5909 \, \pi^2 \, \delta^2}{\alpha}\right]} \qquad 4.62$$

Assuming that the energy dissipated during the breaking process is that amount which will bring the energy density down to the stable limit, one has:

$$\overline{\Delta E} = 0.836 \, \alpha \, \rho_w \, g^3 \, \omega_o^{-4} \qquad 4.63$$

The absence of the steepness criterion in this expression presents somewhat of a paradox, since one might expect the average energy density dissipation to increase with increasing maximum wave steepness. However, this is the logical conclusion from the analysis when one assumes that the energy density does not drop below the minimum breaking level.

Van Dorn (1975) indicates that breaking wave energy dissipation may exceed the amount assumed here when wave growth is rapid. The added complexity of a growth rate-dependent energy dissipation expression does not seem warranted in this model.

Predictions from the wave breaking model include an estimate of the mean temporal interval between the spatial separation of breaking waves on a downwind section of ocean surface. The duration of time for these events to occur has been estimated and the corresponding travel distance determined. Finally, the expected energy dissipation per unit area during an entire wave breaking event has been estimated.

All these predictions are based on the JONSWAP wave spectrum, and forecasting techniques derived for this spectrum suffice to provide the inputs to make forecasts with this wave breaking model. Alternatively, the model can be used with direct measurements of the wind speed, the ocean surface variance (to get Phillips' "constant" α), and the expected frequency ω_0 to assess wave breaking on a real time basis.

4.3.4.1 Detailed Wave Breaking

The wave breaking model proposed in the previous section interprets the actual wave breaking event crudely. If a fine mesh could be held horizontally at a height a_b above the mean surface level, wave-breaking would be considered to be happening everywhere the mesh was in contact with the water. We assume here that waves are not affected by the mesh and that the actual breaking does not occur. The "breaking" wave crests protruding beyond the mesh have the appearance of sine wave crests and remain in contact with the mesh for an average period T_B and over an average length L_B. Figure 4.12a illustrates this crude concept of wave breaking.

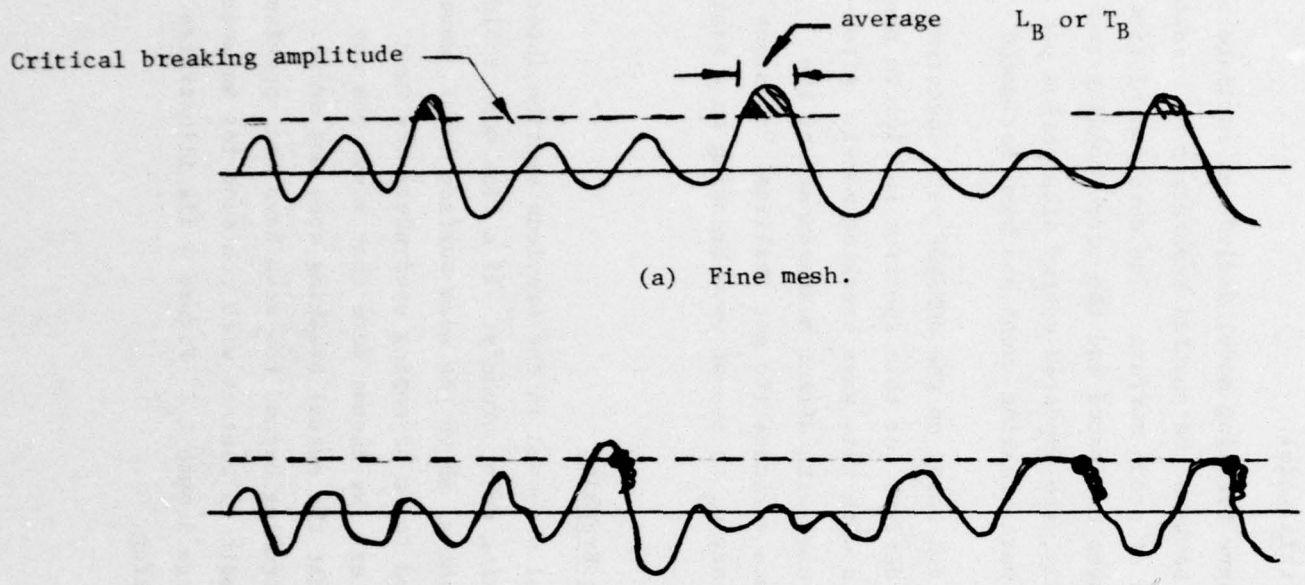

(a) Fine mesh.

(b) Rigid plate

Figure 4.12: Schematic diagram of wave height record showing the critical breaking amplitude and the wave breaking time.

A more realistic picture of breaking is to assume a solid plate at height a_b above the mean as sketched in Figure 4.12b. In this case the wave height is limited and the displaced fluid must be relocated, presumably in front of the wave crest in the form of a white cap. The "breaking" in this case is a disturbance at the point where the whitecap touches the breaking height limit. Although such a model would not affect the time rate of breaking at a point -- which is central to the wave breaking oil droplet dispersion model -- it will alter the interpretation of the spatial extent of breaking, for which one must consider the kinematics of a random wave field.

Figure 4.13 is adapted from Donelan et al. (1972) and illustrates the growth of an individual wave crest. Energy in ocean waves propagates at one-half the speed of the wave crests. A wave can therefore grow by catching up with a slower travelling region of high energy density. In Figure 4.13a, a wave crest is just reaching the breaking height limit. The crest will continue to break between a and partway to b where it has subsided. Notice in b, the deep trough is stable. At the time of c, another crest is at the initial breaking stage.

The concept of high energy regions and wave breaking can be elaborated upon, if one makes certain unproved assumptions concerning the statistics of the envelope and wave elevation functions. Specifically, if one assumes that the rate of upcrossings of the level a_b by the wave elevation is equal to the rate of upcrossings of the magnitude a_b by the amplitude function, a high energy region width (where the envelope function is in excess of the breaking limit) could be determined analogously to the determination of the breaking region of Section 4.3.4. Although this concept of wave breaking at bands of high energy density is supported by field observations and controlled experiments, the assumption concerning the upcrossing rate of the amplitude function is almost certainly in error.

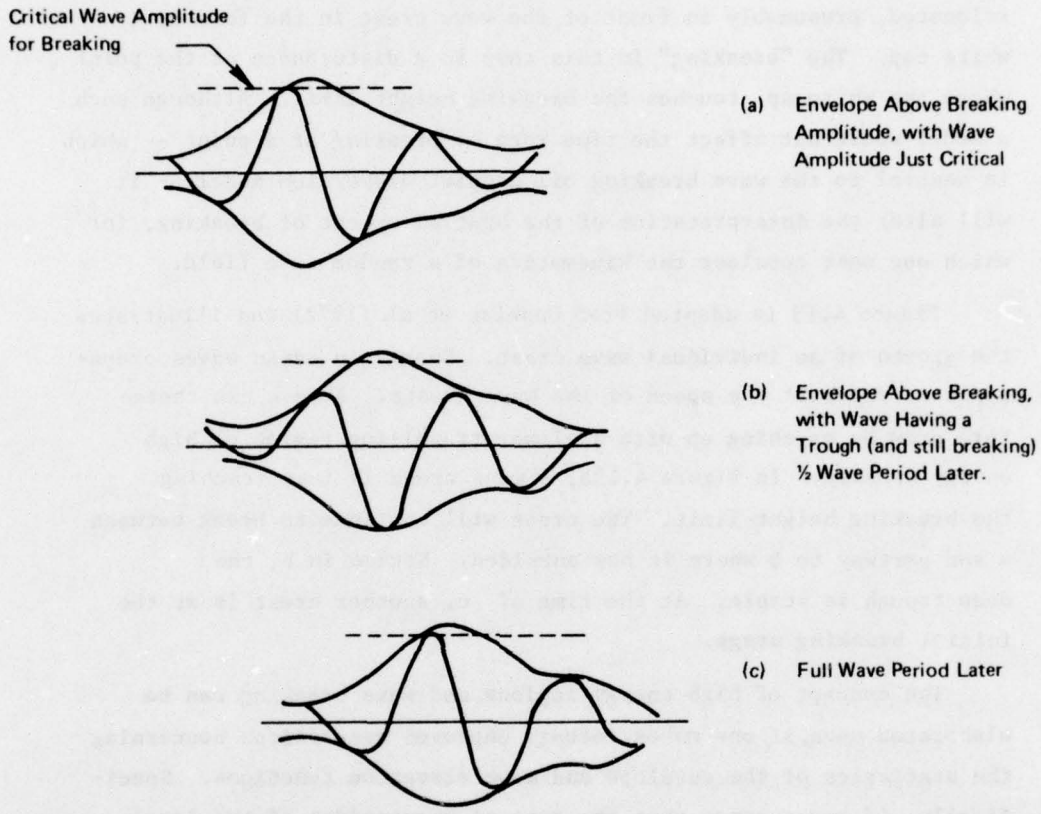

Note: Envelope moves at group speed c_g.

Individual crests move at phase speed c_p.

FIGURE 4–13 ILLUSTRATION OF WAVE BREAKING PHENOMENON WITH INDIVIDUAL WAVES AND WAVE ENVELOPE

Figure 4.14 illustrates what one might expect from such a model if the average width of the energy band were one-quarter wavelength Breaking is assumed to take place at the crest of a wave as it traverses an energy band. Because the relative speed is one-half the phase speed of the crest, the breaking persists over one-half of a wave period. The whole process repeats itself displaced one wavelength in the direction of wave propagation at a frequency equal to half the basic wave frequency.

If the upcrossing rate for the amplitude function can be determined properly, this model could be developed and the details of breaking more fully understood. For the present, however, the estimates from the simpler wave breaking model will be used.

4.3.4.2 A Numerical Example

For fetch limited sea conditions, the JONSWAP spectrum and the wave breaking model readily give the density of breaking waves along a line, the rate of breaking at a point, and the energy density dissipation. In this case the parameters α and ω_m can be expressed in terms of a dimensionless wave age $\xi \equiv Xg/U^2$ (Hasselmann et al., 1976).

$$\alpha = 0.076 \ \xi^{-0.22} \tag{4.64}$$

$$\omega_m = 7 \pi g U^{-1} \ \xi^{-0.33} \tag{4.65}$$

From Equations 4.56, 4.58, and 4.63, the following expressions for fetch limited conditions in deep water can be made:

$$N = \exp (1.2968 \ \xi^{0.22}) \tag{4.66}$$

$$\nu^{+}_{a_b} = 1.2871 \ \frac{g \xi^{-0.33}}{N U} \tag{4.67}$$

$$\overline{\Delta E} = 9.9 \times 10^{-8} \ \rho_w g^{-1} U^4 \xi^{1.1} \tag{4.68}$$

These relations are shown graphically in Figure 4.15.

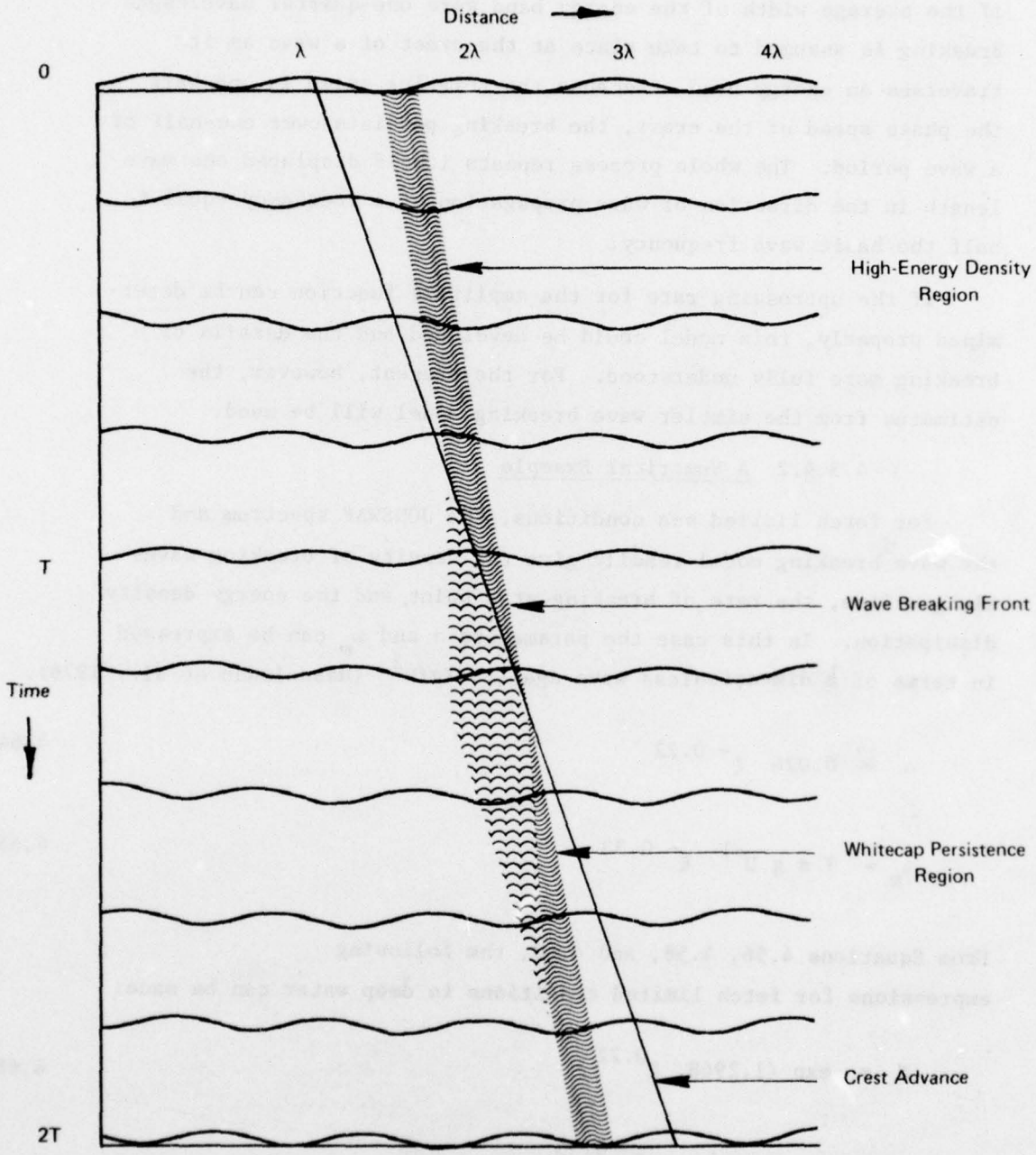

FIGURE 4.14: A POSSIBLE INTERPRETATION OF WAVE BREAKING RELATED TO BANDS OF HIGH ENERGY DENSITY ON THE SEA SURFACE

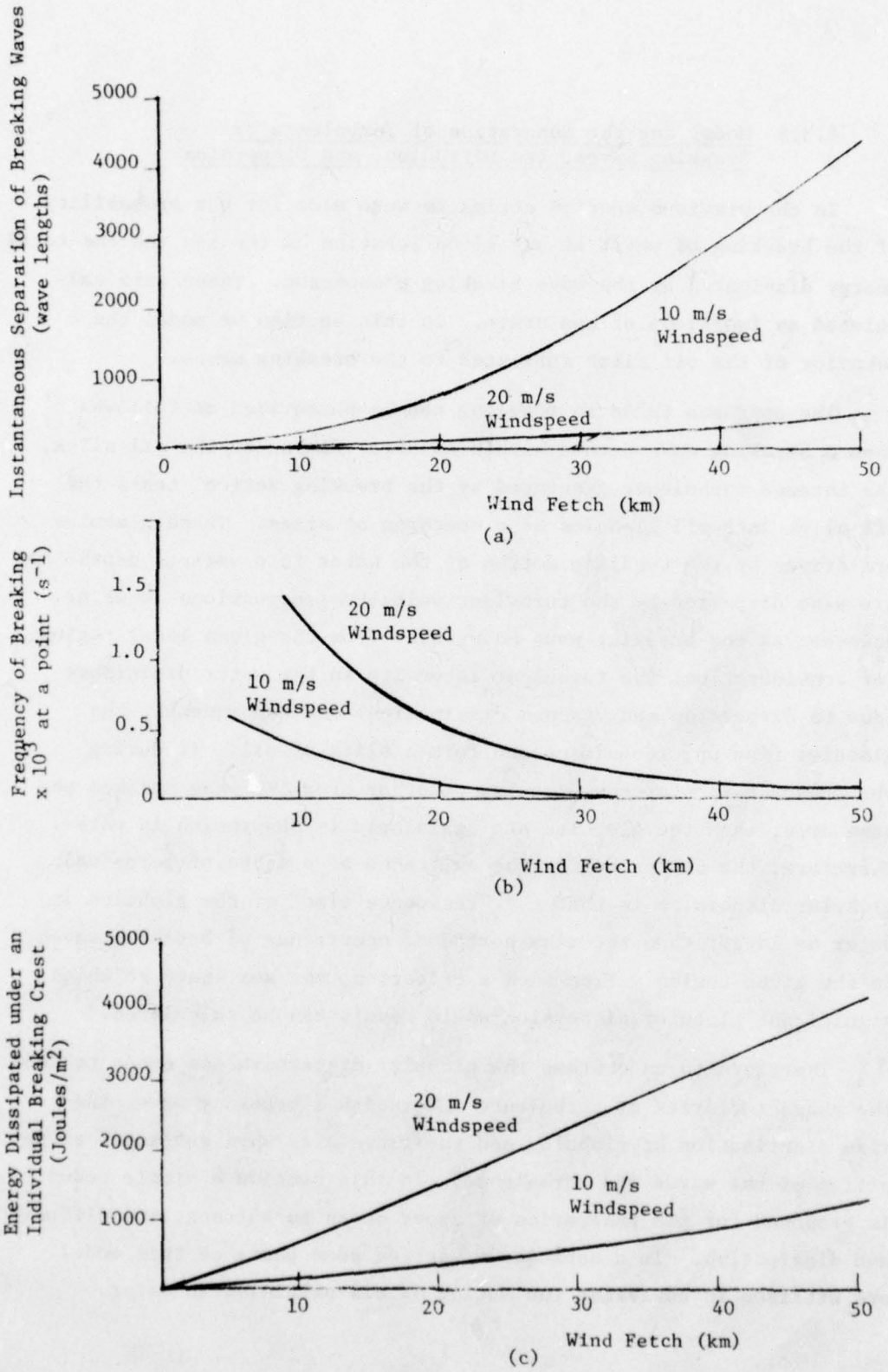

Figure 4.15: Predictions of breaking wave separation, frequency and energy dissipation under fetch limited conditions

4.3.5 Model for the Generation of Turbulence by Breaking Waves, Its Diffusion, and Dispersion

In the previous section estimates were made for the probability of the breaking of waves at any given location on the sea and the total energy dissipated by the wave breaking phenomenon. These were calculated as functions of sea state. In this section we model the behavior of the oil slick subjected to the breaking waves.

The approach taken in modeling can be summarized as follows: When a breaking wave occurs within an area covered by the oil slick, the intense turbulence generated by the breaking action tears the oil slick into oil globules of a spectrum of sizes. These globules are driven by the tumbling motion of the water into various depths and are also dispersed by the turbulent velocity fluctuations in water. However, as the breaking wave moves away from the given local region (of consideration), the turbulent intensity in the water diminishes (due to dispersion and viscous dissipation) and consequently the globules rise up, recoalesce, and form a slick of oil. If during the upward motion of the globules, another breaking wave strikes the same area, then the globules are again held in suspension in water. Therefore, the criterion for the existence of a state of perpetual globular dispersion is that the "residence time" of the globules in water be larger than the mean period of occurrence of breaking waves in the given region. From such a criterion, the sea state at which significant globular dispersion would result can be calculated.

Therefore, to understand the globular dispersion one needs to know the characteristics of turbulence underneath a breaking wave, the size distribution of globules, and their dynamics when subjected to the action of the waves and turbulence. In this section a simple model is proposed for the generation of upper ocean turbulence, its diffusion, and dissipation. In a subsequent section some parts of this model are utilized in analyzing the motion of oil particles in water.

Upper Ocean Turbulence Model -- Physical Concepts

It is not known at the present time whether the turbulence generated in water by the breaking of a wave is small-scale or whether the scale of largest eddies are of comparable magnitude to the wave height (or wavelength). In the absence of such definitive measured results, we postulate that the turbulence is essentially one of small scale (since it is generated by the tumbling action of water).

Because of the nature of wave motion in preferred directions and the effects of the wind, it is highly unlikely that the turbulence in water close to the surface will be isotropic. The physical concepts upon which a turbulence model is proposed for the upper ocean turbulence are schematically illustrated in Figure 4.16a. A breaking wave is moving from left to right and dissipates excess wave energy over a length L. This energy manifests itself as turbulent velocity fluctuations in water. In this model we assume that turbulence is isotropic. Then the mean square velocity fluctuations (intensity of turbulence at the water surface) vary with distance from the crest, as shown qualitatively in Figure 4.16b. The decrease in the surface intensity is due to both diffusion of turbulence and its dissipation. The depth-wise variation is also shown qualitatively in Figure 4.16c.

Assumptions

In developing the turbulence model given below, we make the following assumptions. (It is recognized that all of these assumptions have to be verified experimentally.):

1. Energy dissipation by the breaking wave is at a uniform rate over the length of persistence of the breaking action.
2. All of the energy lost by the wave manifests itself as turbulent kinetic energy.
3. Drift currents in water, generated by the waves, are small and are neglected.
4. Lateral and longitudinal dispersion of turbulence is small compared to the depth-wise diffusion.
5. Presence of the oil does not change the characteristics of turbulence.

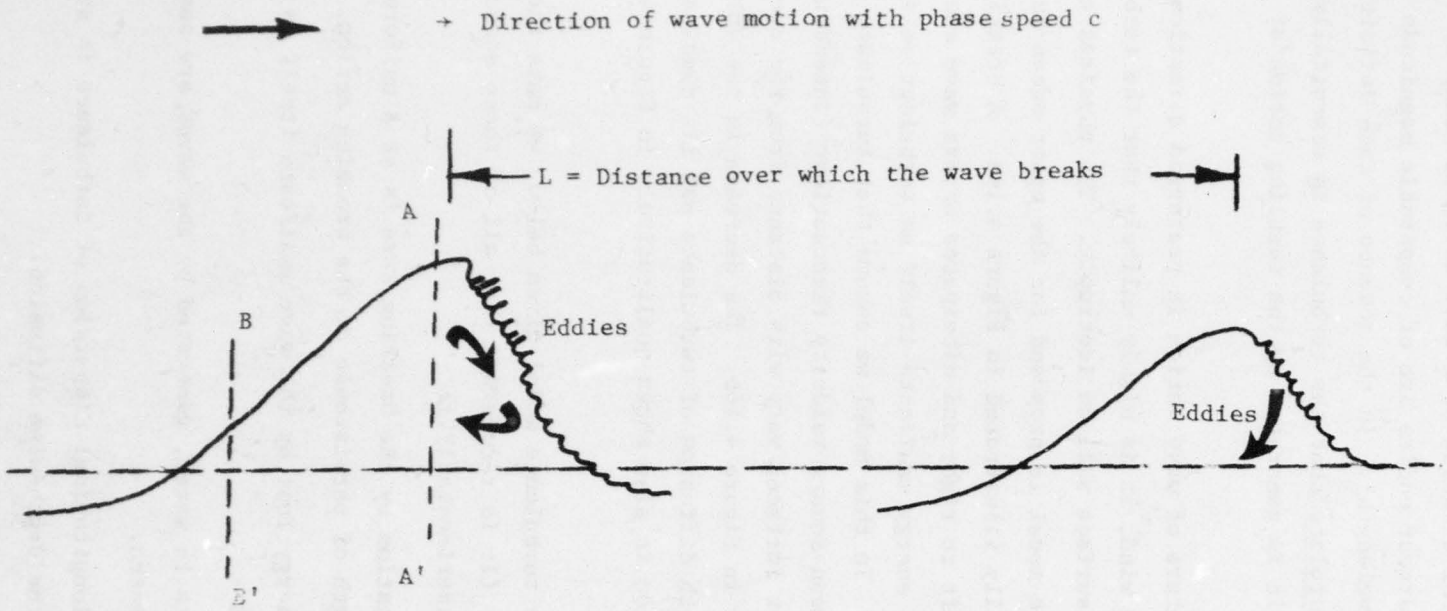

Figure 4.16a Generation of turbulence by a spilling breaker

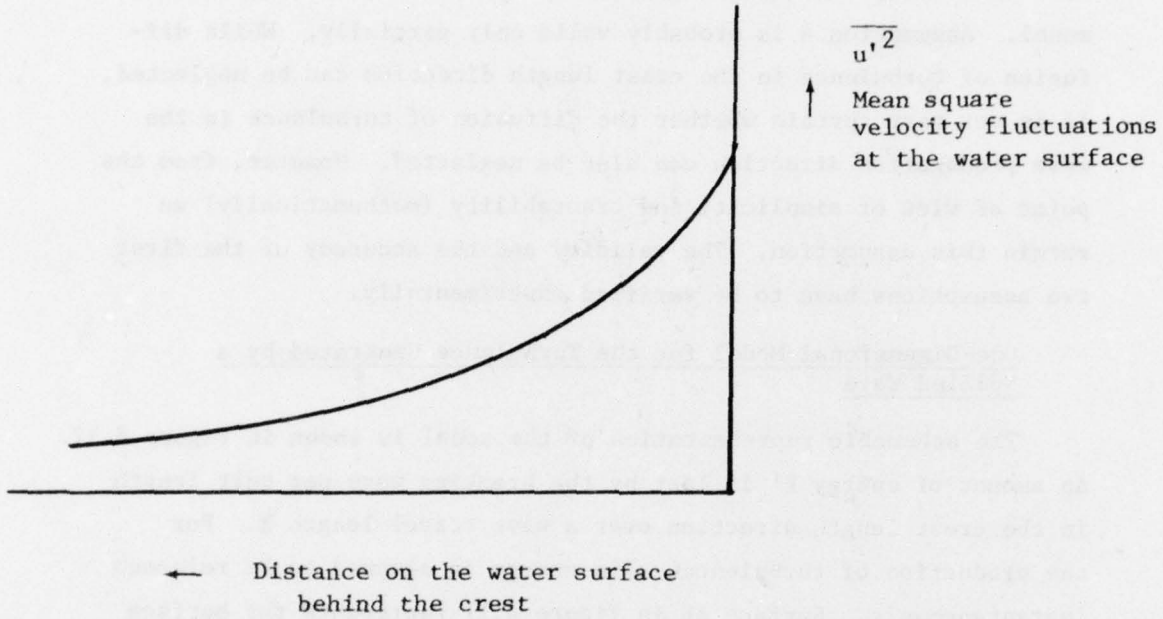

Figure 4.16b: Schematic representation of the variation of intensity of turbulence on the water surface.

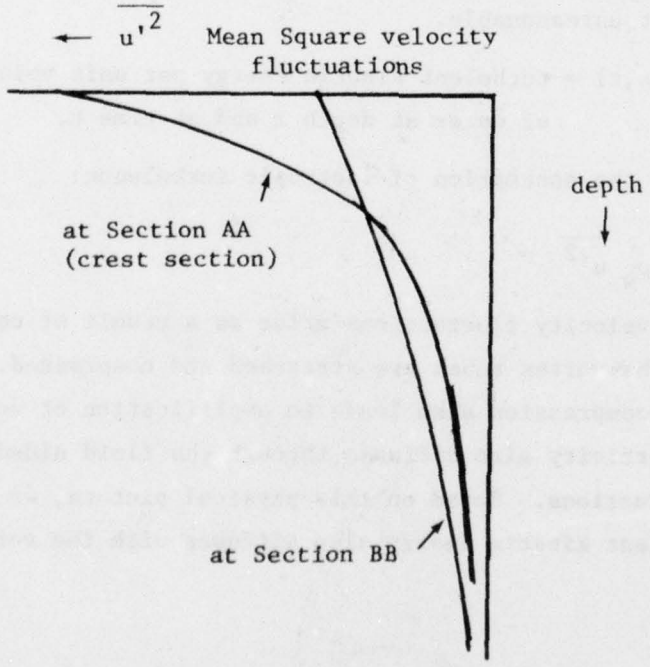

Figure 4.16c: Variation of turbulent intensity with depth

In effect, the turbulence model proposed is a one-dimensional model. Assumption 4 is probably valid only partially. While diffusion of turbulence in the crest length direction can be neglected, it is not very certain whether the diffusion of turbulence in the wave propagation direction can also be neglected. However, from the point of view of simplicity and tractability (mathematically) we retain this assumption. The validity and the accuracy of the first two assumptions have to be verified experimentally.

One-Dimensional Model for the Turbulence Generated by a Spilled Wave

The schematic representation of the model is shown in Figure 4.17. An amount of energy E' is lost by the breaking wave per unit length in the crest length direction over a wave travel length L. For the production of turbulence, this energy is assumed to be released instantaneously. Surface AB in Figure 4.17 represents the surface of undisturbed water and the direction z is the direction of the normal to the surface. Because the wave steepness is seldom larger than 1:10, the assumption that z direction also represents the depth-wise direction is not unreasonable.

Let $e \equiv e(z,t)$ = turbulent kinetic energy per unit volume of water at depth z and at time t.

Because of the assumption of isotropic turbulence:

$$e = (3/2)\ \rho_w\ \overline{u'^2} \qquad 4.69$$

Turbulent velocity fluctuations arise as a result of complex ways in which the vortex tubes are stretched and compressed. This stretching and compression also leads to amplification of vorticity. In addition, vorticity also diffuses through the fluid aided by the turbulent fluctuations. Based on this physical picture, we assume that the turbulent kinetic energy also diffuses with the vorticity.

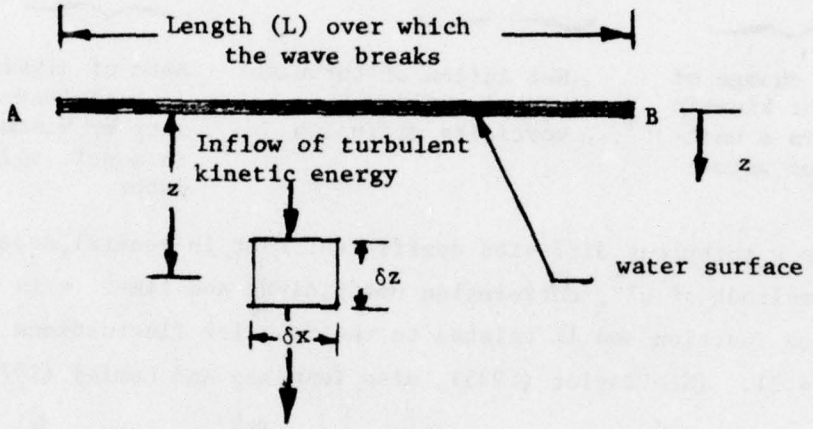

Figure 4.17: Schematic diagram illustrating the one-dimensional model for the generation, diffusion and dissipation of turbulence in the upper ocean.

We now write a kinetic energy balance on an elemental volume of water (Figure 4.17) as follows:

$$\frac{\partial e}{\partial t} = \frac{\partial}{\partial z}\left(D \frac{\partial e}{\partial z}\right) - \varepsilon \qquad 4.70$$

Rate of change of turbulent kinetic energy in a unit volume of water

Net inflow of turbulent kinetic energy by vorticity diffusion

Rate of dissipation of turbulence intensity by viscous friction in a unit volume of water

where D is a turbulent diffusion coefficient that, in general, depends on the magnitude of $\overline{u'^2}$, correlation coefficient and time. ε is the dissipation function and is related to the velocity fluctuations by Equation 4.71. (See Taylor (1935), also Tennekes and Lumley (1974), p. 67.)

$$\varepsilon = 15\, \mu_w \frac{\overline{u'^2}}{\lambda^2} = 10\, \nu_w \frac{e}{\lambda^2} \qquad 4.71$$

where λ is the Taylor microscale of turbulence. It is a measure of the distance over which turbulent velocities are correlated. It is not certain whether λ remains a constant during the production, diffusion and dissipation of ocean turbulence by breaking waves. Since it is possible that the correlation coefficient may vary not only with depth, but also with time, it is entirely possible that λ is also a function (at present unknown) of depth and time. Taylor (1935) makes the argument that in geometrically similar flows the dissipation function ε is directly proportional to $(\overline{u'^2})^{3/2}$. Based on this argument, it is seen that λ is inversely proportional to $(\overline{u'^2})^{1/4}$.

While noting all of the above possibilities, lack of experimental data requires one to make assumptions in developing any model. The constraints we have imposed are that the mathematics be tractable, while at the same time retaining the essential physics. One such simplified model is based on the assumption of a constant diffusion coefficient

and constant decay time (i.e., constant λ). This is given below:

With D = constant, and

λ = constant,

Equation 4.70 reduces to (substituting Equations 4.69 and 4.71):

$$\frac{\partial}{\partial t}\ \overline{u'^2} = D\ \frac{\partial^2}{\partial z^2}\ \overline{u'^2} - \frac{10\ \nu_w}{\lambda^2}\ \overline{u'^2} \qquad 4.72$$

or

$$\frac{\partial e}{\partial t} = D\ \frac{\partial^2 e}{\partial z^2} - \frac{10\ \nu_w}{\lambda^2}\ e \qquad 4.73$$

This equation has to be solved with initial conditions:

$$e(0,z) = 0 \quad \text{for } 0 \le z \le \infty$$
$$e(0,0) = \text{a delta function} \qquad 4.74$$

and boundary condition

$$e(t, \infty) = 0 \text{ for } 0 \le t \le \infty$$

Also the global energy conservation equation is written as

$$E'' = \int_{z=0}^{\infty} e(t,z)\ dz + \int_{t=0}^{t} dt \int_{z=0}^{\infty} \varepsilon\ dz \qquad 4.75$$

total energy per unit nominal sea surface area released instantaneously by the breaking wave	=	total turbulent kinetic energy in the water at any instant t	+	total energy dissipated over the entire field during the time interval between 0 and t.

The solution to Equation 4.73 with constraints 4.74 and 4.75 is given by (Carslaw and Jaeger, 19, page 259, Equation 4):

$$e(t,z) = \frac{3}{2}\rho_w \overline{u'^2} = \frac{E''}{\sqrt{\pi\, Dt}} \exp\left(-\left[\frac{z^2}{4Dt} + \frac{10\,\nu_w\, t}{\lambda^2}\right]\right) \qquad 4.76$$

or with $$t_d = \frac{\lambda^2}{10\,\nu_w} = \text{characteristic viscous dissipation time} \qquad 4.77$$

$$e(t,z) = \frac{E''}{\sqrt{\pi\, Dt}} \exp\left(-\left[\frac{z^2}{4Dt} + \frac{t}{t_d}\right]\right) \qquad 4.78$$

The above solution indicates that the intensity of turbulence is always a maximum at the water surface and varies in a Gaussian way with depth. The magnitude of the maximum intensity (at the surface), however, decreases rapidly with time (faster than at an exponential rate).

If a given location of the sea is subjected to a train of breaking waves of mean period T, then it can be shown (see Appendix E) that the time averaged (over the wave period) kinetic energy of turbulence is given by

$$\bar{e}(z) = \left[\frac{3}{2}\rho_w \overline{u'^2}\right] = \frac{t_d}{T}\,\frac{E''}{\sqrt{Dt_d}} \exp\left(-\frac{z}{\sqrt{Dt_d}}\right) \qquad 4.79$$

Average Over T

Kinetic energy of turbulence per unit volume of water, averaged over a breaking wave period T.

The above value can be construed as a steady-state value of the intensity of turbulence generated in the ocean by breaking waves.

Discussion:

Probably the most important assumption made in developing the model is that the breaking wave-generated turbulence can be characterized by small scales; that is, no large eddies are present. We also assume the diffusion coefficient to be a constant and that the dissipation rate is directly proportional to the intensity of turbulence. Probably a more realistic assumption would have been to make the diffusion coefficient directly proportional to the intensity of turbulence and the dissipation rate proportional to the 3/2 power of the intensity squared [as has been suggested by Taylor (1935)]. These, however, would make the problem highly nonlinear and no known analytical solutions are available. We have also neglected the effects of the energy associated with work done by fluctuating pressure forces and any possible convective terms. Since a high degree of complication is not warranted at the present time, especially in light of the fact that no data exist to compare with the results of any theoretical turbulence model, we have obtained a solution to a much simplified problem which, at least in principle, indicates the nature of the variation of turbulence intensity. It is our contention that, even though the turbulence model is an oversimplification of the realities, its analytical solution affords a guidance for performing appropriate experiments to discern the nature of turbulence generated by ocean wave breaking. Some of these experiments are discussed later in the section on recommendations.

The model proposed indicates that the intensity of turbulence is infinite at zero time. However, in a physical world this does not occur, and therefore, the early time solution should be construed as being approximate. It is also seen that the maximum intensity value

decreases exponentially with time. In fact it may be argued that, if the depth of penetration of the small-scale turbulence is small (neglecting for the moment the presence of any large-scale eddies), then a reasonable representation of the turbulent intensity everywhere underneath the breaking wave may be

$$\overline{u'^2}\,(t) = \overline{u'^2_0} \quad \exp\left(-\frac{t}{t_d}\right) \qquad 4.80$$

where $\overline{u'^2_0}$ is a mean intensity generated initially by the wave breaking and is a function of the energy dissipated (E") by the breaking wave. $\overline{u'^2_0}$ and its relationship to E" and the value of the characteristic dissipation time t_a have to be determined experimentally. The motion of oil globules subjected to the above type of turbulent intensity is discussed in Section 4.3.5.

The steady-state estimate for the turbulent intensity when breaking waves occur repeatedly at intervals of period T is given in Equation 4.79. It is seen that this "d.c." value of the intensity decreases exponentially with depth and, as can be expected, the magnitude at any depth depends on the ratio of the dissipation time scale (t_d) to the wave period T. If the waves occur at a location fairly infrequently (T large), most of the turbulent energy is dissipated before another wave breaks over the same location, with the result the average intensity of turbulence over a wave period is very low. This formula is useful in designing an experiment using a wave tank, for measuring both the dissipation time scale t_d and the diffusion coefficient D. By measuring the time-averaged turbulent intensity at three locations (at least) depthwise in a wave tank wherein wave breaking is induced at regular intervals, values of E", D, and t_d can be measured and extrapolated to the real sea conditions.

In the next section, models are developed for the dynamics of motion and the statistics of oil globules subjected to the breaking waves and the turbulence generated by breaking. The turbulence model developed in this section is utilized.

4.3.6 Motion of the Oil Globules in Water Due to Wave Breaking and Turbulence

The action of the breaking of a wave in the midst of an oil slick is bound to produce two effects. The first one will be the tearing of the slick and formation of globules of oil of various diameters and is caused by the cascading water flow just ahead of the wave crest. The second effect is the vertical dispersion of the oil globules that are formed. The energy lost by the wave in the process of breaking is partitioned many ways. A large fraction of this energy probably manifests itself as upper ocean turbulence, the remainder being partitioned among the nonlinear energy feed to other waves, noise, and the kinetic energy of oil globules. At the present time, there are no quantitative estimates (either by experiment or by theory) that are available for the fractions of wave energy that end up in different modes.

From the point of view of vertical dispersion of oil in the water column, the factors of interest are the initial kinetic energy imparted to the oil globules by the breaking wave and the energy fed to the turbulence. The former results in the penetration of the globules into the water, and the latter (turbulence) disperses the globules vertically. The result of the combined action of initial downward motion and the dispersion by turbulence is that, at every instant of time, there exists a distribution of oil globules as a function of depth. This distribution changes both its shape and the location of its mean. A schematic representation of the events following the occurrence of a breaking wave is illustrated in Figure 4.18.

The downward motion of the globules will be resisted by the hydrodynamic drag due to the motion and the buoyancy force. Because of these two resisting effects, the downward motion of the globules ceases after some time and the globules are accelerated upward by the buoyancy force. The upward motion of the particles, in general, will be at their respective terminal velocities in the absence of a turbulent field. The globules that rise up to the surface may recoalesce to form an oil slick.

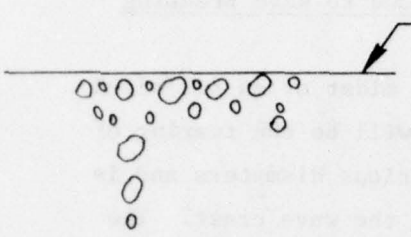

Figure 4–18a Oil globules of all sizes at positions close to the water surface immediately after the occurrence of a breaking wave

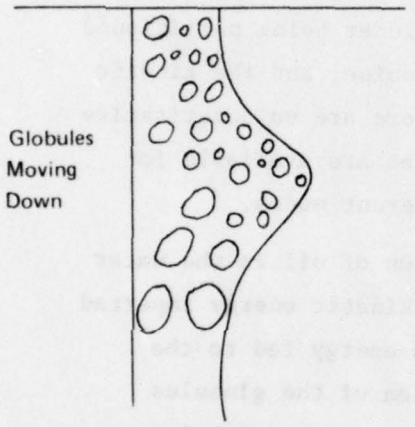

Figure 4–18b Segregation of globules during the downward motion due to the differences in sizes; also the distribution due to turbulence

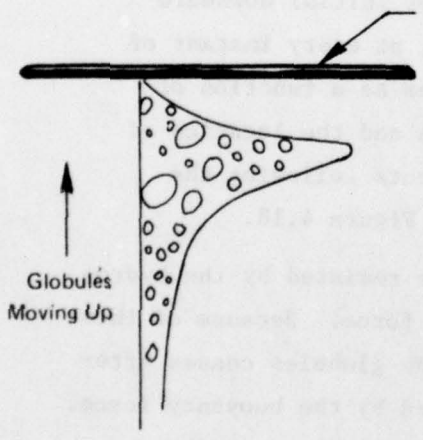

Figure 4–18c Distribution of globules during the upward motion; distribution is the result of turbulent fluctuations in water and due to differences in size

FIGURE 4–18 SCHEMATIC REPRESENTATION OF THE BEHAVIOR OF OIL GLOBULES SUBJECTED TO A BREAKING WAVE

In this physical model of oil globules of a spectrum of sizes, moving initially downward, are considered. The globules, at the same time, are dispersed by the nonstationary and nonhomogeneous turbulence. These globules rise up to reform an oil slick. The parameters of importance that need to be calculated are (i) the maximum depth of penetration, (ii) the dispersion by turbulence, and (iii) the mass of oil (in the form of globules) present in the water as a function of time.

The modeling of the motion of the oil globules in water is performed in two parts. In the first part the deterministic motion of oil particles of a given diameter projected vertically into water with an initial velocity is analyzed. This motion is assumed to be unaffected by the persistence of turbulence. In the second part the dispersion brought about by the turbulence is analyzed.

4.3.6.1 Deterministic Vertical Motion of Oil Globules

Consider an oil globule of density ρ_o and diameter d starting downward into water at an initial speed u_i. It is desired to obtain a description of the motion of the oil globule.

In deriving the description of the motion, given below, we make the following assumptions:

- The motion of the globule can be considered to be at sufficiently high Reynolds' numbers so that the drag coefficient remains a constant.
- The oil globule sizes are small, and therefore the circulatory motion of oil within the globule does not affect the drag law for the motion of the globule through water.
- There is no mixing of oil and water. That is, the properties of oil in the globule and size of the globule do not change during its motion through water.

Writing an equation for the balance of forces on a globule, we have

$$\underbrace{\left(\rho_o + \frac{\rho_w}{2}\right) V \frac{du}{dt}}_{\text{Effective inertia of an accelerating body}} = \underbrace{-(\rho_w - \rho_o) Vg}_{\text{Upward buoyancy force}} - \underbrace{\frac{1}{2} \rho_w u^2 A C_D}_{\text{Drag force resisting motion}} + \text{Forces due to the variation of pressure gradient in water from wave motion.} \qquad 4.81a$$

with $u = u_i$ at $t = 0$ 4.81b

Also $$\frac{dh}{dt} = u \qquad 4.82$$

where u is the downward speed and h the depthwise location at any instant of the oil globule. Other parameters are defined in Appendix A.

The solution to the above equations is derived in Appendix F. The solution is based on the following parameters:

$$s = \frac{\rho_o}{\rho_w} = \text{specific gravity of oil relative to that of water}$$

$$t_{ch} = \frac{u_i \left(s + \frac{1}{2}\right)}{g(1-s)} = \text{characteristic time [time to reach zero speed under a constant deceleration of } g(1-s)/(1/2 + s)]$$

$$\tau = \frac{t}{t_{ch}} = \text{dimensionless time}$$

$$L = u_i t_{ch} = \text{characteristic penetration depth (which is twice the distance traversed by a particle in a constant decelerating field starting with an initial speed } u_i)$$

$$\alpha = \sqrt{\frac{\frac{1}{2} \rho_w u_i^2 A C_D}{V \rho_w g(1-s)}} = \left[\frac{\text{Initial drag force}}{\text{Buoyancy force on the oil globule}}\right]^{\frac{1}{2}} \qquad 4.83$$

The penetration depth at any instant of time during the downward motion is given by (see Equation F-17, Appendix F):

$$\xi = \frac{h}{L} = \frac{1}{\alpha^2} \ln \left[\frac{\cos (\tan^{-1} \alpha - \alpha\tau)}{\cos (\tan^{-1} \alpha)} \right] \qquad 4.84$$

and the downward speed is given by

$$v = \frac{u}{u_i} = \frac{1}{\alpha} \left[\frac{\alpha - \tan (\alpha\tau)}{1 + \alpha \tan (\alpha\tau)} \right] \qquad 4.85$$

The maximum penetration depth and the time to reach the maximum depth are given respectively by

$$\xi_{max} = \frac{h_{max}}{L} = \frac{1}{2\alpha^2} \ln (1 + \alpha^2) \qquad 4.86$$

$$\tau_{sink} = \frac{t_{sink}}{t_{ch}} = \frac{1}{\alpha} \tan^{-1} \alpha \qquad 4.87$$

After the globule reaches the maximum depth, it starts to move back to the surface. This upward motion is essentially at the terminal velocity (a constant for a given size and density). The terminal velocity is given by solving the equation

$$\underbrace{V g (\rho_w - \rho_o)}_{\text{Upward buoyancy force}} = \underbrace{\frac{1}{2} \rho_w u_t^2 A C_D}_{\text{Motion-induced drag force}} \qquad 4.88$$

i.e.,

$$u_t = \frac{u_i}{\alpha} \qquad 4.89$$

Therefore, the position of the particles at any time is given by

$$(h_{max} - h) = u_t (t - t_{sink}) \qquad 4.90$$

where t is the time after the beginning of the motion.

The time to rise from the maximum depth location to the surface is:

$$t_{rise} = \frac{h_{max}}{u_t} = \frac{t_{ch}}{2\alpha} \ln (1 + \alpha^2) \qquad 4.91$$

Total residence time is calculated by

$$t_{residence} = t_{sink} + t_{rise} \qquad 4.92$$

In Appendix F, an example is worked out with assumed numerical values to obtain estimates for the residence time and the depth of penetration. Also, in Appendix F, we discuss the sensitivity of the result to various assumptions and the effect of initial kinetic energy imparted to the globules on the penetration depth.

It is noted that the depth of penetration at any instant (given by Equations 4.84 and 4.90) depends on the initial velocity imparted as well as the diameter of the globules. The initial velocity itself may depend on the size of the globules, if the relative fractions of the breaking wave energy that go into imparting motion to the globules is different for different sizes. This has to be determined by experiment. Because of the distribution of globule sizes and the fact that (even with the same starting velocities of the globules) the motion of the particles depends on their sizes, there would result a distribution of oil in the water column at any instant of time. In addition to the above effect the turbulence would tend to disperse the globules. In analyzing the dispersion by turbulence the penetration depth location (given by Equations 4.84 and 4.90) should be construed as the position of the mean of a probability density distribution of the oil globules. The variance of the probability density distribution will depend (for an ensemble of each size globule) on the characteristics of turbulence and the boundary condition. This is dealt with in the following stochastic model.

4.3.6.2 Stochastic Model for the Vertical Dispersion of Oil Globules by Upper Ocean Turbulence

The objective of the stochastic model developed in this section is to obtain the time history of the probability density distribution for the position of the oil globules in water. This is then used to obtain an estimate for the mass of oil that will be in the water column, as a function of time.

An oil globule that is driven under water by the action of breaking waves will be subjected to the dispersive action of the turbulence in water. As such the position of the oil globules is not predictable deterministically, but only stochastically. The characteristics of probability density distribution of the oil globule position are, therefore, dependent on the characteristics of the turbulence. To this extent the problem is similar in description to the classical "Brownian motion" problem with, however, one major exception. In the case of the classical Brownian motion, the turbulence field is stationary and homogeneous and the particles have zero drift, whereas in the case of oil globules, subjected to breaking wave-generated turbulence, the intensity is, in general, non-stationary and varies with depth. In addition, the oil globules, being buoyant, tend to have a general upward drift. It is because of these additional phenomena that the analysis of globule motion becomes extremely complicated.

The oil globules that rise to the surface of water may be assumed to coalesce to form a film of oil. As more and more globules coalesce with this oil film (due in part to the upward drift of globules, together with the decrease in the turbulent intensity), its thickness grows. From the point of view of the dispersion analysis (that is, the determination of the probability density function), the film at the surface has to be treated as an absorbing boundary. This boundary condition also makes the determination of the density distribution an extremely complicated one. In the model proposed in this section an approximate method of considering the effect of the absorption boundary is indicated.

Model

Consider a situation in which oil globules of a single size (i.e., diameter) are subjected to the turbulence generated by a breaking wave. At some time after the breaking, the probability density distribution of these globules may be as shown schematically in Figure 4.19 (see also Figure 4.18).

If

$f(z, t)$ = probability density function (p.d.f.) for the position of oil globules at time t,

then

$$f(z, t)\, dz = \frac{\text{mass of oil between depths } z \text{ and } z + dz}{\text{total mass of oil in water at any instant of time t, including the surface}} \qquad 4.93$$

Hence:

$$m_d(t) = \int_{z=0}^{\infty} f(z, t)\, dz = \text{fraction of the mass of oil globules of size d that is in the water at at any time t.} \qquad 4.94$$

In general, the behavior of the f function with time and space is influenced, to a considerable extent, by the presence of the absorption boundary. The way to determine the function f is to locate an "underlying" distribution function g (which is the p.d.f. in the absence of an absorption boundary), and then to modify the underlying distribution appropriately to account for the presence of the absorption boundary.

Referring to Figure 4.20, we see that if g is the underlying distribution function and f the actual p.d.f., then the shaded area (shown in the figure) accounts for the "absorbed" part of g by the boundary. How this area can be estimated is treated separately.

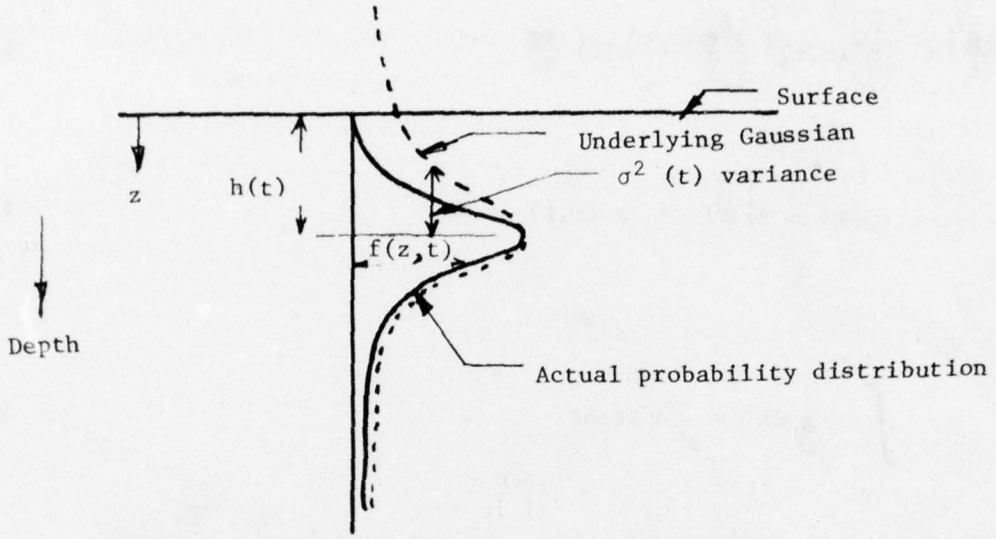

Figure 4.19: Schematic diagram showing the nomenclature for the stochastic analysis.

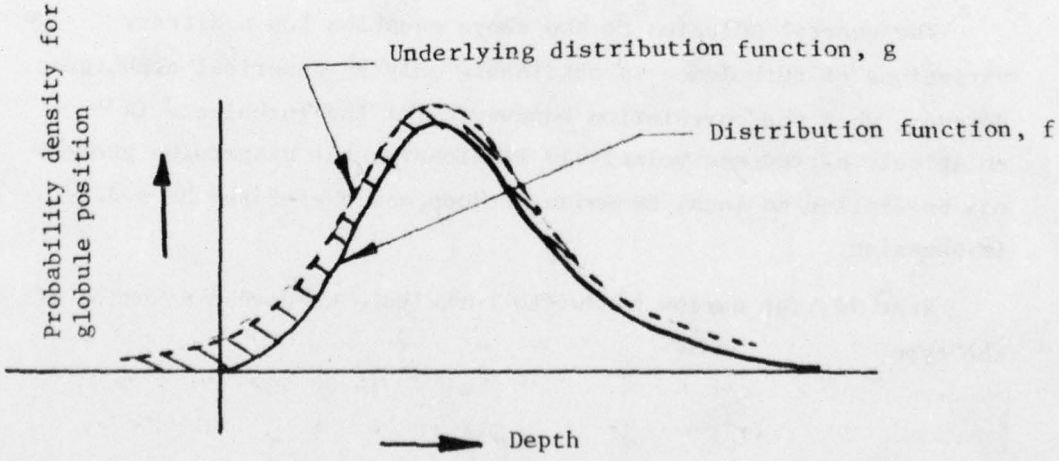

Figure 4.20: Schematic representation of probability density distribution functions z

The general equation for determining the underlying function g is given by

$$\frac{\partial g}{\partial t} = b'(z,t) \frac{\partial^2 g}{\partial z^2} + a(t) \frac{\partial g}{\partial z} \qquad 4.95$$

with $$g(-\infty, t) = g(\infty, t) = 0 \qquad 4.96a$$

and $$\int_{-\infty}^{+\infty} g \, dz = \text{Constant} \qquad 4.96b$$

where $b'(z, t) = \frac{\partial b(z, t)}{\partial t}$

$b(z, t)$ = variance type parameter of the underlying distribution. This parameter depends on the characteristics of the turbulence. (This is the diffusion coefficient in the Brownian motion.)

$a(t)$ = a parameter that indicates a marginal drift of oil globules (for the motion upward, it is the upward terminal velocity).

The general solution to the above equation for arbitrary variations of turbulence is obtainable only by numerical techniques. However, when the correlation bandwidth for the turbulence is relatively narrow and relatively stationary, the dispersion process can be similar to local Brownian motions, and therefore the p.d.f. is Gaussian.

That is, for narrow bandwidth turbulence we have a solution of the type

$$g(z,t) = \frac{1}{\sqrt{2\pi}\,\sigma(t)} \exp\left[-\frac{(z - h(t))^2}{2\sigma^2(t)}\right] \qquad 4.97$$

where

$h(t)$ = depth of the mean for the p.d.f., to be determined from from drift considerations

and

$\sigma^2(t)$ = local time varying variance:

$$\sigma^2(t) = 2t\left[\frac{1}{t}\int_{t_1=0}^{t}\int_{t_2=0}^{t-t_1}\overline{u'(t_1)\,u'(t_1+t_2)}\;dt_1\,dt_2\right] \qquad 4.98$$

where $u'(t_1)$ is the instantaneous value of the fluctuating component of the turbulent velocity in water at time t_1, and the bar on the top of u's denotes time averaging.

We note that the distribution g given in Equation 4.97 is not a stationary Gaussian because of the variation of the variance function $\sigma(t)$ with time.

The quantification of the effect of an absorbing boundary with arbitrary turbulence characteristics is hard to establish. In Appendix G, the effect of the absorbing boundary is calculated for the case of homogeneous, but non-stationary, turbulence. The complicated equation obtained is simplified using some simple physical arguments.

Once the p.d.f. for a given sized globule has been calculated, it is then trivial to calculate the mass of oil in water at any instant of time, if the size distribution of globules is known. An example is given below [for a specific type of turbulence] for calculating the mass of oil in water at any instant of time.

Specific Example

In this example a specific type of turbulence is assumed to illustrate the calculation procedures. Also several other assumptions are made:

- The turbulence is homogeneous and isotropic, but non-stationary.
- The correlation coefficient for the turbulent velocity fluctuations can be approximated by a parabola (see Figure 4.21).

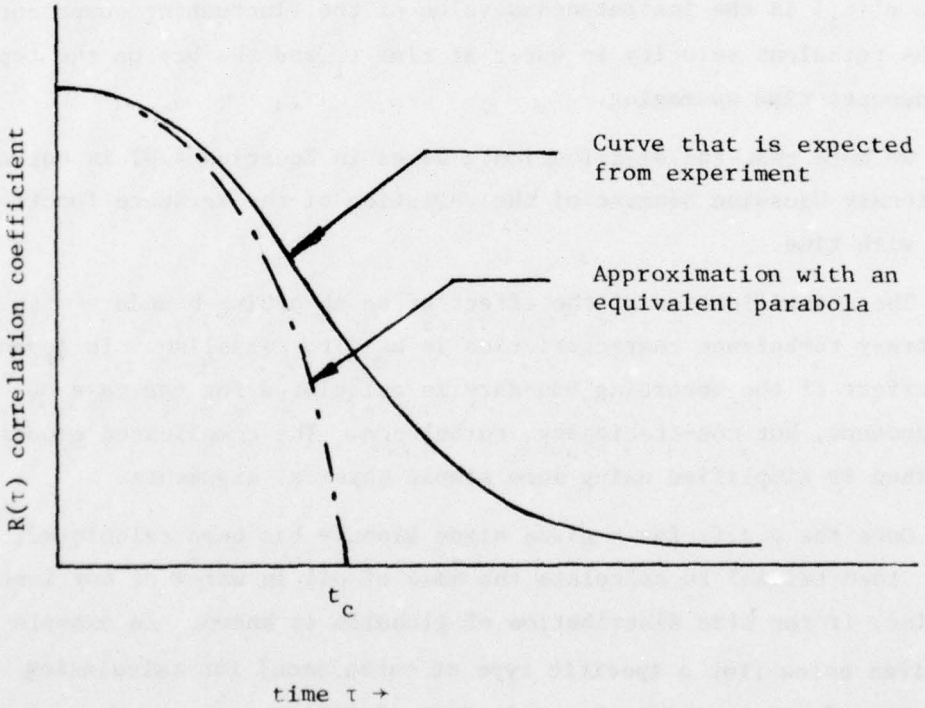

Figure 4.21: Schematic diagram showing the expected variation of coefficient of correlation between turbulent velocity at one instant and another.

- Only oil globules of one size are considered.
- The absorption barrier has no effect on the probability density distribution during the downward motion of the globules.
- The underlying distribution is Gaussian.
- The globule motion is one-dimensional.

We consider a turbulence of the type (see discussion on page 4-72)

$$\overline{u'^2}\,(t) = (u^s)^2 \exp\left(-\frac{t}{t_d}\right) \qquad 4.99$$

where $(u^s)^2$ is the intensity at zero time. Also, we assume

$$R(\tau) = \frac{\overline{u'(t)\,u'(t+\tau)}}{\overline{u'^2}\,(t)} \qquad 4.100$$

where $R(\tau)$ is the correlation function between velocity fluctuations, a time duration τ apart. Figure 4.21 indicates schematically the variation of $R(\tau)$ with τ that may be expected in an actual measurement. The figure also indicates a parabolic approximation used

$$R(\tau) = \begin{cases} 1 - \left(\frac{\tau}{t_c}\right)^2 & ; \quad 0 \le \tau \le t_c \\ 0 & ; \quad \tau > t_c \end{cases} \qquad 4.101$$

where t_c = characteristic correlation time scale.

The mean square deviation σ^2 of the Gaussian distribution is given by

$$\sigma^2\,(t) = 2t\,D(t) \qquad 4.102$$

where

$$D(t) = \frac{1}{t} \int_{x=0}^{t} dx \; \overline{u'^2}(x) \int_{y=0}^{t-x} R(y)\, dy \qquad 4.103$$

D(t) is the coefficeint of diffusion due to the turbulence. Substituting Equations (4.99) and (4.101) in (4.103), we get, for the coefficent of diffusion:

$$D(t) = \frac{(u^s)^2 t_d \, t_c}{t} \left[(a - a^3/3) - e^{-\frac{t}{t_d}} \left\{ ab \left(\frac{1 - a^2}{b} + \frac{2a}{b^2} - \frac{2}{b^3} \right) - \left(\frac{1}{b} - \frac{2}{b^3} \right) \right\} \right] \qquad 4.104$$

where

$$a = \begin{cases} t/t_c & \text{for } t < t_c \qquad 4.105 \\ 1 & \text{for } t > t_c \qquad 4.106 \end{cases}$$

$$b = \frac{t_c}{t_d} \qquad 4.107$$

It is noted from Equation 4.102 that since the σ^2 term is not a function of the position, the underlying distribution g (Equation 4.97) is a normalized Gaussian:

$$g(z,t) = \frac{1}{\sqrt{2\pi}\,\sigma(t)} \exp\left(- \frac{[z - h(t)]^2}{2\sigma^2(t)} \right) \qquad 4.108$$

where $\sigma(t)$ is obtained from Equation 4.102, and h(t) is the position of the mean as determined by the deterministic model (discussed in Section 4.3.6.1).

To obtain the actual distribution function, f, the effect of the absorption boundary has to be accounted for. There are various approximate ways of accounting for the boundary, and

these are discussed in Appendix G. Using these approximate methods, we have

$$f_1(z,t) = \frac{1}{\sqrt{2\pi}\,\sigma(t)}\left[\exp\left(-\frac{[z-h(t)]^2}{2\sigma^2(t)}\right) - \exp\left(-\frac{[z+h(t)]^2}{2\sigma^2(t)}\right)\right] \qquad 4.109$$

$$\text{for } 0 < t < t_{sink}$$

$$f_2(z,t) = \frac{1}{\sqrt{2\pi}\,\sigma(t)}\left[\exp\left(-\frac{[z-h(t)]^2}{2\sigma^2(t)}\right) - \exp\left(-\frac{[z+h(t)+2u_tS]^2}{2\sigma^2(t)}\right)\right] \qquad 4.110$$

$$\text{for } t > t_{sink};\quad z > 0$$

where the parameter S has the dimensions of time and is a function of both time (t) and spatial position (z). The explicit relation between S and the variables t and z is given in Appendix G, Equation G.15.

Equation 4.109 represents the probability density distribution during the time when the mean motion of the oil globules is downward and Equation 4.110 is applicable during the upward motion of the globules.

The fractional mass of oil present in water at any instant of time is given by Equation 4.94. Hence, during the downward (depth-wise) motion of the oil globules, the mass fraction of oil in water at any time is (by substituting f_1 and f_2 from Equations 4.109 and 4.110 into Equation 4.94):

For $0 < t < t_{sink}$,

$$m_d(t) = \frac{1}{\sqrt{2\pi}\,\sigma(t)}\int_{z=0}^{\infty}\left[e^{-\frac{(z-h)^2}{2\sigma^2}} - e^{-\frac{(z+h)^2}{2\sigma^2}}\right]dz = \text{erf}\left[\frac{h(t)}{\sqrt{2}\,\sigma(t)}\right]$$

and for $t \geq t_{sink}$, 4.111

$$m_d(t) = \frac{1}{\sqrt{2\pi}\,\sigma(t)}\int_{z=0}^{\infty}\left[e^{-\frac{(z-h)^2}{2\sigma^2}} - e^{-\frac{(z+h+2u_tS)^2}{2\sigma^2}}\right]dz$$

$$m_d(t) = \text{erf}\ (h/2\sigma) +$$

$$(1/\sqrt{\pi}) \int_{z=0}^{\infty} \frac{\left\{\exp[-(z-h)^2/2\sigma^2] - \exp\ [-(z + h + 2Su_t)^2/2\sigma^2]\right\}}{\sqrt{2\sigma}}\ dz \qquad 4.112$$

The integral in the second term of the above equation cannot be evaluated in terms of elementary functions because of the complicated way in which S is related to z (see Appendix G) and its appearance in the exponent. However, a numerical solution is possible.

When globules of different sizes are considered, we can find the total mass of oil present in water at any time by the relation:

$$M(t) = \int_{d=0}^{\infty} j(d)\ m_d(t)\ dd \qquad 4.113$$

where $j(d)\ dd$ = fraction of the <u>total mass</u> of oil that is contained in globules of size between d and d + dd.

and $m_d(t)$ is defined in Equation 4.94. It is noted that $m_d(t)$ is a function not only of time, but also of the size of the globules (through the variation of h with time and u_t the terminal velocity).

<u>Numerical Example for Calculating the Fraction of Oil Mass in Water</u>

The calculation procedure is best illustrated with a numerical example. All of the data necessary for such a calculation are not available at the present time. However, we have assumed some values <u>which may or may not be realistic</u>. Therefore, the calculations indicated below should be construed only as an illustrative example, and no emphasis should be placed on the actual numerical value <u>per se</u>.

We investigate the dispersion of oil globules of diameter 1 cm, subject to a breaking wave of 3 m amplitude (with critical height for breaking assumed to be 2 m). We assume the following values:

The intensity of homogeneous isotropic turbulence is given by Equation 4.99

t_d = dissipation time = 2 s

$(u^s)^2$ = maximum intensity of turbulence = 1 m^2/s^2

t_c = correlation time = 0.2 s

The calculation procedure involves, for any time instant t:

- Obtaining h(t) from the analysis given in Appendix F (see also the specific example therein),
- Calculating D(t), the coefficient of diffusion from Equation 4.104,
- Obtaining $\sigma(t)$ from equation 4.102, and
- Calculating the mass fraction of oil (of the given diameter globules only) in water $m_d(t)$ from Equations 4.111 and 4.112. To obtain $m_d(t)$ from Equation 4.112 a numerical procedure is used.

Results

The results obtained from using the numerical values are shown in Figure 4.22. Plotted in the figure are:

(i) the depth of penetration of the globules (mean position) as a function of time;

(ii) the standard deviation (σ) of the underlying Gaussian distribution; and

(iii) the calculated mass fraction of oil that is submerged (in the form of globules) in water.

This quantity is calculated in two different ways. In the first case

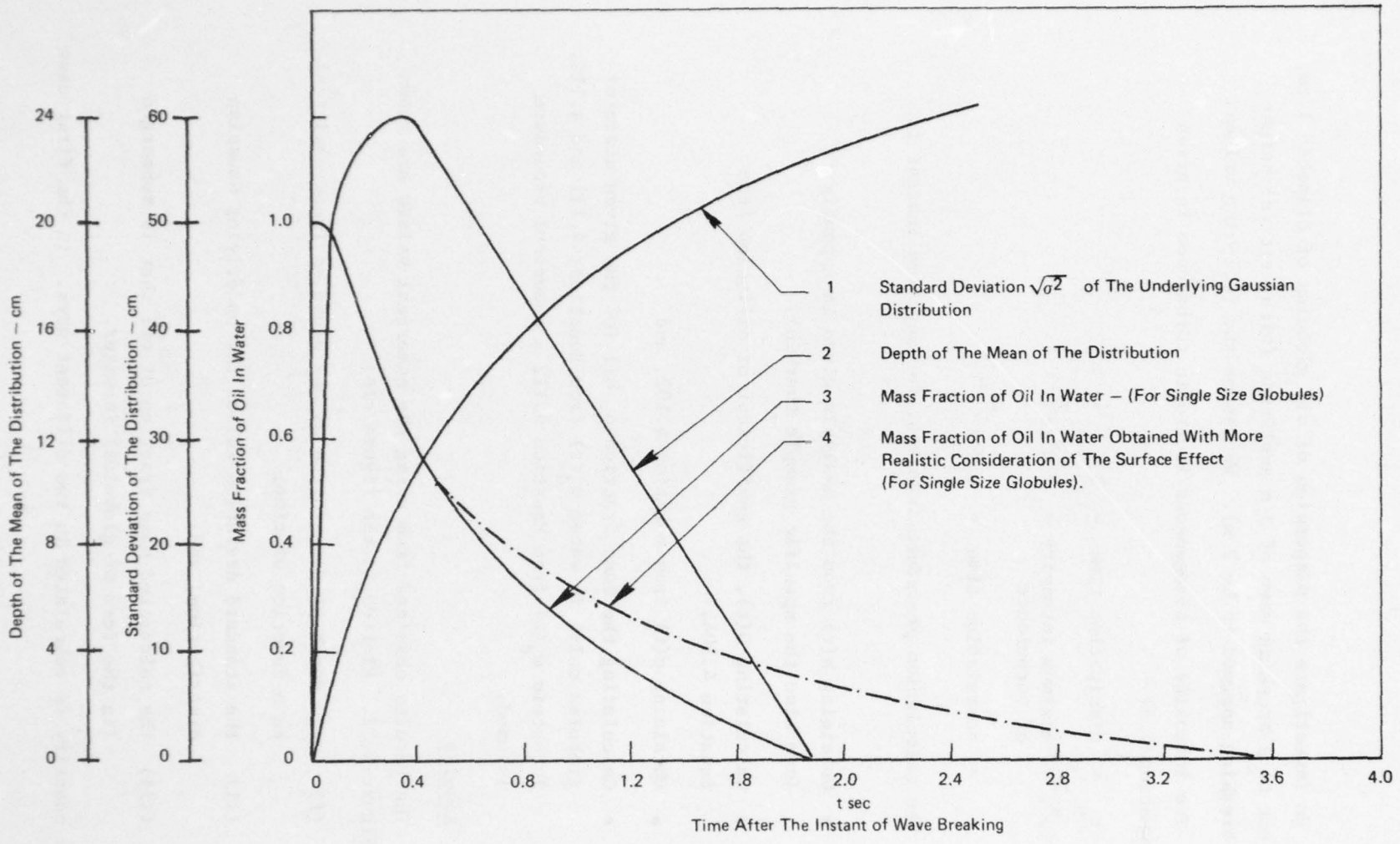

FIGURE 4–22 TIME-WISE VARIATION OF THE FRACTIONAL MASS OF OIL (CONTAINED IN GLOBULES OF A SINGLE SIZE) WHICH IS UNDER WATER

(curve 3) it is assumed that the actual probability density distribution within the water is that part of the Gaussian that is below the water surface minus the part that is above the water. This assumption does not give a very realistic representation of the absorption barrier at the surface of water. The result shown in curve 4 is obtained by using Equation 4.112 and is more accurate.

The result indicates that all of the oil will surface and join the main slick in a time which is about twice the residence time as calculated by a deterministic model (Appendix F). It is, however, to be noted that this estimate may not be applicable if the turbulence is too much different from the one assumed.

The calculations have not been extended to finding the total mass fraction of oil (in the Equation 4.113 sense) which is in water, because this requires data on globule size distributions. The calculations are simple in principle and can be carried out when such data become available.

AD-A049 794 LITTLE (ARTHUR D) INC CAMBRIDGE MASS F/G 6/6
THEORETICAL STUDY TO DETERMINE THE SEA STATE LIMIT FOR THE SURV--ETC(U)
JUN 77 P P RAJ DOT-CG-61505-A
UNCLASSIFIED ADL-79299-F USCG-D-90-77 NL

3 OF 3
AD
A049794

END
DATE
FILMED
3-78
DDC

4.4 Conclusions

The major conclusions from the analyses developed in this chapter are

- Slicklet-type fracturing of oil slicks is highly unlikely, unless the breaking waves have crest lengths comparable in size to the oil slick diameter. Breaking waves of long crest lengths are not generally present in deep waters.
- Langmuir circulation, if present in the area of an oil spill, will be able to carry oil globules deep into the ocean. In about 2 m seas, drops of 7.5 mm diameter would be carried down by such circulations.
- The probability of breaking waves occurring frequently in the same area of the ocean is very low. For example, in a fully developed sea with a 30 km fetch, in 10 m/s wind, only 1 in 2000 waves can be expected to break. However, when a wave breaks, the expected value of the energy input to the sea is of the order of a few kilojoules per square meter.
- In the absence of large eddies under breaking waves, the depth of penetration of oil globules is very small. It is about 30 times the diameter. Also the residence time is short compared to the mean time of occurrence of breaking waves. The residence time is increased by about a factor of 2 due to the vertical dispersion of globules by small-scale turbulence (non-stationary).

CHAPTER 5

SEA-STATE MEASUREMENT IN THE FIELD

5.0 Summary

The parameters used in the sea-state definition in the earlier chapters are identified, and discussions are provided about the types of measurements to be made at any site to evaluate these parameters. The JONSWAP spectrum and its parameters are discussed. The minimum number, type, and the duration of measurements that are necessary to obtain statistically valid values are indicated. Other parameters that are not directly used in the current models, but which have the potential of being used in future models, are identified and some discussion provided on the number of measurements to be made. Forecasting near-term future sea conditions from measurements made at any instant are also discussed briefly.

5.1 Introduction

In the previous chapters the dispersion models have been developed based on the assumption that the sea state can be adequately defined by a spectral description. Two widely accepted correlations have been used, namely, that of Pierson-Moskowitz and the JONSWAP spectrum. Even though these spectra are accepted in the literature, it is noted that the ocean spectra are greatly influenced by local conditions of tidal currents, typography, and meteorology. Therefore, whenever a good estimate is to be made of the environmental problems which depend critically on the state of the sea in a given location, it is imperative to have an accurate description of the sea and the sea state at the particular location. For example, the JONSWAP spectrum is a fetch limited spectrum that has been correlated based on data obtained in the North Sea. The JONSWAP

correlation contains several "free parameters", and it is claimed by the researchers that any sea can be adequately represented by this spectrum, provided the individual parameter values are determined at the particular location. The JONSWAP spectral parameters for the sea in the Gulf of Mexico are not currently available. Therefore, to assess the dispersion of the oil that may be spilled accidentally near a deepwater port in the Gulf Coast, it is necessary to have information about the spectral parameters and the sea state. In this chapter several of these sea state dependent parameters that are used in the models discussed in earlier chapters are identified and some discussion provided as to the minimum number of in situ measurements that are needed to evaluate these parameters in a given location on the sea.

In addition to measuring the parameters for determining the sea state prevalent at any given time, it is desirable to be able to predict the future condition of the sea for times ranging from a few hours to as long a time as a day or two. Such a forecast may result in a more efficient scheduling of the deepwater port operation. The oil off-loading operations will require a certain lead time for shutdown, as will operations designed to put the facility into a minimum risk posture. Ability to forecast the sea state should, therefore, be a necessary part of deepwater port management. The measurement of wave spectral parameters and their rates of change does not provide means of forecasting the immediate future sea state.

5.2 Analyses

We indicate the parameters to be measured with the basic assumption that the JONSWAP spectrum is an adequate representation of a developing or fully developed sea state. The derivation and formulation of this spectrum (which is an elaboration and amplification of Pierson-Moskowitz correlation) is thoroughly described by Hasselman et al. (1976). The spectrum is given by

$$S(\omega) = \alpha \frac{g^2}{\omega^5} \exp\left[-\frac{5}{4}\left(\frac{\omega_m}{\omega}\right)^4 + (\ln \gamma) \exp\left\{ -\frac{1}{2\sigma^2}\left(\frac{\omega}{\omega_m} - 1\right)^2 \right\} \right] \qquad 5.1$$

with,

$$\alpha = 0.032 \left(\frac{\omega_m U}{2\pi g}\right)^{2/3} = 0.0162 \left(\frac{U^2}{X}\right)^{0.2} \qquad 5.2$$

The constant α is termed the Phillips constant and ω_m the spectral peak (i.e., the modal) frequency.

To define the sea state at any particular location the following parameters need to be measured:

1. Phillips Constant α:

This constant is determined provided the wind speed and the fetch are determined (Equation 5.2). Therefore, the following measurements have to be made:

Wind Speed: The wind speed for the spectrum should be measured 10 m above the mean water level at the same site where the wave record is made. To obtain a statistically meaningful value for the near-term wind speed a continuous monitoring of wind speed for at least one-half hour is recommended. However, since the wind speed used in JONSWAP data correlation is really a mean wind speed over the entire fetch distance, we recommend that the wind data measurement be made for a time duration which would be representative of the travel time of wind over the entire fetch distance. It is noted that this duration is itself a function of the wind speed (and the direction from which it is blowing because of the dependence of fetch distance on the compass angle at a given location on the sea). Inherent in this recommendation is the assumption that the wind speed and direction are "reasonably" steady over the fetch travel time. When the wind field is fast changing or has large spatial gradients, as might occur during tropical storms, specialized techniques of wave prediction are necessary. These have been discussed by Ippen (1966).

Fetch: This is also a parameter which influences the value of the Phillips constant. The fetch, in general, varies with compass angle at a given location on the sea. For deep water ports, which are relatively close to the shore (distances of the order of 20 to 40 miles), the distance to the

shoreline in any direction can be considered to be the fetch in that direction. In the seaward direction the fetch may not be fixed, unless for some special geophysical reason a storm always spawns at a particular location on the sea.

In any case, the known fetch can be measured a priori from charts, and information can be stored appropriately (in charts, manuals, or on magnetic tape) in the DWP facility. Where possible the fetch has to be recorded at 5 deg compass angles from the site at which sea state measurements have to be made. It is noted that this measurement is a one time measurement.

In the case of variable fetch (in the seaward direction), there will be a need to analyze historical data on storms and compile a fetch record for each compass angle. There is a likelihood of this being a function of the seasons.

2. Modal Angular Frequency ω_m

The second important parameter in the JONSWAP spectrum is the modal frequency. The modal frequency is related to the mean requency (ω_o) by

$$\omega_m = 0.77694 \ \omega_o \qquad 5.3$$

Therefore measuring ω_o would ensure the determination of ω_m.

The mean frequency (ω_o) in the spectrum can be measured by taking a wave surface elevation record for a sampling period of about 15 minutes to half an hour. From the record the number of upward zero crossings can be counted. The mean frequency is then the number of upcrossings per unit time.

3. Measurement of the Spectrum

The behavior of the sea is affected by the local, site specific conditions such as the water depth and floor gradient, shoreline configurations, or small-scale meteorological peculiarities.

These are not reflected in the spectrum parameters, but the parameter values may require adjustment to suit the local conditions. In order to make such an adjustment it is essential to analyze the wave height record to obtain the complete spectrum.

The wave height record has to be made at least for one-half hour to assure statistically stable conditions. The record can be analyzed by the method of Fast Fourier Transforms, or by a frequency filter method, to provide a complete spectral representation. About 16 to 20 frequency bands may be required to achieve a reasonably accurate approximation. Mean frequency, modal frequency, total energy content, and other spectral shape parameters can be derived. From a record of such characteristics calculated at reasonable time intervals (say, 4 hours), short-term extrapolations of the sea state could be made for near future predictions. In addition, after sufficient data have been accumulated in this fashion, appropriate adjustments to the JONSWAP parameters can be made. These adjustments would apply in particular to the peak augmentation factor (γ) and the two peak width factors (σ), which are the principal shape factors in the JONSWAP spectrum.

4. Breaking Wave Parameters

Power or energy spectrum in itself does not provide any direct information on the frequency of occurrence or the size of breaking waves. It is recalled that the oil dispersion models have identified the breaking waves as the principal cause of oil dispersion in the ocean. In Section 4.3.4, procedures have been indicated for calculating the breaking probability and energy loss in breaking, both quantities being obtained from the sea state spectrum.

It is, however, desirable to measure -- concurrently with determination of the sea spectrum at a specific location -- the parameters of the breaking waves such as their apparent (or dominant) wavelength, wave height, crest length and their

distribution in the horizontal plane. These measurements also could be a one-time measurement (like the fetch distances), so long as the relationships between sea spectral parameters and the breaking wave parameters are determined.

The measurements of breaking wave parameters are probably the most difficult to achieve with accuracy. Probably they would depend upon visual or photographic methods, or upon the development of highly specialized equipment, in contrast to the other sensors which could be drawn from a large reservoir of oceanographic and meteorological instrumentation.

It is difficult to estimate a priori how many sets of data have to be measured to obtain a reasonable correlation between the breaking wave parameters and the sea spectrum parameters. The ultimate objective of these measurements should be to obtain enough data to correlate the breaking probability (i.e., the number of breaking waves per unit sea surface) with the sea state represented (approximately) by the wind speed and fetch, similar to that presented in Figure 4.15.

5. Other On-site Measurements

The dispersion of the oil slick is influenced by the nature of the oil and its physical properties. In addition, there are several other variables which influence the dispersion of oil, but which have not been fully accounted for in the first generation dispersion models discussed in this report. Similarly, the significance of some of the parameters that influence the sea spectrum and the wave breaking process has not been fully established, or at least their effects have not been explicitly incorporated into the dispersion models. However, it is our contention that these parameters should be measured at a given sea station, not only to obtain a better understanding of the sea state conditions, but also to provide inputs into future and more accurate oil dispersion models. These parameters include:

Oil and Water Density: The dispersion of oil, both in the horizontal and in the vertical direction, is influenced to a considerable extent by oil and water densities. It is, therefore, necessary to measure these quantities at the deep-water port site.

The water density is a relatively easy parameter to measure. Also, for the depths of concern (upper 2 to 3 meters of the ocean) the water density is expected to be uniform, and its dependence on surface temperature and salinity concentration is not large. However, we recommend that water samples be taken often (once a day if feasible) for density analysis.

The density of the oil (and other physical properties including the type of crude, etc.) should be analyzed from the samples of oil taken from the ship before the oil transfer takes place. In addition, the sea water temperature should be measured in the area. Should any oil spill occur at the DWP site, the oil temperature will quickly equilibrate with the sea temperature and consequently the properties (especially the viscosity and vapor pressure) will change. The property change affects both the evaporation process and the dispersion process.

Air Temperature and Barometric Pressure: The air temperature and pressure have relatively low influence on the oil evaporation process, compared to the water temperature. Their main effect is to change the air density which influences the mass transfer rates from the oil to the air stream. The currently generated models do not use these parameters explicitly. It is conceivable that future models, especially those dealing with the air/sea interactions in the presence of large oil slicks may utilize these data. As such, these data need to be measured. Air temperature and barometric pressure measurements may be taken at the standard 10 m height (above the mean water level). Continuous monitoring of these quantities is recommended.

Tidal and Surface Currents: The effect of tidal currents on oil spill dispersion (other than the surface movement of the slick en masse) is not known. Also tidal currents influence the wave breaking probability at any given location. Tidal current data are, in general, available from precalculated astronomical tide tables, or can be measured by standard oceanographic current meters.

Surface ocean current speed and direction will also need to be known to predict the drift of oil slicks. Detailed descriptions of the local weather and currents for coastal areas are given in issues of the Coast Pilot and in an atlas or in special studies that describe in detail the surface circulation on the continental shelf. Where such data are not available, they can be measured through the use of drift bottles or Rhodamine dye techniques widely used by oceanographers, Charnel (1975) and Coastal Hydrologists (1968).

Forecasting Sea State Conditions: Prediction of future sea state involves the prediction of the sea spectrum. The wind speed and direction can be predicted from meteorological forecasts. Since the spectral shape parameters (γ and σ for the JONSWAP spectrum) are known for a particular location from previous measurements, the prediction of the spectrum reduces to the prediction of the Phillips constant and the modal frequency. The former is determined from the relationship given in Equation 5.2 and the forecast wind and fetch (wind direction). The latter is estimated also from Equation 5.2; that is from the relationship

$$\nu = \frac{U\ \omega_m}{2\pi\ g} = \left(\frac{\alpha}{0.032}\right)^{3/2} \qquad 5.4$$

These brief computations give the values necessary to define the spectrum or to be used directly in the wave breaking probability and energy models.

A different approach to prediction would lie in a mathematical extrapolation process, for each of the significant parameters or variables, based upon a set of data points derived from measurements taken at a specific sampling interval. Neither of the predictive approaches requires any additional measurements.

APPENDIX A

NOMENCLATURE

Symbol	Details	Formula or Equation #	Units
a	Wave amplitude		m
a^*	Root mean square amplitude		m
$\overline{a^2}$	Mean square wave in a given sea $\int_0^\infty e(\omega)d\omega$		m^2
a_b	Breaking amplitude of wave	4.5.1	m
A	Area of oil slick		m^2
A	Also parameter defined in equation 4.3	$\frac{1 - (\pi S)^2}{2\pi S}$	
A	Also used for the cross-sectional area of a globule normal to the direction of motion	4.38 and Appendix F	m^2
b	Oil layer thickness	3.1	m
c	Wave phase speed	Table 2.1	m/s
C	Volume concentration of oil globules in water at any depth	2.16	kg/m^3
C_0	Volume concentration of oil globules at the water surface	2.16	kg/m^3
C_D	Drag coefficient between wind and water	2.6	
C_D	Also hydraulic drag coefficient for the motion of oil globles in water	4.38	
C_I	Intertia coefficient--due to the accelerated motion of globules	4.44	
d	Mean diameter of oil globules	-	m
D	Molecular diffusivity of the soluble fractions of oil in water	2.15	m^2/s
D	Also diffusion coefficient due to turbulent fluctuations	4.70	m^2/s

NOMENCLATURE (continued)

Symbol	Details	Formula or Equation #	Units
e	Turbulent kinetic energy per unit volume of water Also represents the base of natural logarithm	4.69	J/m^3
$e(\omega)$	Spectral energy density between frequencies ω and $\omega + d\omega$	2.3, 2.5	$m^2 s$
E	Wave energy per unit sea surface area $= \frac{1}{2}\rho_w g \int_0^\infty e(\omega)\, d\omega$	Table 3.2	J/m^2
E'	Energy lost by a breaking wave over a wave travel length, expressed per unit length in the crest length direction	P 4-66	J/m
E''	Wave energy per unit area of sea $= \frac{1}{2} \rho_w g \overline{a^2}$		J/m^2
E''	Also total energy released under a breaking wave per unit area, that goes to produce turbulence	4.75	J/m^2
$\bar{E}_B$	Expected energy density of waves that break	4.61	J/m^2
$\dot{E}''_{wind}$	Rate of energy input by wind into unit area of sea	Section 3.2.2	J/m^2 s
ΔE	Expected value for the energy dissipated by breaking action	4.62	J/m^2
f	Ratio of r.m.s. turbulent speed to the orbital speed of water particle	3.40	
f(z,t)	Probability density function for the position of a given oil globule	4.93	
$\vec{F}_{AI}$	Added inertia force on globules	4.44	N
F_m	Minimum fetch distance to establish a fully developed sea	Table 2-2	km

NOMENCLATURE (continued)

Symbol	Details	Formula or Equation #	Units
g	Gravitational acceleration	Table 2-1	m/s^2
g	Also used to represent the underlying Gaussian distribution	4.97	m^{-1}
h	Film thickness of oil	4.9	m
h	Water depth	Table 2-1	m
h	Also depth to which oil globules sink into the water	Section 4.3.6.1	m
h_c	Critical film thickness for slick fracture	4.37	m
h_{max}	Maximum depth to which an oil globule of a given diameter penetrates	4.86	m
h(t)	Depthwise location of the mean of the probability density distribution function (denoting the globule positions).	4.97	m
H	Wave height	2.1	m
Ha	Average height of all waves	Table 2-2	m
H_f	Most probable wave height	Table 2-2	m
H_s	Significant wave height	2.2	m
j(d)	Size distribution function of oil globules	4.113	
K	Turbulent diffusion coefficient	2.17	m^2/s
ℓ	Integral scale of turbulence, i.e., the size of eddy	3.29	m
$\sqrt{\overline{\ell^2}}$	r.m.s. value of the crest lengths for breaking waves	Section 4.2.2	m
L	Length of slick normal to wave propagation direction	4.20	m
L	Also used as a characteristic length scale for the motion of oil globules in water	4.83	m
L	Also used for distance between crests of breaking waves on a sloping beach	P. 2-8	
L	Also length of slot	Appen. D	m

NOMENCLATURE (continued)

Symbol	Details	Formula or Equation #	Units
L_a^*	Average length between wave crests	Table 2-2	m
m_d (t)	Fractional mass of oil globules of size d that is in water at time t.	4.94	
M (t)	Total mass fraction of oil present in water (when all sizes of globules are included) at time t. Note this is the fraction of the mass of oil that was within the area in which breaking wave occurred.	4.113	
N	Number of oil globules formed per unit area of the sea	Section 3.2	
N	Number of distinct slots present within an oil slick at any given instant	4.11	
N	Number of breaking waves per expected wave length in a fully developed sea	4.58	
N_j	Number of moles of j^{th} specie in the oil film	3.5	k moles
p(a)	Probability density at the wave amplitude a	3.35	
p'	Fluctuating pressure in water	P. 3-13	N/m^2
p*	r.m.s. value of pressure fluctuations due to turbulence in water	3.15	N/m^2
p_{atm}	Atmospheric pressure	4.7	N/m^2
p_{vap}	Vapor pressure	4.7	N/m^2
P	Percent of waves that break	2.8	
P (t)	Total probability of slick fracture at any given time	4.15	
P_{uf}	Transition probability for change from uncut to fractured state	4.12	
P_N	Transition probability for slick fracture at any given time with N waves	4.29	
P_N^o	Probability of uncut with all N waves necessary	4.32	

NOMENCLATURE (continued)

Symbol	Details	Formula or Equation #	Units
Re_t	Reynolds number at terminal speed of motion	4.40	
$R(\tau)$	Speed correlation function	4.100	
s	Ratio of densities of upper and lower fluids (*oil density/water density*)	Table 2-1	
s	Also used for shear-strain rate in the water surface due to wind shear stress	3.27	s^{-1}
S	Wave steepness	$\frac{2a}{\lambda}$	
S	Also total entropy of the oil film	3.5	J/K
S	Also used as a parameter representing the effect of absorption boundary at water surface, for the motion of oil globules	4.110 & Appendix G	s
$S(\omega)$	Wave spectral energy density per unit area of sea surface		J s/m^2 rad
t	Elapsed time		s
t_c	Characteristic of time for slick fracture	4.19	s
t_c	Also characteristic correlation time scale	4.101	s
t_{ch}	Characteristic globule motion time	4.83	s
t_d	Time scale for the dissipation of turbulent kinetic energy	4.77	s
t_m	Minimum wind duration to establish a FDS	Table 2-2	hrs
t_r	Residence time of globules	4.92, 3.3	s
t_{sink}	Time for the oil globules to sink to the maximum depth	4.87	s
T	Wave Period. Also used for the time between the occurrences of breaking at a point.	4.78	s
T	Also temperature of film	Section 3.3	K

NOMENCLATURE (continued)

Symbol	Details	Formula or Equation #	Units
T_c	Average closing time for a slit in the oil slick	Section 4.2.2	s
T_m	Period associated with highest waves in the spectrum	Table 2-2	s
T_s	Significant wave period	2.5	s
T_w	Mean period between the occurrence of breaker waves	Section 4.2.2	s
T_B	Average length of time over which a wave continues to break	4.56	s
T_a^*	Average observable wave period	Table 2-2	s
u	Vertical speed of oil globules	4.43	m/s
u_t	Also terminal speed of rise of oil globules	3.3, 3.4, 4.38	m/s
u*	Friction velocity due to wind stress = 0.04 U	2.7	m/s
u^s	r.m.s. value of initial turbulent intensity	4.99	m/s
u'	Fluctuating velocity in water due to turbulence	4.71	m/s
$\sqrt{u'^2}$	r.m.s. velocity of turbulent fluctuations in water		m/s
U	Orbital velocity of water particle due to wave motion. Also, group speed of waves.	Table 2-1	m/s
$\underline{U}$	Total internal energy of a film	3.5	J
$\overline{U_w^2}$	Mean square water speed amplitude	3.43	$(m/s)^2$
U_s	Significant water speed amplitude	3.40	m/s
U, U_{wind}	Wind speed	2.3	m/s
v	Vertical speed of water surrounding an oil globule	4.47	m/s
v	Also used for dimensionless vertical velocity	4.85	
V	Volume of oil spilled	2.15	m^3

NOMENCLATURE (continued)

Symbol	Details	Formula or Equation #	Units
V	Also used for volume of an individual oil globule	4.81	m^3
V	Also speed with which a fractured part of an oil slick spreads	4.9	m/s
x	Length sticks (also used as x_1 and x_2)	Appen. D	m
X	Fetch distance	P. 4-59, 5-2	m
z	Depthwise coordinate (z = 0 is the water surface)		m
z_0	Mixing depth	2.16	m

NOMENCLATURE (continued)

Symbol	Details	Formula or Equation #	Units
α	Equilibrium spectrum constant (related to the wind-water drag coefficient)	2.9, 2.12	dimensionless
α	Also used as a characteristic parameter for the motion of oil globule	4.84	
α	Also a parameter defined in Appendix D	D-9	
β	Parameter in the spectral energy density distribution	2.12	
γ	Also parameter appearing in the JONSWAP spectrum	4.48, 5.1	
γ	Interfacial tension	3.8	N/m
Γ	Strain rate of stretching or compression of oil film	4.1 Appendix C	s^{-1}
δ	Wave steepness	$2a\ \lambda^{-1}$	
ε	Turbulent energy dissipation function (rate dissipation of turbulent energy per unit volume of water)	3.29, 4.70	J/s m^3
η (t)	Elevation record of waves	4.46	m
$\overline{\eta^2}$	Mean square elevation	4.45, 4.59	m^2
θ	Polar coordinate of a point on the oil film	Appendix C	degrees
κ	Wave number $= \frac{2\pi}{\lambda}$	4.71	m^{-1}
λ	Wave length		m
λ	Also used for Taylor microscale of turbulence		m
μ	Chemical potential	3.5	
μ_o	Oil viscosity		N s/m^2

NOMENCLATURE (continued)

Symbol	Details	Formula or Equation #	Units
μ_j	Chemical potential of j^{th} specie	3.5	
$\nu^+_{a_b}$	Rate of upcrossing at level a_b	4.56	s^{-1}
ν_w	Kinematic viscosity of water	2.15	m^2/s
ξ	Wave age Also used for dimensionless depth location of an oil globule	4.64 4.84	
ρ_a	Density of air	2.1	kg/m^3
ρ_n	Area molar density of the n^{th} specie in the film	3.10	k moles/m^2
ρ_o	Density of oil		kg/m^3
ρ^*	Critical surface density for thermodynamic stability of a film of a pure component	Page 3-10	k moles/m^2
ρ_w	Density of water		kg/m^3
σ	Surface tension of oil		N/m
σ	Also in a parameter occuring in the JONSWAP spectrum	4.48	
σ	Also used to denote the standard deviation of the probability density distribution function for the position of oil globules in water.	4.97 4.98	
τ	Dimensionless time for slick fracture and also for motion of oil globules	4.19, 4.83	
τ	Shear stress at the air-water interface due to wind	Section 3.5	N/m^2
τ_{sink}	Dimensionless time for the oil globules to sink to the lowest depth in water	4.87	

NOMENCLATURE (continued)

Symbol	Details	Formula or Equation #	Units
ψ	Normal tensile stress in the oil film	4.5	N/m^2
ω	Wave frequency		rad/s
ω_m	Modal frequency in the wave energy spectrum	4.48	rad/s
ω_o	Expected frequency of zero mean, narrow band, random process	4.49	rad/s
ω_c	Cut off frequency for the spectrum in a developing sea		rad/s
$\tilde{\omega}$	Ratio of the energy lost in a breaker wave to the total energy possessed by the wave for one wave cycle	Page 2-26	
Ω	Vorticity	Section 3.5	rad/s
Ω'	Fluctuating component of vorticity	Section 3.5	rad/s

APPENDIX B

RELATIONSHIP BETWEEN VARIOUS SEA STATE PARAMETERS

In this appendix several parameters are derived from a spectral correlation for a fully developed sea. The widely used Pierson-Moskowitz spectral representation is used. This representation is also applicable to the International Ship Structures Congress' spectrum (ISSC - Michael 1968).

The average wave energy per unit nominal surface area of the sea is given by (see Lamb 1932, Michael 1968).

$$E'' = \frac{1}{2}\rho_w g \overline{a^2} = \frac{1}{2}\rho_w g \int_{\omega=0}^{\infty} e(\omega)\, d\omega \qquad \text{B.1}$$

where $e(\omega)$ = spectral energy density (in units of m^2 s) at frequency ω.

The Pierson-Moskowitz (P.M.) and ISSC spectra for $e(\omega)$ have the form*

$$e(\omega) = \alpha \frac{g^2}{\omega^5} \; Exp - \left[\beta\left(\frac{g}{\omega U_{WIND}}\right)^4\right] \qquad \text{B.2}$$

U = Amplitude of water particle velocity = $a\omega$

(where a is the wave amplitude)

Hence $$\overline{U^2} = \overline{a^2\omega^2} \qquad \text{B.3}$$

i.e., $$\overline{U^2} = \int_{\omega=0}^{\infty} \omega^2 e(\omega)\, d\omega \qquad \text{B.4}$$

---

*Commonly accepted values are $\alpha = 1.62 \times 10^{-2}$, $\beta = 0.74$ for P.M. spectrum

Substituting Equation B.2 into B.4 and integrating we get

$$\overline{U^2} = \frac{\sqrt{\pi}}{4} \quad \frac{\alpha}{\sqrt{\beta}} \quad U_{WIND}^2 \qquad \text{B.5}$$

For a Rayleigh distribution of particle velocity amplitudes, we have

$$U_s^2 = 2\,\overline{U^2} \qquad \text{B.6}$$

Hence $$U_s = f\, U_{WIND} \qquad \text{B.7}$$

where* $$f = \left[\frac{\pi \alpha^2}{4\beta}\right]^{\frac{1}{4}} \qquad \text{B.8}$$

If the heights of waves are Rayleigh distributed then it can be shown that the significant wave height H_s is related to the mean square amplitude $\overline{a^2}$ (see Equation B.1) by

$$H_s = \sqrt{\frac{2\alpha}{\beta}} \quad \frac{U_{WIND}^2}{g} \qquad \text{B.9}$$

From Equations B.5 and B. 9, it can be shown that

$$\overline{U^2} = \sqrt{\frac{\alpha \pi}{32}} \quad g H_s \qquad \text{B.10}$$

The modal frequency, ω_o, is that frequency at which the energy density is highest, that is:

$$\left.\frac{de(\omega)}{d\omega}\right]_{\omega = \omega_o} = 0 \qquad \text{B.11}$$

*With the α and β values corresponding to Pierson-Moskowitz spectrum f = 0.129

using the equation B.2 for $e(\omega)$, it can be shown that

$$\frac{1}{e(\omega)} \frac{de(\omega)}{d\omega} = 0 = -\frac{5}{\omega_0} + \frac{4\beta}{\omega_0} \left(\frac{g}{\omega_0 U_{WIND}} \right)^4$$

Hence

$$\frac{U_{WIND}\,\omega_0}{g} = \left[\frac{4}{5} \beta \right]^{1/4} \qquad \text{B.12}$$

APPENDIX C

EVALUATION OF STRAIN RATES IN AN OIL FILM SUBJECTED TO A SIMPLE TRAVELING WAVE

Objective:

The objective of the analysis presented in this appendix is to obtain the strain rates in a thin film of oil subjected to the action of a traveling wave.

Analysis:

Section C.1: Evaluation of Oil Film Length Changes

Let us consider an oil film present on a calm body of water. We concentrate our analysis on a length $\frac{\lambda}{2}$ of this oil film. Let P_1', P_2' . . . P_9' be oil "particles" located equally spaced on this length whose x-coordinate positions are designated by $x_1^{(i)}$, $x_2^{(i)}$ . . . This situation is schematically illustrated in Figure C.1a.

Let now this oil slick be subjected to a travelling wave of wavelength λ. The oil particles move along circles of radius "a" which is the amplitude of the wave (see Lamb, 1932, page 368). Figure C.1b represents a condition in which particle P_1 is at the crest of the wave, particle P_9 is at the trough of the wave, and P_5 is at the level of the undisturbed slick. The profile lengths P_1P_5 and P_5P_9 need to be calculated and compared with initial lengths $P_1'P_5'$ and $P_5'P_9'$.

From the small amplitude potential wave theory (see Lamb, 1932, Ch. IX. p. 368), for the disturbed position of a particle on the wave, we have:

$$x(t) = x_i - a \sin(kx_i - \omega t) \qquad \text{C.1}$$

$$y(t) = y_i + a \cos(kx_i - \omega t) \qquad \text{C.2}$$

where (x,y) are the coordinates of a particle of oil (which is the same as that of the water surface particle) whose initial coordinates before being

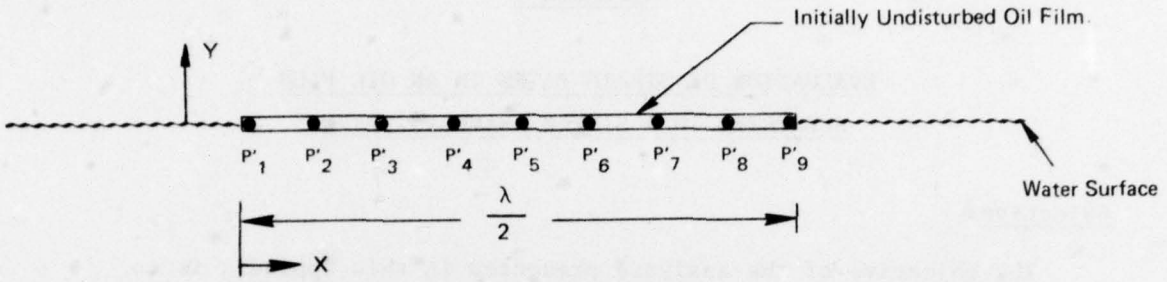

FIGURE C–1a SCHEMATIC REPRESENTATION OF AN OIL SLICK NOT SUBJECTED TO WAVE ACTION, INDICATING THE POSITIONS OF EQUALLY-SPACED POINTS IN A LENGTH λ/2.

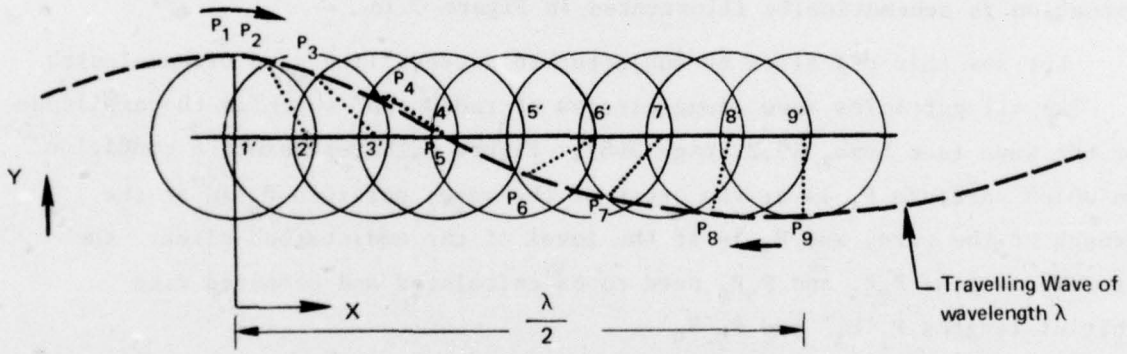

LENGTH BETWEEN P_1 AND P_5 IS UNDER COMPRESSION AND BETWEEN P_5 AND P_9 IS STRETCHED

FIGURE C–1b POSITIONS OF THE PARTICLES AFTER BEING SUBJECTED TO A PROGRESSIVE WAVE OF WAVELENGTH λ

disturbed by the wave are (x_i, y_i). Also κ is the wave number $(2\pi/\lambda)$ and ω is the radian frequency of the wave.

The length of the oil film at any time instant t is given by

$$dl = \sqrt{[d(x(t))]^2 + [dy(t)]^2} \; ; \qquad \text{C.3}$$

i.e., $$\frac{dl}{dx_i} = \sqrt{\left(\frac{dx}{dx_i}\right)^2 + \left(\frac{dy}{dx_i}\right)^2} \qquad \text{C.4}$$

Substituting Equations C.1 and C.2 and C.4 and simplifying, we get

$$\frac{dl}{dx_i} = \sqrt{[1+(ak)^2] - 2ak\cos(\kappa x_i - \omega t)} \qquad \text{C.5}$$

The picture shown in Figure C.1b corresponds to t = 0. (This can be easily seen by substituting t = 0 and obtaining the positions of particles P_1 through P_9 from Equations C.1 and C.2.) Therefore, substituting t = 0 in Equation C.5, for the specific condition represented by Figure C.1b, we get:

$$\left(\frac{dl}{dx_i}\right)_{t=0} = \sqrt{[1+(ak)^2] - 2ak\cos(\kappa x_i)} \qquad \text{C.6}$$

Let

$$\ell_1 = \text{length } P_1P_5 \qquad \text{C.7}$$

$$\ell_2 = \text{length } P_5P_9$$

Hence, integrating equation C-6, we have:

$$\ell_1 = \int_{x_i=0}^{\lambda/4} \sqrt{1+(ak)^2 - 2ak\cos kx_i}\; dx_i \qquad \text{C.8}$$

$$\ell_2 = \int_{x_i=\frac{\lambda}{4}}^{\frac{\lambda}{2}} \sqrt{1+(ak)^2 - 2ak\cos kx_i}\; dx_i \qquad \text{C.9}$$

Simplifications of Equations C.8 and C.9

Noting that $ak = \pi \frac{2a}{\lambda} = \pi S$ which is a measure of the wave steepness, we define the following parameters:

$$\theta = kx_i \qquad \text{C.10}$$

$$A = \frac{1+(ak)^2}{2ak} = \frac{1+(\pi S)^2}{2\pi S} > 1 \qquad \text{C.11}$$

= wave steepness parameter

$$L = \frac{k\ell}{\sqrt{2ak}} = \text{dimensionless length} \qquad \text{C.12}$$

Substituting equations C.10 through C.12 into C.8 and C.9, and after some algebraic manipulations, we get

$$L_1 = \frac{K\ell_1}{\sqrt{2ak}} = \int_{\theta=0}^{\pi/2} \sqrt{A - \cos\theta}\ d\theta \qquad \text{C.13}$$

$$L_2 = \frac{K\ell_2}{\sqrt{2ak}} = \int_{\phi=0}^{\pi/2} \sqrt{A + \cos\phi}\ d\phi \qquad \text{C.14}$$

The above two integrals can be expressed in terms of incomplete elliptic functions of the second kind and the details are given in Section C.3 of this appendix. Incomplete elliptic functions are tabulated by Abramowitz and Stegun (1964, page 616) for various values of the parameters.

Table C.1 indicates the calculation of L_1 and L_2 for various values of the steepness ratio $\frac{2a}{\lambda}$.

Also presented in the table are the values of percent of contraction and percent of stretching of the film. These are defined by

$$\% \text{ Contraction} = \frac{\ell_1 - \frac{\lambda}{4}}{\lambda/4} \times 100 = 100\left[\sqrt{\frac{8}{\pi}S}\ L_1 - 1\right] \qquad \text{C.15}$$

$$\% \text{ Expansion} = \frac{\ell_2 - \lambda/4}{\lambda/4} \times 100 = 100\left[\sqrt{\frac{8}{\pi}S}\ L_2 - 1\right] \qquad \text{C.16}$$

where S is the steepness ratio, given by $S = \frac{\lambda}{2a}$ C.17

The variations in % contraction and % stretching with the wave steepness are shown in Figure C.2.

Table C.1

Calculations of the Stretching and Contraction of Oil Film Length Due to a Traveling Wave

Wave Steepness Ratio $S=\frac{2a}{\lambda}$	$A=\frac{1+(\pi S)^2}{2\pi S}$	Δ In Degrees	ν In Degrees	Eliptic Functions		L_1	L_2	% Contraction	% Stretching
				$E(\Delta,\nu)$	$E(\pi/4,\nu)$				
$\frac{1}{30}$	4.827	50.978	35.864	0.8387	0.760	3.139	3.669	- 8.546	6.895
$\frac{1}{20}$	3.262	53.927	43.24	0.899	0.7495	2.605	3.095	- 7.063	10.424
$\frac{1}{15}$	2.492	56.829	49.182	0.918	0.743	2.164	2.777	-10.839	14.414
$\frac{1}{10}$	1.749	62.441	58.541	0.953	0.729	1.649	2.417	-16.844	21.987
$\frac{1}{7}$	1.338	69.170	67.638	0.992	0.720	1.305	2.202	-21.313	32.802

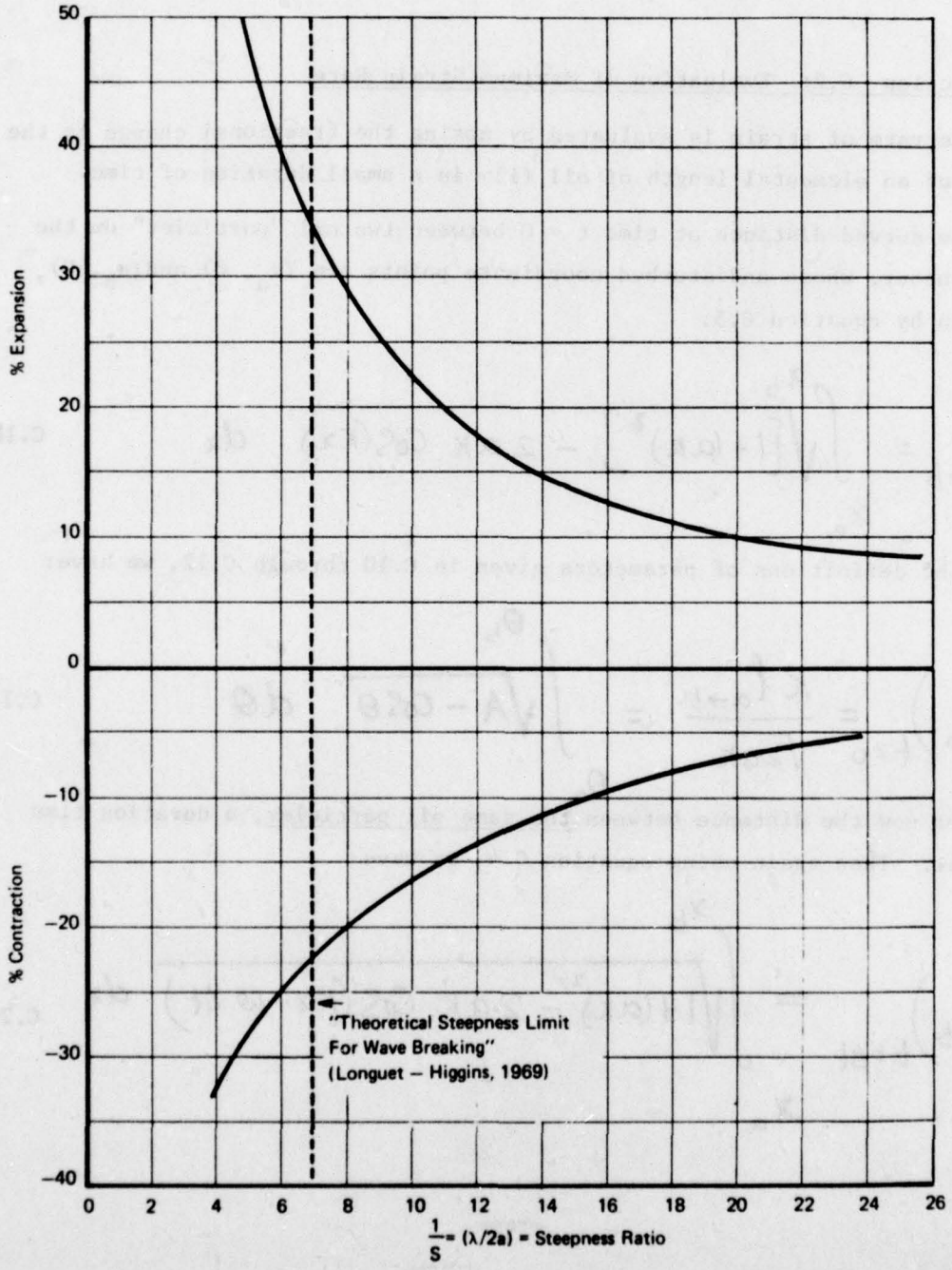

FIGURE C.2 VARIATION OF THE FRACTIONAL CONTRACTION AND STRETCHING OF OIL FILM WITH WAVE STEEPNESS

Section C.2: Evaluation of Maximum Strain Rate

The rate of strain is evaluated by noting the fractional change in the length of an elemental length of oil film in a small duration of time.

The curved distance at time t = 0 between two oil "particles" on the wave contour, whose undisturbed coordinate points are $(x_a, 0)$ and $(x_b, 0)$, is given by equation C.5:

$$\ell_{a\to b} = \int_{x_a}^{x_b} \sqrt{\left[1+(ak)^2\right] - 2ak\cos(kx)}\; dx \qquad \text{C.18}$$

Using the definitions of parameters given in C.10 through C.12, we have:

$$\left(L_{a\to b}\right)_{t=0} = \frac{k\,\ell_{a\to b}}{\sqrt{2ak}} = \int_{\theta_a}^{\theta_b} \sqrt{A-\cos\theta}\; d\theta \qquad \text{C.19}$$

Consider now the distance between the same oil particles, a duration time Δt later. Then again using equation C.4, we have

$$\left(\ell_{a\to b}\right)_{t=\Delta t} = \int_{x_a}^{x_b} \sqrt{1+(ak)^2 - 2ak\cos(kx-\omega\,\Delta t)}\; dx \qquad \text{C.20}$$

or

$$\left(L_{a\to b}\right)_{t=\Delta t} = \frac{\kappa\left(l_{a\to b}\right)_{\Delta t}}{\sqrt{2a\kappa}} = \int_{\theta_a}^{\theta_b} \sqrt{A - \cos(\theta - \omega\Delta t)} \qquad \text{C.21}$$

Hence,

$$\text{strain rate} = \Gamma = \frac{1}{\Delta t}\left[\frac{\text{final length}}{\text{initial length}} - 1\right] \qquad \text{C.22}$$

i.e.,

$$\Gamma = \lim_{\Delta t \to 0} \frac{1}{\Delta t}\left[\frac{\left(L_{a\to b}\right)_{\Delta t}}{\left(L_{a\to b}\right)_{t=0}} - 1\right] \qquad \text{C.23}$$

We consider the points a and b very close to each other (i.e., the length of film between them is very small).

Hence,

$$\left.\begin{aligned} \left(L_{a\to b}\right)_{t=0} &= \sqrt{A - \cos\theta}\; d\theta \\ \left(L_{a\to b}\right)_{t=\Delta t} &= \sqrt{A - \cos(\theta - \omega\Delta t)}\; d\theta \end{aligned}\right\} \qquad \text{C.24}$$

Substituting C.24 in C. 23 and expanding cos $(\theta - \omega\,\Delta t)$ and simplifying, we get

$$\Gamma(\theta) = \lim_{\Delta t \to 0} \frac{1}{\Delta t} \left\{ \sqrt{1 - \omega\,\Delta t \frac{\sin\theta}{(A - \cos\theta)}} - 1 \right\}$$

$$\Gamma(\theta) = -\frac{1}{2}\,\omega\,\frac{\sin\theta}{(A - \cos\theta)} \qquad \text{C.25}$$

Equation C.25 indicates that strain rate is proportional to ω and varies with θ (which is essentially a measure of the position of the particle in the undisturbed slick).

In fact equation C.25 can be generalized to any time t as

$$\Gamma(\theta, t) = -\frac{1}{2}\,\omega\,\frac{\sin(\theta - \omega t)}{[A - \cos(\theta - \omega t)]} \qquad \text{C.26}$$

The right hand side function of equation C.25 has a maximum value for a given angle θ. It is shown in Section C.4 of this appendix that the maximum value of the tensile strain rate occurs at

$$\theta = \pi - \cos^{-1}\left(\frac{1}{A}\right) \qquad \text{C.27}$$

where the principal value of the $\cos^{-1}$ is used.

The maximum tensile strain rate is

$$\Gamma_{\substack{max \\ tensile}} = \frac{\omega}{2}\,\frac{1}{\sqrt{A^2 - 1}} \qquad \text{C.28}$$

Section C.3: Expressions for the integrals etc. in terms of standard mathematical functions.

In this section, the mathematical formulae derived in the earlier sections are expressed in terms of standard mathematical functions.

$$L_1 = \int_0^{\pi/2} \sqrt{A - \cos\theta}\, d\theta \qquad A > 1 \text{ (See equation C.13)} \qquad \text{C.29}$$

Referring to equation (2), §2.576, page 156 of Gradshteyn and Rhyzik (1965), we have

$$L_1 = \left[2\sqrt{A+1}\; E(\delta, \nu) - \frac{2\sin\theta}{\sqrt{A-\cos\theta}} \right]_{\theta=0}^{\pi/2} \qquad \text{C.30}$$

where

$$\delta = \sin^{-1}\sqrt{\left[\frac{(A+1)(1-\cos\theta)}{2(A-\cos\theta)}\right]} \qquad \text{C.31}$$

$$\nu = \sin^{-1}\sqrt{\frac{2}{(1+A)}} \qquad \text{C.32}$$

and E (δ, ν) = incomplete elliptic function of the second kind defined by (see page 905 of the above reference)

$$E(\delta, \nu) = \int_{\alpha=0}^{\delta} \sqrt{1 - \sin^2\nu \sin^2\alpha}\; d\alpha \qquad \text{C.33}$$

Hence, equation C.30 becomes

$$L_1 = \left[2\sqrt{A+1}\; E(\Delta, \nu) - \frac{2}{\sqrt{A}} \right] \qquad \text{C.34}$$

where

$$\Delta = \sin^{-1} \sqrt{\frac{1+A}{2A}} \qquad \text{C.35}$$

and ν is defined by equation C.32.

The equation C.14 is expressed by

$$L_2 = \int_0^{\pi/2} \sqrt{A + \cos\theta}\; d\theta \qquad \text{C.36}$$

Referring to equation (1), §2.576 of page 156 in Gradshteyn and Rhyzik (1965), the above expression can be written as

$$L_2 = \left[2\sqrt{(1+A)}\; E\left(\frac{\theta}{2}, \nu\right) \right]_{\theta=0}^{\pi/2} \qquad \text{C.37}$$

i.e.,

$$L_2 = 2\sqrt{(1+A)}\; E\left(\pi/4, \nu\right) \qquad \text{C.38}$$

Section C.4 : Determination of the maximum strain rate -- Mathematical details

From equation C.25, we find that

$$\Gamma(\theta) = -\frac{\omega}{2} \frac{\sin\theta}{(A-\cos\theta)} \; ; \; A > 1 \qquad \text{C.39}$$

Let

$$\epsilon(\theta) = \frac{2}{\omega}\Gamma(\theta) = -\frac{\sin\theta}{(A-\cos\theta)} \qquad \text{C.40}$$

Therefore ,

$$\frac{d\epsilon}{d\theta} = \frac{1-A\cos\theta}{(A-\cos\theta)^2} \qquad \text{C.41}$$

Hence, maximum value of ϵ occurs at $\theta = \theta^*$, where

$$\cos\theta^* = \frac{1}{A} \qquad \text{C.42}$$

Now,

$$\frac{d^2\epsilon}{d\theta^2} = \frac{(A-\cos\theta)A\sin\theta - 2\sin\theta(1-A\cos\theta)}{(A-\cos\theta)^3} \qquad \text{C.43}$$

Substituting equation C.42 in C.45, we have

$$\left(\frac{d^2\epsilon}{d\theta^2}\right)_{\theta=\theta^*} = \pm \left[\frac{A}{(A^2-1)}\right]^2 \sqrt{(A^2-1)} \qquad \text{C.44}$$

Where the plus sign should be taken with the principal value of θ^* from equation C.42 and the minus sign with the first harmonic value (i.e., $\pi - \theta^*$).

Hence, maximum strain rate occurs at

$$\dot{\theta} = \theta^* = \cos^{-1}\left(\frac{1}{A}\right) \qquad 0 \leq \theta^* \leq \pi/2 \qquad \text{C.45}$$

and its value is (substituting equation C.33 in C.30 and simplifying)

$$\dot{\Gamma}_{max} = \pm \frac{\omega}{2} \frac{1}{\sqrt{(A^2-1)}} \qquad \text{C.46}$$

where plus sign implies stretching and minus sign implies compression.

Note that the stretching maximum occurs at $\theta = (\pi - \theta^*)$ where θ^* is the principal value of equation C.42.

APPENDIX D

EVALUATION OF THE PROBABILITY THAT N SLOTS OCCURRING SIMULTANEOUSLY BUT LOCATED AT RANDOM WILL FORM A CUT OF TOTAL LENGTH L

SUMMARY

The probability that N simultaneous breaking waves, occurring within an oil slick of width L, will form a continuous cut across the slick is determined in this appendix. The analysis developed is restricted to the case of one dimension and N less than 10.

The results indicate that the probability of fracture is sensitive to the ratio of the width of oil slick to the root mean square crest length of the waves.

ANALYSIS

The problem is analyzed by considering an analogous one dimensional problem. The analogy is with sticks and slots.

The problem can then be posed as follows:

"A slot of fixed length L and N sticks of various lengths are given. The sticks are dropped at random along the length of the slot (sticks are arranged to be collinear with the slot). What is the probability that the N sticks taken together will bridge the length of the slot L?"

A schematic representation of the problem with N = 3 is shown in Figure D.1. It is noted that whenever the center of a stick lies within the length L of the slot, the stick is considered in the calculation. A bridge (or cut in the case of oil) is said to occur if one or more of the N sticks (waves) cover the whole length of the slot.

A bridge can occur with a single stick, two sticks, three sticks, or a combination thereof. The number of possibilities increases very rapidly as the number of sticks considered increases. It may be stated qualitatively, that the probability of bridging (or cutting the slick) increases as the number of sticks (waves) increases. Given below is an analysis to determine quantitatively the probability.

We define the following probabilities:

P_i^0 the probability that i sticks will bridge the slot, using up all the sticks to do so (no stick can be removed without eliminating the bridge).

P_i the probability that i sticks will bridge the slot; includes the chances that a single stick will make a bridge, the chances that a pair will, etc. D.1

Clearly, therefore, the probability that one stick will bridge the slot is identical to the probability a single stick alone will bridge the slot. That is:

$$P_1 = P_1^0 \qquad \text{D.2}$$

We consider now the case of two sticks. Since P_1^0 is the probability that a single stick will bridge the gap, $(1 - P_1^0)$ is the chance that a single stick will not bridge the slot. Hence,

the probability that either of the two sticks individually will not bridge the slot. $= (1 - P_1^0)^2$

Similarly, the probability that both sticks together will not bridge the slot. $= (1 - P_2^0)$

Therefore, the combined probability that the two sticks, either individually or combined will not bridge the slot. $= (1 - P_1^0)^2 (1 - P_2^0)$

Noting the definition of P_2 from equation D.1, and noting the above discussions we get

$$P_2 = 1 - (1-P_2^0)(1-P_1^0)^2 \qquad \text{D.3}$$

where the right-hand side represents the probability that a bridge will occur by either single sticks or their combination.

By induction, a similar formula can be derived for other numbers of sticks. For the general case of N sticks, it can be shown by similar arguments that,

$$P_N = 1 - (1-P_1^0)^N (1-P_2^0)^{\frac{N(N-1)}{2!}} (1-P_3^0)^{\frac{N(N-1)(N-2)}{3!}} \ldots\ldots \qquad \text{D.4}$$

The exponents on the individual probability terms (i.e., terms such as $N(N-1)/2!$) in the above formula represent the total number of ways in which N sticks can be arranged when taken two at a time, three at a time, etc. These exponents are simply the binomial coefficients. The values for these exponents are given in table D-1 for different values of N between 1 and 10.

We now make an assumption* that the probability that N sticks together bridge the slot and N-1 do not is very small for any $N > 2$. For example, if 8 sticks together bridge the gap, chances are that just 7 of them may also bridge the gap. In other words, the probability that 8 bridge the gap and 7 do not is rather small. The mathematical expression of this assumption is given by:

$$P_N^0 \ll 1 \qquad \text{for} \quad N>2 \qquad \text{D.5}$$

Based on the above approximation equation, D.4 is reduced to

$$P_N \simeq 1 - (1-P_1^0)^N (1-P_2^0)^{\frac{N(N-1)}{2}} \qquad \text{D.6}$$

* The justification for this assumption is that not only is the phenomenon physically possible, but that the assumption leads to considerable simplification in the mathematical analysis.

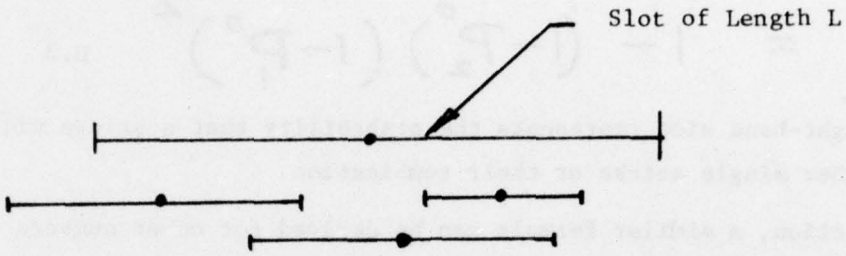

FIGURE D.1: ILLUSTRATION OF STICKS AND SLOT MODEL WITH 3 STICKS AND SLOT OF LENGTH L

Table D-1

Values of Binomial Coefficients

	N	$\frac{N(N-1)}{2!}$	$\frac{N(N-1)(N-2)}{3!}$	$\frac{N(N-1)(N-2)(N-3)}{4!}$	$\frac{N(N-1)(N-2)(N-3)(N-4)}{5!}$
N = 1	1				
2	2	1			
3	3	3	1		
4	4	6	4	1	
5	5	10	10	5	1
6	6	15	20	15	6
7	7	21	35	35	21
8	8	28	56	70	56
9	9	36	84	126	126
10	10	45	120	210	252

Once the values of P_1^0 and P_2^0 are determined the total probability P_N can be determined from the above equation.

DETERMINATION OF P_1^0 AND P_2^0

In order to determine the above probabilities it is necessary to know the distribution of lengths of sticks. We assume that the stick lengths are Rayleigh distributed. That is,

$$p(x) = \frac{2x}{\overline{\ell^2}} \exp\left(-\frac{x^2}{\overline{\ell^2}}\right) \qquad \text{D.7}$$

where

$p(x)$ = probability density of the length being between x and $x + dx$.

$\overline{\ell^2}$ = mean square length of the sticks (or waves)

x = length of the stick.

Integrating $p(x)\,dx$ between any limits, say between x_1 and x_2, gives the probability that a given stick will have a length between x_1 and x_2. That is:

$$P(x_1 : x_2) = \int_{x_1}^{x_2} \frac{2x}{\overline{\ell^2}} \exp\left(-\frac{x^2}{\overline{\ell^2}}\right) dx \qquad \text{D.8}$$

$P(x_1 : x_2)$: Probability that the stick length is between x_1 and x_2.

We now define a parameter

$$\alpha = \frac{L}{\sqrt{\overline{\ell^2}}} \qquad \text{D.9}$$

α is the length of the slot expressed as a multiple of the r.m.s. length of the stick size distribution.

EVALUATION OF P_1^0

A single stick will bridge the slot* if its length is sufficient to cover the slot of length L and the center of the stick lies within the slot. These two conditions can be satisfied in the following ways:

i) stick length (x) is greater than 2L

ii) stick length is between L and 2L and the stick center lies in a region of width (x - L) centered at L/2.

We note that no bridging occurs if $x < L$.

The probability P_1^0 is then given by:

$$P_1^0 = \underbrace{P\ (x \geq 2L)}_{\text{Probability that stick length is larger than 2L}} + \underbrace{P(L \leq x \leq 2L/\text{center within L})}_{\text{Probability that stick length is between L and 2L and that its center is within the slot.}} \quad \text{D.10}$$

Now

$$P(x \geq 2L) = \int_{2L}^{\infty} \frac{2x}{l^2} \exp\left(-\frac{x^2}{l^2}\right) = e^{-4\alpha^2} \quad \text{D.11}$$

Assuming that the position of the stick center is equally likely to be located at any point within the slot length L, the probability that the stick center will lie in a region of width (x - L) is equal to (x - L)/L.

Therefore, the probability that the center is within the slot and that the length of the stick is between L and 2L is given by:

---

* It is implicitly assumed that the center of the stick falls always within the slot. If this is not satisfied, only that length of the stick which laps over the slot is considered in the counting.

$$P(L \le x \le 2L \mid \text{center within } L) = \int_{L}^{2L} \frac{(x-L)}{L} \frac{2x}{\ell^2} \exp\left(-\frac{x^2}{\ell^2}\right) dx \qquad \text{D.12}$$

$$= -e^{-4\alpha^2} + \frac{\sqrt{\pi}}{2\alpha}\left[\text{erf}(2\alpha) - \text{erf}(\alpha)\right]$$

Substituting D.11 and D.12 in D.9 we get:

$$P_1^0 = \frac{\sqrt{\pi}}{2\alpha}\left[\text{erf}(2\alpha) - \text{erf}(\alpha)\right] \qquad \text{D.13}$$

EVALUATION OF P_2^0

The evaluation of P_2^0 contains two steps. First the probability of bridging gap L with the length of stick #1 being less than L is evaluated. Secondly, the probability of bridging when the length of stick #1 is between L and 2L is determined. The total probability of bridging with both sticks 1 and 2 being necessary is then the sum of the above two probabilities. It is noted that the probability of length of stick #1 being larger than 2L is not considered because then stick #1 is itself enough to bridge the gap. Such a possibility is not taken into account in defining P_2^0. Therefore,

$$P_2^0 = \underbrace{P(x_1 \le L)}_{\text{Probability that with the length } x_1 \text{ of stick \#1 being less than L, the slot is bridged.}} + \underbrace{P(L \le x_1 \le 2L)}_{\text{Probability that with the length } x_1 \text{ of stick \#1 being between L and 2L the slot is bridged}} \qquad \text{D.14}$$

Each of the probability terms on the right-hand side of the above equation contains three subsets as described below.

Case 1: Length x_1 of stick #1 is less than or equal to L.

The probability that some part of stick #1 touches one end or the other of the slot is x_1/L.

Case 1a: Length x_2 of stick #2 satisfies the following constraints.

$$\left.\begin{aligned} x_2 &\le L \\ x_1 + x_2 &\le 2L \end{aligned}\right\} \qquad \text{D.15}$$

Note that if $x_1 + x_2 < L$, no bridging of the slot is possible. The chance that the stick #2 touches the other end of the slot is $x_2/2L$. Given this arrangement, the chance that sticks 1 and 2 overlap and bridge the slot is given by:

$$\text{Overlap chance} = \frac{\text{max separation of centers to cut - min separation of centers to cut}}{\text{max separation of centers - min separation of centers}}$$

$$= \frac{\frac{x_1+x_2}{L} - \left(L - \frac{x_1+x_2}{2}\right)}{L - \left(L - \frac{x_1+x_2}{2}\right)} = \frac{2(x_1+x_2-L)}{(x_1+x_2)} \qquad \text{D.16}$$

Let

P_{1a} = Probability that a bridging of the slot occurs under the above subcase condition,

then

$$P_{1a} = \int_0^L \frac{2x_1\,dx_1}{l^2}\ \frac{x_1}{L}\, e^{-\frac{x_1^2}{l^2}} \int_{L-x_1}^{L} \frac{2x_2\,dx_2}{l^2}\ \frac{x_2}{2L}\ \frac{2(x_1+x_2-L)}{(x_1+x_2)}\, e^{-\frac{x_2^2}{l^2}} \qquad \text{D.17a}$$

$$= \frac{4}{\alpha^2} \int_0^{\alpha} \phi_1^2\, e^{-\phi_1^2}\, d\phi_1 \int_{\alpha-\phi_1}^{\alpha} \phi_2^2\ \frac{(\phi_1+\phi_2-\alpha)}{(\phi_1+\phi_2)}\, e^{-\phi_2^2}\, d\phi_2 \qquad \text{D.17b}$$

Subcase 1b: Length x_2 of stick #2 satisfies:

$$\left.\begin{aligned} L \le x_2 \le 2L \\ x_1 + x_2 = 2L \end{aligned}\right| \qquad \text{D.18}$$

The stick #2 cannot bridge the slot alone. The chance that stick #2 touches the other end of the slot only is equal to $(2L - x_2)/(2L)$. The chance that sticks 1 and 2 overlap is the same as given in subcase 1a. Hence, the probability P_{1b} of bridging the slot together is given by

$$P_{1b} = \int_0^L \frac{2x_1\,dx_1}{\ell^2}\,\frac{x_1}{L}\,e^{-x_1^2/\ell^2} \int_L^{2L-x_1} \frac{2x_2}{\ell^2}\,\frac{(2L-x_2)}{2L}\,\frac{2(x_1+x_2-L)}{(x_1+x_2)}\,e^{-x_2^2/\ell^2}\,dx_2 \qquad \text{D.19a}$$

$$= \frac{4}{\alpha^2}\int_0^{\alpha} \phi_1^2 e^{-\phi_1^2}\,d\phi_1 \int_{\alpha}^{2\alpha-\phi_1} \phi_2(2\alpha-\phi_2)\,\frac{(\phi_1+\phi_2-\alpha)}{(\phi_1+\phi_2)}\,e^{-\phi_2^2}\,d\phi_2 \qquad \text{D.19b}$$

Subcase 1c: Length x_2 of stick #2 satisfies

$$\left.\begin{aligned} L \le x_2 \le 2L \\ x_1 + x_2 > 2L \end{aligned}\right| \qquad \text{D.20}$$

The chance that stick 2 touches the other end of the slot is the same as given in 1a. In this configuration the sticks always overlap. The probability P_{1c} that a bridging of the slot occurs is given by:

$$P_{1c} = \int_0^L \frac{2x_1\,dx_1}{\ell^2}\,\frac{x_1}{L}\,e^{-\frac{x_1^2}{\ell^2}} \int_{2L-x_1}^{2L} \frac{2x_2\,dx_2}{\ell^2}\,\frac{(2L-x_2)}{2L}\,e^{-x_2^2/\ell^2} \qquad \text{D.21a}$$

$$= \frac{2}{\alpha^2}\int_0^{\alpha} \phi_1^2 e^{-\phi_1^2} \int_{2\alpha-\phi_1}^{2\alpha} \phi_2(2\alpha-\phi_2)\,e^{-\phi_2^2}\,d\phi_1\,d\phi_2 \qquad \text{D.21b}$$

Therefore, the total probability of bridging when $x_1 < L$ is obtained from equations D.17a, D.19a, and D.21a. This is given by:

$$P(x_1 \leq L) = P_{1a} + P_{1b} + P_{1c} \qquad \text{D.22}$$

Case 2: Length x_1 of stick #1 satisfies $L \leq x_1 \leq 2L$.

The probability that stick #1 touches one end of slot is $(2L - x_1)/2L$. As before in this case also there are 3 subcases to consider.

Subcase 2a: Length x_2 of slick 2 satisfies:

$$x_2 \leq L$$

$$L \leq x_1 + x_2 \leq 2L \qquad \text{D.23}$$

Then the probability P_{2a} of bridging the slot is given by:

$$P_{2a} = \int_L^{2L} \frac{2x_1\,dx_1}{\ell^2} \; \frac{2L-x_1}{L} \; e^{-\frac{x_1^2}{\ell^2}} \int_0^{2L-x_1} \frac{2x_2\,dx_2}{\ell^2} \; \frac{x_2}{2L} \; \frac{2(x_1+x_2-L)}{(x_1+x_2)} \times e^{-\frac{x_2^2}{\ell^2}} \qquad \text{D.24a}$$

$$= \frac{4}{\alpha^2} \int_\alpha^{2\alpha} \phi_1(2\alpha-\phi_1)\, e^{-\phi_1^2} \int_0^{2\alpha-\phi_1} \phi_2^2 \; \frac{\phi_1+\phi_2-\alpha}{\phi_1+\phi_2} \; e^{-\phi_2^2}\, d\phi_1\, d\phi_2 \qquad \text{D.24b}$$

Subcase 2b: Stick #2 length x_2 satisfies:

$$x_2 \leq L$$

$$x_1 + x_2 \geq 2L \qquad \text{D.25}$$

The probability P_{2b} of bridging is given by

$$P_{2b} = \int_{L}^{2L} \frac{2x_1\,dx_1}{\ell^2}\,\frac{2L-x_1}{L}\,e^{-\frac{x_1^2}{\ell^2}} \int_{2L-x_1}^{L} \frac{2x_2\,dx_2}{\ell^2}\,\frac{x_2}{2L}\,e^{-\frac{x_2^2}{\ell^2}} \qquad \text{D.26a}$$

$$\frac{2}{\alpha^2}\int_{\alpha}^{2\alpha} \phi_1\,(2\alpha-\phi_1)\,e^{-\phi_1^2} \int_{2\alpha-\phi_1}^{\alpha} \phi_2^2\,e^{-\phi_2^2}\,d\phi_1\,d\phi_2 \qquad \text{D.26b}$$

Subcase 2c: Length x_2 of stick #2 satisfies

$$L \le x_2 \le 2L \qquad \text{D.27}$$

$$x_1 + x_2 \ge 2L$$

The bridging probability P_{2c} is given by

$$P_{2c} = \int_{L}^{2L} \frac{2x_1\,dx_1}{\ell^2}\,\frac{2L-x_1}{L}\,e^{-\frac{x_1^2}{\ell^2}} \int_{\alpha L}^{2L} \frac{2x_2}{\ell^2}\,dx_2\,\frac{(2L-x_1)}{2L}\,e^{-\frac{\dot{x}_2^2}{\ell^2}} \qquad \text{D.27a}$$

$$= \frac{2}{\alpha^2}\int_{\alpha}^{2\alpha} \phi_1\,(2\alpha-\phi_1)\,e^{-\phi_1^2} \int_{\alpha}^{2\alpha} \phi_2\,(2\alpha-\phi_2)\,e^{-\phi_2^2}\,d\phi_1\,d\phi_2 \qquad \text{D.27b}$$

From the above results the probability of bridging of the slot when $L \leq x_1 < 2L$ can be determined using the formula:

$$P(L \leq x_1 \leq 2L) = P_{2a} + P_{2b} + P_{2c} \qquad \text{D.29}$$

Using equations D.14, D.22, and D.29, P_2^0 can be determined.

NUMERICAL VALUES

The values of P_1^0, P_2^0, and P_N have been obtained from equations D.13, D.14, and D.6, respectively, for a range of values of N from 1 through 10. Six values of α have been considered ($\frac{1}{\alpha}$ varies from 0.4 to 0.9 in intervals of 0.1). The results obtained are shown in table D-2.

Two values are given for each value of N and α. The first number gives the total probability of bridging the gap with a N stick system. The second number gives a dimensionless time (τ_N) for achieving the closure of the slot. This time is defined by:

$$\tau_N = \frac{-1}{\ln(1-P_N)} \qquad \text{D.30}$$

We also note that the P_N values obtained by the approximation represented by equation D.6 gives the lower bound for the numerical value of P_N. This is because all of the truncated term of the factors in equation D.5 are all smaller than unity.

Table D-2

Values of P_N and τ_N Calculated from the Truncated Series*

	α =	1.1111	1.2500	1.4286	1.6667	2.0000	2.5000
P10		0.092276	0.054778	0.026984	0.009819	0.002075	0.000144
P20		0.137530	0.119347	0.091146	0.057177	0.025947	0.006450
N = 1	P_N =	0.092276	0.054778	0.026984	0.009819	0.002075	0.000144
	τ_N =	10.3290	17.7507	36.5563	101.3414	481.3984	6929.8701
2		0.289356	0.213186	0.139534	0.075002	0.029986	0.006737
		2.9275	4.1708	6.6542	12.7206	32.8467	147.9335
3		0.520163	0.423213	0.308422	0.186357	0.081581	0.019651
		1.3618	1.8173	2.7116	4.8489	11.7507	50.3873
4		0.720565	0.627639	0.494824	0.324791	0.152995	0.038638
		0.7843	1.0123	1.4645	2.5463	6.0223	25.3781
5		0.859651	0.788302	0.664619	0.471709	0.239124	0.063358
		0.5093	0.6441	0.9153	1.5671	3.6592	15.2828
6		0.939203	0.894007	0.797639	0.610294	0.334230	0.093290
		0.3571	0.4456	0.6259	1.0612	2.4581	10.2111
7		0.977286	0.953265	0.889829	0.728961	0.432564	0.127946
		0.2642	0.3264	0.4549	0.7660	1.7648	7.3044
8		0.992681	0.981853	0.944692	0.822272	0.528923	0.166687
		0.2034	0.2494	0.3454	0.5789	1.3265	5.4841
9		0.997966	0.993794	0.974947	0.890122	0.619067	0.208844
		0.1614	0.1968	0.2712	0.4528	1.0361	4.2688
10		0.999512	0.998131	0.989686	0.935953	0.699953	0.253712
		0.1311	0.1592	0.2186	0.3639	0.8307	3.4171

* $P_N = 1 - (1 - P_1^0)^N \; (1 - P_2^0)^{\frac{N(N-1)}{2}}$ $\qquad \tau_N = -1/\ln (1 - P_N)$

APPENDIX E

TIME AVERAGED TURBULENT KINETIC ENERGY IN WATER SUBJECTED TO REPEATED BREAKING WAVE ACTION

In this appendix, the details of derivation are given to calculate the steady state turbulent intensity in the upper levels of the ocean, when the turbulence is generated by a series of breaking waves equally spaced in time. The application of this result has been discussed in section 4.3.5.

Analysis

Let us consider an ocean, where breaking waves occur every T seconds.

Let the energy dissipation/breaker (in the breaking regions) per unit area be $= E''$ E.1

Average rate of energy input to turbulence per unit area per unit time $= \dot{E}'' = \frac{E''}{T}$ E.2

Let $\bar{e}$ = time averaged kinetic energy of turbulence per unit volume

Hence the equation for spatial variation of time averaged turbulence is

$$D \frac{d^2 \bar{e}}{dz^2} = \epsilon = \frac{10 \nu_w}{\lambda^2} \bar{e} \qquad \text{E.3}$$

with boundary conditions $z = 0, \quad -D \frac{d\bar{e}}{dz} = \dot{E}''$

$z = \infty \quad \bar{e} = 0$

We rewrite equation E.3 in dimensionless form using the parameters defined below.

t_d = dissipation time = $\frac{\lambda^2}{10\ \nu_w}$

$L = D\ t_d$ = characteristic diffusion distance

$\xi = z/L$ = dimensionless distance

E.4

Hence, equation E.3 becomes

$$\frac{d^2\bar{e}}{d\xi^2} = \bar{e} \quad \text{with conditions}$$

$$\xi = 0 \; ; \; \frac{d\bar{e}}{d\xi} = -\frac{\dot{E}'' L}{D}$$

$$\xi = \infty \; ; \; \bar{e} = 0 \qquad \text{E.5}$$

The solution to equation E.5 is given by

$$\bar{e}(\xi) = \frac{\dot{E}'' L}{D} \exp(-\xi) \qquad \text{E.6}$$

$$\text{i.e.,} \quad \bar{e}(z) = \frac{t_d}{T} \frac{E''}{\sqrt{D t_d}} \exp\left(-\frac{z}{\sqrt{D t_d}}\right) \qquad \text{E.7}$$

Note z is the depth below the water surface at any time.

APPENDIX F

ESTIMATION OF THE RESIDENCE TIME OF OIL GLOBULES SUBJECTED TO BREAKING WAVES

OBJECTIVE

The objective of the analysis is to obtain an estimate for the depth to which oil globules of a given size would be sunk and the total residence time of the globules in water, when an oil slick is subjected to the action of a breaking wave.

INTRODUCTION

The breaking action of waves in the open ocean is produced primarily by two mechanisms, viz, the nonlinear interaction of waves and by the action of the wind on developing seas. The intensity of breaking depends on the severity of sea conditions. The result of wave breaking is a loss of the wave energy. This energy lost by the wave manifests itself in the form of increased agitation of the water surface locally (turbulence), some of it goes to enhance the energy in other wave frequencies and a small fraction ends up as noise. The magnitude of the energy loss depends on the size of the breaking wave. The length over which the breaking action takes place is of the order of 1/4 of the mean wave length of the breaker. (Milgram,1976)

When an oil slick is subjected to the breaking waves, there is a high probability that at least some oil will be driven beneath the water surface. The oil slick may be torn by the breaking action resulting in the formation of globules of a spectrum of sizes. These globules, being buoyant, would tend to rise to the water surface after they are driven below the water surface. If, before the globules reach the surface, another wave hits the same area of the sea, the globules

may be held in suspension for a longer time. Hence, by knowing the total residence time of the oil globules due to the action of a single breaking wave and the probability of breaking in a given area, the average residence time of oil globules in a given sea condition can be calculated.

It is, therefore, the purpose of the analysis presented below to obtain an estimate of the residence time of an oil globule of a given size subjected to a breaking wave action. Because of the lack of the knowledge of the total energy lost by a breaker and the fraction of this energy that may be imparted to the oil globules, the direction of motion of the globules etc., suitable conservative assumptions are made.

ANALYSIS

To make the problem tractable we assume the following:

1. Energy dissipated by the breaking wave per unit area of sea surface underneath the breaking wave is constant (and equal to "E)
2. All of this energy goes to impart initial downward momentum to oil particles
3. Only one size oil particles are formed, and these do not form an emulsion with water
4. Analysis can be considered to be one dimensional (i.e., no edge effects).

The effect of the above assumptions and their impact on the results are discussed in a later section.

Let $\bar{\lambda}$ = mean wavelength of the breaking waves

a_b = minimum amplitude for breaking (based on the breaking criterion)

a = amplitude of the wave if it were not breaking

Hence energy lost by the breaking wave/unit area = $E_1'' = \frac{1}{2} \rho_w g (a^2 - a_b^2)$ (F.1)

However, this is the energy loss density averaged over a wavelength.

It is, however, known that waves break typically over a quarter of their wave length. Assuming that this energy is uniformly lost over $\lambda/4$, the total energy loss rate is

$$E'' = 4E_1'' = 2\rho_w g (a^2 - a_b^2) \qquad \text{(F.2)}$$

Let us assume the following
undisturbed oil thicknesss = b

The size of globules (dia) formed = d

Total number of globules formed per unit surface area = $N = \frac{b}{(\pi/6)d^3} = \frac{b}{V}$

Energy imparted to each globule (see assumption 2) = $\frac{E''}{N} = E^*$

Initial downward speed of oil globule = $u_i = \left[\frac{2E^*}{\rho_o V}\right]^{\frac{1}{2}}$ (F.3)

We now write the equation of motion of the particle

$$\left(\rho_o + \frac{\rho_w}{2}\right) V \frac{du}{dt} = -(\rho_w - \rho_o) V g - C_D \frac{1}{2} \rho_w u^2 A$$

+ pressure gradient terms that depend on the mean wave frequency. (F.4)

with $u = u_i$ at $t = 0$ (F.5)

where C_D is a constant drag coefficient (for oil gloubles a globule larger than 1 mm diameter), A is the cross-sectional area of and V its volume.

The pressure gradient term is dependent on the wave frequency, the location beneath the water surface and the phase within a wave cycle. This term will be small if the residence time of oil in water is small compared with the wave period.

For our analysis we assume a priori that the residence time is small compared to wave period. Hence we neglect the additional pressure gradient term.

To solve equation F.4 with condition 5 we define the following characteristic and dimensionless parameters

$$
\left\{
\begin{array}{lll}
t_{ch} = \dfrac{u_i\left(s+\frac{1}{2}\right)}{g\,(1-s)} & = & \text{Characteristic time, i.e. time to reach zero velocity under a constant deceleration of } g\left(\dfrac{s+\frac{1}{2}}{1-s}\right) \\
L = u_i\, t_{ch} & = & \text{characteristic depth (depth to which a constantly decelerating particle would go in time } t_{ch}) \\
s = \rho_o/\rho_w & = & \text{Specific gravity of oil relative to that of water} \\
\alpha^2 = \dfrac{\frac{1}{2} C_D \rho_w U_i^2 A}{\rho_w V g\,(1-s)} & = & \dfrac{\text{initial drag force}}{\text{buoyancy force on oil globule}} \\
\tau = t/t_{ch} & = & \text{dimensionless time} \\
v = u/u_i & = & \text{dimensionless velocity} \\
\xi = z/L & = & \text{dimensionless depth}
\end{array}
\right\} \qquad \text{(F.6)}
$$

Hence equation (F.4) can be written as

$$\frac{dv}{d\tau} = -(\alpha^2 v^2 + 1) \qquad \text{(F.7)}$$

with

$$v = 0 \quad \text{at} \quad \tau = 0 \qquad \text{(F.8)}$$

The solution to equation F.7 with F.8 is: (See Gradshteyn and Rhizhik, 1965).

$$(\tan^{-1}\alpha - \tan^{-1}\alpha v) = \alpha\tau \qquad \text{(F.9)}$$

i.e., $$v = \frac{1}{\alpha} \tan\left[\tan^{-1}\alpha - \alpha\tau\right] \qquad \text{(F.10)}$$

$$v = \frac{1}{\alpha}\left[\frac{\alpha - \tan\alpha\tau}{1 + \alpha\tan\alpha\tau}\right] \qquad \text{(F.11)}$$

From equation F.11 it can be seen easily that v = 0, i.e., the drop has reached the lowest position, when,

$$\tan\alpha\tau = \alpha \qquad \text{(F.12)}$$

$$\text{i.e.} \quad \tau_{sink} = \frac{1}{\alpha}\tan^{-1}\alpha \qquad \text{(F.13)}$$

To evaluate the depth of penetration:

We write the following kinematic equation of motion

$$\frac{d\zeta}{dt} = u. \qquad \text{(F.14)}$$

Using the definitions given in equation F.6, we have

$$\frac{d\xi}{d\tau} = v \qquad \text{(F.15)}$$

$$\text{with} \quad \xi = 0 \quad \text{at} \quad \tau = 0 \qquad \text{(F.16)}$$

Substituting the value for v from equation (F.10) in equation F.15 and rearranging we get

$$\int_{\xi=0}^{\xi} d\xi = \int_{\tau=0}^{\tau} \frac{1}{\alpha} \tan\left[\tan^{-1}\alpha - \alpha\tau\right] d\tau \quad \text{(see note below)}$$

$$\text{i.e.,} \quad \xi = \frac{1}{\alpha^2} \ln\left\{\frac{\cos(\tan^{-1}\alpha - \alpha\tau)}{\cos(\tan^{-1}\alpha)}\right\} \quad \text{(F.17)}$$

It can easily be shown that equation F.17 reduces to

$$\xi = \frac{1}{\alpha^2} \ln(\cos\alpha\tau + \alpha\sin\alpha\tau) \quad \text{(F.18)}$$

Hence, ξ_{max} is given by substituting the value of τ_{sink} from equation F.12

$$\xi_{max} = \frac{1}{2\alpha^2} \ln(1+\alpha^2) \quad \text{(F.19)}$$

$$\text{and} \quad \tau_{sink} = \frac{1}{\alpha} \tan^{-1}\alpha \quad \text{(F.13)}$$

---

* The solution to this integral is given by Selby (1967), page 377, equation 238.

CALCULATION OF RISE TIME:

After the oil globule reaches the maximum depth it is pushed back up by buoyancy force. However, a very short time later, the speed of the oil globule reaches its terminal velocity. No appreciable error will result if one assumes that the entire rise is at constant speed equal to the terminal velocity.

It can be shown that in the dimensionless parameterisation scheme defined by equation F.6 the terminal velocity is

$$v_{terminal} = \frac{1}{\alpha} \qquad (F.20)$$

Using equation F.15 and considering $v = v_{terminal}$ = constant we have (see equation F.19)

$$\tau_{Rise} = \frac{\varepsilon_{max}}{v_{terminal}} = \frac{1}{2\alpha} \ln(1+\alpha^2) \qquad (F.21)$$

Hence the total residence time is

$$\tau_{residence} = \tau_{sink} + \tau_{rise}$$

i.e., $$\tau_{res} = \frac{1}{\alpha}\left[\tan^{-1}\alpha + \frac{1}{2}\ln(1+\alpha^2)\right] \qquad (F.22)$$

NUMERICAL CALCULATIONS

We assume the following values for illustration purposes

Wave Parameters

Mean wavelength = $\bar{\lambda}$ = 28 m ($\bar{\kappa}$ = 0.21 m^{-1})

Critical breaking amplitude = a_b = 28/14 = 2 m

Consider the situation for a wave of amplitude = a = 3 m

Mean radian frequency of wave = $\bar{\omega} = \sqrt{\frac{2\pi g}{\lambda}}$ = 1.43 rad/s

Mean phase speed = $\bar{c} = \bar{\omega}/\bar{\kappa} = \frac{1.43}{0.21}$ = 6.83 m/s

Average energy lost by wave/ per unit sea area (equation F.1) = $E_1'' = \frac{1}{2} \times 1000 \times 9.8 \ (3^2 - 2^2)$ = 2.45×10^4 J/m^2

Energy density of lost energy over the breaking length (equation F.2) = $E'' = 4 \times 2.45 \times 10^4$ = 9.8×10^4 J/m^2

Oil Film Parameters

Oil density = ρ_o = 900 kg/m^3

Assume initial oil film thickness = b = 2cm = 2×10^{-2} m

Assume diameter of oil globules formed = d = 1 cm = 10^{-2} m

Volume of each globule = V = $\pi/6 \times 10^{-6}$ = 5.24×10^{-7} m^3

Hence number of globules (equation F.3) = $N = \frac{2 \times 10^{-2}}{5.24 \times 10^{-7}}$ = 3.82×10^4

Energy imparted to each globule (equation F.3) = $E'' = \frac{9.x \times 10^4}{3.82 \times 10^4}$ = 2.566 J

Initial speed of each globule (equation F.3) = u_i = 104.32 m/s

First we calculate the following force estimates on the particle.

Buoyancy force = $\rho_o V g(1 - s)$ = $10^3 \times 5.24 \times 10^{-7} \times 9.8 \times 0.1$ = 5.135×10^{-4} N

Initial drag force = $\frac{1}{2} C_D \rho_w u_i^2 A$ = $\frac{1}{2} \times 0.5 \times 10^3 \times 104.32^2 \times \left(\frac{\pi \times 10^{-4}}{4}\right)$ = 213.7 N

It is seen from the above that the drag force is about seven orders of magnitude larger than the buoyancy. Hence the buoyancy can be completely neglected in the calculations without appreciable error.

Order of magnitude of the depth to which oil globule would penetrate if drag were the only force resisting oil motion

$$= \frac{E''}{\text{Initial drag}} = \frac{2.566}{213.7} = 1.2 \times 10^{-2} \text{ m}$$

More Exact Calculations Using the Analysis Characteristic Parameters

t_{ch} (see equation F.6) $= \frac{104.32}{9.8} \frac{(0.9 + 0.5)}{(1 - 0.9)} = 149.03$ s

$L = 104.32 \times 149.03 = 15546.7$ m

$$\alpha = \left[\frac{213.7}{5.135 \times 10^{-4}}\right]^{\frac{1}{2}} = 645.0$$

dimensionless time for sinking (equation F.13) $= \tau_{sink} = \frac{1}{645} \tan^{-1} 645 = 2.433 \times 10^{-3}$

dimensionless terminal velocity (equation F.20) $= v_{terminal} = \frac{1}{645} = 1.55 \times 10^{-3}$

dimensionless sinking depth (equation F.19) $= \xi_{max} = \frac{1}{2 \times 645^2} \ln (1 + 645^2) = 1.555 \times 10^{-5}$

dimensionless rise time (equation F.21) $= \tau_{rise} = \frac{1.555 \times 10^{-5}}{1.55 \times 10^{-3}} = 1.003 \times 10^{-2}$

Hence,

dimensionless residence time (equation F.22) $\tau_{residence} = (2.433 \times 10^{-3} + 1.003 \times 10^{-2})$

$= 1.246 \times 10^{-2}$

Dimensionless Values

sinking time = $t_{sink} = 2.433 \times 10^{-3} \times 149.03 = 0.363$ s

rise time = $t_{rise} = 1.003 \times 10^{-2} \times 149.03 = 1.495$ s

Total residence time = $t_{residence} = 0.363 + 1.495 = 1.858$ s

maximum depth of penetration $z_{max} = 1.555 \times 10^{-5} \times 15546.7 = 0.242$ m

RESULTS AND DISCUSSION

The depth of penetration and the residence time of oil globules calculated for a variety of conditions are shown in Table F.1. The results in the table are arranged to indicate the sensitivity of the final answers to variations in the parameter values. The variation of residence time with initial drop speed is plotted in Figure F.1 and the change in the maximum depth of penetration with drop speed is indicated in Figure F.2.

The results indicate some interesting features. For example, it is seen that the depth of penetration is somewhat insensitive to the initial speed. (At an initial speed of 104 m/s the depth of penetration is 25 cm whereas at 7 m/s the penetration is 17 cm). Though this seems somewhat odd, it is easy to explain if one notes the high drag force (which is dependent on the square of the speed) initially for high speed. The result of the high drag is to reduce

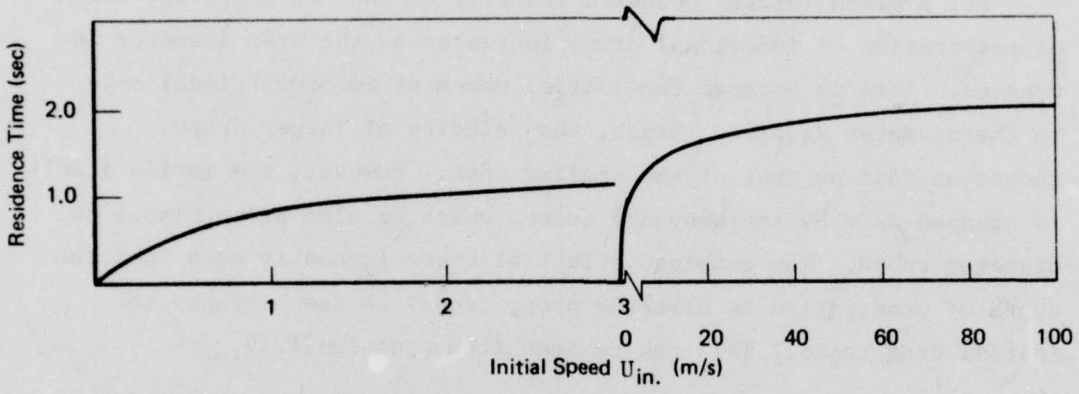

FIGURE F–1 VARIATION OF TOTAL RESIDENCE TIME OF 1 CM DIAMETER OIL DROP IN WATER AS A FUNCTION OF INITIAL DOWNWARD VELOCITY

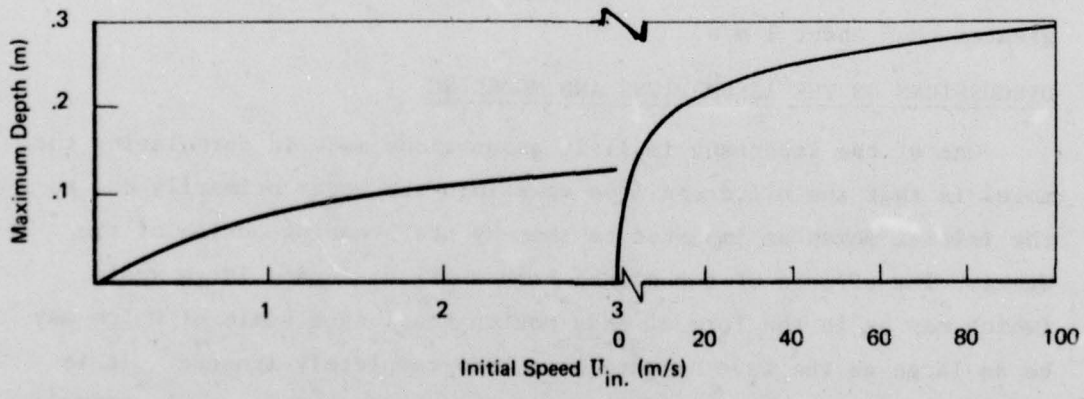

FIGURE F–2 MAXIMUM DEPTH OF PENETRATION AS A FUNCTION OF INITIAL VELOCITY

rapidly the speed. In effect most of the penetration occurs at very low speed, under a condition of retarding buoyancy force and a comparable drag force. Figures F.1 and F.2 indicate that for initial speed larger than about 20 m/s, the residence time and penetration depth for 1 cm diameter drop do not change appreciably. However, if the starting speed is very low, say less than 1 m/s, the penetration depth is also small (less than 10 cm).

For a given initial downward velocity of the oil drops the depth of penetration of individual drops increases as the drop diameter increases. This is because the initial momentum is proportional only to the diameter squared. Hence, the velocity of larger drops reduce as fast as that of the smaller ones. However, the motion itself is stopped only by the buoyancy force, which is also proportional to diameter cubed. The combined effect of these forces is such that the depth of penetration is directly proportional to the buoyancy to initial drag ratio. This can be seen from equation F.19.

The changes in the values of other parameters such as the drag coefficient and gravity (which is a manifestation of the accelerating water due to wave action) do not result in substantial changes in the values of the penetration depth.

The one important observation that can be made from the sensitivity analysis results given in Table F.1 is that the ratio of the depth penetration to the diameter is almost invariant for speeds of drops greater than about 1 m/s.

DISCUSSIONS ON THE ASSUMPTIONS AND MODELING

One of the important implicit assumptions made in formulating the model is that the oil drops move down into the water primarily due to the initial momentum imparted to them by the breaking action of the waves. The effects of turbulence both small scale and large scale (which may be in the form of eddy motion the length scale of which may be as large as the wave height) have been completely ignored. It is not certain whether such a drastic assumption is valid -- only experiments can provide answers to these unknowns. If indeed large-scale eddy motions do result as a consequence of repetitive breaking waves at a location (and the accumulation of vorticity in the water), the depth to which oil drops may be carried down will then be comparable to the eddy sizes.

Table F.1

Sensitivity of depth penetration and residence time to changes in the values of various parameters

Relative density of oil $s=\rho_o/\rho_w$	Diameter of oil globule d (m)	Drag coefficient C_D	Initial downward speed of globules u_i (m/s)	Gravitational acceleration g (m/s^2)	Oil residence time t_{res} (s)	Depth of penetration h_{max} (m)	$\frac{h_{max}}{d}$	Remarks
0.9	$1x10^{-2}$	0.4	104.3	9.8	2.05	$29.7x10^{-2}$	29.7	Variation of oil specific gravity
0.95	$1x10^{-2}$	0.4	104.3	9.8	3.13	$32.4x10^{-2}$	32.4	
0.99	$1x10^{-2}$	0.4	104.3	9.8	7.89	$37.3x10^{-2}$	37.3	
0.9	$1x10^{-2}$	0.4	0.25	9.8	0.38	$2.5x10^{-2}$	2.5	Variation of initial downward speed of oil drops
0.9	$1x10^{-2}$	0.4	1.00	9.8	0.81	$8.1x10^{-2}$	8.1	
0.9	$1x10^{-2}$	0.4	10.00	9.8	1.44	$18.7x10^{-2}$	18.7	
0.9	$1x10^{-2}$	0.4	100.00	9.8	2.04	$29.5x10^{-2}$	29.5	
0.9	$1x10^{-3}$	0.4	104.3	9.8	0.74	$3.5x10^{-2}$	35	Variation with diameter
0.9	$2x10^{-2}$	0.4	104.3	9.8	2.77	$56.1x10^{-2}$	28	
0.9	$1x10^{-2}$	0.4	104.3	4.9	3.02	$31.3x10^{-2}$	31.3	Buoyancy and diameter variation. Gravity variation assumed because of the accelerating effects of water motion
0.9	$1x10^{-2}$	0.4	104.3	7.35	2.41	$30.3x10^{-2}$	30.3	
0.9	$1x10^{-3}$	0.4	104.3	7.35	0.87	$3.6x10^{-2}$	35.7	
0.9	$2x10^{-3}$	0.4	104.3	7.35	1.18	$6.8x10^{-2}$	34.1	
0.9	$2x10^{-2}$	0.4	104.3	7.35	3.26	$57.5x10^{-2}$	28.7	
0.9	$1x10^{-2}$	0.5	104.3	9.8	1.86	$24.2x10^{-2}$	24.2	Drag coefficient variation

The merit of developing a model for the motion of oil drops in the absence of turbulence (as is done in the present case) lies in obtaining an order of magnitude estimate of the depths to which globules of oil would be driven when only the traditional retarding forces exist.

The second important assumption made was on the total energy that goes into generating the initial motion of the oil globules. We assumed that all of the energy lost by the breaking wave manifests itself as the kinetic energy of the oil globules. This is clearly not true, and there results unreasonably high initial speeds of the oil globules (104 m/s in the example given). What is more appropriate, probably, is to assume the initial speed of the globules to be equal to (or of the same order of magnitude as) the phase speed of the breaking wave. However, we note that the starting speed has very little effect on the penetration depth. In the example considered, if we had assumed that only 1% the wave loss energy goes into oil globules (therefore initial speed of the order of 10 m/s) we would still predict a penetration depth of about 20 cm . As a matter of fact, it is entirely probable that nature indeed will partition the energy such that 99% goes into inducing turbulence in the water with a small amount going into the oil globule production and motion. What this means is that by measuring the depth of penetration of oil globules in an experiment, it is impossible to estimate the energy partition.

We have also assumed tacitly that oil globules start moving vertically down through the water column. However, an observation of the white cap region of a spilling wave would indicate that the water particles (in the white cap) have a rolling motion, rolling on the steep side of the breaking wave. If oil were present, the oil particles produced by the surface breaking action would probably be projected at an angle somewhere between the wave surface and vertical. Therefore, the oil particles in real situation may not reach the depths predicted by the simple model proposed. Hence, the model is conservative in that the residence time predicted will be longer, and consequently lower sea states (producing breaking waves long periods apart) may keep the globules in suspension.

In the analysis presented, the accelerations of water due to the wave motion and the resulting pressure gradient opposing or aiding (depending on the wave phase) the oil drop motion have been neglected. This does not seem to affect the result as evidenced by the insensitivity of the penetration depth to variations in the g value. Besides the residence time seems to be quite small compared to wave periods.

CONCLUSIONS

The major conclusions from this analysis are

- it is unrealistic to account for all of the wave energy lost by a breaking wave by initial kinetic energy of oil globules.
- most of the wave energy loss has to be assigned to water turbulence, and its effect on downward dispersion of oil has to be considered.
- the maximum initial speed of oil globules is probably comparable to the water particle speeds in a breaking wave; this speed is in the range 1 to 10 m/s.
- for a three orders-of-magnitude variation in downward speed of the globules the ratio of penetration depth to diameter varies only by about an order of magnitude. This ratio is insensitive to initial velocity for velocities greater than a critical value.
- the possibility of large-scale motion induced by eddies of wave height size moving the oil drops down en masse should be explored.

APPENDIX G

CHARACTERIZATION OF THE ABSORBING BOUNDARY CONDITION PRESENTED BY THE OIL FILM FOR THE MOTION OF OIL GLOBULES IN WATER

1. Introduction

In this appendix the detailed analysis is given for mathematically modeling the absorption condition posed by the presence of an oil slick on the water surface and for the stochastic determination of the motion of oil globules underneath it. The statistics of the oil globule motion have already been discussed in Section 4.3.6.2. It is recalled that the globule number density distribution function is assumed to be given by an underlying Gaussian function suitably modified by the absorption barrier effect of the (progressively growing) oil film at the water surface. It is this effect on the distribution function that is discussed in this appendix.

The presence of an absorbing barrier affects the probability density function (pdf; also termed the distribution) in two ways. The first way is by the truncation of the distribution at the point of absorption. This is explained by the physical boundary condition that no particle can travel beyond the barrier (that is,cross the barrier). The second effect of the barrier is to reduce the density function within the field of particle motion (which for the case of oil globules in water is below the water surface). This effect is explained in detail below.

Consider the Gaussian distribution of particles at a given time t which can be assumed to be the distribution in the absence of the barrier. Associated with a specific spatial location, which for the purposes of discussion can be identified as "depth z" in figure G.1, is the probability density value. This value in a sense represents the relative chances of a particle's being at location between z and z + dz at the given time t. Figure G.1 shows schematically some particle

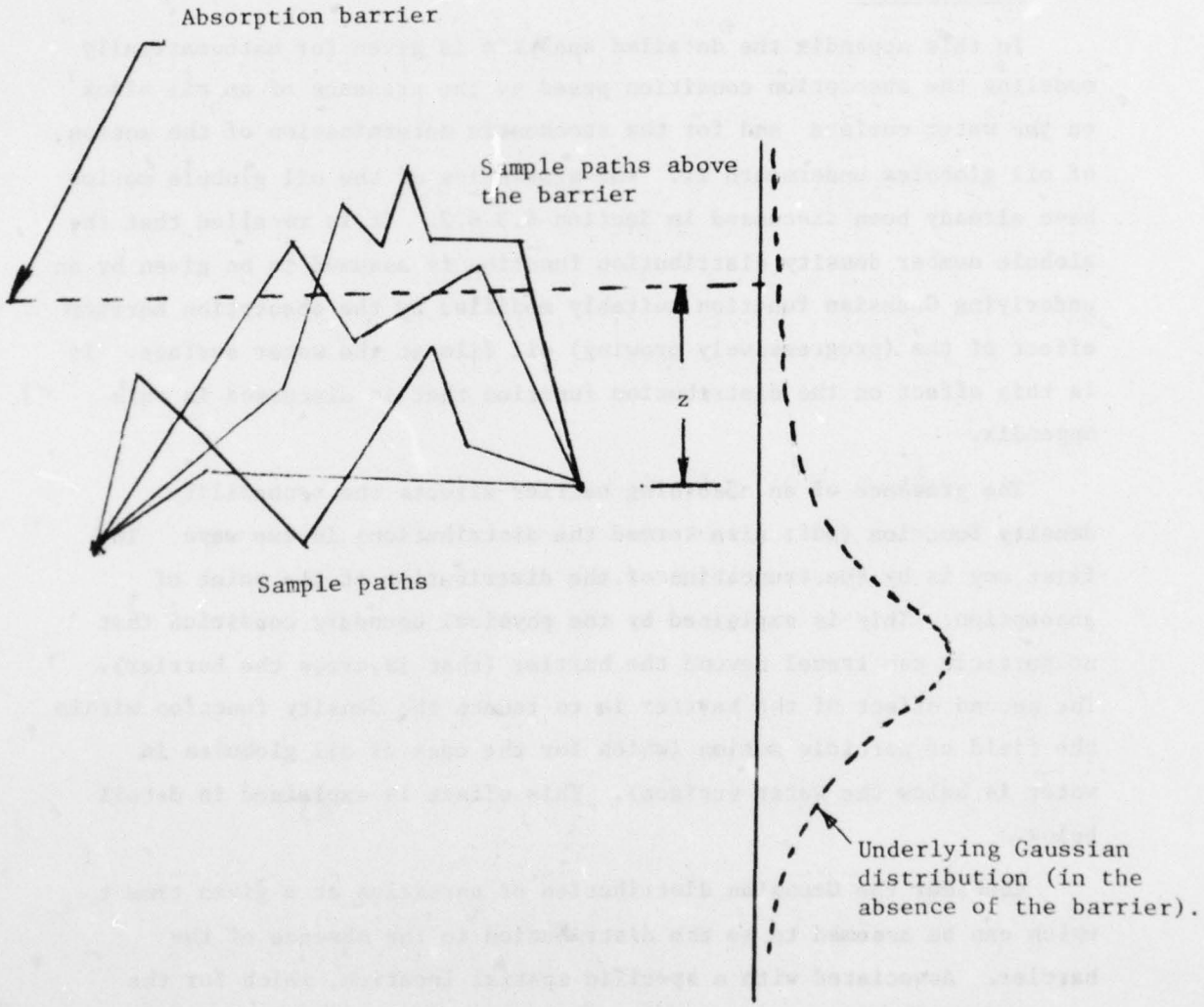

Figure G.1: Schematic representation of the effect of barrier on sample paths of the particle.

traces (called sample paths) by which a particle may reach z. If an absorbing barrier is introduced at the location shown, certain sample paths are eliminated. That is, it is no longer possible for a particle to go above the barrier and then reach z. The chances of reaching z are hence reduced which, in effect, results in the reduction of the probability distribution function (p.d.f.).

The behavior of the boundary is also dependent on the characteristics of the motion of the particles in the field. If the particle motion is similar to a simple Brownian motion with a fixed location for the mean position of the distribution function, the effect of the boundary can be analyzed easily. However, in the case of the motion of the oil globules subjected to ocean turbulence, there is a mean upward drift of particles, because of the lower density of oil relative to water. This phenomenon introduces further complications in the mathematics for the evaluation of the absorption boundary effect.

2. Analyses

2.1 Brownian Motion with Zero Mean Drift

Let us consider a process which has no mean drift and whose distribution function (Gaussian) has the mean at the depth h. Let the absorbing barrier be at depth zero. These are shown schematically in Figure G.2.

The normalized density function in the absence of the barrier is given by

$$f^*(\xi) = \frac{1}{\sqrt{2\pi}\,\sigma(t)}\, e^{-\frac{(\xi-\lambda)^2}{2\sigma^2}} \qquad \text{G.1}$$

$$(-\infty < \xi < \infty)$$

We now examine a sample path that terminates at point P which is at a depth z below the barrier. This is presented in Figure G.2 as the path ABCDP. This would be one possible path by which a particle from A may reach P in the absence of the barrier. However, in the presence of the barrier this path is not allowable and is, therefore, termed an "absorbed path".

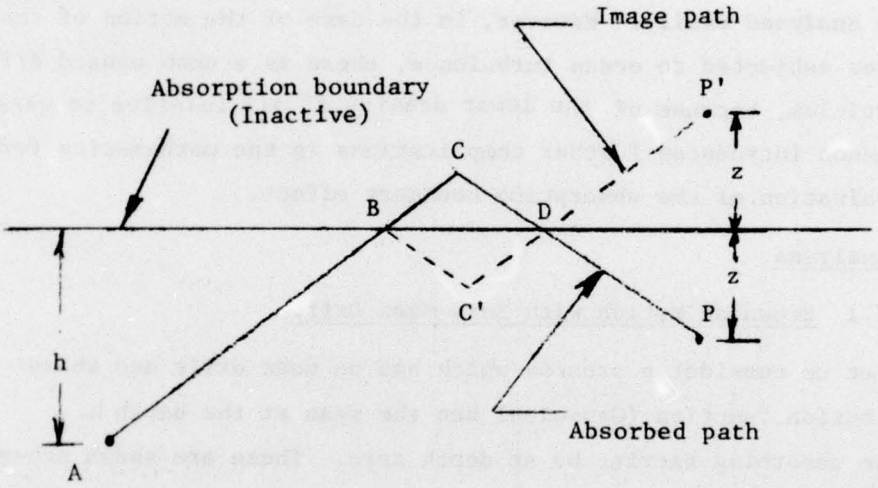

Figure G.2: Schematic representation of absorbed and image paths for a stationary mean (position) Brownian process.

We now consider in addition to the absorbed path ABCDP, its mirror reflection (in the barrier) path ABC'DP', which, in the absence of barrier results in a particle ending up at point P' (which is exactly z distance above the barrier). This path is termed the "imaged path".

The Brownian motion has the mathematical property of independent increments. That is, the distribution of increments occurring after a time t is independent of the same path before t. Thus the relative probability measure of the imaged path ABC'DP' is the same as that of the absorbed path ABCDP. It then follows that there is a one-to-one correspondence between the theoretical sample paths ending at P (within the field of motion) and those ending at P' (at the image positions). Hence the density of the absorbed paths normally terminating at P is equal to the unabsorbed density of paths terminating at image positions P'. That is

Prob (Cross zero, terminate at depth z, z + dz)
= prob (cross zero, terminate at position z, z + dz above the barrier) G.2

Hence, the reduction in the p.d.f. in the field of motion is obtained by removing from the underlying Gaussian function that part of the probability represented by sample paths terminating at the image positions. Hence, the actual probability density distribution in the presence of an absorbing barrier is

$$f(z) = \frac{1}{\sqrt{2\pi}\,\sigma}\left[\exp\left(\frac{(z-h)^2}{2\sigma^2}\right) - \exp\left(-\frac{(z+h)^2}{2\sigma^2}\right)\right] \qquad \text{G.3}$$

2.2 Absorption Effect in the Presence of a Mean Drift

a) General Approach

In the presence of a mean drift, so that the position of the mean (h) of the underlying Gaussian distribution is a function of time, the reduction in the probability density cannot be determined by simply considering absorbed and image paths as in the previous section.

Consider now a time varying underlying Gaussian function given by

$$f^*(z,t) = \frac{1}{\sqrt{2\pi}\,\sigma(t)} \exp\left\{-\frac{[z-h(t)]^2}{2\sigma^2}\right\} \qquad \text{G.4}$$

where z is considered positive in the increasing depth direction.

For constant upward drift velocity u_t of the mean of the distribution we have,

$$h(t) = h(t_i) - u_t (t - t_i) \qquad \text{G.5}$$

The absorption barrier is at position x = 0. The reduction in the p.d.f is calculated in this case also by considering sample paths but accounting properly for the times elapsed in particular motions.

Instead of allowing the barrier to be stationary and the mean position to move up to the barrier, the problem is transformed to a coordinate system in which the barrier is moving towards the mean position. This transformation does not alter the physics of the problem but makes the mathematics relatively simpler.

Consider a sample path starting at the position of the mean. This is represented by the point A in Figure G.3. At time t = 0, the point A is at a depth h(0) below the barrier. This sample path terminates at point P which is at location z below the barrier. The time taken for a particle travel between A and P is t. As the particle is moving upward, the barrier is also moving down (in the sense of the coordinate transformation discussed above) and the particle path intersects the barrier at point B at time, say, s. In the absence of the barrier the particle path would then be BCDP, terminating at P.

As in the previous section, we calculate the probability absorption by calculating the probability of the image path. However, in this case the image path is BC'DP' where P' is the image of P in the line BG. (Note B is the position of the barrier at the time s of "impact"

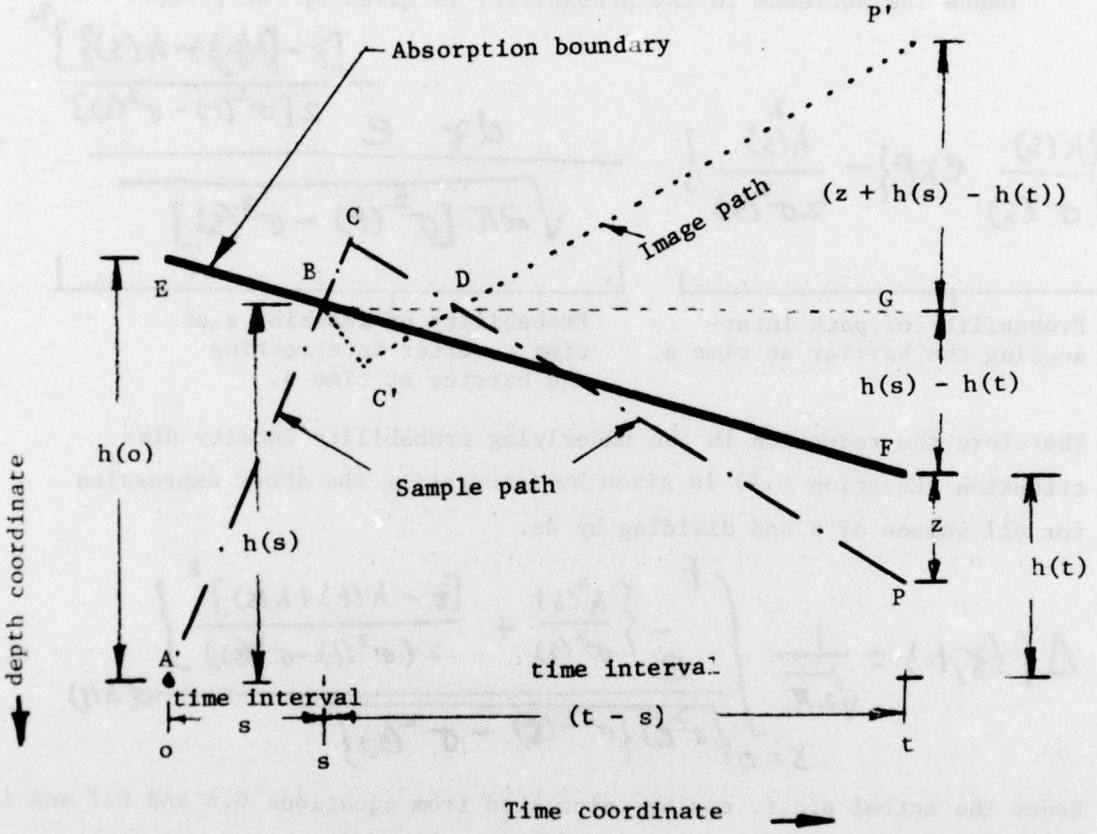

Figure G.3: Schematic diagram showing the particle paths used in the evaluation of the effect of absorption barrier when there is a mean drift of particles.

of the sample path with the barrier). Therefore the probability of absorption is the combined probability of reaching the barrier at time s and then terminating at position P' [whose distance from the barrier at time t is z + 2 (h(s)-h(t)) as can be seen from Figure G.3]. Since s is any arbitrary time, all possible values of s between zero and t have to be considered.

Hence the decrease in the probability is given by the product

$$\underbrace{\frac{dh(s)}{\sqrt{2\pi}\,\sigma(s)}\exp\left\{-\frac{h^2(s)}{2\sigma^2(s)}\right\}}_{\text{Probability of path intersecting the barrier at time s.}}\quad\underbrace{\frac{d\gamma\; e^{-\frac{[\gamma-\{h(t)-h(s)\}]^2}{2[\sigma^2(t)-\sigma^2(s)]}}}{\sqrt{2\pi[\sigma^2(t)-\sigma^2(s)]}}}_{\text{Probability of reaching z at time t, after intersecting the barrier at time s.}} \qquad \text{G.6}$$

Therefore the reduction in the underlying probability density distribution (Equation G.4) is given by integrating the above expression for all values of s and dividing by dz.

$$\Delta f(\gamma,t) = \frac{1}{\sqrt{2\pi}}\int_{s=0}^{t} \frac{e^{-\left\{\frac{h^2(s)}{\sigma^2(s)}+\frac{[\gamma-h(t)+h(s)]^2}{2(\sigma^2(t)-\sigma^2(s))}\right\}}}{\sqrt{\sigma^2(s)\{\sigma^2(t)-\sigma^2(s)\}}}\,dh(s) \qquad \text{G.7}$$

Hence the actual p.d.f. can be calculated from equations G.4 and G.7 and is given by

$$f(\gamma,t) = f^*(\gamma,t) - \Delta f(\gamma,t) \qquad \text{G.8}$$

The expression in Equation G.7 is the most general value for the effect of the absorption boundary on the distribution function in a Brownian motion. For constant drift speed of the mean, equation G.5 can be substituted in the integrand of equation G.7.

b) Simplified Approach

The evaluation of the effect of the absorbing boundary on the density function, in general, involves the calculation of the integral given in Equation G.7. In most problems, with complicated time dependent turbulence characteristics (i.e., σ), the determination of the integral value can be achieved only by numerical means. However, a simple and approximate value for the effective reduction in the p.d.f. can be obtained by the analysis given below. The analysis retains all of the physics of the problem, but by making judicious simplifying assumptions reduces the mathematics to solving a quadratic equation.

The principle of this approach is based on the ideas developed in Section G.2.2, but considering the effect of mean drift. This is accomplished by considering a single particle path as shown in Figure G.4.

Consider the path ABP where P is the position at a distance z below the barrier. The particle leaving A reaches P in time t after intersecting the barrier at time* $(t-s)$.

The total vertical distance travelled by the particle in time $\hat{t}$ is given by (see Figure G.4),

$$L = H - u_t(\hat{t}-s) + z + u_t s. \qquad \text{G.9}$$

where $\hat{t} = t - t_{dm}$ G.10

t_{dm} = time at which the depth of the mean of the density distribution is a maximum (this is obtained by the methods illustrated in Section 4.3.6 and Appendix F).

Hence the average speed $= \frac{\text{distance travelled}}{\text{time}} = \frac{L}{\hat{t}}$ G.11

*It is to be noted that this intersection time is termed $(\hat{t}-s)$ instead of s as was used in the previous case. This slightly confusing change is made for mathematical convenience.

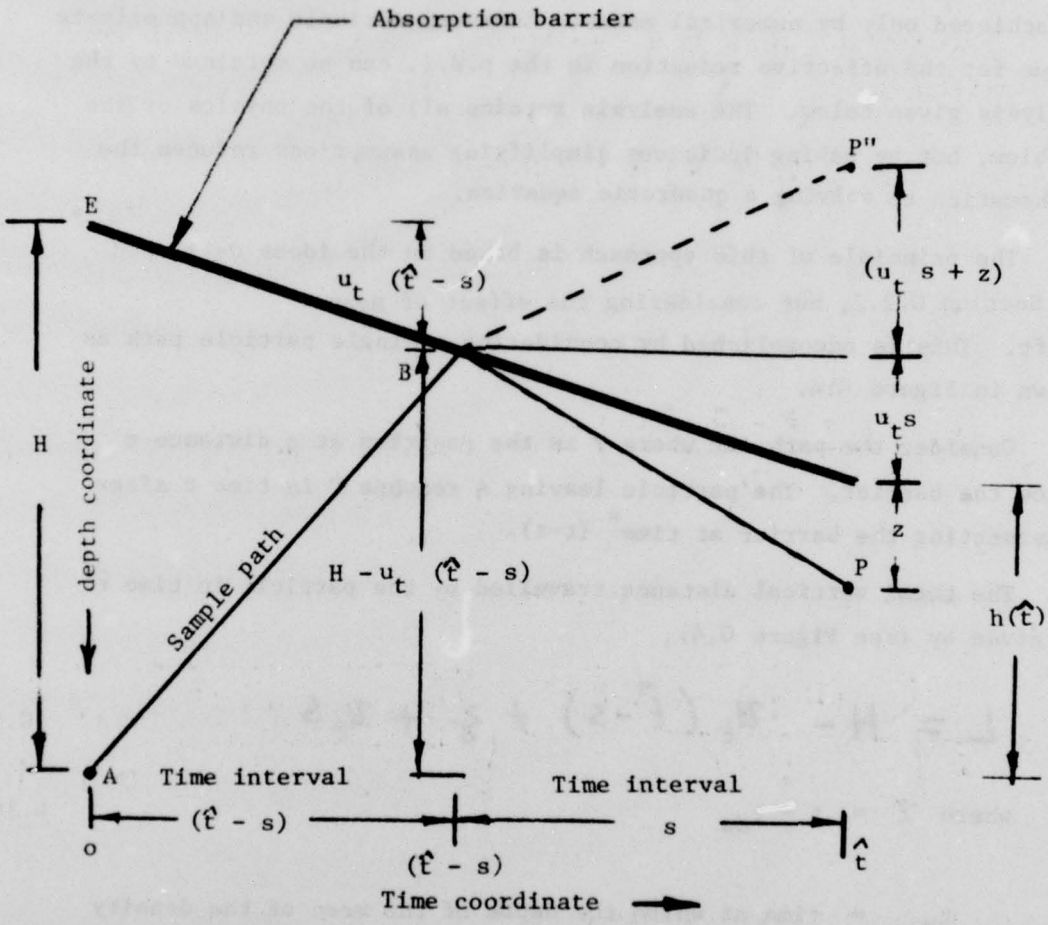

Figure G.4: Schematic diagram showing the principle involved in calculating the barrier effect, using the approximate approach.

Assuming that the average speed of the particle is the same before and after encounter with the barrier we have

$$\frac{L}{\vec{t}} = \frac{H - u_t(\vec{t}-s)}{(\vec{t}-s)} \qquad \text{G.12}$$

Substituting for L from equation G.9 in G.12 we get after some simplification

$$\frac{H - u_t(\vec{t}-s) + \delta + u_t s}{\vec{t}} = \frac{H}{\hat{t}-s} - u_t \qquad \text{G.13}$$

i.e.,

$$s^2 + \left(\frac{H+\delta-2u_t\vec{t}}{2u_t}\right)s - \frac{\delta\vec{t}}{2u_t} = 0 \qquad \text{G.14}$$

Solving this quadratic for s we have

$$s = \frac{1}{2}\left[-\frac{(H+\delta-2u_t\vec{t})}{2u_t} + \sqrt{\frac{(H+\delta-2u_t\vec{t})^2}{(2u_t)^2} + \frac{4\delta\vec{t}}{2u_t}}\right] \qquad \text{G.15}$$

where the positive sign is taken in front of the square root to conform to the condition that at $\hat{t} = 0$, $s = 0$. G.16

Therefore the reduction in the underlying probability function is determined by calculating the probability of the presence image path ABP' in the absence of the barrier. That is,

$$\Delta f(\delta,t) \simeq \frac{1}{\sqrt{2\pi}\,\sigma(t)} \exp\left[-\frac{(\delta+h(t)+2u_t s)^2}{2\sigma^2(t)}\right] \qquad \text{G.17}$$

where s is given by equation G.15.

It is noted that the value of Δf in equation G.17 changes with z not only due to the appearance of z in the exponent but because of the dependence of s on z. Also the value H should be interpreted as the maximum depth of penetration of the particles in the sense of the analyses presented in Section 4.3.6 and in Appendix F.

The actual density function is, therefore, given by equation G.8 where for Δf the expression in equation G.17 is used.

BIBLIOGRAPHY

Abramowitz, M., and I.A. Stegun, "Handbook of Mathematical Functions," National Bureau of Standards, Applied Mathematics Series -55, June 1964.

Banner, M.L., and Phillips, O.M. "On the Incipient Breaking of Small Scale Waves," J. Fluid Mech., 65, Part 4, 1974, pp. 647-656.

Barger, W.R., Garrett, W.D., Mollo-Christensen, E.L., and Ruggles, K.W., "Effects of an Artificial Sea Slick upon the Atmosphere and the Ocean," J. Appl. Meteorology, 9, No. 3, June 1970, pp. 396-400.

Barnett, T.P., "On the Generation, Dissipation and Prediction of Ocean Wind Waves," J. Geo. Phys. Res., 73, No. 2, Jan. 1968, pp. 513-529.

Bauer, W.H., and Bulloff, J.J., "Chemical Additives to Control Oil Spills - A State of the Art Summary, Interim Technical Report to USCG on Contract No. DOT-CG-33, 755-A, Jan. 1974.

Beegle, B.L., Modell M., and Reid R.C., "Thermodynamic Stability Criterion for Pure Substances and Mixtures," *AICHE J.*, 21, 1974, p. 1200.

Belyeav, V.S., Lubimtzev, M.M., and Ozmidov, R.V., "The Rate of Dissipation of Turbulent Energy in the Upper Layer of the Ocean," J. Phys. Ocean, 5, July 1975, pp. 499-505.

Bigelow, H.B., and Edmondson, W.T., "*Wind Waves at Sea, Breakers and* Surf," H.O. Pub #602, U.S. Navy Hydrographic Office, Washington, D.C., 1952.

Brunnock, J.V., Duckworth, D.F., and Stephens, G.C., "Analysis of Beach Pollutants," J. Inst. Petroleum, 54, No. 539, Nov. 1968, p. 324.

Carslaw, H.S., and Jaeger, J.C., "Conduction of Heat in Solids," 2nd Edition, Oxford, Clarendon Press, 1967.

Coles, "Heavy Weather Sailing," John De Graff, Tuckahoe, N.Y., 1972.

Crandall and Mark, "Random Vibration in Mechanical Systems," Academic Press, New York, 1963.

Davis, S.J., and Gibbs, C.F., "The Effect of Weathering on a Crude Oil Residue Exposed at Sea," Water Research, 9, 1975, pp. 275-285.

Dean, R.A., "The Chemistry of Crude Oils in Relations to Their Spillage on the Sea," Symp. Proc., "Biological Effects of Oil Pollution on Littoral Communities," Field Studies Council, London, July 1968.

Donelan, Longuet-Higgins, and Turner, "Periodicity in Whitecaps," Nature, 239, 1972, pp. 449-451.

Donnaly, R., Experiments Demonstrated at USCG Headquarters, Washington, October 15, 1976.

Fallah, M.H., and Stark, R.M., "Literature Review - Movement of Spilled Oil at Sea," Marine Tech Soc. J., 10-N1, Jan. 1976, pp. 3-18.

Faller, A.J., "Oceanic Mixing and the Langmuir Circulation," Technical Note #BN683, Institute for Fluid Dynamics and Applied Mathematics and Graduate Meteorology Program, University of Maryland, College Park, Maryland, March 1971.

Falvey, H.T., "Prediction of Wind Wave Heights," ASCE J., Hyd. Div., 100 (WWI), Feb. 1974, pp. 1-12.

Fay, J.A., "Physical Processes in the Spread of Oil on Water Surface," Prevention and Control of Oil Spills, Am. Petrol. Inst., Washington, D.C., 1970, pp. 463-467.

Gradshteyn, I.S., and I.M. Ryzhik, "Table of Intergrals Series and Products," Fourth Edition, Academic Press, 1965.

Harrison, W., Winnik, M.A., Kwong, P.T.Y., and MacKay, D., "Disappearance of Aromatic and Aliphatic Components from Small Sea Surface Slicks," Env. Sci. Tech., 9, No. 3, March 1975.

Hasselmann et al., "Measurements of Wind-Wave Growth and Swell Decay during the Joint North Sea Wave Project, "Deutsches Hydrographiches Institute, Hamburg, 1973.

Hasselmann et al., "A Parametric Wave Prediction Model," J. Phys. Oceanography, 6, 1976, pp. 200-228.

Hinze, J.O., "Turbulence - An Introduction to Its Mechanism and Theory," McGraw Hill, 1959.

Jeffreys, H., "On the Formation of Water Waves in a Wind," Proc. Royal Soc. London, Ser. A, 1924, pp. 107-189.

Jones, W.T., "Instability at an Interface between Oil and Flowing Water," J. Basic Engineering, 1972, pp. 874-878.

Kinsman, B., "Wind Waves: Their Generation and Propagation on the Ocean Surface," Prentice Hall, Englewood Cliffs, N.J., 1965.

Kolesnichenko, S.G., Derzhavets, A. Ya, and Chebanyuk, L.K., "An Investigation of Wave Transformation in the Presence of a Whole Oil Film on the Sea Surface," Odessa Marine Research Institute, USSR,

Lamb, H., "Hydrodynamics," 6th Edition, Dover Publications, N.Y., 1932.

Leibovich, S., "Oil Slick Instability and the Entrainment Failure of Oil Containment Booms," ASME, 75-FE-8, 1975.

Leibovich, S., "A Natural Limit to the Containment and Removal of Oil Spills at Sea," Ocean Eng., 3, 1975, pp. 29-36.

Levich, V.G., "Physico-Chemical Hydrodynamics," Prentice Hall, New York, 1962, pp. 433 and 452.

Longuet-Higgins, M.S., "On the Statistical Distribution of the Heights of Sea Waves," J. Marine Res., XI, No. 3, 1975, pp. 245-266.

Longuet-Higgins, M.S., "A Model of Flow Separation at a Free Surface," J. Fluid Mech., 57, Part I, 1973, pp. 129-148.

Longuet-Higgins, M.S., "On Wave Breaking and Equilibrium Spectrum of Wind Generated Waves," Proc. Royal Soc. London, Ser. A, 310, 1969, pp. 151-159.

Longuet-Higgins, M.S., and Turner, J.S., "An Entrainment Model of a Spilling Breaker," J. Fluid Mech., 63, Part I, 1974, pp. 1-20.

Longuet-Higgins and Cartwright, "The Statistical Distribution of the Maxima of a Random Function," Proc. Royal Soc. London, A 237, 1956, pp. 212-232.

Longuet-Higgins, "On the Joint Distribution of the Periods of Amplitudes of Sea Waves," J. Geophys. Res., 80, 1975, pp. 2688-2694.

McLean, A.Y., and Betancourt, O.J., "Physical and Chemical Changes in Spilled Oil Weathering under Natural Conditions," Paper No. OTC-1748, Offshore Technology Conf., Dallas, 1973.

Michael, W.H., "Sea Spectra Simplified," Marine Technology, Jan. 1968, pp. 17-30.

Milgram, J.H., Dept. of Ocean Engineering, MIT, Personal Communication, May 1976.

Milgram, J.H., and Van Houten, R.J., "Hydrodynamics of the Containment of Oil Slicks," 10th Symp. on Naval Hydrohynamics, MIT, June 1974.

Osborn, T.R., "Report on the Symposium on Turbulence in the Ocean," 11-14 June 1968, Report #25, Institute of Oceanography, University of British Columbia, Vancouver, B.C., July 1970.

Phillips, O.M., "The Equilibrium Range in the Spectrum of Wind-Generated Waves," J. Fluid Mech., 4, 1958, pp. 426-434.

Price, R.K., "Detailed Structure of the Breaking Wave," J. Geo. Phys. Res., 75, No. 27, Sept. 1970, pp. 5276-5278.

Price, R.K., "The Breaking of Water Waves," J. Geo. Phys. Res., 76, No. 6, Feb. 1971, pp. 1576-1581.

Regnier, Z.R., and Scott, B.F., "Evaporation Rates of Oil Components, Env. Sci. Tech., 9, No. 5, May 1975.

Ruggles, K.W., "The Vertical Mean Wind Profile over the Ocean for Light to Moderate Winds," J. Appl. Meteorology, 9, No. 3, June 1970, pp. 389-395.

Schlichting, H., "Boundary Layer Theory," Fourth Edition, McGraw-Hill, 1962.

Scott, J.T. et al., "On the Mechanisms of Langmuir Circulations and Their Role in Epilimion Mixing," Limnology and Oceanography, 14, 1969, pp. 493-503.

Selby, S.M., "Standard Mathematical Tables," 15th Edition, The Chemical Rubber Co., Ohio, 1967.

Slattery J., Northwestern University, Evanston, Illinois, 1975 (class notes).

Stewart and Grant, "Determination of the Rate of Dissipation of Turbulent Energy near the Sea Surface in the Presence of Waves," J. Geophys. Res., 67, 1962, pp. 3177-3180.

Svedrup, H.V., and Munk, W.H., "Wind, Sea and Swell, Theory of Relations for Forecasting," Hydrographic Office, Pub. CK. No. 601, U.S. Dept. of Navy, 1947.

Taylor, G.I., "Statistical Theory of Turbulence I-III," Proc. Royal Soc. London, A 151, No. 874, 1935a, pp. 421-464.

Tennekes, H., and Lumley, J.L., "A First Course in Turbulence," The MIT Press, 3rd printing, Dec. 1974.

Van Dorn, W.G., "Oceanography and Seamanship," Dodd, Mead, and Co., New York, 1974.

Van Dorn, W.G., and Pazan, "Laboratory Investigations of Wave Breaking," Scripps Institution of Oceanography, Ref. #75-21, 1976.

Waldman, G.D., Johnson, R.A., and Smith, P.C. "The Spreading and Transport of Oil Slicks on the Open Ocean in the Presence of Wind, Waves and Currents," Final Report to USCG, Contract DOT-CG-20617-A, AVCO Corp., Wilmington, Mass., July 1973.

Wicks, M., "Fluid Dynamics of Floating Oil Containment by Mechanical Barriers in the Presence of Water Currents," Proceedings of the Joint Conference on Prevention and Control of Oil Spills, American Petroleum Institute, 1969, pp. 55-106.

Wilson, B.W., "Note on Surface Wind Strees over Water at Low and High Wind Speeds", J. Geo. Phys. Res., 65, No. 10, Oct. 1960, pp. 3377-3382.

Zalosh, R.G., and Jensen, D.S., "A Numerical Model of Droplet Entrainment from a Contained Oil Slick," Symp. Fluid Mechanics in the Petroleum Industry, Houston, Dec. 1975.

*U.S. GOVERNMENT PRINTING OFFICE: 1978 733-306/410 1-3